Thesis Entitled

Manganese Substituted Polyoxometalates and their Functionalization: Synthesis, Characterization and Oxidation of Alkenes

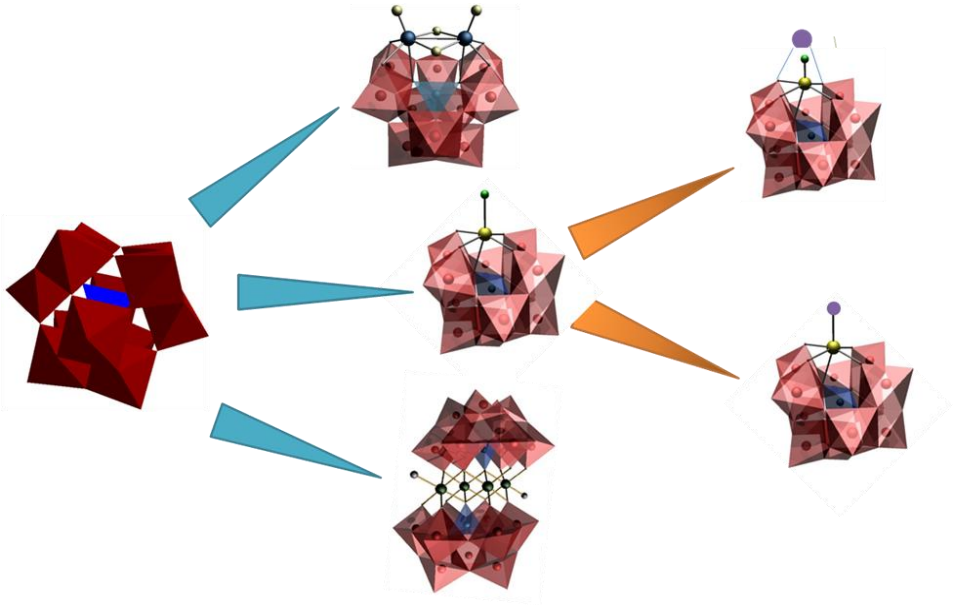

Submitted to
The Maharaja Sayajirao University of Baroda

For the Degree of

DOCTOR OF PHILOSOPHY
IN
CHEMISTRY

By
Mr. Ketan R. Patel

Department of Chemistry, Faculty of Science
The Maharaja Sayajirao University of Baroda, Vadodara 390 002
INDIA

August 2012

Department of Chemistry
Centre of Advanced Studies in Chemistry
& DST-FIST sponsored Department
Faculty of Science, Vadodara 390 002
India
Tel: +91-265-2795552
E-mail: chemistry_msu@yahoo.com
The Maharaja Sayajirao University of Baroda

CHL\ Date:

CERTIFICATE

This is to certify that the thesis entitled, "**Manganese Substituted Polyoxometalates and their Functionalization: Synthesis, Characterization and Oxidation of Alkenes**", submitted for Ph. D. degree in chemistry by **Mr. Ketan R. Patel** contains original research work and no part of the thesis has been submitted for any other degree.

(Dr. Anjali Patel)
Research Supervisor

(Prof. B. V. Kamath)
Head
Chemistry Department

(Prof. Nikhil Desai)
Dean
Faculty of Science

Dedicated to

My Late Mom
and
My Dad

I especially wish to thank my advisor, Dr. Anjali Patel, Associate Professor, Department of Chemistry, Faculty of Science, M. S. University of Baroda, for offering me the opportunity to work with her in such a productive group and in such an interesting area of chemistry. She has given me a continuous flow of freedom and encouragement throughout my whole research period. With her great support, I have obtained exceptional achievements in my academic career. She has truly influenced my life in a positive way and helped me to develop both as a person and as a scientist, for this I will always be grateful. It is really fortunate for me to present this work with the contributions from an outstanding Guide like her.

Ketan Patel

ACKNOWLEDGEMENTS

I would like to thank Department of Science and Technology (DST, New Delhi), for providing financial support, in form of project fellow.
I avail this opportunity to render my sincere thanks to Prof. B. V. Kamath, Head, Chemistry Department, M. S. University of Baroda, Vadodara for providing infrastructure facility.

I am thankful to the following persons for helping me during the different stages of my research work

Dr. Amitava Das	Cyclic Voltammetric studies	Analytical Division, CSMCRI
Prof. Shobhana K. Menon	Cyclic Voltammetric studies	Chemistry Department, Gujarat University
Prof. Samar Das	Crystal Structure refinement	School of Chemistry, University of Hyderabad
Dr. Vandana Rao	SEM and EDAX analysis	Metallurgy Department, M. S. University of Baroda

I take this opportunity to thank my seniors, Dr. Pragati Shringarpure-Joshi for helping me in all the difficulties during the research period. I would also like to thank my colleagues, Miss. Varsha Brahmakhatri, Mr. Soyebkhan Pathan, Nilesh Narkhede and Sukriti Singh for their kind co-operation during the work.

I am thankful to all non-teaching staff of the Chemistry Department for their helping hand throughout my research work.

Last but not the least, I wish to express my deep sense of gratitude to my family members and friends for their moral support, constant encouragement and co-operation throughout my work.

.

Ketan Patel

PART –B Functionalization of Transition Metal Substituted Polyoxometalates

List of Abbreviations

PW_{12}	Dodecatungstophosphate
PW_{11}	Undecatungstophosphate
PW_{10}	Decatungstophosphate
$PW_{11}Mn$	Mono Mn(II) substituted phosphoyungstate
$PW_{10}Mn_2$	Di Mn(II) substituted phosphotungstate
PW_9Mn_4	Tetra-Mn(II) substituted sandwich type phosphotungstate
S	Salen
$PW_{11}Mn$--S	Functionalized $PW_{11}Mn$ by salen
SBA	(S)-(+)-sec-butylamine
$PW_{11}Mn$-SBA	Functionalized $PW_{11}Mn$ by SBA
Cy	(R)-(-)-1-cyclohexylethylamine
$PW_{11}Mn$-Cy	Functionalized $PW_{11}Mn$ by Cy
Sty	Styrene
StyO	Styrene oxide
BA	Benzaldehyde
Cy6	Cyclohexene
Cy6O	Cyclohexene oxide
Cy8	*cis*-Cyclooctene
Cy8O	Cyclooctene oxide
TBHP	*tert*-Butyl hydrogen peroxide

General Introduction

The great majority of inorganic compounds are constructed of metallic atoms as principal entities. Inorganic molecules have great potential because the numbers of elements in purely inorganic molecules, combined with structural diversity, make them more powerful, particularly as far as their application is concerned. In fact, the search for new properties puts more importance on the elements in a framework than on the structure itself. In this regard, Polyoxometalates (POMs) chemistry offers opportunities, insights, properties and applications that cannot be matched by any other single group of compounds. Polyoxometalates form a large and distinctive class of molecular inorganic compounds of unrivaled electronic versatility as well as structural variation that impacts the various fields of science and technology and there have been major developments in this respect [1-3].

What are Polyoxometalates?

Polyoxometalates are discrete anionic metal oxygen clusters which can be regarded as soluble oxide fragments [3] and have come up as a key emerging area that promises to allow the development of sophisticated design molecule-based materials. They are a distinctive class with unique properties of topology, size, electronic versatility as well as structural diversity. Due to the combination of their added value properties such as redox properties, large sizes, high negative charge, nucleophilicity they play a great role in various fields such as medicine, material science, photochromism, electrochemistry, magnetism as well as catalysis.

POMs have the general formula $[X_xM_mO_y]^{q-}$, in which X is the hetero atom, usually a main group element (e.g., P, Si, Ge, As), and M is the addenda atom, being a d-block element in high oxidation state, usually $V^{IV,V}$, Mo^{VI} or W^{VI}. These compounds are always negatively charged although the negative density is widely variable depending on the elemental composition and the molecular structure.

POMs are polymeric oxoanions formed by different mononuclear oxoanions as shown in the following equation.

$$12MO_4^{m-} + XO_4^{p-} + 23H^+ \longrightarrow [XM_{12}O_{40}]^{n-} + H_2O$$

The free acids or acidic forms of POMs are known as heteropolyacids.

POMs are gaining much more attention because of the following reasons [1-3].

- Chemical properties of POMs such as redox potentials, acidities, and solubilities in various media (aqueous as well as organic) can be tuned by choosing constituent elements and counter cations.
- POMs are thermally and oxidatively stable in comparison with common organometallic complexes and enzymes.
- Metal-substituted POMs with "controlled active sites" can easily be synthesized.

History of Polyoxometalates

The polyoxometalates have been known since the work of Berzelius [4] on the ammonium 12-molybdophosphate in 1826.

After the discovery of this first polyoxometalates, the field of POMs chemistry progressed significantly [2].

1. About 20 years later, Svanberg and Struve showed that the insoluble ammonium salt of this complex could be used for the gravimetric analysis of phosphate.

2. However, the study of polyoxoanions chemistry did not accelerate until the discovery of the tungstosilicic acids and their salts in 1862 by Marignac [5].

3. Thereafter, the field developed rapidly, so that over 60 different types of heteropoly acids (giving rise to several hundred salts) had been described by the end of first decade of this century.

4. In 1908, A. Miolati suggested a structural hypothesis for heteropoly compounds based on coordination theory. According to his hypothesis, the heteroatom was considered to have octahedral coordination with MO_4^{2-} or $M_2O_7^{2-}$ ligands.

5. In the mid 1930's, A. Rosenheim had given a laboratory perspective for the synthetic and descriptive research of Miolati.

6. The first steps towards understanding the structure of polyoxometalates anions was taken by L. C. Pauling in 1929. Pauling [6] proposed a structure for 12:1 complexes based on an arrangement of twelve MO_6 octahedra surrounding a central XO_4 tetrahedron. He proposed the structure of 12-tungstoanions based on the central PO_4 or SiO_4 tetrahedrons surrounded by WO_6 octahedrons. In order to minimize electrostatic repulsions, he proposed that all the polyhedral linkages involved sharing of vertices rather than edges. As a result the resulting formula required 58 oxygen atoms i.e. $[(PO_4)W_{12}O_{18}(OH)_{36}]^{3-}$.

7. After Pauling's proposal, in 1933 Keggin [7,8] solved the structure of $H_3PW_{12}O_{40}.5H_2O$ by powder X-ray diffraction and showed that the anion was indeed based on WO_6 octahedral units. As suggested by Pauling, these octahedra being linked by shared edges as well as corners. The application of X-ray crystallography to the determination of polyoxometalate structures accelerated the development of polyoxometalate chemistry.

8. An year later in 1934, Signer and Gross demonstrated that $H_4SiW_{12}O_{40}$, $H_5BW_{12}O_{40}$ and $H_6[H_2W_{12}O_{40}]$ were structurally isomorphous with Keggin's structure [9].

9. Bradley and Illingworth confirmed Keggin's work in 1936, by studying the crystal structure of $H_3PW_{12}O_{40}.29H_2O$.

10. These results of (Bradley's and Illingworth's) were largely supported by the single crystal experiments of Brown and co-workers, which were reported in 1977.

With the development of polyoxometalate chemistry various types of structures were discovered and listed in Table 1 and Figure 1.

Table 1. Different types of POMs families [3]

Structure	[a]General Formula	Charge	X^{n+}
Keggin	$XM_{12}O_{40}$	8-n	P^{5+}, As^{5+}, Si^{4+}, Ge^{4+}
Silverton	$XM_{12}O_{42}$	8-	Ce^{4+}, Th^{4+}
Dawson	$X_2M_{18}O_{62}$	6-	P^{5+}, As^{5+}
Waugh	XM_9O_{32}	6-	Mn^{4+}, Ni^{4+}
Anderson (Type A)	XM_6O_{24}	12-n	Te^{6+}, I^{7+}

[a]where M= Mo^{VI},W^{VI},$V^{V,\ VI}$ etc.

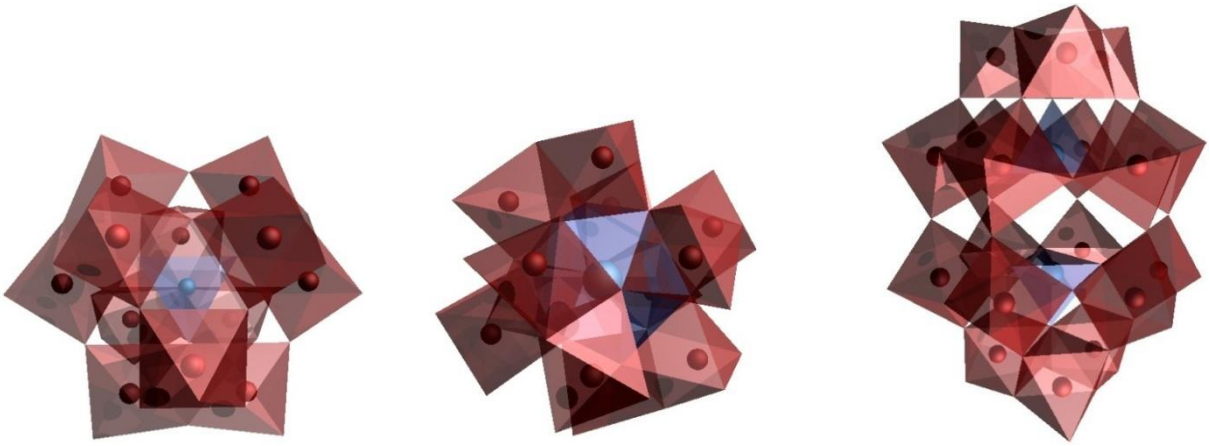

(a) Keggin (b) Silverton (c) Dawson

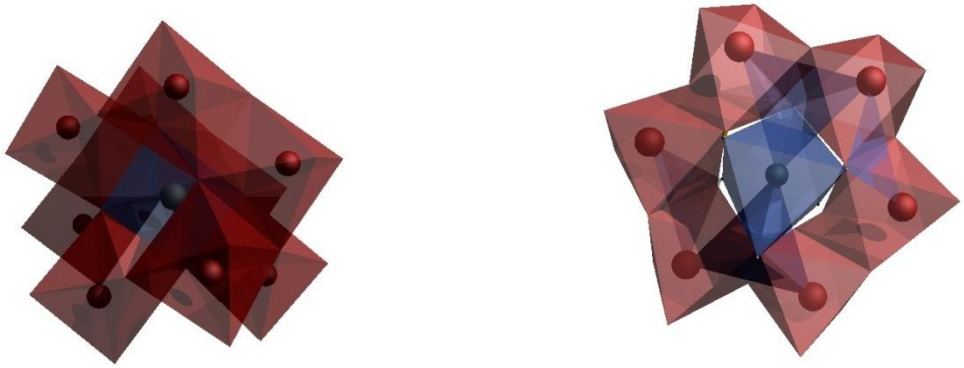

(d) Waugh (e) Anderson

Figure 1. Polyhedral representation of different types of POMs/ polyanions

After that, an extensive literature on their synthesis, structure and properties has been accumulated and summarized in the form of reviews as well as books namely:

1. “Heteropoly and Isopoly Oxometalates” by M.T. Pope, (Eds.) C. K. Jorgensen, Springer-Verlag, Berlin, (1983).

2. Inorganic solid acids and their use in acid catalyzed hydrocarbon reactions had studied by A. Corma, *Chem. Rev.*, 95, 559, (1995).

3. The catalytic properties of heteropoly compounds have been studied and reviewed by T. Okuhara, N. Mizuno, M. Misono, *Adv. Catal.*, 41, 113, (1996).

4. Issue on Polyoxometalates, Eds. C. L. Hill, *Chem. Rev.*, 98, 1, (1998).

5. “Metal-oxygen clusters: The surface and catalytic properties of heteropolyoxometalates”, by J. B. Moffat, (Eds.) M. V. Twing, M. S. Spencer, Kluwer Academic plenum, New York, (2001).

6.“Polyoxometalate chemistry: From topology via self assembly to applications” by M.T.Pope and A. Muller, (Eds.) M. T. Pope and A. Muller, Kluwer Academic, (2001).

7. “Catalysts for fine chemical synthesis: Catalysis by polyoxometalates”, I. V. Kozhevnikov, Vol. 2, Wiley (2002).

8. "Polyoxometalate Molecular Science" by M. T. Pope, A. Muller, Kluwer Academic Publishers, (2003).

9. "Mechanisms in homogeneous and heterogeneous epoxidation catalysis", Ch 4 "Activation of hydrogen peroxide by polyoxometalates" by N. Mizuno, (Eds) S. Ted Oyama, Elesvier Publications, (2008)

10. “Modern heterogeneous oxidation catalysis”, Ch 6 “Liquid-Phase Oxidations with Hydrogen Peroxide and Molecular Oxygen Catalyzed by Polyoxometalate-Based Compounds” by N. Mizuno, (Eds) N. Mizuno, Wiley (2009)

11. Green Oxidation Reactions by Polyoxometalate-Based Catalysts: From Molecular to Solid Catalysts by Mizuno, *Top. Catal.*, 53, 876, (2010).

12. Polyoxometalates: Building blocks for functional nanoscale systems by L. Cronin, *Angew. Chem.*, 49, 1736, (2010).

13. Hybrid Organic-Inorganic Polyoxometalate Compounds: From Structural Diversity to Applications by Anne Dolbecq, *Chem. Rev.,* 110, 6009, (2010).

14. Polyoxometalates containing late transition and noble metal atoms by Frederic Lefebvre, *Coordination. Chem. Rev.,* 255, 1642, (2011).

Structure of Polyoxometalates

The structure of $[PW_{12}O_{40}]^{3-}$ was first reported by Keggin in 1933. It consists of a central XO_4 tetrahedron (X = heteroatom or central atom) surrounded by twelve MO_6 octahedra (M = addenda atom). The twelve MO_6 octahedra comprise four groups of three edge-shared octahedra, the M_3O_{13} triplet [7, 8], which have a common oxygen vertex connected to the central heteroatom.

The oxygen atoms in this structure fall into four classes of symmetry-equivalent oxygens: X-O_a-$(M)_3$, M-O_b-M, connecting two M_3O_{13} units by corner sharing; M-O_c-M, connecting two M_3O_{13} units by edge sharing; and O_d-M, where M is the addenda atom and X the heteroatom. The simplest representation is showing in Figure 2.

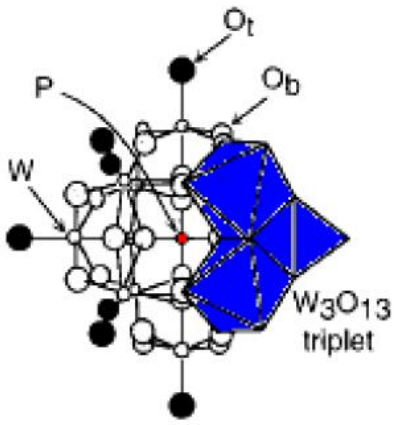

Figure 2. Keggin type $[PW_{12}O_{40}]^{3-}$

Geometrically, five isomers have been proposed by Baker and Figgis [10]. The α isomer, which has the overall T_d symmetry, is the most prevalent and thermodynamic stable isomer. Rotating one of the triads by 60° forms the β-Keggin, and the overall symmetry changes from T_d to C_{3v}. The γ, δ and ε isomers are formed by successive 60° rotation of two, three or four W_3O_{13} groups, respectively. They are less stable than the α- and β-isomers due to the increasing numbers of coulombically-unfavorable edge-shared contacts of two highly charged metal ions. Once all four triads are rotated, the overall symmetry of the resulting ε-isomer goes back to T_d.

Polyoxometalate compounds, in the solid state, are composed of polyoxoanions, cations such as protons, metals and water of crystallization. Sometimes in additions they contain neutral organic molecules. From the view point of catalysis based on POMs, it is very important to distinguish between the primary, secondary and tertiary structure [11-15]. It has also been realized that, in addition to these structures, tertiary and higher-order structures influence the catalytic function [14]**.** The different types of structures for the polyoxoanion are represented in Figure 3.

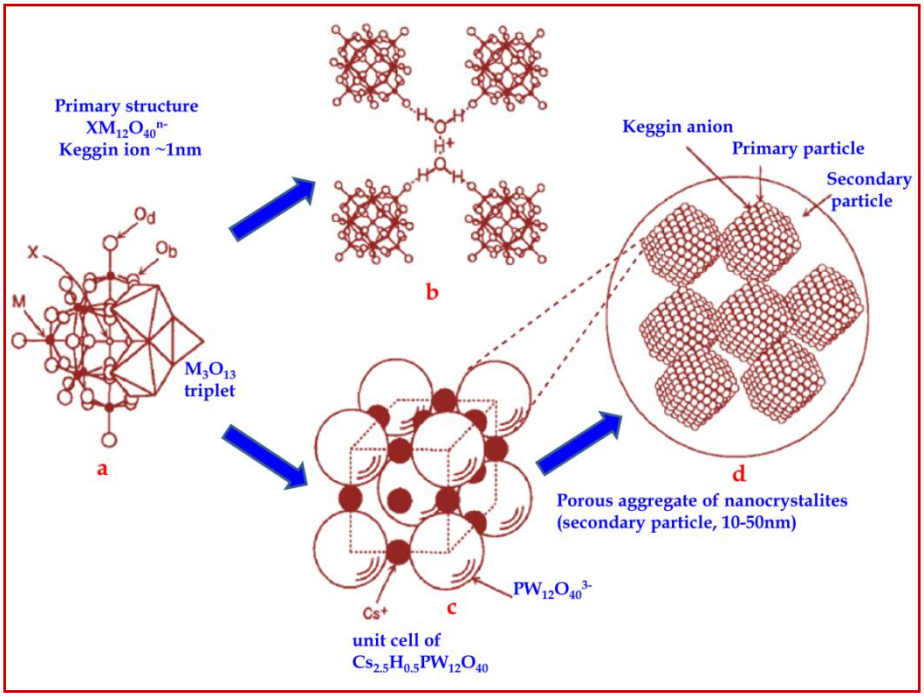

Figure 3. Primary, secondary, and tertiary structures of Keggin type polyoxometalate; (a) Primary structure (Keggin structure, $XM_{12}O_{40}$); (b) Secondary structure ($H_3PW_{12}O_{40}.6H_2O$); (c) Secondary structure for unit cell of ($Cs_3PW_{12}O_{40}$); (d) Tertiary structure with porous aggregates [$Cs_{2.5}H_{0.5}PW_{12}O_{40}$]; {Taken from "Advances in Catalysis", by M. Misono and N. Mizuno, 41, 113, (1996)}

The basic structure of a polyoxoanion molecule itself is called a "primary structure" and is formed from the condensation of oxoanions (Figure 3a). The

secondary structure of the solid POMs is formed from the coordination of the polyoxoanion with acidic protons, other cations and/or water molecules of hydration (Figure 3b). A stable form contains six water molecules of hydration per Keggin unit, forming a body centered cubic (bcc) structure with Keggin units at the lattice points and $H_5O_2^+$ bridges along the faces. Each terminal oxygen atom is bound to a hydrogen atom of an $H_5O_2^+$ bridge. In this structure, the acidic protons are located in the $H_5O_2^+$ bridges between lattice points. If less than six water molecules are present, acidic protons may be located in remaining $H_5O_2^+$ bridges, in H_3O^+ or may be directly coordinated to oxygen atoms of the Keggin unit. The tertiary structure is the structure of solid POMs as assembled. The size of the particles, pore structure, distributions of protons in the particle etc. is the elements of the tertiary structure (Figure 3c).

Properties of Polyoxometalates

Polyoxometalates have usually low surface area (1-10 m^2/g) reflecting their high solubility in water. The pores of POMs are inter-particle, not intra-crystalline. Considering the size and shape of the Keggin anion and the crystal structure, there is no open pore through which nitrogen molecule can penetrate.

Thermal Stability

There are various kinds of stabilities, for example, thermal stability and hydrolytic stability in solution, and those stabilities change very much depending on the type of POMs [11-13]. Some solid POMs in acidic form are thermally stable and applicable to vapor phase reactions conducted at high temperatures. The thermal stability of these polyoxometalates changes with heteroatom, polyatom and polyanion structure as follows:

$$PW_{12}O_{40}^{3-} > PMo_{12}O_{40}^{3-} > SiMo_{12}O_{40}^{4-}$$

But the thermal stability of mixed addenda heteropolyanions is generally low. The thermal stability of polyoxometalate type compounds is studied extensively by TGA, DTA, XRD, etc.

The Differential Thermal Analysis (DTA) results of different POMs shows an endotherm at lower temperature and an exotherm at higher temperature (Table 2). The low temperature endotherm is due to removal of water. The high temperature exotherm is ascribed to the decomposition of cage like structure of heteropolyanion compound to yield a more compact crystalline product consisting large oxides of Mo(VI) and W(VI).

Table 2. DTA results of various Heteropolyacids

Heteropolyacids	Endotherm (K)	Exotherm (K)
$H_3PW_{12}O_{40}$	448-569	853-868
$H_4SiW_{12}O_{40}$	413-551	743-773
$H_3PMo_{12}O_{40}$	336-432	663-681
$H_4SiMo_{12}O_{40}$	337-453	609-628

Herve et al. investigated the thermal changes of structures by means of XRD, TGA and DTA for Keggin type polyoxoanions e.g., $H_3PW_{12}O_{40}.29H_2O$,

$H_3PMo_{12}O_{40}.29H_2O$ and $H_4PMo_{11}O_{40}.29H_2O$. FT-IR of $H_4PMo_{11}O_{40}.29H_2O$ showed the release of V atoms to form $H_3PMo_{12}O_{40}$ and V_2O_5 species.

From TGA and DTA two types of water are observed in POMs compounds i.e., water of crystallization and constitutional water molecules. The former usually lost at temperature below 473K. The constitutional water molecules (acidic protons bound to oxygen of the polyanion) of $H_3PW_{12}O_{40}$ and $H_3PMo_{12}O_{40}$ are lost at 623K and 543K respectively.

In situ XRD, ^{31}P NMR and thermoanalysis, it was concluded that thermolysis of $H_3PMo_{12}O_{40}$ proceeds in two steps, as shown below:

$$H_3PMo_{12}O_{40}.nH_2O \underset{nH_2O}{\overset{473-623\,K}{\rightleftharpoons}} H_3PMo_{12}O_{40} \underset{-1.5H_2O}{\overset{658\,K}{\rightleftharpoons}} H_xPMo_{12}O_{38.5+\frac{x}{2}(x=0.01)}$$

The MoO_3 phase appears at temperature higher than 573 K.

Hodnett and Moffat assumed that the same decomposition proceeded via $H_3PW_{12}O_{40}$. Thermal gravimetric analysis of $H_3PW_{12}O_{40}$ and $Cs_{2.5}H_{0.5}PW_{12}O_{40}$ showed that entire water molecules of crystallization are lost at temperature as low as 573K and acidic groups are removed as water is formed from protons and lattice oxygens at temperatures exceeding 623 K. The number of protons lost, x, in $Cs_{2.5}H_{0.5-x}PW_{12}O_{40-x}$ were 0.24, 0.31 and 0.32 after treatment at 623K, 673K and 773K respectively. Similar removal of protons of $K_{2.5}H_{0.5}PMo_{12}O_{40}$ begins by 500K. The thermal stability of $H_3PMo_{12}O_{40}$ and its salts changes with counter cations. Bi and tetravalent metal salts are not stable. The hydrogen form and ammonium salts decomposed at 693 and 743 K respectively. Cs and K salts are stable up to their melting point.

Adsorption and Absorption properties

A remarkable characteristic property of some of the solid POMs is the ability to absorb easily a large quantity of polar or basic molecules such as alcohols and nitrogen bases in the solid bulk [16-18]. The absorption depends on basicity and the size of the molecule to be absorbed and the rigidness of the secondary

structure. While in case of desorption, alcohols absorbed can readily leave the bulk, but desorption of pyridine and ammonia needs a high temperature.

Acidic properties [19]

It was proved that acidic forms of POMs such as $H_3PW_{12}O_{40}$ and $H_3PMo_{12}O_{40}$ in the solid state are pure Bronsted acids and are stronger acids than the conventional solid acids such as SiO_2-Al_2O_3, H_3PO_4/SiO_2, HX and HY zeolites [17, 20]. Heteropolyacids are much stronger than the oxoacids of constitute elements and ordinary mineral acids (Table 3). The strong acidity is caused by:

1. Dispersion of the negative charge over many atoms of the polyanion
2. The fact that the negative charge is less distributed over the outer surface of the polyanion owing to the double-bond character of the M=O bond, which polarizes the negative charge of O_t to M.

Table 3. Dissociation Constants of various acids and acidic form of POMs [19]

Sr. No.	Acids	pK1	pK2	pK3
1	$H_3PW_{12}O_{40}$	1.6	3.0	4.0
2	$H_4PW_{11}VO_{40}$	1.8	3.2	4.4
3	$H_3PMo_{12}O_{40}$	2.0	3.6	5.9
4	$H_4SiMo_{12}O_{40}$	2.1	3.9	5.9
5	H_2SO_4	6.6	-	-
6	HCl	4.3	-	-
7	HNO_3	9.4	-	-

The key to the effectiveness of polyoxoanions as catalysts is the high Bronsted acidity associated with them. This high Bronsted acidity is due to the large polarization of negative charge on the polyoxoanionic species. They are complex Bronsted acids, with very strong Brønsted acidity, approaching the superacid region [19]. Their acid–base properties can be varied over a wide range by changing the chemical composition. This unique structure exhibits

extremely high proton mobility, while heteropolyanions can stabilize cationic organic as well as inorganic intermediates. On top of that POMs have a good thermal stability in the solid state, far better than other strong acids.

In aqueous solution, of acidic forms of POMs i.e. heteropolyacids are strong, fully dissociated acids [21]. $SiW_{12}O_{40}^{4-}$, $PW_{12}O_{40}^{3-}$, anions remain deprotonated even after accepting two and three extra electrons respectively. In solution, POMs are stronger than the usual mineral acids such as H_2SO_4, HCl, HNO_3. The central atom is the important factor in determining the acid strength and the acidity is related to the total charge on the anion than to the type of metal atom in the shell of heteropoly acids. The acid strength is found to follow the order

$$H_3PW_{12}O_{40} > H_4SiW_{12}O_{40} > H_3AsW_{12}O_{40} > H_4GeW_{12}O_{40}$$

Redox properties

The addenda metal atoms in most POMs are in their highest oxidation states (d^0) and it is therefore clear that these complexes are in general capable of acting as oxidizing agents [2]. It was noted that certain polyanions, especially the 12-molybdo Keggin type species were readily reduced to form blue species more commonly known as "heteropoly blues" or "molybdenum blues". In most of the POMs structures the addenda (i.e. metal) atoms occupy "octahedral" sites with either one or two terminal oxygen atoms. As a result, they can undergo facile reversible reduction to yield species of the type $\{MOL_5\}$ in which one or more of the metal centers has a reduced i.e. d^1 configuration.

Depending on the solvent, the acidity of the solution and the charge of the polyanion, the reductions involve either single electron or multi electron steps often accompanied by protonation. The oxidation potential is strongly dependent on the addenda atom and is not much influenced by central hetero atom. The oxidation potentials of polyanions containing Mo and V are high as these ions are easily reduced. It has been reported that oxidative ability decreases in the order V - > Mo - > W – containing heteropolyanion.

Redox properties of dodecapolyoxoanions depend on both the constituent elements of polyanions and counter cations. The oxidizing ability (or reducibility) has been estimated from the reduction of POMs compounds by H_2, CO and organic compounds. The methods involve measurements of the reduction rate at a constant temperature, the temperature-programmed reduction and the EPR signal formed by the reduction. Also the binding energy of the XPS peaks has been examined. Although the orders of oxidizing ability observed differ a little for the various methods adopted and the investigators, the following trends have been observed:

When the activation of a reducing agent proceeds easily, the reduction rate of polyanions approximately parallels the oxidation potential in solution. For example, in the case of heteropolyanions mixed with Pd/carbon powders, the order for the reduction by H_2 was

$$PMo_{12} > SiMo_{12} > PW_{12} > SiW_{12}$$

Oxidation reactions in which POMs compounds are efficient solid catalysts are oxidative dehydrogenation of aldehydes, carboxylic acids, ketones, nitriles, etc. to form C=C bonds at α position to a C=O or C=N group and dehydrogenation of alcohols and amines to form C=O and C=N bonds, as well as oxidation of aldehydes to produce carboxylic acids.

Apart from these, the use of POMs in oxidation catalysis is much more complicated and diverse. The basic importance of using POMs in various homogeneous as well as heterogeneous oxidation chemistry is due to their inherent stability towards strong oxidants as well as their ability to retain their structures at high temperatures.

Applications of Polyoxometalates

Since the discovery of POMs, they found significant importance in various fields of science and technology. The field of POMs chemistry is about more than two centuries old but still they are a large and rapidly growing class of compounds, especially because of their large domains of applications. The

applications of POMs based on combinations of so-called “value-adding properties” are summarized in Table 4.

Table 4. Applications of POMs based on "Value adding properties" [22]

Sr.No.	Application fields
1	Coatings
2	Analytical chemistry
3	Processing radioactive waste
4	Separations
5	Sorbents of gases
6	Membranes
7	Sensors
8	Dyes/pigments
9	Electrochemistry/electrodes
10	Capacitors
11	Dopants in nonconductive polymers
12	Dopants in conductive polymers
13	Dopants in sol-gel matrixes
14	Cation exchangers
15	Flammability control
16	Bleaching of paper pulp
17	Clinical analysis
18	Food chemistry
19	Catalysis

Some of the most important fields where POMs have played a significant role are described in the Table 5.

Table 5. Areas of applications involving acidic form POMs/POMs

Sr. No.	**POMs**	**Application field**	**Reference**
1	$H_4PMo_{11}VO_{40}$ $K_xH_{4x}PMo_{11}VO_{40,}$ $H_5PMo_{10}V_2O_{40}$	modification of carbon electrodes, capacitors	23
2	$H_3PMo_{12}O_{40}$,$H_3PW_{12}O_{40}$	electrolytic capacitors	24, 25
3	$H_3PMo_{12}O_{40}$,$H_4SiW_{12}O_{40}$	colorants for pigmenting paints, printing inks and plastics	26
4	$H_4SiMo_{12}O_{40}$,$H_4SiW_{12}O_{40}$	dyes for polyester and polyacrylonitrile fibers	27
5	$H_3PW_{12}O_{40}$	electrochromic-ion conducting gels, films, xerogels, photochromic coatings for copiers	28-32
6	$H_4SiW_{12}O_{40}$	treatment of cathode electrodes (vitreous C and graphite) dopant of polyaniline and polypyrrole	33
7	$H_3PMo_{12}O_{40}$	dopant of poly(*N*-ethylpyrrole)	34
8	$H_3PW_{12}O_{40}nH_2O$	liquid H_2-O_2 fuel cell	35
9	$H_4SiW_{12}O_{40}$ Au/*n*-Sb_2S_3	Schottky barrier solar cells	36
10	$[\gamma\text{-}SiW_{10}O_{36}]^{8-}$,$Rb_8K_2[\{Ru_4O_4(OH)_2(H_2O)_4\}$ $(\gamma\text{-}SiW_{10}O_{36})_2]$	water splitting	37-39

11	Keggin; $H_{3+x}PV_xMo_{12-x}O_{40}$ (x=0, 2)	micelle-directed nanoparticles	40
12	$\{[XW_9O_{34}]_2[Mn^{III}_4Mn^{II}_2O_4(H_2O)_4]\}[ErW_{10}O_{36}]^{9-}$	Single molecular magnet	41,42
13	$[iPrNH_3]_6[Mo_7O_{24}]$, $K_7[PTi_2W_{10}O_{40}]$,$K_7[PTi_2W_{10}O_{40}]$, $[iPrNH_3]_6[PTi_2W_{10}O_{38}(O_2)_2]$ $K_{10}Na[(VO)_3(SbW_9O_{33})_2]$, $K_{12}[(VO)_3(AsW_9O_{33})_2]$ $K_6[P_2W_{18}O_{62}]$,$K_4[SiMo_{12}O_{40}]$	Antiviral activity	43-48
14	$H_5PMo_{10}V_2O_{40}$,$Na_4PVW_{11}O_{40}$, $H_9P_2V_3W_{15}O_{62}$,$Na_6V_{10}O_{28}$ $K_5SiVW_{11}O_{40}$	wood pulp bleaching	49-51
15	$H_3PMo_6W_6O_{40}$	porous support for the purification of vent air	52
16	$H_5PV_2Mo_{10}O_{40}$	decontamination of mustard (HD) analogues	53

Thus, as mentioned above, in last two decades POMs have attracted significant interest in variety of fields. Among the numerous applications, catalysis is by far the most important and it forms the major bulk of the total fields of applications. POMs based catalysts have played an important role in the field of acid as well as oxidation catalysis due to their high Bronsted acidity as well as their tendency to exhibit fast reversible multi-electron redox transformations under rather mild conditions and their inherent stability towards strong oxidants.

Hence they are widely used as a model system for fundamental research providing unique opportunities for mechanistic studies on the molecular level. At the same time they become increasingly important for applied catalysis.

They provide good basis for the molecular design of mixed oxide catalyst and they have high capability in practical uses.

The advantage of POMs as catalysts [54]:

1. Catalyst can be designed at molecular levels based on the followings

I. Acidic and redox properties

These properties of catalyst can be controlled by choosing appropriate elements (type of polyanion, heteroatom counter cation etc.)

II. Multi-functionality

Acid-Redox, Acid-Base, multielectron transfer etc.

III. Tertiary structure, bulk type behaviour for solid state

These are well controlled by counter cations

2. Molecularity-metal oxides cluster

I. Molecular design of catalyst

II. Cluster models of mixed oxide catalyst and relationships between solution and solid catalyst

III. Description of catalytic processes at atomic/molecular level.

Spectroscopic study and stoichiometry are realistic

3. Unique reaction field

I. Bulk type catalysis

"Pseudo-liquid" and bulk type-II behaviour provide unique three dimensional reaction environment for catalysis

II. Pseudo-liquid behavior

This makes spectroscopic and stoichiometric studies feasible and realistic.

III. Phase transfer catalysis

IV. Shape selectivity.

4. Unique basicity of polyanion

I. Selective co-ordination and stabilization of reaction intermediates in solution and in pseudo-liquid phase, possibly also on the surface.

II. Ligands and supports for metals and organometallics.

About 80-85% of patents and applied literature claims about applications of POMs in the field of catalytic activity [22]. Their popularity can be attributed to the abundant study and their commercial availability.

The first attempts to use POMs as catalysts were tracked way back in the 19th century. Systematic investigation of catalysis by POMs began in the early 1970's.

Some of the major achievements of POMs based compounds in the field of catalysis have been reviewed by number of groups.

1. Inorganic solid acids and their use in acid catalyzed hydrocarbon reactions had studied by A. Corma, *Chem. Rev.*, 95, 559, (1995).
2. The catalytic properties of heteropoly compounds have been studied and reviewed by T. Okuhara, N. Mizuno, M. Misono, *Adv. Catal.*, 41, 113, (1996).
3. Different reactions such as hydration, esterification, condensation, miscellaneous reactions, polymerization, alkylation, oxidation of various organic compounds have been studied and reviewed by I. V. Kozhevnikov, *Chem. Rev.*, 98, 171, (1998).
4. Structural and catalytic properties of heteropolyacids have also been studied and reviewed by N. Mizuno and M. Misono, *Chem. Rev.,* 98, 199, (1998).
5. Use of different heteropolyacids for oxidation of alcohols using molecular oxygen has been demonstrated by T. Mallat, *Chem. Rev.*, 104, 3037, (2004).
6. Catalytic evaluation of different organic substrates over supported polyoxometalates has been studied by Y. Ren, B. Yue, M. Gu and H He, *Materials*, 3, 764, (2010).

As discussed earlier, the acidic as well as redox properties of POMs can be tuned at molecular level which can lead to development of a new class of materials with unique structural as well as electronic properties. One of the most significant properties of modified precursors is their ability to accept and release specific numbers of electrons reversibly, under marginal structural rearrangement [55-57]. As a result, they are expected to play an important role in catalysis. Thus, the modification of parent POMs are likely to help in

development of new generation catalysts with enhanced properties of acidity, redox potential and stability.

The modification of properties can be basically done by tuning the structural properties at the atomic or molecular level in two ways (i) By creating defect (lacuna) in parent POMs structures (i.e. Lacunary Polyoxometalates, LPOMs) and (ii) Incorporation of transition metal ions into the defect structures (i.e. Transition Metal Substituted Polyoxometalates, TMSPOMs).

Transition metal substituted polyoxometalates (TMSPOMs) are of excellent candidate in POMs chemistry due to their unique electrochemical, magnetic, medicinal and catalytic properties [1-3, 58-68]. They can be rationally modified at molecular level including size, shape, charge density, redox states as well as stability [58-66] and hence they act as an excellent building block for expansion of targeted architecture.

Parallel to this domain, the area of functionalization (Inorganic-organic hybrid) has followed similar importance and expansion in last few years. In this context, a significant attention continues to focus on the functionalization of TMSPOMs [69-75]. Modification in TMSPOMs may help in various fields such as photo- and electrochromism, magnetism, medicine and catalysis [71-75].

Functionalization is a matter for POMs reactivity and provides structural and spectroscopic model for substrate binding to have better catalytic activity. The incorporation of organic substructures into inorganic oxide framework provides a powerful method for structural modification and synthesis of novel organic-inorganic hybrid materials. This combines the unique features of both the organic and inorganic components. Functionalization may result in the activation of surface oxygen. Functionalization might provide multifunctional oxidation catalysts that display selective recognition of substrates and provide higher selectivity.

The thesis is divided into two parts.

(A) Transition metal substituted Polyoxometalates (B) Functionalization of Transition metal substituted POMs.

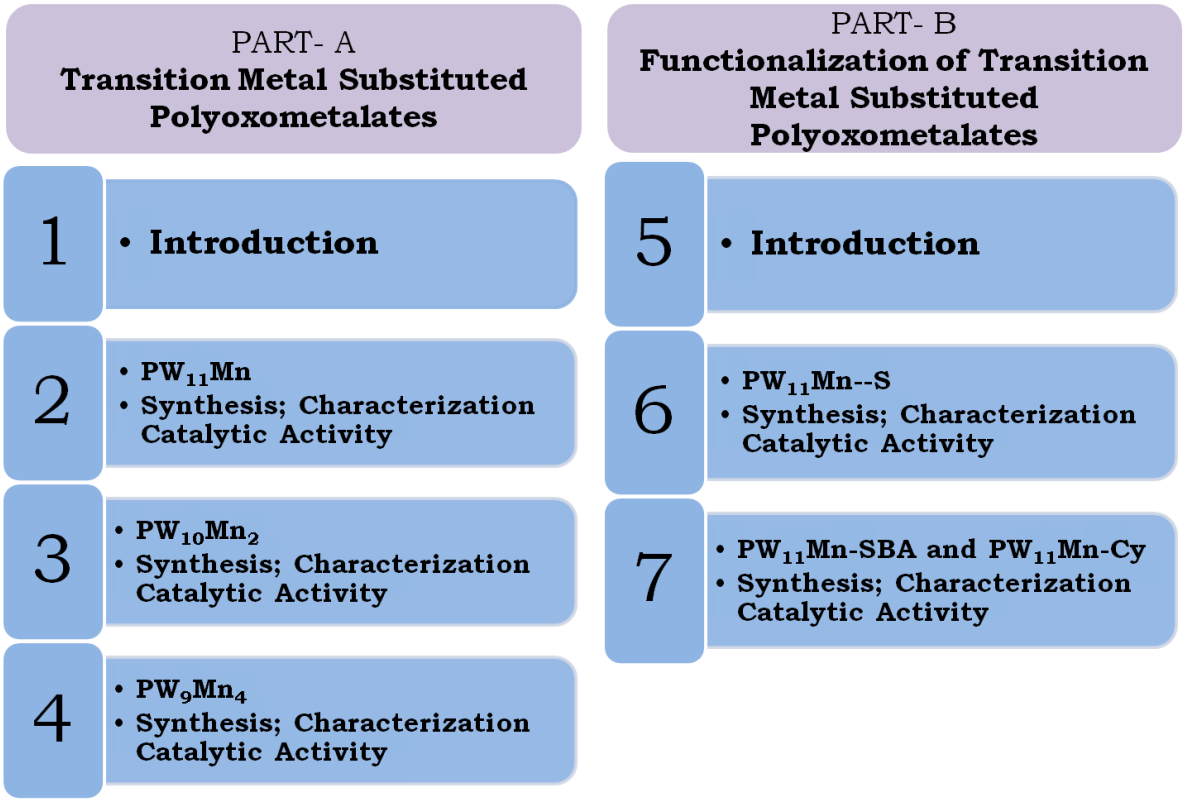

Chapter 1 consists of detailed introduction of transition metal substituted phosphotungstate and description for selecting Mn as substituting transition metal amongst whole Ist series of transition metals. It also describes properties and applications of TMSPOMs, especially in the field of homogeneous as well as heterogeneous catalysis.

Chapter 2 deals with one-pot *in situ* synthesis and detail characterization of cesium salt of Mn(II) substituted phosphotungstate ($PW_{11}Mn$) based on mono lacunary POMs. The catalytic activity was evaluated for solvent free liquid phase oxidation of alkenes using environmentally benign oxidants such as H_2O_2 and O_2. A study on the kinetic behavior was also carried out and the various kinetics parameters such as order of reaction, rate constant as well as activation energy was determined.

Chapter 3 deals with one-pot *in situ* synthesis as well as characterization of cesium salt Mn(II) substituted phosphotungstate based on di lacunary POMs ($PW_{10}Mn_2$). The catalytic activity was evaluated for solvent free liquid phase oxidation of alkenes using environmentally benign oxidants such as H_2O_2 and O_2. A study on the kinetic behavior was also carried out and the various kinetics parameters such as order of reaction, rate constant as well as activation energy was determined.

Chapter 4 deals with one-pot *in situ* synthesis and characterization of tetranuclear Mn(II) substituted sandwich compound based on tri lacunary POMs (PW_9Mn_4). The catalytic activity was evaluated for solvent free liquid phase oxidation of alkenes using environmentally benign oxidants such as H_2O_2 and O_2. A study on the kinetic behavior was also carried out and the various kinetics parameters such as order of reaction, rate constant as well as activation energy was determined.

Chapter 5 describes detailed introduction of functionalization of TMSPOMs and their application in oxidation catalysis. Designing of active and selective oxidation catalysts can be done by proper selection of the organic ligand.

Chapter 6 consist of functionalization of $PW_{11}Mn$ by salen via *noncovalent* interaction while **Chapter 7** consist functionalization $PW_{11}Mn$ by Chiral organic ligands ((S)-(+)-sec-butylamine and (R)-(-)-cyclohexylethylammine) via *covalent* interaction. The synthesized complexes were characterized in solid as well as solution state by various spectroscopic techniques. The catalytic activity was evaluated for solvent free liquid phase oxidation of alkenes using environmentally benign oxidants such as H_2O_2 and O_2.

References

1. M. T. Pope, A. Muller (Eds.), *Polyoxometalate Chemistry: From Topology via Self-Assembly to Applications*, Kluwer, Dordrecht, (2001)
2. "*Polyoxometalate Molecular Science*", M. T. Pope, A. Muller, Kluwer Academic Publishers, (2003)
3. M. T. Pope, *Inorganic Chemistry Concepts Vol. 8: Heteropoly and Isopoly Oxometalates*, Springer, Berlin, (1983)
4. J. J. Berzelius, *Pogg. Ann. Phys. Chem.*, 6, 369, (1826)
5. C. Marignac. *Ann. Chim.*, 25, 362, (1862)
6. L. C. Pauling. *J. Am. Chem. Soc.*, 51, 2868, (1929)
7. J. F. Keggin. *Nature*, 131, 908, (1933)
8. J. F. Keggin. *Proc. Roy. Soc. A*, 144, 75, (1934)
9. Signer R, Gross H., *Helv. Chim. Acta*, 17, 1076, (1934)
10. L. C. W. Baker, J. S. Figgis, *J. Am. Chem. Soc.*, 92, 3794 (1970)
11. M. Misono, K. Sakata, Y. Yoneda, W. Lee, *in* "Proc. 7th Int. Congr. Catal., Tokyo, 1980," p. 1047. Kodansha, Tokyo, Elsevier, Amsterdam, (1981)
12. M. Misono, *Catal. Rev.Sci. Eng.,* 29, 269 (1987)
13. M. Misono, *Catal. Rev.Sci. Eng.,* 30, 339 (1988)
14. M. Misono, *in* "Proc. 10th Int. Congr. Catal., Budapest, 1992," p. 69. Elsevier, Amsterdam, and Akademiai Kiado, Budapest, (1993)
15. T. Okuhara, N. Mizuno, M. Misono, *Adv. Catal.*, 41, 113, (1996)
16. M. Misono, In Proc. Climax 4th Intern. Conf. Chem. Uses Molybdenum; Barry, H. F., Mitchell, P. C. H., Eds.; p 289, (1982)
17. M. Misono, N. Mizuno, K. Katamura, A. Kasai, Y. Konishi, K. Sakata, T. Okuhara, Y. Yoneda, *Bull. Chem. Soc. Jpn.*, 55, 400, (1982)
18. T. Okuhara, S. Tatematsu, K. Y. Lee, M. Misono, *Bull. Chem. Soc. Jpn.* 62, 717, (1989)
19. M. Furuta, K. Sakata, M. Misono, Y. Yoneda, *Chem. Lett.*, 31, (1979)
20. I. V. Kozhevnikov, *Chem. Rev.*, 98, 171, (1998)
21. I. V. Kozhevnikov, *Russ. Chem. Rev.*, 56, 811, (1987)

22. D. Katsoulis, *Chem. Rev.*, 98, 359, (1998)
23. J. Calahan, E. Cueller, M. Desmond, J. Currie, U.S. Patent 4633372 A, (1986)
24. T. Morimoto, T. Matsubara, Y. Hamaya, N. Iwano, Japanese Patent JP 62114207 A2, (1987)
25. R. S. Alwitt, German Patent DE 2618616, (1976); (English equivalent, U.S. Patent 4031436)
26. F. Closs, B. Albert, H. Wienand, European Patent EP 619346
27. R. A. Clarke, U.S. Patent 3387916, (1968)
28. D. E. Katsoulis, J. R. Keryk, Abstract ACS National Meeting, Inorganic Chemistry Section, Aug 20-24, Chicago, (1995)
29. M. Tasumisago, H. Honjo, Y. Sakai, T. Minami, B. Orel, U. Lavrencic-Stangar, M. G. Hutchins, *Solid State Ionics,* 59, 171, (1993)
30. K. Kalcher., *J. Non-Cryst. Solids.,* 175, 251 (1994)
31. A. Averbach, U.S. Patent 3623866, (1971); *Chem. Abstr.* 76, 66324, (1971).
32. A. Averbach, U.S. Patent 3687672, (1972); *Chem. Abstr.* 77, 171261, (1972)
33. L. Nadjo, B. Keita, French Patent FR 2573779 A1, (1986); *Chem. Abstr.* 106, 75016, (1986) (Equivalent, Canadian Patent CA1275385)
34. G. Bidan, E. Genies, M. Lapkowski, European Patent EP 323351 A1, 1989; *Chem. Abstr.* 1989, *111,* 207397 (English equivalent, Canadian Patent CA1332643)
35. N. Giordano, P. Staiti, S. Hocevar, A. S. Arico, *Electrochim. Acta.,* 41, 397 (1996)
36. O. Savadogo, K.C. Mandal, *Electron. Lett.*, *28,* 1682 (1992)
37. A. Sartorel, M. Carraro, G. Scorrano, R. De-Zorzi, S. Geremia, N. D. McDaniel, S. Bernhard, M. Bonchio, *J. Am. Chem. Soc.*, 130, 5006 (2008)
38. Y. V. Geletii, B. Botar, P. Kogerler, D. A. Hillesheim, D. G. Musaev, C. L. Hill., *Angew. Chem.*, 120, 3960 (2008)

39. Y. V. Geletii, B. Botar, P. Kogerler, D. A. Hillesheim, D. G. Musaev, C. L. Hill, *Angew. Chem.*, 47, 3896 (2008)
40. G. Maayan, R. Popovitz-Biro, R. Neumann, *J. Am. Chem. Soc.*, 128, 4968 (2006)
41. C. Ritchie, A. Ferguson, H. Nojiri, H. N. Miras, Y. F. Song, D.-L. Long, E. Burkholder, M. Murrie, P. Kogerler, E. K. Brechin, L. Cronin, *Angew. Chem.*, 120, 5691 (2008)
42. M. A. Aldamen, J. M. Clemente-Juan, E. Coronado, C. Marti- Gastaldo, A. Gaita-Ario, *J. Am. Chem. Soc.,* 130, 8874 (2008)
43. H. Yanagie, A. Ogata, S. Mitsui, T. Hisa, T. Yamase, M. Eriguchi, *Biomed. Pharmacother.*, 60, 349 (2006)
44. S. Mitsui, A. Ogata, H. Yanagie, H. Kasano, T. Hisa, T. Yamase, T. M. Eriguchi, *Biomed. Pharmacother.*, 60, 353 (2006)
45. R. Prudent, V. Moucadel, B. Laudet, C. Barette, L. Lafanechre, B. Hasenknopf, J. Li, S. Bareyt, E. Lacote, S. Thorimbert, M. Malacria, P. Gouzerh, C. Cochet, *Chem. Biol.*, 15, 683 (2008).
46. K. Dan, T. Yamase, *Biomed. Pharmacother.*, 60, 169 (2006)
47. S. Shigeta, S. Mori, T. Yamase, N. Yamamoto, *Biomed. Pharmacother.*, 60, 211 (2006)
48. M. Inoue, T. Suzuki, Y. Fujita, M. Oda, N. Matsumoto, T. Yamase, *J. Inorg. Biochem.*, 100, 1225 (2006)
49. I. A. Weinstock, R. H. Atalla, U. P. Agarwal, J. L. Minor, C. Petty, *Spectrochim. Acta: Part A.*, 49A, 819 (1993)
50. I. A. Weinstock, R. H. Atalla, R. S. Reiner, M. A. Moen, K. E. Hammel, C. J. Houtman, C. L. Hill, *New J. Chem.*, 20, 269 (1996).
51. I. R. Weinstock, C. L. Hill, World Patent WO 9405849 A1, 1994; *Chem. Abstr.*, 121, 233328 (1994).
52. A. Fukuda, Y. Fukuda, M. Inoue, M. Maki, Y. Kaneko, M. Waki, Japanese Patent JP 04035716 A2, 1992; *Chem. Abstr., 117,* 117592 (1992)
53. R. D. Gall, C. L. Hill, Walker, J. E. *Chem. Mater., 8*, 2523 (1996)

54. N. Mizuno, M. Misono, *Chem. Rev.* 98, 199, (1998)
55. R. Thouvenot, A. Proust, P. Gouzerh, *Chem. Comm.*, 1837, (2008)
56. I. A. Weinstock, *Chem. Rev.*, 98, 113, (1998)
57. M. Sadakane and E. Steckhan, *Chem. Rev.*, 98, 219, (1998)
58. Issue on "Polyoxometalates", *Chem. Rev.* 98, 1, (1998)
59. M. T. Pope and A. Müller (Eds.), *Polyoxometalates: From Platonic Solids to Anti-Retroviral Activity*, Kluwer, Dordrecht, The Netherlands, (1994)
60. D. -L. Long, E. Burkholder, L. Cronin, *Chem. Soc. Rev.,* 36, 105, (2007)
61. I. V. Kozhevnikov, Catalysts for fine chemical synthesis-Catalysis by polyoxometalates, John Wiley and Sons, Chichester, UK, p 117, (2002)
62. M. T. Pope, A. Müller, *Angew. Chem.*, 30, 34, (1991)
63. P. J. Hagrman, D. Hagrman, J. Zubieta, *Angew. Chem.*, 38, 2638, (1999)
64. E. Burkholder, J. Zubieta, *Chem. Commun.* 2056, (2001)
65. C. D. Wu, C. Z. Lu, H. H. Zhuang, J. S. Huang, *J. Am. Chem. Soc.* 124, 3836, (2002)
66. K. Fukaya, T. Yamase, *Angew. Chem.* , 42, 654, (2003)
67. H. Q. Tan, Y. G. Li, Z. M. Zhang, C. Qin, X. L. Wang, E. B. Wang, Z. M. Su, *J. Am. Chem. Soc.* 129, 10066, (2007)
68. J. Thiel, C. Ritchie, C. Streb, D.L. Long, L. Cronin, *J. Am. Chem. Soc.* 131, 4180, (2009)
69. U. Kortz, *Chem. Comm.,* 2962 (2005)
70. L. De-Liang, R. Tsunashima, L. Cronin, *Angew. Chem.*, 49, 1736 (2010)
71. A. Dolbecq, E. Dumas, C. R. Mayer, P. Mialane, *Chem. Rev.*, 110, 6009 (2010).

72. C. Besson, J. H. Mirebeau, S. Renaudineau, S. Roland, S. Blanchard, H. Vezin, C. Courillon, A. Proust., *Inorg.Chem.*50, 2501, (2011).
73. B. Matt, C. Coudret, C. Viala, D. Jouvenot, F. Loiseau, G. Izzet, A. Proust., *Inorg. Chem.*, 50, 7761, (2011).
74. B. Matt, J. Moussa,L. M. Chamoreau, C. Afonso, A. Proust, H. Amouri, G. Izzet., *Organomettalics.*, 31, 35, (2012).
75. A. Proust, B. Matt, R. Villanneau, G. Guillemot,P. Gouzerh, G. Izzet, *Chem. Soc. Rev.*, DOI: 10.1039/c2cs35119f

PART A

Transition Metal Substituted
Polyoxometalates

CHAPTER

1

Introduction

In the last few years, more and more attention is given to the development of new generation materials using a rational and molecular engineering approach which allows development of the active sites, uniform composition and distribution [1-11]. However, successful designing is impossible without fundamental knowledge about the structure of the active species and the nature of their reactivity. The establishment of so called "structure–reactivity relationships" is highly important to formulate requirements to the composition and structure of an optimal new generation material.

As a new generation materials, over the last few years, the chemistry of POMs has continued its rapid development not only as a pure chemical science, but in a multidisciplinary manner, interacting with other areas such as materials science, magnetism, medical, bio- and nanotechnology as well as catalysis [12-20]. The permanent interest in POMs chemistry is largely due to the versatile nature of POMs, in terms of their structure, size, redox activity, solubility, thermal stability and charge density.

As mentioned in General Introduction, the modification of the precursors of parent POMs can lead to development of a new class of compounds with unique structural as well as electronic properties. This can be accomplished by modification in parent POMs via incorporation of transition metal ions into the defect structures. The oxo ligands at the vacant sites are basic enough to react with metal cations forming a new class of compounds more commonly known as Transition Metal Substituted POMs (TMSPOMs).

TMSPOMs have attracted continuously growing attention in the domain of POMs chemistry [12-22]. This mostly due to the fact that TMSPOMs can be rationally modified at molecular level including size, shape, charge density, acidity, redox states, stability and solubility resulting in their outstanding chemical properties. It affords convenient platforms for the stabilization of unusually high oxidation state metal-oxo species. TMSPOMs have advantages over organometallic complexes such as (i) they are robust under oxidation conditions, under which most organic ligands decompose (ii) their solubility is tunable by changing counter cations (iii) their redox properties are adjustable by changing the central (hetero) atom

and the incorporated transition metal [23]. This unique class of metal oxygen clusters are outstanding inorganic building blocks due to their undisputed structural beauty and controllable sizes, shapes and high negative charges [14, 24-30]. They exhibit an enormous variety of structures, which leads to interesting and unexpected properties that give rise to many applications in magnetism, medicine and catalysis [13, 14, 31].

The known TMSPOMs are mono-, di-, tri-substituted or sandwich type derivatives of Keggin type POMs, e.g. $[M'(H_2O)XM_{11}O_{39}]^{n-}$, $[M'_2(H_2O)_2XM_{10}O_{38}]^{m-}$ and $[M'_3(H_2O)_3XM_9O_{37}]^{p-}$ or $[M'_4(H_2O)_2(XM_9O_{34})_2]^{q-}$ (where $X=P^{5+}$, Si^{4+}; $M=W^{6+}$, Mo^{6+} and M'=transition metal). The reports on synthesis and characterization involving different TMSPOMs are well documented in art. In the present work we have restricted ourselves to transition metal substituted phosphotungstates, mainly because of two reasons (i) lot of work has been carried out on transition metal substituted silicotungstates and germanotungstate, to some extent. (ii) The available literature would result in increasing the bulk of the thesis.

What are Lacunary Polyoxometalates?

Controlled hydrolysis of parent POMs with base under appropriate conditions (temperature, ionic strength, etc.) can form defect structures. This defect structures are commonly known as "*lacunary POMs*". These lacunary POMs are a class of inorganic ligands with a set of unique properties such as multidenticity, rigidity, thermal and oxidative stability [1-4]. Further, these lacunary POMs are typically stable in a certain pH range and can generally incorporate a wide variety of transition metals to restore the parent structures or serve as building blocks for constructing larger metal oxide architectures.

Removal of one, two or three MO units from the parent POMs, gives rise to mono-, di- or tri lacunary POMs. When the solution of $[XM_{12}O_{40}]^{n-}$ are treated with base, a series of hydrolysis reactions occurs leading to the formation of lacunary polyoxometalates (Scheme 1).

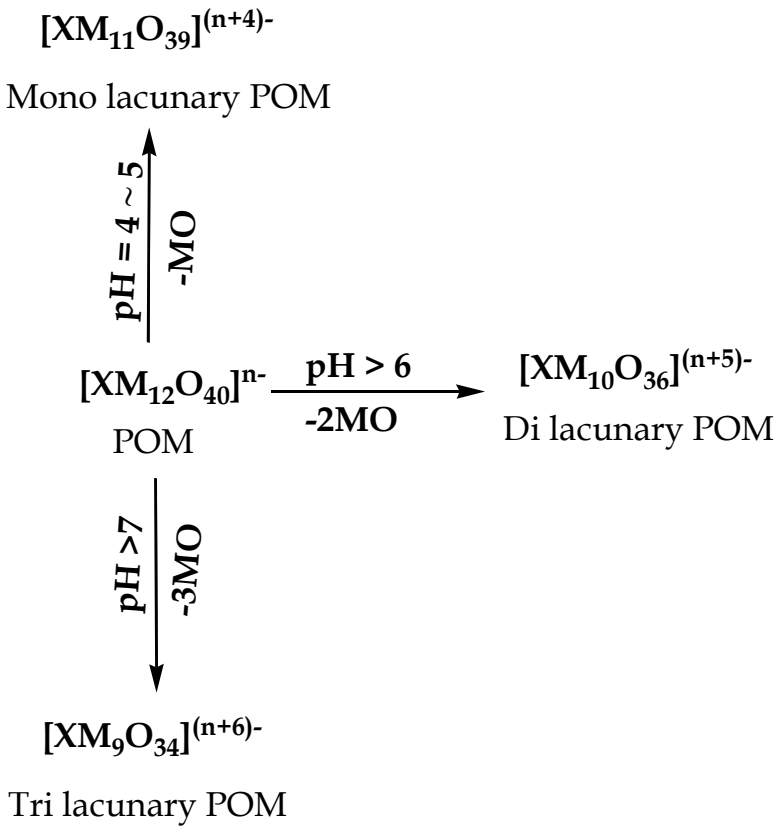

Scheme 1. Formation of Lacunary polyoxometalate

All the lacunary species derived from the parent Keggin type structure, are obtained from the three Baker-Figgis (α, β and γ) isomers by means of the elimination of a variable number of octahedral [32]. The structural rearrangement of one of the 4 triads leads to the formation of different types of lacunary POMs.

In the case of phosphotungstate system, the reaction patterns are similar to those of the silicotungstates, not as thermodynamically stable with equilibria between the different possible isomers and producing isomeric mixtures. The formation of lacunary phosphotungstates are visualised in Figure 1.

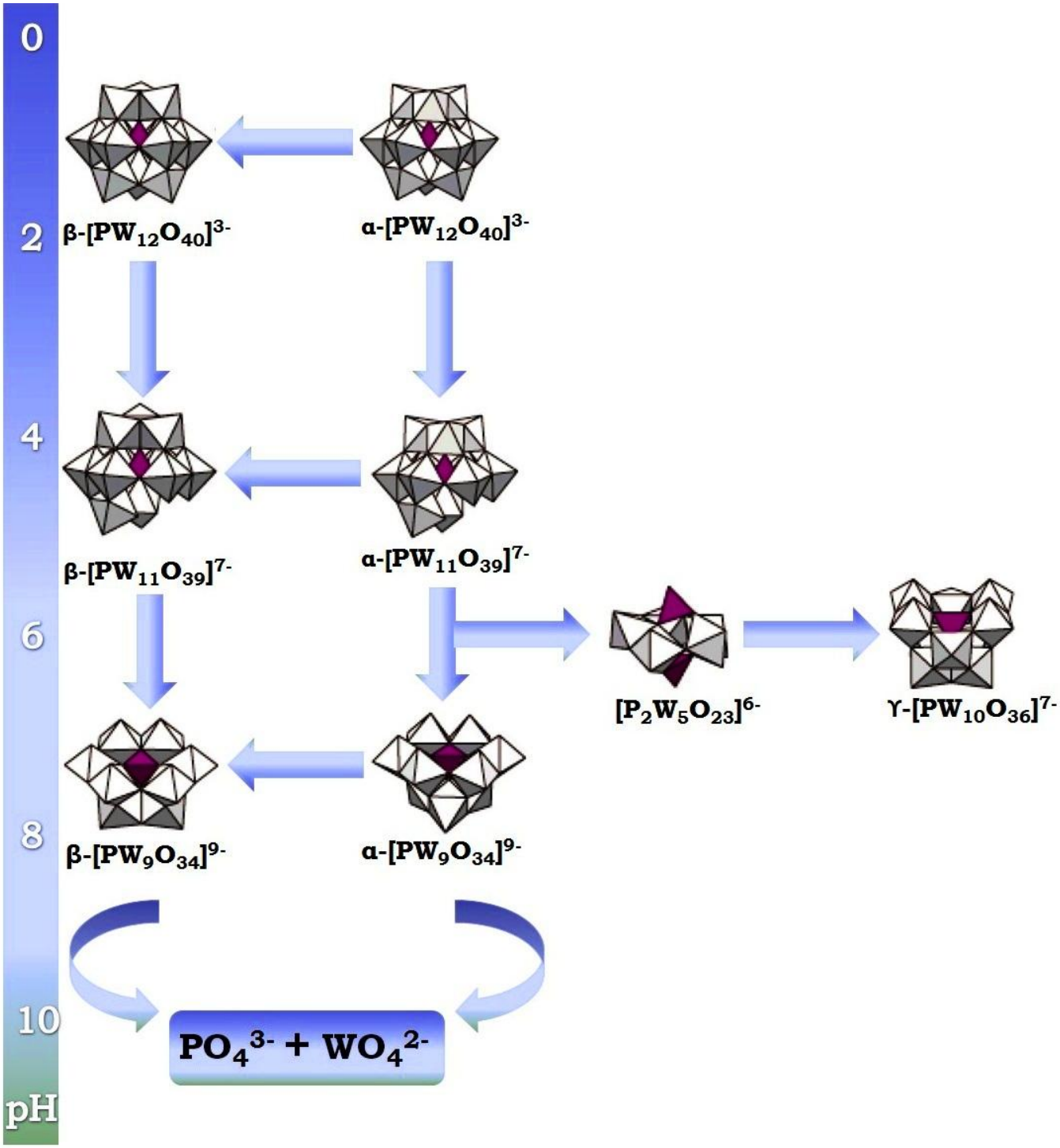

Figure 1. pH dependent formation of lacunary phosphotungstates

As seen, it is clear that the formation of mono, di or tri lacunary phosphotungstates is mainly pH dependent, each possessing its own reactivity and stability trend. Hence, synthetically, special attention is paid to fine changes in reaction conditions such as pH, temperature, buffer

capacity, ionic strength, and cation size: all having the potential to exert a considerable effect on the polyanion equilibria and formation of products [33, 34].

Classification and Properties of lacunary POMs

The structures of the lacuna obtained with the lacutary POMs are mainly dependent on the number of vacancies generated in the parent 'saturated' structure. The classical examples of geometries observed in lacunary POMs are shown in Figure 2.

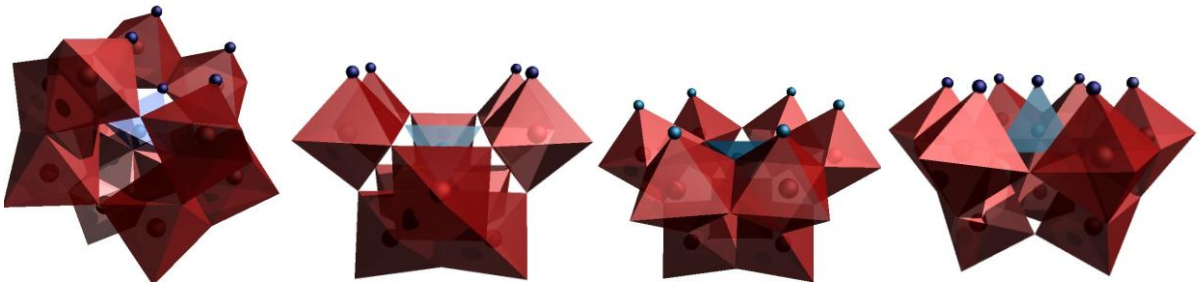

Figure 2. Different types of lacunary polyoxometalate structures derived from parent Keggin unit

The monovacant ligand $[\alpha\text{-}PW_{11}O_{39}]^{7-}$ is obtained from its parent Keggin $[PW_{12}O_{40}]^{3-}$ structure by the loss of one $[W(VI)=O]^{4+}$ unit at pH 4-5. In monovacant species, total five oxygen atoms are available, of which four oxygen atoms are accessible at the surface of the lacuna. These four oxygen atoms present a slightly distorted square geometry. This lacunary POMs is stable in solution over a wide range of pH values and ionic strengths, and can coordinate with most transition metal ions ($M^{2+/3+}$) to form the mono-substituted Keggin complexes, $[M(OH_2)PW_{11}O_{39}]^{n-}$. In Keggin structure all-tungsten usually crystallize in high symmetry cubic system as a result the crystallographically imposed symmetry causes the incorporated transition metal ion and the eleven tungsten atoms to be positionally disordered over the twelve heavy atom sites. As a consequence, each heavy atom position is occupied by 1/12 M and 11/12 W, which makes the absolute structural

determination, including the key bond distances and angles around M center, less informative.

In divacant species, γ-$[XW_{10}O_{36}]^{n-}$(X = P, Si, Ge), the four nearly coplanar oxygen atoms of the lacuna define a rectangular geometry. Considerable attention has been given on the di-vacant because it can bind two transition metal groups adjacent to one another and might, as a consequence, reveal new features in the now well established field of POM-catalyzed homogeneous and heterogeneous catalytic oxidation [35-39]. In addition, recent research has established that this moiety and its di-metal-substituted form readily, yielding diverse POMs structures [40-48].

These di-metal substituted structures contain two d metals in adjacent positions as either “in-pocket” or “out-of-pocket” isomers. The in-pocket isomers contain bonds between the central hetero atom oxygens and the incorporated d- electron metal centre. In contrast, the out-of-pocket isomers do not contain this bond, and consequently the d-electron metals are displaced from the centre of the polyoxoanion and frequently multiply bonded to other adjacent polyoxoanions or distinct structural units.

In trivacant, $[XW_9O_{34}]^{n-}$, six nearly coplanar oxygen atoms define a distorted hexagon. The trivacant derivatives are formed by removing three neighbouring WO_6 octahedra and are classified as A-type and B-type. For trivacant species, the nature of the isomer (A- or B-$[XW_9O_{34}]^{n-}$) and the nature of the hetero element are crucial parameters that will influence the type of derivatization that can occur at the vacant site. Removal of three corner sharing octahedral W units leads to the formation of A-isomer and removal of one of the four edge-sharing W_3 triads leads to the formation of B-isomer. It has been shown that [A-α-$PW_9O_{34}]^{9-}$ undergoes a solid-state isomerization to form [B-α-$PW_9O_{34}]^{9-}$ upon heating at 150 °C for days [49]. The thermal transformation process can be easily monitored by FT-IR spectroscopy and it is believed that the unheated complex, the starting material $Na_9[PW_9O_{34}]$, is predominantly [A-α-$PW_9O_{34}]^{9-}$, and the thermolyzed product is mainly [B-α-$PW_9O_{34}]^{9-}$. In the structure of A-α-{PW_9}, all phosphorus oxygens of the central tetrahedral PO_4 unit are connected to tungsten atoms, while there is a free P-O oxygen in the structure of B-α-

{PW_9}. Both A and B isomers having reactive open coordination sites consisting of nucleophilic oxygen atoms and the structural difference makes their coordination chemistry with transition metals quite different. The A-α-[PW_9] usually reacts with three M to form the trinuclear complexes [A-$M_3(H_2O)_3XW_9O_{37}]^{n-}$ or trinuclear sandwich complexes $[M_3(H_2O)_3$(A-$XW_9O_{34})_2]^{n-}$, whereas B-α-[PW_9] generally incorporates four transition metals to give sandwich complexes $[M_4(OH_2)_2$(B-$PW_9O_{34})_2]^{n-}$,where two M atoms are located at the saturated internal site and the other two at the external positions. For each external M, the sixth aqua ligand is labile and can be easily replaced by other strong σ-donating ligands.

Mono substituted POMs

Mono-substituted Keggin derivatives are recognized as inorganic analogs of metalloporphyrin complexes [50]. They have distinct advantages over the metalloporphyrin and organometallic complexes that they are rigid, hydrolytically stable and thermally robust. The non-oxidizable tungsten-oxo framework of polyanions acts as an inert, multi-dentate ligand which can accommodate a multitude of transition metal centers [51-54].

The reaction of the mono lacunary $[XM_{11}O_{39}]^{n-}$ anion with transition-metal cations M' in aqueous solution leads to the formation of mono transition-metal-substituted POMs (TMSPOMs) $[XM_{11}M'(L)O_{39}]^{m-}$, (where M' = d- electron transition metal and L = monodentate ligand, generally H_2O) (Scheme 2).

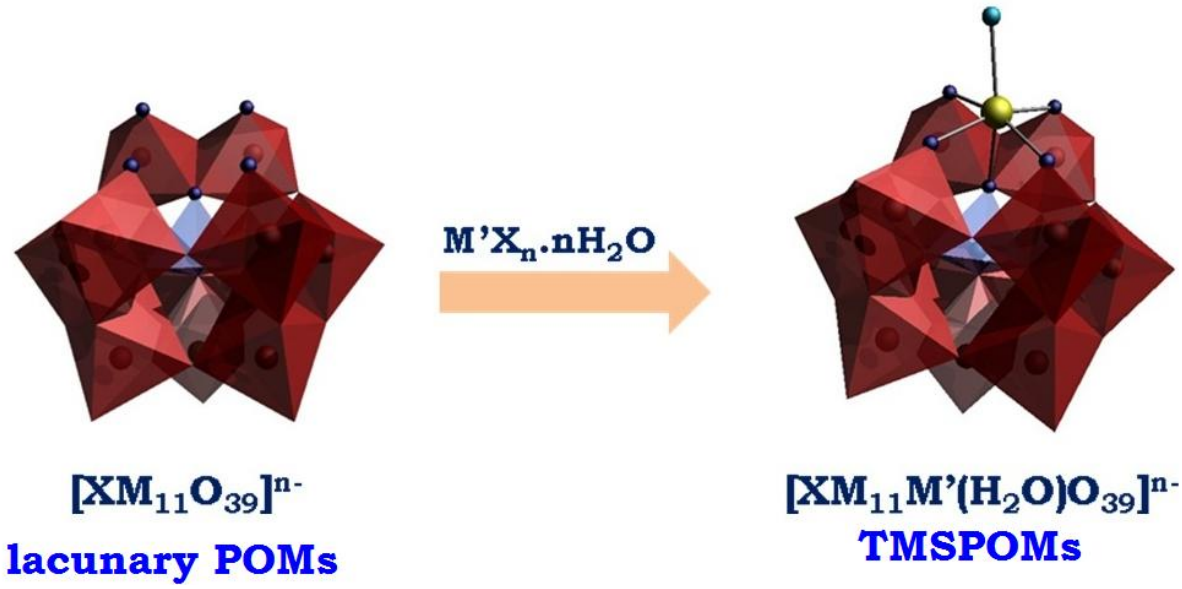

Scheme 2. Formation of mono-substituted POMs from lacunary POMs

The environment around the substituted cation M' in the metal substituted polyanions $[XM_{11}M'(H_2O)O_{39}]^{n-}$ is considered to be near octahedral. In particular, the complexes of the type $[XM_{11}M'(H_2O)O_{39}]^{n-}$ show many analogies to metalloporphyrins [50, 55-57].

As mentioned earlier (In general introduction), here we will concentrate on phosphotungstate derivative only. In 1956, Baker et al. first time reported the synthesis of alkali salts of $[Co^{2+}Co^{3+}W_{12}O_{42}]^{7-}$ from $NaWO_4.2H_2O$ and cobaltous acetate tetrahydrate at neutral pH and

characterized for elemental analysis, oxidation state, electrochemical properties, powder XRD as well as for Single crystal analysis [58]. Afterwards in 1966, on the basis of crystal structure, the presence of Co ions was confirmed in the outer sphere of the polyoxotungstates rather as a central hetero atom [59] by the same group.

Weakley and Malik in 1967 extended the work of Baker et al. by synthesizing a series of mono cobalt substituted polyoxotungstates, especially cobalt substituted silicotungstate was synthesized from 12-tungstosilicic acid and metal salt at pH 6. The obtained deep red crystal was analyzed for single crystal X-ray, powder XRD and UV visible spectroscopy [60]. Tourne, Weakly and Malik in 1970's jointly reported the synthesis of triheteropolyanions consisting of $XZW_{11}O_{40}H_2$"- (X = B, Zn, P, Si, Ge; Z = Cu(II) , Mn(II), Mn(III)). The synthesized complexes were characterized by elemental, magnetic susceptibility, potentiometric titrations, spectroscopic techniques and powder X-ray diffraction patterns [61]. After Baker's work, Ripen et al. reported Ni-subsituted derivative for silico and phosphotungstates as well as their pyridine derivatives [62]. Weakly group reported electronic properties of a series of cobalt substituted polyoxotungstates by varying the hetero atom. Examples include $[BCoW_{11}O_{40}H_2]^{7-}$, $[AsCoW_{11}O_{40}H_2]^{5-}$, $[PCo^{II}W_{11}O_{40}H_2]^{5-}$ and $[PCo^{III}W_{11}O_{40}H_2]^{6-}$ [60, 63], as well as the pyridinium salt of $[PW_{11}O_{39}Co^{II}(py)]^{5-}$ [63].

A Japanese group confirmed the work of Baker and Figgis and they have investigated the chemical as well as spectroscopic properties of the $[PW_{11}O_{39}Co^{II}(H_2O)]^{5-}$ [64]. The exchange of the water molecule by various inorganic groups ($[Fe(CN)_6]^{4-}$, SCN-, SO_3^{2-}) in $[PW_{11}O_{39}Co^{II}(py)]$ was then studied by Zonnevijlle and Tourne in 1983 [65]. Klevtsova et al. in 1991 then described crystal structure of the cesium salt of $[PW_{11}Co^{II}(H_2O)O_{39}]^{5-}$ [66]. The complex was synthesized in a two step process, the first step involved the formation of 11-phosphotungstate and the second step involved the incorporation of cobalt from the individual salt of the metal ion. Later, Rong and Pope showed the reaction of $[PW_{11}O_{39}Ru^{II}(H_2O)]^{5-}$ with pyridine, sulfoxides, dialkyl sulfides, and active alkenes and their characterization by electronic absorption spectroscopy, ^{31}P and ^{183}W NMR spectroscopy in 1991

[67] whereas EPR spectra for $[PW_{11}O_{39}Ru^{III}L]^{4-}$ (L = H_2O, dmso, py) derivate was reported in 2009 [68]. Zhang and Pope in 1995, also synthesized the aqueous and non-aqueous soluble salts of $[PW_{11}O_{39}Mn^{IV}(H_2O)]^{3-}$ by chemical and electrolytic oxidation of corresponding Mn(II) and Mn(III) ions and characterized by elemental, spectroscopic analysis, magnetic moment, ESR, EXAFS and X-ray absorption near edge spectroscopy [69]. In 1995, Anson et al. reported the electrochemical analysis for $Cs_m[PW_{11}O_{39}Ru^{III}(L)]$, {L = pyridine (m = 4), pyrazine (m =4), N-methylpyrazinium (m = 3)} [70].

At the same time, Galan-Mascaros et al. for the first time reported X-ray analysis for tetraethylene salt of $[PW_{11}Mn^{II}O_{39}]^{5-}$, indicating the formation of chain like structure [71]. Afterwards the crystal structure for tetra ethyl ammonium salt of $[PW_{11}O_{39}Co^{II}(H_2O)]^{5-}$ was described by Weakley and coworkers in 1996 [72]. They found the monosubstituted Keggin groups were assembled into straight chains through W-O-Co linkages.

In 2000, Bonchio et al. have reported synthesis of dmso derivative of $[PW_{11}\ Ru^{II}LO_{39}]^{5-}$ (L=DMSO) by microwave technique and their characterization [73]. Proust and coworkers reported the synthesis of $[PW_{11}O_{39}\{Re^{V}NC_6H_5\}]^{4-}$ [74]. J. Peng and Z. Zhang's group reported the hydrothermal synthesis of $[PW_{11}O_{39}Co^{II}(L)]^{5-}$, (where M= W, Mo and L=pbpy,5-phenyl-2-(4-pyridinyl)pyridine and 4,4′-bipy) [75, 76]. In 2007, Proust's group reported the synthesis, characterization of $[PW_{11}O_{39}\{Ru^{V}NPPh_3\}]^{3-}$ [77] and further its reaction with hydroxide in 2009 [78]. Cavaleiro and co-workers reported the use of extended X-ray absorption fine structure (EXAFS) as a structural characterization tool for $[PW_{11}O_{39}M(H_2O)]^{n-}$, (M= Co, Mn, Fe) [79]. The synthesis and structural as well as spectroscopic characterization of $[PW_{11}O_{39}M(H_2O)]$, (where M= Ca and Sr) involving alkaline earth metals was reported by J. Wang and group [80].

Recently, Sokolov et al. has successfully incorporated Ir into $PW_{11}O_{39}$ framework and studied the substitutional lability at the Ir(III) site using ESI-MS and multinuclear NMR [81].

Di-Substituted POMs

The coordination between the divacant POMs and transition metals under different conditions can lead to saturated disubstituted POMs [42, 82] disubstituted dimmers [83], and many other complexes [47, 84-87], which can crystallized in low symmetry disorder-free space groups.

Kortz and co-workers have significantly contributed in the field of di-substituted POMs, mainly silicotungstate and germanotungstate of monomer, dimer, trimer and tetramer form of di-substituted POMs [87]. Apart from him, number of groups, Pope [41, 88], Lunk [44], Mizuno [82, 89, 90], Hill [91] and Proust [92] have also contributed towards disubstituted POMs. But as our main concern is about the monomeric form of di-substituted phosphotungstates, the relevant references for the same have been included only.

The reaction of the di lacunary $[PW_{10}O_{36}]^{n-}$ anion with transition-metal cations M in aqueous solution leads to the formation of di transition-metal-substituted POMs $[PM_2(H_2O)_2W_{10}O_{38}]^{n-}$, (where M= d-electron transition metal).

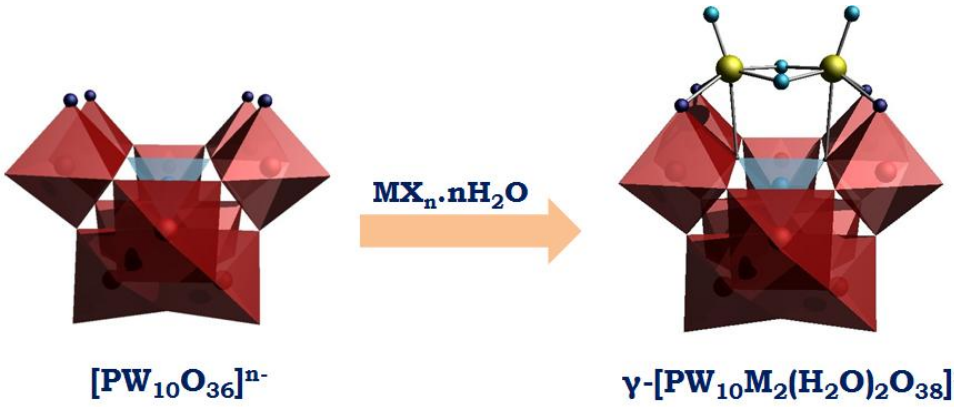

Scheme 3. Formation of monomeric form of di-substituted POMs

In 1983 Domaille et. al. synthesized di-substituted phosphotungstate from individual salts at pH 8.2 and identified the formation of $K_7[PW_{10}Ti_2O_{40}]$ structure using FT-IR and ^{183}W NMR [93]. Afterwards in 1986, on the basis of multinuclear NMR [94] and crystal structure [95], the presence edge

shared VO polyhedra joining the adjacent W_30_{13} units in caesium salt of γ-$[PV_2W_{10}O_{40}].xH_2O$ were confirmed by the same group.

Ozeki and Yamase crystallized $[PW_{10}Ti_2O_{40}]^{7-}$ [96] following Domaille's procedure [93] and found that $[PW_{10}Ti_2O_{40}]^{7-}$ preserved its C_2 symmetry with distinguishable substituted sites. Coronado et al. reported di-substituted copper complex $[PW_{10}Cu_2(H_2O)_2O_{38}]^{7-}$, with a mixture of corner- or edge shared $Cu^{II}O_6$ octahedra on the basis of Crystal structure and magnetic study [97]. In 1996 Secheresse et al. demonstrated that the stereospecific addition of the di-cation $[M_2S_2O_2]^{2+}$ (M= Mo, W) to the divacant POMs leads to the formation of oxo-thio POMs, γ-$[PW_{10}M_2S_2O_{38}]^{6-}$ [98, 99] in DMF.

In 2001 Nomiya's group reported reaction of tri-lacunary precursors $[PW_9O_{34}]^{9-}$ with $Ti(SO_4)_2$ resulted in formation of monomeric form of [α-1,2-$PW_{10}Ti_2O_{40}]^{7-}$ in less acidic conditions (pH 7.8) and dimer under more acidic conditions (pH 1.0-2.2) [100].

A literature survey shows that since last 10 years, no work has been carried out on the synthesis of monomeric form of di-substituted phosphotungstate.

Sandwich type compound based on trilacunary POMs

The coordination between the tri-vacant POMs and transition metals can generally lead to tri-substituted POMs [101-104] and sandwich type POMs [105]. Here, we have restricted ourselves to the sandwich type phosphotungstates. However for reader's acquaintance we would like to mention that various groups Robert [106], Tourne [107], Krebs [108], Kortz [45, 53, 109, 110], Mialana [111], Wang [112], Niu [113], Yamase [114], Xu [115], Liu [116] have contributed in this field of sandwich type POMs based on trilacunary POMs.

The sandwich-like phosphotungstate derived from tri-vacant phosphotungstate are of two types; (i) A-type sandwich POMs containing three corner-sharing MO_6 octahedra between two $[A\text{-}\alpha\text{-}XW_9O_{34}]^{n-}$ units and (ii) B-type sandwich POMs containing four edge-sharing octahedra between two B-α-trivacant units. The A-α-$[PW_9]$ usually reacts with three M to form trinuclear sandwich complexes $[M_3(H_2O)_3(A\text{-}XW_9O_{34})_2]^{n-}$ and B-α-$[PW_9]$ generally incorporates four transition metals to give the $[M_4(OH_2)_2$(B-

$PW_9O_{34})_2]^{n-}$,where two M atoms are located at the saturated internal site and the other two at the external positions (Scheme 4) [105].

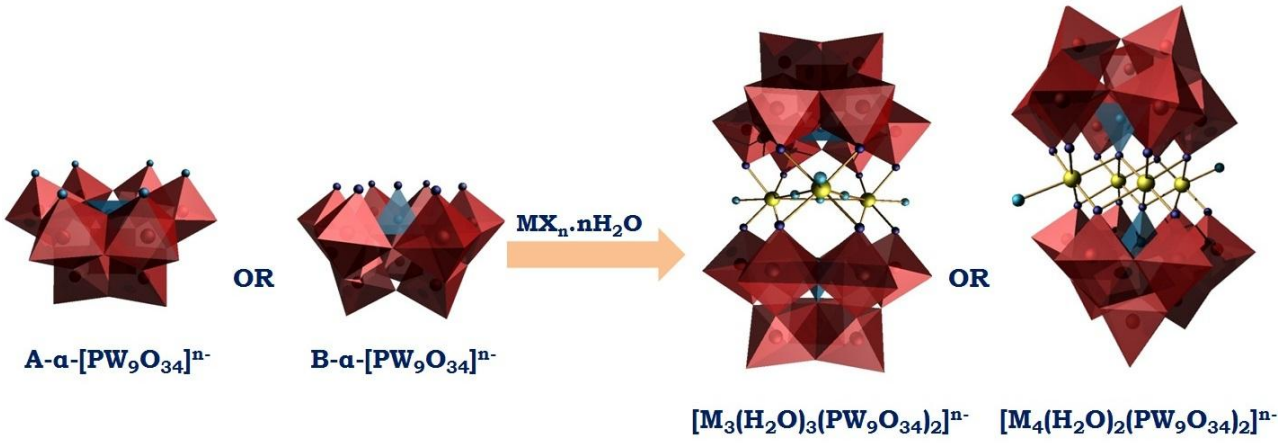

Scheme 4. Formation of sandwich type POMs from trilacunary POMs

This new class of complexes were discovered by Weakly, Evans and Tourne in 1973 named as "Sandwich" type POMs. They obtained single crystal of $K_{10}P_2W_{18}Co_4(H_2O)_2O_{68}$ complex [117] by reacting either $PW_{11}Co(H_2O)O_{39}$ with Co^{2+} at pH 7-7.5 in aqueous solution, *or* H^+: HPO_4^-: Co^{2+}: WO_4^{2-} mixture of composition 11:2:4:18 at 100°C.

Finke et. al. in 1981 extended the work of Weakly by synthesizing a series of sandwich type phosphotungstates, $P_2W_{18}M_4(H_2O)_2O_{68}^{10-}$ (M=Cu^{2+},Co^{2+},Zn^{2+}) using trilacunary phosphotungstate and various metal salts [118]. The C_2h symmetry of synthesized complexes was determined by various spectral techniques. Knoth et. al. reported the synthesis of $[(RM)_3P_2W_{18}O_{68}]^{n-}$ and $[M_3P_2W_{18}O_{68}]^{n-}$ by reacting A-type trilacunary phosphotungstate with $RMCl_3$ (RM=PhSn, $CpFe(CO)_2Sn$, CpTi) along with series of transition metals (Co(II), Mn(II), Fe(II), Ni(II), Cu(II), Zn(II) and Pd(II)) [119, 120].

Further, in 1987 Finke et. al. reinvestigated the same complexes ($[P_2W_{18}M_4(H_2O)_2O_{68}]^{10-}$ (M=Cu^{2+},Co^{2+},Zn^{2+})) as reported in 1981 and synthesized the same complexes in pure isomeric form with high yield and characterized by IR spectra, P-XRD patterns, ^{31}P NMR and 2D ^{183}W NMR [49]. Weakly and Finke reported the X-ray analysis for mixture of sodium-

potassium salt of $[Cu_4(H_2O)_2(PW_9O_{34})_2]^{10-}$ with two B-$PW_9O_{34}^{9-}$ units linked via four coplanar Cu^{2+} atoms and carrying aqua ligands [121].

Coronado and co-workers reported X-ray analysis and magnetic properties of potassium salt of $[Mn_4(H_2O)_2(PW_9O_{34}]$ [122] and mixture of sodium-potassium salt of $[Ni_4(H_2O)_2(PW_9O_{34}]$ [123] by reacting trilacunary phosphotungstate and metal salts. Pope et. al. synthesized low valence potassium salt of $[Mn^{II}_4(H_2O)_2(PW_9O_{34})_2]^{10-}$, mix valence potassium salt of $[Mn^{II,III}_4(H_2O)_2(PW_9O_{34})_2]^{10-}$ and high valence potassium-ceasium salt of $[Mn^{III}_4(H_2O)_2(PW_9O_{34})_2]^{10-}$ complexes and observed that the later two species are one- and three-electron oxidized derivatives of $[Mn^{II}_4(H_2O)_2(PW_9O_{34})_2]^{10-}$ [124]. Zhang and Hill reported X-ray analysis for tetrabutyl ammonium chloride salt of $[Fe_4(H_2O)_2(PW_9O_{34})_2]^{10-}$ synthesized from trilacunary precursors and metal salt and further characterized by various spectroscopic techniques [125].

Kortz and co-workers have contributed significantly towards Si and Ge derivative of sandwich type POMs. But as we have restricted ourselves to the synthesis of sandwich type phosphotungstates only related references have been included.

Kortz and co-workers reported the presence of three transition metals between two B-trivacant phosphotungstate with sodium ion in the free coordination site, $[Ni_3Na(H_2O)_2(PW_9O_{34})_2]^{11-}$ by reacting trilacunary phosphotungstate and metal salt at pH 6.9 and characterized by various spectral techniques [126]. The same group reported the X-ray analysis for caesium salt of $[\{PhSbOH\}_3(A\text{-}\alpha\text{-}PW_9O_{34})_2]^{9-}$ complex by direct interaction of Ph_2SbCl_3 with three different lacunary phosphotungstate precursors, (A-α-$[PW_9O_{34}]^{9-}$, $[PW_{11}O_{39}]^{7-}$ or $[P_2W_{20}O_{70}(H_2O)_2]^{10-}$, in an aqueous acidic medium under hydrothermal condition with idealized D_3h symmetry [127].

Hill group has reported the synthesis of the carbonate-encapsulated A-type sandwich complex of $Y^{(III)}$ ions, $(YOH_2)_3(CO_3)(A\text{-}PW_9O_{34})_2^{11-}$ and characterization by X-ray analysis and NMR [128]. The same group demonstrated that the decomposition of sandwich type phosphotungstate $[(M(OH_2)_2)_3(A\text{-}\alpha\text{-}PW_9O_{34})_2]^{12-}$ (where M= $Mn^{(II)}$ or $Co^{(II)}$), giving a new family of transition metal substituted phosphotungstate of general formula

$[((MOH_2)M_2PW_9O_{34})_2(PW_6O_{26})]^{17-}$ (where M= $Mn^{(II)}$ or $Co^{(II)}$) [129]. These group in 2010 presented a new family of sandwich-type phosphotungstate containing two types of metals in the central belt: $M'_2M_2(PW_9O_{34})_2^{12-}$ (M'= Na or Li, M= Mn^{2+}, Co^{2+}, Ni^{2+} and Zn^{2+}) which were characterized by elemental analysis, FT-IR, ^{31}P NMR, X-ray analysis and magnetic susceptibility [130].

Catalysis by TMSPOMs

Majority of applied work was carried out in field of catalysis, especially oxidation of various organic substrates. Because the catalytically active site is at the substituted transition metal centre and POMs functions as a ligand with a strong capacity for accepting electrons. The substituting metal center is thus pentacoordinated by the "parent" POMs. The octahedral coordination sphere is completed by an additional sixth labile ligand, L (usually L= H_2O). This lability of the sixth ligand allows the interaction of the substituting transition metal atom reacting with substrate and/or oxidant. In analogy with organometallic chemistry the "pentadentate" POMs acts as an inorganic ligand. This analogy led to transition metal-substituted polyoxometalates being termed "inorganic metalloporphyrins" and have distinct advantages over organometallic species, *e.g.* they are rigid, hydrolytically stable and thermally robust. Further, the "active sites" of their transition metals and countercations can undergo extensive synthetic modifications.

In 1986, Hill and Brown [50] reported the following mechanism for oxidation process.

$$\underset{\text{oxometal}}{\mathbf{M{=}O}} + \underset{\substack{\text{alkene or}\\ \text{alkane}}}{\mathbf{Sub}} \xrightarrow{k_{ox}} \mathbf{M + SubO} \quad \underset{\text{epoxide}}{} \qquad \text{-- (1)}$$

This proposed mechanism is related to the work through earlier investigations of analogous metalloporphyrin systems by the Hill group (catalytic profiles, characterization of intermediates, product distributions, kinetics and other studies in many papers) [131-140].

In 2001, Pope and coworkers showed that the POMs catalyzed oxidations may be categorized by the principle mode of the catalytic reaction. There are two major reaction mechanisms [15]. In the first case, the catalytic cycle can be best described by the division of the reaction into two stages (Eq 2).

Initially, the substrate is oxidized by the POM to yield the product and the reduced POM catalyst. The reduced POM catalyst is then reoxidized, often by oxygen to form water, hence completing the catalytic cycle.

$$\text{Substrate} + \text{POM}_{ox} \longrightarrow \text{Product} + \text{POM}_{red} + 2H^+$$

$$\text{POM}_{red} + O_2 + 2H^+ \longrightarrow \text{POM}_{ox} + H_2O \qquad \text{-- (2)}$$

In the liquid phase, the oxidation of the substrate is often a dehydrogenation (electron and proton transfer from the substrate to the catalyst) and regeneration of the catalyst implies electron donation of oxygen to the catalyst with co-formation of water or insertion.

The second reaction type views the oxidation catalyzed by the POM as an interaction with a primary oxidant (Eq 3). This interaction yields an activated catalyst intermediate e.g. peroxo, hydroperoxo or high valent oxo species which can be used to oxidize the organic substrate

$$\text{Oxidant} + \text{POM} \longrightarrow [\text{POM-Ox}]_{activated}$$

$$[\text{POM-Ox}]_{activated} + \text{Substrate} \longrightarrow \text{POM} + \text{Product} \qquad \text{-- (3)}$$

In this second type of oxidation reactions, the actual reaction mechanism certainly varies as a function of the transition metal and oxidant, but can be considered as taking place via a general intermediate "transition metal - oxidant" species.

Hill and coworkers have given a significant contribution in this field of oxidation catalysis. They have reported the use of $[PW_{11}O_{39}M(H_2O)]$, (where M = Co^{II}, Mn^{II}, Fe^{II} and Cu^{II}) for oxidation of alkanes using *tert*-butyl hydrogen peroxide as an oxidant [141]. They have reported selective oxygenation of alkenes by iodosylarenes catalyzed by $[PW_{11}O_{39}M^{II}]^{5-}$, M=Co(II) or Mn(II) [50]. The quarternary ammonium salt of $[SiW_{11}O_{39}Ru^{III}(H_2O)]$ was used for oxidation of alkanes as well as epoxidation of alkenes using different oxidants such as PhIO, $NaIO_4$, etc. by R. Neumann and his co-workers [142, 143]. The oxidation of alkanes by O_2 facilitated by several TMSPOMs complexes including $K_5CrPW_{11}O_{39}N_3$ has been reported by Lyons and Ellis [144, 145].

Further, Rong and Pope reported alkene epoxidation over $[PW_{11}O_{39}Ru^{III}(H_2O)]$ using acetonitrile as a solvent with PhIO as an oxidant [67]. Hill et al. then demonstrated the efficient catalytic activity for the $[SiW_{11}O_{39}Cr^{III}(H_2O)]$ for oxidation of alkenes and alcohols by using chromium oxide as an oxidant [146]. They have also reported the use of a series of, $[XMW_{11}O_{39}]$, (M = Fe, Co, Ni, Zn, Mn, Cu) and (X= P, Si), for oxidation of H_2S to get elemental sulphur [147]. Hill [50, 141], Finke [148], Neumann [142, 143, 149] and their co-workers have explored the use of Mn^{II} or Mn^{III} substituted $[PW_{11}O_{39}M(H_2O)]$ as epoxidation catalysts with iodosylbenzene and hydrogen peroxide as oxidants. Pope and co-workers reported the use of $[PW_{11}O_{39}Mn^{IV/V}(L)]^{4-/3-}$ for oxidation of alkenes [69]. Anson et al. demonstrated the use of $Cs_m[PW_{11}O_{39}Ru^{V}(L)]$, for alcohol oxidation [71]. Mizuno and coworkers studied the effect of several TMS POMs catalysts $[PMW_{11}O_{39}]$, (where M = Co, Mn, Fe, Cu and Ni) several aldehydes, and different solvents on the aerobic oxidation of cyclohexene to epoxide (major product), and allylic alcohol and ketone (minor products) [150].

Kholdeeva et al. reported alkene epoxidation of tetra butylammonium salts of $[PW_{11}MO_{39}]$ (where, M = Co^{II}, Mn^{II}, Cu^{II}, Pd^{II}, Ti^{IV}, Ru^{IV}, and V^{V}) by dioxygen [151] in the presence of isobutyraldehyde (IBA) using acetonitrile as solvent.

Epoxidation of alkenes using $[PW_{11}CoO_{39}]^{5-}$ was reported by W Nam et al. using buffered potassium monopersulfate [152]. Mizuno and coworkers also reported oxidation of alkanes and alcohols using $[SiW_{11}\ Ru(H_2O)O_{39}]^{5-}$ [153].

Mizuno and coworkers have given a significant contribution in the field of oxidation catalysis using di-substituted POMs. They reported the use of $[SiW_{10}Mn^{III}_2(H_2O)_2O_{38}]^{6-}$, for the oxygenation of cyclohexane to cyclohexanol and cyclohexanone using 1 atm of molecular oxygen in dichloromethane-acetonitrile mixture [154]. The same group reported epoxidation of various alkenes catalyzed by $[XW_{10}O_{39}M_2(H_2O)_2]$, (where X= P, Si and M = Fe, V and Ti) in the presence of H_2O_2 with high yields of epoxide under mild reaction condition using of acetonitrile as solvent [38, 155-159]

Mizune et. al. also reported efficiency of diiron-substituted silicotungstate, $[\gamma(1,2)\text{-}SiW_{10}\{Fe(OH)_2\}_2O\text{-}]^{6-}$ in the O_2-based epoxidation of alkenes [35, 36, 82].

The sandwich-type POMs have received much attention because of their superior catalytic performance for the oxidation with hydrogen peroxide [108, 124, 160-171] and molecular oxygen [172,173]. Furthermore, sandwich-type POMs have been considered to be more thermodynamically stable as compared other substituted Keggin-type POMs [160, 161, 124, 40, 114, 115]. Neumann and co-workers reported an efficient biphasic H_2O_2-based epoxidation system catalyzed by $[WZnM_2(H_2O)_2(ZnW_9O_{34})_2]^{q-}$ ($M=Mn^{II}$, Zn^{II}, etc.), [160]. The same group reported oxidative and hydrolytic stability of manganese containing $[WZnMn_2(H_2O)_2(ZnW_9O_{34})_2]^{12-}$ complexes for epoxidation of cyclooctene [160, 161].

Krebs and co-workers reported the potentiality of manganese substituted POMs in regioselective epoxidation of *R*-(+)-limonene to 1,2- epoxide at ambient temperature in a biphasic system [108].

Hill and co-workers reported the epoxidation of alkenes catalyzed by iron substituted sandwich type POMs, $[Fe_4(H_2O)_2(PW_9O_{34})_2]^{10-}$ using H_2O_2 in presence of acetonitrile as solvent [124]. Kala raj et. al. reported epoxidation

of *R*-(+)-limonene catalyzed by cobalt-containing sandwich-type POMs, $[WCo_3(H_2O)_2(CoW_9O_{34})_2]^{10-}$ using H_2O_2 [167].

The methyltricaprylammonium salt of $[((Mn^{II}OH_2)Mn^{II}_2PW_9O_{34})_2(PW_6O_{26})]^{17-}$ complexes effectively catalyzed the epoxidation of cyclooctene, cyclohexene, and 1-hexene reported by Hill [127].

Thus a literature survey shows that most of the reported articles describe synthesis of the transition metal substituted phosphotungstate derivative either from lacunary POMs or from individual salts. A careful survey also shows that all the reported articles dealing with catalysis are in homogeneous medium using solvents and hence they suffer from the traditional drawbacks of homogeneous catalysis. It was also observed that very few articles are available on the oxidation of alkenes using mono, di and tetra nuclear (sandwich) manganese substituted phosphotungstate as catalyst.

So, considering these aspects, it was thought of interest to design a new easy synthetic pathway for synthesis of transition metal substituted phopshotungstates, especially manganese substituted phosphotungstate and to use them as catalysts for solvent free oxidation reaction. As Mn is most important metal from the view point of oxidation catalysis, it was selected for the present work.

Considering the all the aspects following objectives have been set.

Objectives

1. To tailor 12-Tungstophosphoric acid at molecular level.
2. Modification in the traditional two step synthetic approach by developing an uncomplicated in-situ “one Pot” synthetic approach for synthesis of TMSPOMs.
3. To minimize complex solution speciation processes arising from the presence of a multi-equilibrium situation and depends on a multitude

of factors (such as pH, ionic strength, reaction time, temperature, counterions and concentration of starting materials).

4. To establish the use of manganese substituted phosphotungstates as catalysts for solvent free liquid phase oxidation of alkenes with economically and environmentally benign oxidants, H_2O_2 and O_2.
5. To study the effect of manganese substitution on the catalytic activity of different substrates and propose the best catalyst among them.
6. To study kinetic behavior of all the catalysts using H_2O_2 as an Oxidant

Chapter 2 deals with one-pot *in situ* synthesis of cesium salt of Mn(II) substituted phosphotungstate based on mono lacunary POMs ($PW_{11}Mn$). The synthesized complex was characterized by single crystal analysis. It was also characterized in solid as well as solution by various spectral as well as electrochemical techniques. The catalytic activity was evaluated for solvent free liquid phase oxidation of alkenes using environmentally benign oxidants such as H_2O_2 and O_2.

Chapter 3 deals with one-pot *in situ* synthesis of cesium salt Mn(II) substituted phosphotungstate based on di lacunary POMs ($PW_{10}Mn_2$). The synthesized complex was characterized in solid as well as solution by various spectral and electrochemical techniques. The catalytic activity was evaluated for solvent free liquid phase oxidation of alkenes using environmentally benign oxidants such as H_2O_2 and O_2.

Chapter 4 deals with one-pot *in situ* synthesis of sandwich compound based on tri lacunary POMs (PW_9Mn_4). The synthesized complex was characterized by single crystal analysis. It was also characterized in solid as well as solution by various spectral. The catalytic activity was evaluated for solvent free liquid phase oxidation of alkenes using environmentally benign oxidants such as H_2O_2 and O_2.

For all catalysts, kinetic study was carried out using H_2O_2 as an oxidant. All the catalysts were regenerated after a simple workup and reused.

Finally, comparison in mono, di and tetra manganese substituted phosphotungstate was carried out to study effect of Mn centre on oxidation of alkenes using O_2 and H_2O_2 in form of % conversion as well as % selectivity.

References

1. J. M. Thomas, *J. Mol. Catal. A: Chem.,* 115, 371, (1997)
2. J. M. Thomas, C. R. A. Catlow, G. Sankar, *Chem. Commun.,* 2921, (2002)
3. F. Lefebvre, J.-M. Basset, *Curr. Topics Catal.,* 3, 215, (2002)
4. Z. L. Lu, E. Lindner, H. A. Mayer, *Chem. Rev.,* 102, 3543, (2002)
5. T. Don Tilley, *J. Mol. Catal. A: Chem.,* 182, 17, (2002)
6. R. Raja, J. M. Thomas, *J. Mol. Catal. A: Chem.,* 181, 3, (2002)
7. M. A. Barteau, J. E. Lyons and K. Song, *J. Catal.,* 216, 236, (2003)
8. J. M. Thomas, R. Raja, *J. Organomet. Chem.,* 689, 4110, (2004)
9. J. -M. Basset, J. -P. Candy, C. Coperet, F. Lefebvre and E. A. Quadrelli, *Nanotechnol. Catal.,* 2, 447, (2004)
10. D. K. Bohme, H. Schwarz, *Angew. Chem. Int. Ed.* 44, 2336, (2005)
11. O. Kholdeeva, *Top. Catal.,* 40, 229, (2006)
12. M. T. Pope, *Inorganic Chemistry Concepts Vol. 8: Heteropoly and Isopoly Oxometalates*, Springer, Berlin, (1983)
13. M. T. Pope and A. Müller (Eds.), *Polyoxometalates: From Platonic Solids to Anti-Retroviral Activity*, Kluwer, Dordrecht, The Netherlands, (1994)
14. Issue on "Polyoxometalates", *Chem. Rev.* 98, 1, (1998)
15. M. T. Pope, A. Muller (Eds.), *Polyoxometalate Chemistry: From Topology via Self-Assembly to Applications*, Kluwer, Dordrecht, 2001
16. *Polyoxometalate Chemistry for Nano-Composite Design*, ed. T. Yamase and M. T. Pope, Kluwer, Dordrecht, The Netherlands, (2002)
17. M. T. Pope, *Comput. Coord. Chem. II*, 4, 635, (2003)
18. C. L. Hill, *Comput. Coord. Chem. II*, 4, 679, (2003)
19. J. J. Borras-Almenar, E. Coronado, A. Mueller, M. T. Pope (Eds.), *Polyoxometalate Molecular Science*, Kluwer, Dordrecht, The Netherlands, (2004)
20. D. -L. Long, E. Burkholder, L. Cronin, *Chem. Soc. Rev. 36*, 105, (2007)
21. L. Bi, U. Kortz, B. Keita, L. Nadjo, *Dalton Trans.,* 3184, (2004)
22. N. Vankova, T. Heine and U. Kortz, *Eur J. Inorg Chem.,* 5102, (2009)

23. M. Sadakane, D. Tsukuma, M. Dickmann, B. Bassil, U. Kortz, M. Higashijima, W. Ueda, *Dalton Trans.,* 4271, (2006)
24. M. T. Pope, A. Müller, *Angew. Chem. Int. Ed. Engl.* 30, 34, (1991)
25. P. J. Hagrman, D. Hagrman, J. Zubieta, *Angew. Chem. Int. Ed.* 38, 2638, (1999)
26. E. Burkholder, J. Zubieta, *Chem. Commun.* 2056, (2001)
27. C. D. Wu, C. Z. Lu, H. H. Zhuang, J. S. Huang, *J. Am. Chem. Soc.* 124, 3836, (2002)
28. K. Fukaya, T. Yamase, *Angew. Chem. Int. Ed.* 42, 654, (2003)
29. H. Q. Tan, Y. G. Li, Z. M. Zhang, C. Qin, X. L. Wang, E. B. Wang, Z. M. Su, *J. Am. Chem. Soc.* 129, 10066, (2007)
30. J. Thiel, C. Ritchie, C. Streb, D.L. Long, L. Cronin, *J. Am. Chem. Soc.* 131, 4180, (2009)
31. I. V. Kozhevnikov, *Catalysts for fine chemical synthesis-Catalysis by polyoxometalates*, John Wiley and Sons, Chichester, UK, p 117, (2002)
32. L.C.W. Baker, J. Figgis. *J. Am. Chem. Soc*, 92, 3794 (1970).
33. N. H. Nsouli, A. H. Ismail, I.S. Helgadottir, M.H. Dickman, J. M. Clemente-Juan, U. Kortz, *Inorg. Chem.*, 48, 5884, (2009).
34. S. G. Mitchell, H. N. Miras, D. Long, L. Cronin, *Inorg. Chim. Acta*, 363, 4240, (2010)
35. K. Kamata, K. Yonehara, Y. Sumida, K. Yamaguchi, S. Hikichi, N. Mizuno, *Science.*, 300, 964 (2003)
36. Y. Nishiyama, Y. Nakagawa, N. Mizuno, *Angew. Chem. Int. Ed.*, 40, 3639 (2001)
37. N. Mizuno, C. Nozaki, I. Kiyoto, M. Misono, *J. Am. Chem. Soc.*, 120, 9267 (1998)
38. N. Mizuno, K. Yamaguchi, K. Kamata, *Coord. Chem. Rev.*, 249, 1944 (2005)
39. B. Botar, Y. V. Geletii, P. Kögerler, D.G. Musaev, K. Morokuma, I. A. Weinstock, C. L. Hill, *J. Am. Chem. Soc.*, 128, 11268 (2006)
40. J. Canny, A. Tézé, R. Thouvenot, G. Hervé, *Inorg. Chem.*, 25, 2114 (1986)

41. J. Canny, A. Tézé, G. Hervé, M. Leparulo-Loftus, M. T. Pope, *Inorg. Chem.*, 30, 976 (1991)
42. F. Xin, M. T. Pope, *Inorg. Chem.*, 35, 5693 (1996)
43. F. Xin, M. T. Pope, G. J. Long, U. Russo, *Inorg. Chem.*, 35, 1207 (1996)
44. K. Wassermann, H. J. Lunk, R. Palm, J. Fuchs, N. Steinfeldt, R. Stosser, M. T. Pope, *Inorg. Chem.*, 35, 3273 (1996)
45. U. Kortz, S. Isber, M. H. Dickman, D. Ravot, *Inorg. Chem.*, 39, 2915 (2000)
46. U. Kortz, S. Matta, S., *Inorg. Chem.*, 40, 815 (2001)
47. B. S. Bassil, U. Kortz, A. S. Tigan, J. M. Clemente-Juan, B. Keita, P. D. Oliveira, L. Nadjo, *Inorg. Chem.*, 44, 9360 (2005)
48. Z. Zhang, Y. Li, E. Wang, X. Wang, C. Qin, H. An, *Inorg. Chem.*, 45, 4313 (2006).
49. R. G. Finke, M. W. Droege, P. J. Domaille, *Inorg. Chem.*, 26, 3886 (1987)
50. C. L. Hill and R. B. Brown, *J. Am. Chem. Soc.*, 108, 536, (1986)
51. L. -H. Bi, M. Reicke, U. Kortz, B. Keita, L. Nadjo and R. J. Clark, *Inorg. Chem.*, 43, 3915, (2004)
52. F. Hussain, B. S. Bassil, L. -H. Bi, M. Reicke and U. Kortz, *Angew. Chem., Int. Ed.*, 43, 3485, (2004)
53. U. Kortz, S. Nellutla, A. C. Stowe, N. S. Dalal, U. Rauwald, W. Danquah and D. Ravot, *Inorg. Chem.*, 43, 2308, (2004)
54. U. Kortz, S. Nellutla, A. C. Stowe, N. S. Dalal, J. Vantol, B. S. Bassil, *Inorg. Chem.*, 43, 144, (2004)
55. A. Proust, R. Thouvenot, P. Gouzerh, *Chem. Comm.,* 1837, (2008)
56. D. E. Katsoulis and M. T. Pope, *J. Chem. Soc., Chem. Comm.,* 1186, (1986)
57. C. L. Hill, C.M. Prosser-McCartha, *Coord. Chem. Rev.,* 143, 407, (1995)
58. L. C. W. Baker and T. P. McCutcheon, *J. Am. Chem. Soc.,* 78, 4503, (1956)
59. L. C. W. Baker, V. S. Baker, K. Eriks, M. Pope, M. Shibata, O. Rollins, J. Fang, L. Koh, *J. Am. Chem. Soc.,* 88, 2329, (1966)

60. T. J. R. Weakley, S. A. Malik, *J. Inorg. Nucl. Chem*, 29, 2935, (1967)
61. C.M. Torne, G. F. Tourne, S. A. Malik, T. G. R. Weakly. *J. Inorg. Nucl. Chem.* 32, 3875, (1970).
62. R. Ripan, N. Pucasu, D. Stanescu, P. Z. Boian, *Anorg. Allgem. Chem.* 384, 297, (1971)
63. T. J. R Weakley, *J. Chem. Soc. Dalton. Trans.*, 341, (1973)
64. A. Komura, M. Hayashi, H. Imanaga, *Bull. Chem. Soc. Jpn.,* 49, 87, (1976)
65. F. Zonnevijlle, C. M. Tourne, G. F. Tourne, *Inorg. Chem. 22*, 1198, (1983)
66. R. F. Klevtsova, E. N. Yurchenko, L. A Glinskaya, L. I. Kuznetsova, L. G. Detusheva, T. P. Lazarenko, *Zh. Strukt., Khim.*, 132, 102, (1991)
67. C. Rong, M. T. Pope, *J. Am. Chem. Soc.* 114, 2932, (1992)
68. C. Rong, H. So., M. T. Pope., *Eur. J. Inorg. Chem.,* 5211, (2009)
69. X. Zhang, M. T. Pope, M. R. Chance, G. B. Jameson, *Polyhedron.,* 14, 1381, (1995)
70. J. Bart., F. Anson, *J. Electroanal. Chem.,* 390, 11, (1995)
71. J. R. Galan-Mascaros, C. Gimenez-Saiz, S. Triki, C. J. Gomez-Garcia, E. Coronado , L. Ouahab, *Angew. Chem. Int. Ed.* Engl. 34, 1460, (1995)
72. H. Evans Jun., T. J. R Weakley, G. B. Jameson, *Dalton Trans.,* 2537, (1996)
73. A. Bagno, M. Bonchio, A. Sartorel, G. Scorrano, *Eur. J. Inorg. Chem.* 17, (2000)
74. C. Dablemont, A. Proust, R. Thouvenot, C. Afonso, F. Fournier, J. C. Tabet, *Inorg. Chem. 43*, 3514, (2004)
75. Z. Han, Y. Zhao, J. Peng, H. Ma, Q. Liu, E. Wang, *J. Mol. Struct.* 738, 1, (2005)
76. Y. B. Huang, J. X. Chen, T. Y. Lan, X. Q. Lu, C. X. Wei, Z. S. Li, Z. C. Zhang, *J. Mol. Struct.* 783, 168, (2006)
77. V. L. Lahootun, C. Besson, R. Villanneau, F. Villain, L. M. Chamoreau, K. Boubekeur, S. Blanchard, R. Thouvenot, A. Proust, *J. Am. Chem. Soc.,* 129, 7127, (2007)

78. C. Besson, Y. Geletii, F. Villain, R. Villanneau, C. Hill, A. Proust, *Inorg. Chem.,* 48, 9436, (2009)
79. M. Balula, I. Santos, J. Gamelas, M. Cavaleiro, N. Binsted, W. Schlindwein, *Eur. J. Inorg. Chem.,* 1027, (2007)
80. J. P. Wang, K. H. Wang, J. Y. Niu, *J. Mol. Struc.,* 886, 183, (2008)
81. M.N. Sokolov, S. A. Adonin, D. A. Mainichev, C. Vicent, N. F. Zakharchuk, A. M. Danilenkoa, V. P. Fedin, *Chem Comm.*, 47, 7833 (2011).
82. C. Nozaki, I. Kiyoto, Y. Minai, M. Misono, N. Mizuno, *Inorg. Chem.*, 38, 5724 (1999).
83. Y. V. Geletii, B. Botar, P. Kogerler, D. A. Hillesheim, D. G. Musaev, C. L. Hill, *Angew. Chem. Int. Ed.*, 47, 3896 (2008).
84. Z. Luo, P. Kogerler, R. Cao, C. L. Hill, *Polyhedron,* 28, 215 (2009).
85. Z. Luo, P. Kogerler, R. Cao, I. Hakim, C. L. Hill, *Dalton Trans.*, 54 (2008).
86. B. S. Bassil, S. Nellutla, U. Kortz, A. C. Stowe, J. V. Tol, N. S. Dalal, B. Keita, L. Nadjo, *Inorg. Chem.*, 44, 2659 (2005).
87. B. S. Bassil, U. Kortz, *Dalton. Trans.*, 40, 9649, (2011)
88. X. Zhang, C. J. O'Connor, G. B. Jameson, M. T. Pope, *Inorg. Chem.*, *35*, 30 (1996).
89. Y. Nakagawa, K. Uehara, N. Mizuno, *Inorg.Chem.*, 44, 14 (2005).
90. Y. Kikukawa, S. Namaguchi, Y. Nakagawa, K. Uehara, S. Yuchida, K. Yamaguchi, N. Mizuno, *J. Am. Chem. Soc.*, 130, 15872 (2008).
91. D. Quinonero, Y. Wang, K. Morokuma, L. A. Khavrutskii, B. Botar, Y. V. Geletii, C. L. Hill, D. G. Musaev, *J. Phys. Chem. B,* 110, 170 (2006).
92. C. Besson, D. G. Musaev, V. Lahootun, R. Cao, L. M. Chamoreau, R. Villanneau, F. Villain, R. Thouvenot, Y. V. Geletii, C. L. Hill, A. Proust, *Chem. Eur. J.*, 15, 10233 (2009).
93. P. J. Domaille, W. H. Knoth, *Inorg. Chem.*, 22, 818 (1983).
94. P. J. Domaille, G. Watunya, *Inorg. Chem.*, 25, 1239 (1986).
95. P. J. Domaille, R. L. Harlow, *J. Am. Chem.* Soc., 108, 2108 (1986).
96. T. Ozeki, T. Yamase, *Acta Cryst.,* C47, 693 (1991).

97. C. J. Gomez-Garcia, E. Coronado, P. Gomez-Romero, N. Casaii-Pastor, *Inorg. Chem.*, *32,* 89 (1993).
98. E. Cadot, V. Bereau, B. Marg, S. Halut, F. Secheresse, *Inorg. Chem.,* 35, 3099 (1996).
99. E. Cadot, V. Bereau, F. Secheresse, *lnorg. Chim. Acta.* 252, 101 (1996).
100. K. Nomiya, M. Takahashi, J. A. Widegren, T. Aizawa, Y. Sakai, N. C. Kasuga., *J. Chem. Soc, Dalton. Trans.,* 3679 (2002).
101. R. G. Finke, M. W. Droege, *J. Am. Chem. Soc.,* 106, 7274 (1984).
102. R. G. Finke, B. Rapko, R. J. Saxton, P. J. Domaille., *J. Am. Chem. Soc.,* 108, 2947 (1986).
103. N. Mizuno, C. Nozaki, T. Hirose, M. Tateishi, M. Iwamoto., *J. Mol. Catal. A* :*Chemical.*, 117, 159 (1997).
104. A. Kishida, A. Taguchi, N. Mizuno., *Chemistry Letters*, 1374 (2000).
105. Y. Hou, L. Xu, M. J. Cichon, S. Lense, K. I. Hardcastle, C. L. Hill, *Inorg. Chem.*, 49, 4125 (2010).
106. F. Robert, M. Leyrie, G. Herve, *Acta Crystallogr.,* B38, 358 (1982).
107. C. M. Tourne, G. F. Tourne, F. Zonnevijlle., *J. Chem. Soc. Dalton. Trans.*, 143 (1991).
108. M. Bo1sing, A. Noh, I. Loose, B. Krebs, *J. Am. Chem. Soc.*, 120, 7252 (1998).
109. U. Kortz, N. K. Al-assem, M. G. Savelieff, N. A. Al Kadi, M. Sadakane, *Inorg. Chem.*, 40, 4742 (2001).
110. L. H. Bi, U. Kortz, B. Keita, L. Nadjo, H. Borrmann, *Inorg. Chem.,* 43, 8367 (2004).
111. P. Mialane, J. Marrot, E. Riviere, J. Nebout, G. Herve, *Inorg. Chem.*, 40, 44 (2001).
112. L. H. Bi, R. D. Huang, J. Peng, E. B. Wang, Y. H. Wang, C. W. Hu, *Dalton Trans.,* 121 (*2001*).
113. J. Wang, P. Ma, Y. Shen, J. Niu, *Cryst. Growth. Des.*, 7, 603 (2007).
114. T. Yamase, H. Abe, E. Ishikawa, H. Nojiri, Y. Ohshima, *Inorg. Chem.,* 48, 138 (2009).
115. N. Jiang, F. Li, L. Xu, Y. Li, J. Li, *Inorg. Chem. Comm.,* 13, 372 (2010).

116. Y. Liu , J. Dou , D. Wang , X. Zhang, D. Li , Y. Jia, *J. Chem. Crystallogr.* 41, 186 (2011).
117. T. J. R Weakley, H. T. Evans, Jr. J. S. Showell, G. F. Tourne, C. M. Tourne, *J. Chem. Soc. Chem. Comm.*, 139, (1973)
118. R. G. Finke, M. Droege, *J. Am. Chem. Soc.*, 103, 1587 (1981).
119. W. H. Knoth, P. J. Domaille, R. D. Farlee, *Organometallics*, 4, 62 (1985).
120. W. H. Knoth, P. J. Domaille, R. L. Harlow, *Inorg. Chem.*, 25, 1577 (1986).
121. T. J. R. Weakley, R. G. Finke, *Inorg. Chem.,* 29, 1235 (1990).
122. C. J. Gomez-Garcia, E. Coronado, P. Ghez-Romero, N. Casafi-Pastor, *Inorg. Chem.*, 32, 3378 (1993).
123. J. M. Clemente-Juan, E. Coronado, J. R. Galan-Mascaros, C. J. Gomez-Garcıa *Inorg. Chem.,* 38, 55 (1999).
124. X. Y. Zhang, G. B. Jameson, C. J. O'Connor M. T. Pope, *Polyhedron*, 15, 917 (1996).
125. X. Zhang, Q. Chen, D. C. Duncan, R. J. Lachicotte, C. L. Hill., *Inorg. Chem.*, 36, 4381 (1997).
126. U. Kortz, I. M. Mbomekalle, B. Keita, L. Nadjo, P. Berthet, *Inorg. Chem.,* 41, 6412 (2002).
127. L. F. Piedra-Garza, M. H. Dickman, O. Moldovan, H. J. Breunig, U. Kortz, *Inorg. Chem.,* 48, 411 (2009).
128. X. Fang, T. M. Anderson, W. A. Neiwert, C. L. Hill, *Inorg. Chem.,* 42, 8600 (2003).
129. M. D. Ritorto, T. M. Anderson, W. A. Neiwert, C. L. Hill, *Inorg. Chem.,* 43, 44 (2004).
130. Y. Hou, L. Xiu, M. J. Cichon, S. Lense, K. I. Hardcastle, C. L. Hill, Inorg. Chem., 49, 4125, (2010).
131. J. A. Smegal, C. L. Hill, *J. Am. Chem. Soc.,* 105, 3515, (1983)
132. B. C. Schardt, C. L. Hill, *J. Am. Chem. Soc.,* 102, 6374, (1980)
133. B. C. Schardt, F. J. Hollander, C. L. Hill, *J. Am. Chem. Soc.,* 104, 3964, (1982)

134. M. J. Camenzind, F. J. Hollander, C. L. Hill, *Inorg. Chem.,* 21, 4301, (1982)
135. C. L. Hill, F. J. Hollander, *J. Am. Chem. Soc.,* 104, 7318, (1982)
136. J. A. Smegal, B. C. Schardt, C. L. Hill, *J. Am. Chem. Soc.,* 105, 3510 (1983)
137. J. A. Smegal, C. L. Hill, *J. Am. Chem. Soc.,* 105, 2920, (1983)
138. C. L. Hill, J. A. Smegal, T. J. Henly, *J. Org. Chem.,* 48, 3277, (1983)
139. M. J. Camenzind, F. J. Hollander, C. L. Hill, *Inorg. Chem.,* 22, 3776, (1983)
140. C. L. Hill, M. M. Williamson, *Inorg. Chem.,* 24, 3024, (1985)
141. M. Faraj, C. Hill, *Chem. Commn.,* 1487, (1987)
142. R. Neumann, *Chem. Comm.,* 1324, (1989)
143. R. Neumann, C. Abu-Gnim, *J. Am. Chem. Soc.,* 112, 6025, (1990)
144. J. E. Lyons, P. E. Ellis Jr., V.A. Durante, R. A. Grasselli and A. W. Sleight (eds.), *Stud. Surf. Sci. Catal.*, Elsevier Scientific, Amsterdam, p. 99, (1991)
145. J. E. Lyons, P. E. Ellis Jr., H. K. Myers Jr., G. Suld, W. A. Langdale, U.S. Patent 4, 803, 187, Feb. 7, (1989)
146. C. L. Hill, *J. Am. Chem. Soc.,* 115, 8178, (1993)
147. M. K. Harrup, C. L. Hill, *Inorg. Chem.,* 33, 5448, (1994)
148. D. Mansuy, J. Bartoli, P. Battioni, D. Lyon, R. Finke, *J. Am. Chem. Soc.,* 113, 7222, (1991)
149. R. Neumann, *Dioxygen Activation and Homogeneous Catalytic Oxidation*, Eds, L.I. Simandi, Elsevier Science Publishers, Amsterdam (1991)
150. N. Mizuno, T. Hirose, M. Tateishi, M. Iwamoto, *Chem. Lett.* 1839, (1993)
151. O. Kholdeeva, V. A. Grigoriev, G. M. Maksimov, M. A. Fedotov, A.V. Golovin, K. I. Zamaraev, *J. Mol. Catal. A: Chem.*, 114, 123, (1996)
152. S. Choi, H. Lee, H. Kim, W. Nam, *Bull. Korean Chem. Soc.,* 23, 1039, (2002)
153. K. Yamaguchi, N. Mizuno, *New J. Chem.,* 26, 972, (2002)
154. T. Hayashi, A. Kishida, N. Mizuno, *Chem. Comm.*, 381, (2002)

155. N. Mizuno, K. Kamata, K. Yamaguchi, *Top Catal.*, 53, 876, (2010)
156. Y. Nakagawa, K. Kamata, M. Kotani, K. Yamaguchi, N. Mizuno, *Angew Chem Int Ed.*, 44, 5136, (2005)
157. Y. Nakagawa, N. Mizuno, *Inorg Chem.*, 46, 1727, (2007)
158. N. Mizuno, Y. Nakagaw, K. Yamaguchi, *J .Mol. Catal. A: Chemical.*, 251, 286, (2006)
159. N. Mizuno, S. Hikichi, K. Yamaguchi, S. Uchida, Y. Nakagawa, K. Uehara , K. Kamata, *Catal. Today.*, 117 , 32, (2006).
160. R. Neumann, M. Gara, *J. Am. Chem. Soc.*, 117, 5066, (1995)
161. R. Neumann, M. Gara, *J. Am. Chem. Soc.*, 116, 5509, (1994)
162. R. Neumann, A.M. Khenkin, *Inorg. Chem.*, 34, 5753, (1995)
163. R. Neumann, H. Miller, *J. Chem. Soc., Chem. Commun.*, 2277, (1995)
164. R. Neumann, D. Juwiler, *Tetrahedron.*, 52, 8781, (1996)
165. R. Neumann, A.M. Khenkin, *J. Mol. Catal. A: Chem.*, 114, 169, (1996)
166. G. Maayan, R.H. Fish, R. Neumann, *Org. Lett.*, 5, 3547, (2003)
167. N.K. Kala Raj, V.G. Puranik, C. Gopinathan, A.V. Ramaswamy, *Appl. Catal. A.*, 256, 265, (2003)
168. W. Adam, P.L. Alsters, R. Neumann, C.R. Saha-Moller, D. Sloboda-Rozner, R. Zhang, *J. Org. Chem.*, 68, 1721, (2003)
169. M.V. Vasylyev, R. Neumann, *J. Am. Chem. Soc.*, 126, 884, (2004)
170. D. Sloboda-Rozner, P. Witte, P.L. Alsters, R. Neumann, *Adv. Synth. Catal.*, 346, 339, (2004)
171. P.T. Witte, P.L. Alsters, W. Jary, R. Mullner, P. Pochlauer, D. Sloboda-Rozner, R. Neumann, *Org. Proc. Res. Dev.*, 8, 524, (2004)
172. R. Neumann, M. Dahan, *Nature.*, 388, 353, (1997)
173. R. Neumann, M. Dahan, *J. Am. Chem. Soc.*, 120, 11969, (1998)

CHAPTER

2

Mono Manganese(II) Substituted Phosphotungstate: Synthesis, Structural and Spectroscopic Characterization as well as Solvent free Liquid Phase Oxidation of alkenes

- **Paper Published**

  Trans. Met. Chem., 36, 171-177, (2011).

Transition Met Chem (2011) 36:171–177
DOI 10.1007/s11243-010-9450-2

One-step synthesis of a Keggin-type manganese(II)-substituted phosphotungstate: structural and spectroscopic characterization and non-solvent liquid phase oxidation of styrene

Ketan Patel · Pragati Shringarpure · Anjali Patel

Received: 11 October 2010 / Accepted: 8 December 2010 / Published online: 24 December 2010

Abstract The Keggin-type Cs salt of a mono Mn(II)-substituted phosphotungstate ($Cs_5[PMnW_{11}O_{39}]$) was synthesized from $H_3PW_{12}O_{40}$, $MnCl_2$ and CsCl. The complex was characterized in solution as well as in the solid state by spectroscopic, magnetic and electrochemical techniques. The complex crystallized in tetragonal phase. X-ray structural analysis shows two types of disorder in which the Mn and W atoms are distributed over the 12 positions, and the Mn atom could not be distinguished from the 11 W atoms distributed equally over the 12 addenda atoms in the Keggin structure. The catalytic activity of the complex was evaluated for non-aqueous oxidation of styrene using molecular oxygen. The complex gave >99.0% selectivity towards benzaldehyde and could be reused.

Introduction

Among the various TMSPOMs, the manganese-substituted POMs are of considerable interest because of their redox properties and variable oxidation states, which makes them important for various catalytic processes. The synthesis, characterization and catalytic activity of mono manganese-substituted phosphotungstate have been reported by number of groups [1-7].

The first manganese substituted polyoxotungstates were synthesized by Weakly et. al. in 1970 [1]. They reported the synthesis of sodium, potassium, ammonium, guanidinium and alkyl ammonium salts of Mn(II) and Mn(III) polyoxotungstates using three different methods. The first method involves the synthesis from XW_{11} and $MnCl_2.4H_2O$. The second method involves the synthesis from the individual salts (i.e. $Na_2WO_4.2H_2O$ and $MnCl_2.4H_2O$). The third method describes one pot synthesis from the parent POMs, i.e. from XW_{12} by in situ generation of XW_{11} (where X = Si, P and Ge) species and then substituting the metal ion into the vacant cavity. The synthesized complexes were characterized by elemental and spectrochemical techniques. The oxidation states were determined from the magnetic susceptibility which was further confirmed by potentiometric titrations. The powder X-ray patterns were also recorded for all the complexes based on which the lattice parameters were determined.

Afterwards, the synthesis of potassium and guanidinium salts of manganese(II) substituted phosphotungstates as well as the silicotungstates was also reported by Katsoulis and Pope [2]. The synthesized complexes were characterized by absorption spectra and ESR analysis. In 1995, Pope and coworkers synthesized the aqueous and non-aqueous soluble salts of Mn(IV) substituted phosphotungstates by chemical and electrolytic oxidation of corresponding Mn(II) and Mn(III) ions and characterized by elemental, spectroscopic analysis, magnetic moment, ESR and X-ray absorption near edge spectroscopy [3]. In the same year, Coronado et al. reported for the first time the single crystal data for the organic derivative of Mn(II) substituted phosphotungstate, $(ET)_{8n}[PMnW_{11}O_{39}]$, indicating the formation of chain like

structure [4]. In 1998 Coronado and co-workers reported the synthesis, crystal structure and magnetic properties of series of radical salts with bis(ethylene dithio) tetrathiafulvalene and monosubstituted POMs of formula $[XZ(H_2O)M_{11}O_{39}]^{5-}$ (XZM_{11}= $SiFe^{III}Mo_{11}$, $SiCr^{III}W_{11}$, $PCo^{II}W_{11}$, $PNi^{II}W_{11}$, $PCu^{II}W_{11}$, $PZn^{II}W_{11}$, $PMn^{II}W_{11}$ and $PMn^{II}Mo_{11}$) [5]. Nowiska et. al. studied ESR spectra of lacunary phosphotungstate modified with Mn(II) ions ($[PW_{11}Mn_x]^{5-}$, x=1-0.02) and point out the presence of two manganese species with different symmetry [6]. In 2007 Cavaleiro et al. applied EXAFS technique to understand the local environment around W and other substituted metal (Fe,Mn,Ru) in lacunary phosphotungstate and transition metal substituted phosphotungstate and compared with that of parent Keggin anion $[PW_{12}O_{40}]^{3-}$ [7].

Thus, all the reports to date focus on the two-step synthesis of the manganese-substituted phosphotungstates at almost neutral pH. To the best of our knowledge, only Weakely et al. have reported one-pot synthesis of sodium, potassium, ammonium, guanidinium or alkylammonium salts of $XMnW_{11}$ from XW_{12} (where X = Si, P or Ge). The isolation of a cesium salt of the Mn(II)-substituted phosphotungstate as well as its single-crystal analysis along with systematic characterization has not yet been reported.

The catalytic activity of the above mentioned derivative of manganese substituted phosphotungstate, has been explored for oxidation of various substrates by Hill. Hill and Brown have reported selective oxygenation of alkenes by iodosylbenzene and pentaflouroiodosylbenzene catalyzed by $[PW_{11}\ MnO_{39}]^{5-}$ using acetonitrile as solvent [8]. Further, Hill and Mc-Cartha described the catalytic oxidation of alkanes, alkenes and alcohols over quarternary ammonium salts of manganese (II) substituted phospho as well as silicotungstates [9]. They reported the oxidation of alkenes at lower temperatures using different oxidants such as molecular oxygen, PhIO, $Na_2S_2O_3$ and H_2O_2 under inert atmosphere.

Literature survey shows that all reported articles on catalytic activity of manganese substituted phosphotungstates are in presence of solvents. Further, no reports are available on oxidation of styrene. So it was thought

of interest to evaluate the catalytic activity for the same by carrying out solvent free liquid phase oxidation of alkenes, especially styrene.

In the present work, for the first time we have come up with the one pot in situ synthesis of cesium salt of mono Mn(II)-substituted phosphotungstate ($PW_{11}Mn$), starting from a commercially available 12-tungstophosphoric acid. The synthesized complex was systematically characterized in solid as well as in solution by single crystal analysis, elemental analysis, TGA, FT-IR, UV-Visible, ESR, powder XRD, ^{31}P NMR and cyclic voltammetry. The catalytic activity was evaluated for solvent free liquid phase oxidation of alkenes using environmentally friendly oxidants, H_2O_2 and O_2. Oxidation of alkenes was carried out by varying different parameters such as mole ratio of alkene to H_2O_2, reaction temperature, catalyst amount, and reaction time. The catalyst was regenerated after a simple workup and reused. The kinetics of the reaction was also studied. The rate of reaction and order of reaction was determined. The effect of temperature on rate constant was studied, and the activation energy was calculated by fitting the results into Arrhenius equation.

2.1 Experimental

Materials

All the chemicals used were of A. R. grade. $H_3PW_{12}O_{40}.nH_2O$ was obtained from Loba Chemie, Mumbai. NaOH, $MnCl_2.4H_2O$, CsCl, styrene, benzaldehyde, 30% aqueous H_2O_2, TBHP, cyclohexene, Cis-cyclooctene and dichloromethane were obtained from Merck and used as received.

Synthesis of $PW_{11}Mn$

The pH of a solution of $H_3PW_{12}O_{40}.nH_2O$ (2.88 g, 1 mmole) in water (10 ml) was adjusted to 4.8 using NaOH (Scheme 1). The solution was heated to 90°C with stirring. A solution of $MnCl_2$ (0.197 g, 1 mmole) in water (10 ml) was added to this hot solution. The final pH of the solution was adjusted to 4.8. The solution was heated at 90°C with stirring for 1h and filtered hot. 10 ml of a saturated solution of CsCl was added to the hot filtrate. The resulting mixture was allowed to stand overnight at room temperature. The solution was filtered, and the orange crystals (yield 88%) were dried at 50°C. The filtrate was used for the estimation of tungsten and manganese, in order to see the loss during the synthesis.

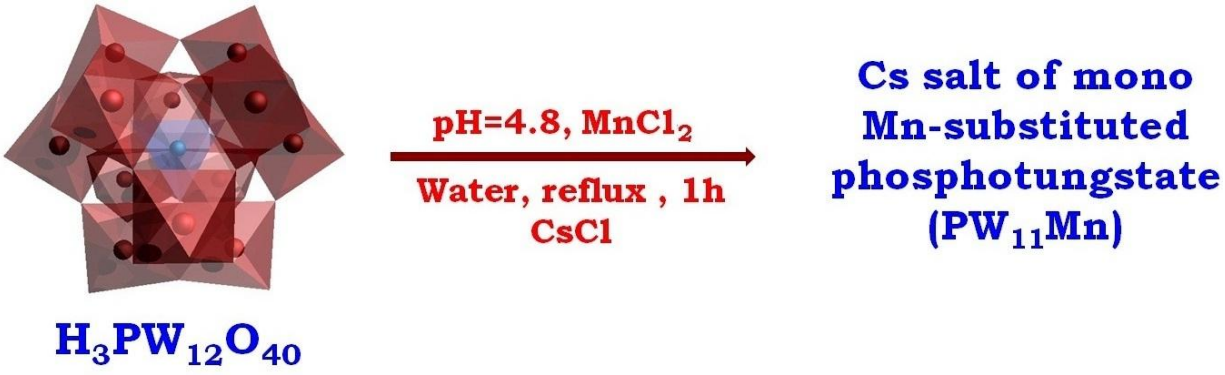

Scheme 1. Synthesis of $PW_{11}Mn$

2.2 Characterization

Elemental analysis was carried out using a JSM 5610 LV instrument combined with an INCA EDX-SEM analyzer for the quantitative identification of metals. TGA was carried out with a Mettler Toledo Star SW 7.01 up to 600^{o}C. FTIR spectra were recorded as KBr pellets on a Perkin-Elmer instrument. UV–Vis spectra were recorded at ambient temperature on Perkin–Elmer 35 LAMDA instrument using 1 cm quartz cells. ESR spectra were recorded on a Varian E-line Century series X-band ESR spectrometer (room temperature scanned from 2,000 to 4,000 Gauss and liquid nitrogen temperature scanned from 2,000 to 3,200 Gauss). Cyclic voltammetry was performed on a CH-660 instrument, USA at room temperature. A glassy carbon working electrode and an Ag/AgCl reference electrode were used. ^{31}P solution NMR spectra were recorded in D_2O on a Bruker ACF 300-MHz instrument. The analysis of the product mixtures for any leaching of Mn was carried by using atomic absorption spectrometer AAS GBC-902 instrument.

2.3 Results and discussion

2.3.1 X-ray Diffraction Techniques

Single Crystal Analysis

The single-crystal X-ray analysis was performed at 298(2) K on a Bruker SMART APEX CCD area detector system [λ(Mo - Ka) = 0.71073 A°], with a graphite monochromator. Two thousand and four hundred frames were recorded with ω scan width of 0.3^{o}, each for 10s, crystal-detector distance 60 mm and collimator 0.5 mm. The data were reduced using SAINTPLUS [10], and a multi-scan absorption correction using SADABS [10] was performed. Structure solution and refinement were done using SHELX-97 [11]. All non-hydrogen atoms were refined anisotropically. During the crystallography, 39093 reflections were collected, amongst which, 2463 were unique and used to solve the structure [R (int) = 0.1477].

The details of the crystal data are presented in Table 1.

Table 1. Crystal Data for $PW_{11}Mn$ and collection parameters

Empirical formula	**Cs_5 $MnO_{44}P$ W_{11} H_8**
Formula weight	3484.87
Temperature	273(2) K
Crystal system	Tetragonal
space group	P4(2)/ncm
Unit cell dimensions	a = 20.968(4) A alpha = 90 b = 20.968(4) A beta = 90 c = 10.427(4) A gamma = 90
Z, Calculated density	4, 5.049 Mg/m^3
Absorption coefficient	31.792 mm^-1
F(000)	5956
Theta range for data collection	1.37 to 26.56 deg.
Completeness to theta =26.56	98.6 %
Absorption correction	Empirical
Max. and min.transmission	0.1432 and 0.0376
Refinement method	Full-matrix least-squares on F^2
Data / restraints / parameters	2463 / 0 / 158
Goodness-of-fit on F^2	1.061
Final R indices [I>2sigma(I)]	R1 = 0.0437, wR2 = 0.1167
R indices (all data)	R1 = 0.0683, wR2 = 0.1244

Orange block type single crystals were obtained by re-crystallization from hot water. A suitable crystal with dimensions of 0.30 x 0.16 x 0.10 mm was assigned to the tetragonal system with a = b = 20.968(4) A, c = 10.427(4) A, V = 4,584(2) A^3, d_{cal} = 5.039 Mg/m^3, d_{exp} = 5.049 Mg/m^3. The observed space group for the crystal was P4(2)/ncm. This is as expected (since Co, Ni, Mn are isostructural and crystallize within the same space group and phase) and is in good agreement with the reported crystal structure of $Cs_5[PNi(H_2O)W_{11}O_{39}]$ [12]. The final cycle of refinement for structure including the atomic coordinates and anisotropic thermal parameters (Cs, P, W and O) converged at 0.0437 [I>2 sigma(I)] and Rw = 0.0683]. In the final difference map, the deepest hole was -2.539 located at 0.67 A ° from O_{11} and the highest peak was 3.802 A ° located at 3.25 A ° from O_6.

The crystal structure analysis shows that the manganese atoms are not present as counter cations. The Cs atoms were present as counter cations with Cs–P distance of 5.9149 and 6.430 A°. The crystallographic refinement of the complex suggests the presence of 5.75 Cs atoms per Keggin unit as counter ions, while the elemental analysis confirms the presence of five Cs atoms for each polyanion. The single-crystal X-ray analysis shows the presence of $3H_2O$, while the thermal analysis indicates the presence of $5H_2O$. This difference may be due to the loss of water in the process of single crystal XRD data collection and is consistent with previous observations [13].

Thus, based on the structural and elemental analysis, the formula of the complex is proposed as:

$$Cs_5[PW_{11}Mn(H_2O)O_{39}].4H_2O$$

The structural analysis shows two types of disorders in the crystal (Figure 1). Firstly, the Mn and W atoms were distributed over the 12 positions and the Mn atom could not be distinguished from the 11 W atoms distributed equally over the 12 addenda atoms in the Keggin structure, and secondly, the Keggin polyanion is distributed over two orientations related by a centre of symmetry.

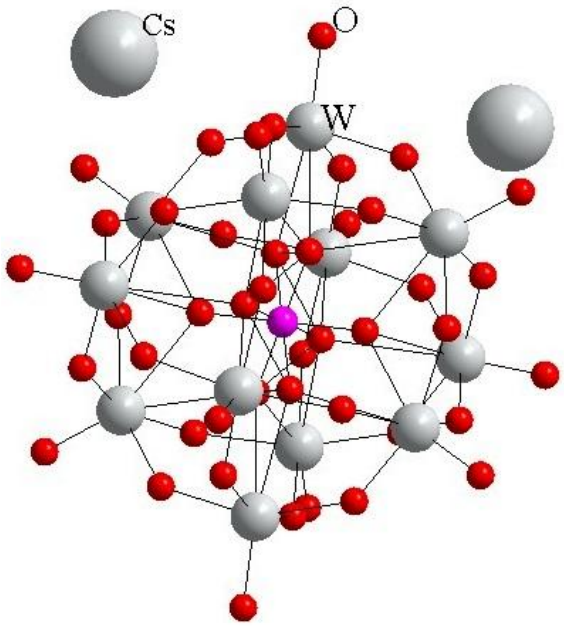

Figure 1. Disordered Keggin type POMs

The packing structure of the polyanion indicates that the Cs atoms occupy the voids (Figure 2) created due to the close packing. At the same time, H_2O molecules are also expected to be present in the voids. During the final refinement cycle, the isotropic thermal parameters for the atomic coordinates of O indicated the presence of 4 different O atoms, apart from the O atoms of the Keggin unit. These O atoms are thought to originate from the adsorbed water molecules. Due to the large difference in the electron densities of H and W, the presence of H could not be confirmed from the structural data. On the other hand, the presence of $5H_2O$ molecules was confirmed by thermal analysis.

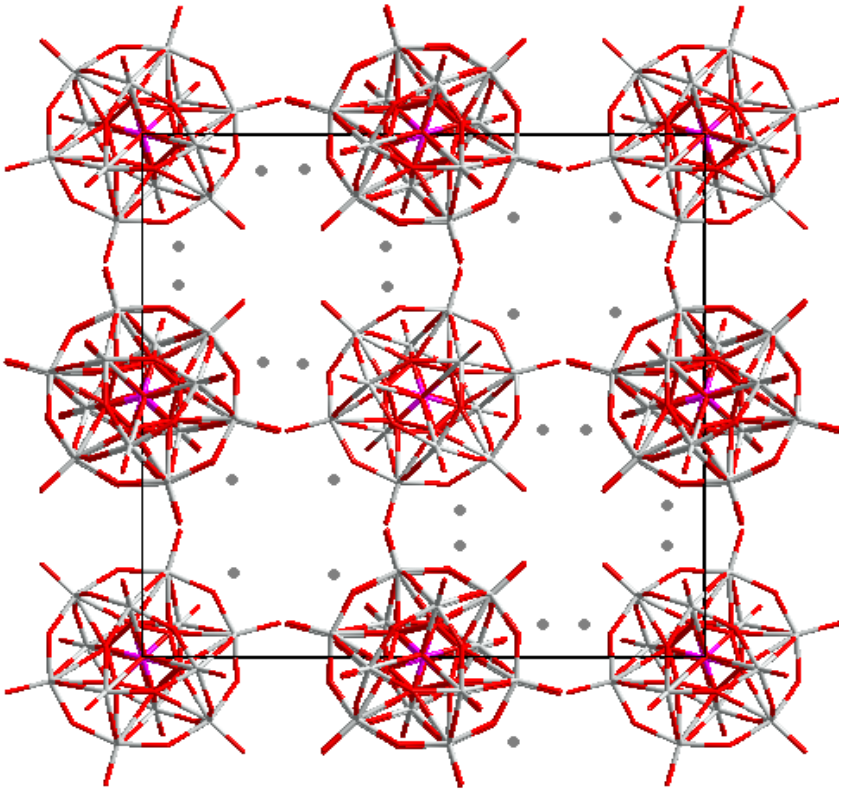

Figure 2. Cs cations fill the voids between the POMs

The typical Keggin structure in which all W–W contacts have equal distances (~3.57 A°) but there are different W–O distances were obtained. The three different types of W–O bond distances correspond to the O-terminal (1.69 A°), O-cis bridging (1.90A°) and O-trans bridging (2.47A°) atoms, respectively.

In the Keggin-type POMs, the central tetrahedral PO_4 is surrounded by twelve WO_6 octahedra in four groups of W_3O_{13} units. If the structure is totally symmetrical, PO_4 has T_d symmetry with all P–O bond lengths equal (1.52 A°). In the present structure, the central four oxygen atoms (bonded to three W atoms and one P atom) are disordered over eight positions, from which three different types of P–O bonds are obtained. Two of these have almost the same bond length of 1.49 and 1.52 A°, respectively, while the third P–O bond has a longer length of 1.60 A° (involving O_{12}), indicating a distortion in PO_4 T_d symmetry. This may be due to the change in the environment around the corresponding W_3O_{13} unit. Hence, the change in

the environment due to the substitution of Mn in the corresponding W_3O_{13} and P–O_{12}–W_3O_{13} moieties is as expected. The three W atoms attached to O_{12} are W_1, W_1 and W_3. The bond length of W_3–O_{12} is 2.50 A°. The corresponding terminal oxygen attached to W_3 is O_6. So, as mentioned earlier in the discussion, the presence of disorder in the crystal structure is at O_6, and hence, the probability of Mn substitution is maximum at W_3.

The Cs cations show a number of contacts with the anions. It seems likely that extensive cooperation between cations throughout the crystal is important to form a continuous network that stabilizes the structure and makes the crystals stable in air (Figure 3).

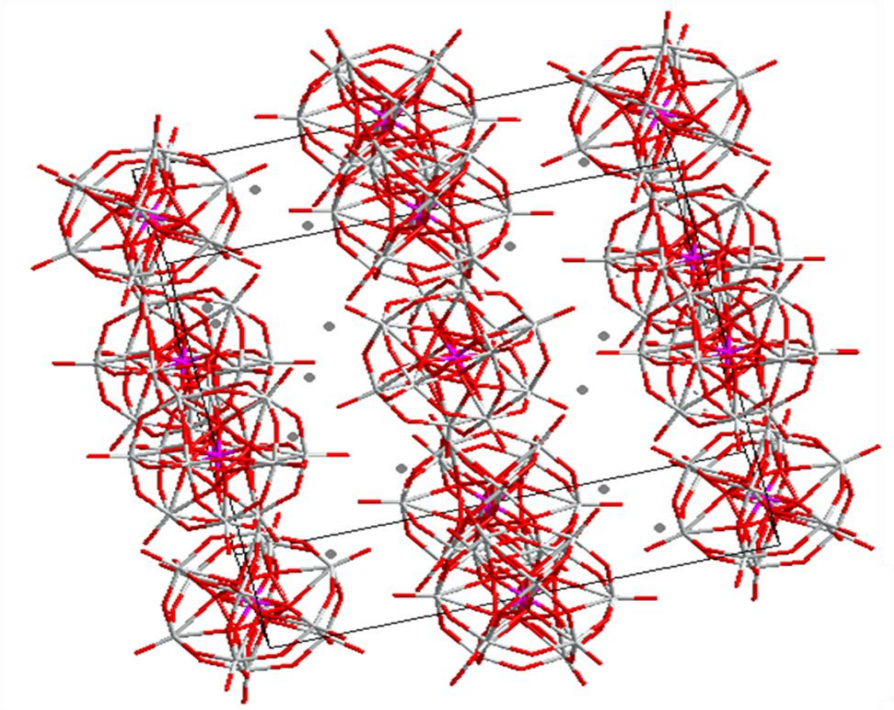

Figure 3. Extensive cooperation between cations and POMs anions

PXRD

The powder XRD pattern of $PW_{11}Mn$ is presented in Figure 4 together with the simulated pattern using the data set obtained by single crystal analysis. The experimental and simulated patterns are similar indicating that the single crystal and bulk structures are identical.

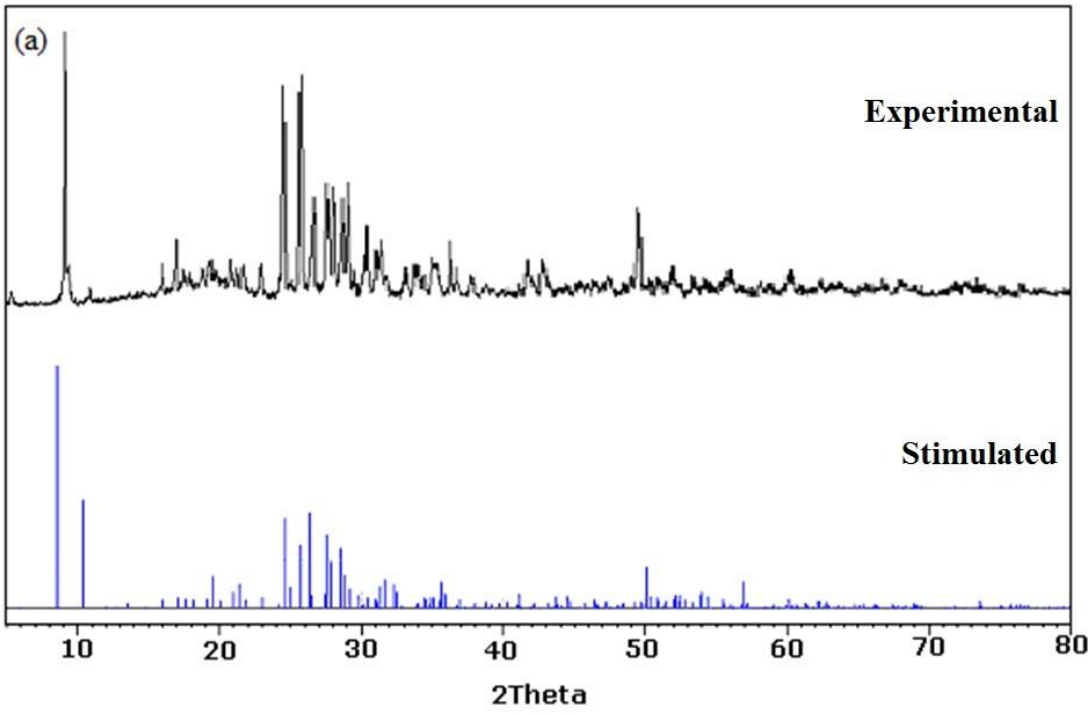

Figure 4. (a) Experimental and (b) Stimulated PXRD pattern of $PW_{11}Mn$

2.3.2 Spectroscopic Analysis

Elemental Analysis

Elemental analysis for tungsten and manganese was carried out in the filtrate by gravimetry and volumetric methods, respectively [14]. The observed proportion of W in the filtrate was 0.68% [2.2 g of W (i.e., 100% was taken for synthesis. Out of that 0.0149gm i.e., 0.68% of W remained unreacted in the filtrate)], which corresponds to loss of one equivalent of tungsten from $H_3PW_{12}O_{40}.nH_2O$. The proportion Mn in the filtrate was 0.091%, corresponding to incorporation of one equivalent of manganese into the lacunary species created by the removal of one W. The observed values for the elemental analysis for the isolated complex were in good agreement with the theoretical values. Found: Cs, 19.8; W, 56.7; P, 0.9; Mn, 1.5; O,

20.1; Calc: Cs, 19.1; W, 57.9; P, 0.9; Mn, 1.6; O, 20.2. The proportion of H_2O was calculated from the TGA curve; the total observed weight loss (2.5%) corresponds to loss of $5H_2O$ molecules.

FT-IR

The presence of manganese in the $PW_{11}Mn$ was confirmed by spectral as well as electrochemical techniques.

The frequencies of FT-IR bands for $[PW_{12}O_{40}]^{3-}$, PW_{12}; $[PW_{11}O_{39}]^{7-}$, PW_{11}; and $[PW_{11}MnO_{39}]^{5-}$, $PW_{11}Mn$ are shown in Table 2. There is a splitting and shifting of the P–O frequency for PW_{11} when compared to that of PW_{12}. Thus, the P–O band at 1080 cm^{-1} for PW_{12} is split into two bands at 1085 and 1043 cm^{-1} for PW_{11}. The observed splitting value $\Delta\upsilon$ of 42 cm^{-1} is near to the reported [6] value, indicating the formation of lacunary PW_{11}. Thouvenot et al. [15, 16] have reported values of $\Delta\upsilon$ for P–O bonds where different transition metals are introduced into the octahedral lacuna of PW_{11}. The frequency data for $PW_{11}Mn$ showed characteristic splitting for the P–O bond frequency (1077 and 1053 cm^{-1}) with $\Delta\upsilon$ 24 cm^{-1}. This clearly indicates that Mn(II) was introduced into the O_h lacuna. The difference in the $\Delta\upsilon$ value is lower for $PW_{11}Mn$ than for PW_{11}. This may be due to pseudosymmetric environment that results from exchange of a W atom to Mn(II).

Table 2. FT-IR Frequency Data

POMs	**FTIR band frequencies (cm^{-1})**			
	P-O	**W=O**	**W-O-W**	**Mn-O-W**
PW_{12}	1080	982	893, 812	-
PW_{11}	1085, 1043	952	863, 808	-
$PW_{11}Mn$	1077, 1053	955	884, 813	438

There is also a shift in the stretching vibration of W=O from 952 to 955cm^{-1} and in the W–O–W vibration from 863 to 884cm^{-1}, indicating the complexation of the Mn. An additional band at 438cm^{-1} is attributed to the Mn–O vibration. Thus, the FTIR spectra clearly show the incorporation of

Mn into the Keggin framework. It is not present as a counter cation since no appreciable shifting would be expected in this case.

UV-Visible

The UV–vis spectrum of $PW_{11}Mn$ recorded in water showed two peaks (Figure 5). An intense peak at 293 nm is assigned to O → W charge transfer, indicating the formation of $PW_{11}O_{39}$ lacuna in the synthesized complex. A broad band in the visible region around 400–405nm corresponds to the presence of Mn(II) in the complex. No bands were observed in the region of 450–500 nm, typical of Mn(IV) and Mn(III) [17]. The presence of Mn(II) was further confirmed by ESR, ^{31}P NMR and cyclic voltammetry.

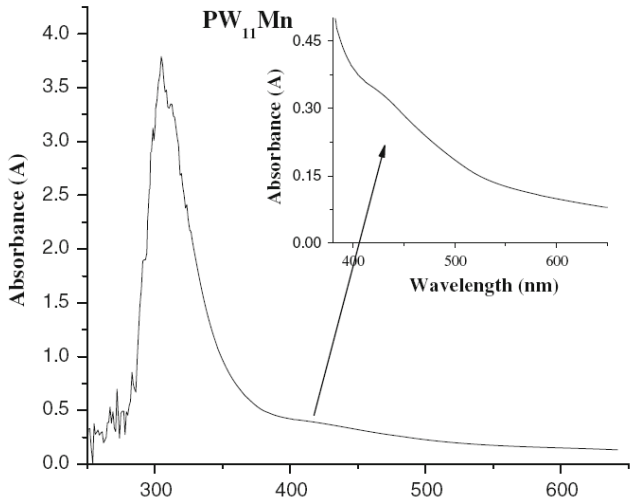

Figure 5. UV-visible spectra of $PW_{11}Mn$

ESR

The full-range (4,000–2,000 G) X-band room temperature ESR spectrum of $PW_{11}Mn$ shows one broad, weak and poorly resolved signal at g ~ 1.9, which can be assigned to Mn(II). It has been reported by Nowinska et al. that Mn(II) introduced into octahedral lacuna of the Keggin structure should give rise to a signal at g ~ 2, which is attributed to octahedral or distorted octahedral environment [6]. The broadness of the signal may be due to the fast relaxation of unpaired electrons [17]. Since the fast relaxation of electrons can be restricted by low-temperature ESR, the ESR spectrum was also

recorded at (298 K) in the range of 3,200 to 2,000 G. The low-temperature ESR shows (Figure 6) a well-resolved six-line spectrum with g ~ 2.3, corresponding to the octahedral environment of Mn(II).

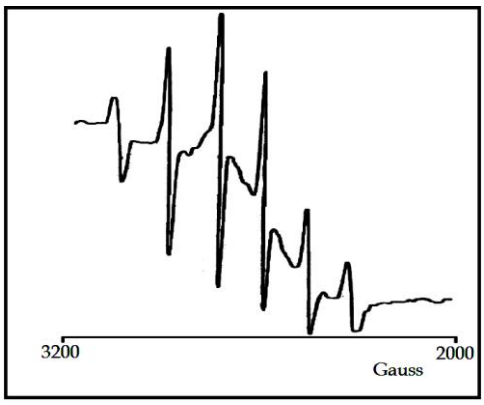

Figure 6. Low Temperature ESR Spectra of $PW_{11}Mn$

^{31}P Solution NMR

The ^{31}P NMR spectrum of $PW_{11}Mn$ was recorded in D_2O. The chemical shift for PW_{11} was -10.5 ppm which is in good agreement with the literature [18]. For $PW_{11}Mn$, an appreciable downfield shift of -13.65 ppm (Figure 7) was observed.

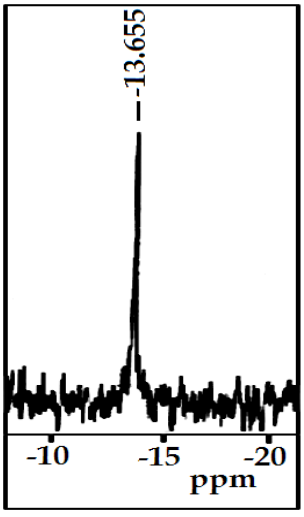

Figure 7. ^{31}P NMR spectra of $PW_{11}Mn$ recorded in D_2O

This may be due to the presence of Mn(II). As mentioned earlier, due to the presence of paramagnetic Mn(II), the P–O–Mn bond is elongated. Also due to the electron-withdrawing effect of Mn(II), the stretching of the P–O–

Mn bond is favoured. This result in deshielding of the P–O bond, giving rise to a downfield NMR signal compared to the PW_{11} species.

Electrochemical studies

The cyclic voltammograms of PW_{11} and $PW_{11}Mn$ were recorded in buffer medium at pH 5 (Figure 8a, b). It has been reported that the lacunary anion (PW_{11}) having a formal charge of 7 features one reversible redox process in aqueous buffered media [19]. The obtained values of Epa and Epc (-0.5 and -0.55 V, respectively,) are in good agreement with the literature, indicating one electron reduction in the lacunary anion.

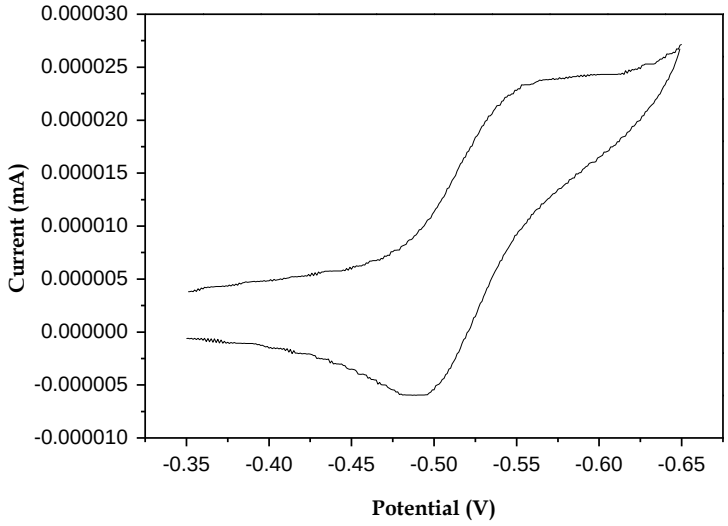

Figure 8a. Cyclic Voltammogram of PW_{11} in acetate buffer (pH 5)

The cyclic voltammogram of $PW_{11}Mn$ showed three redox potentials (Figure 8b). The reversible redox wave in the positive potential corresponds to the Mn(II) species, and the other two reversible redox couples obtained in the negative potential correspond to $PW_{11}O_{39}$ species. The reduction couples obtained at -0.8 and -0.4 V are characteristic of the phosphotungstate anions. It has been reported by Sadakane et al. [20] that the Mn(II/III) redox potential is pH independent in the pH range of 3–7. The cyclic voltammogram of $PW_{11}Mn$ (pH 5.0 in acetate buffer) shows one reversible redox couple at +1.1 V. The effective redox potential determined from the

anodic and cathodic peak potentials corresponds to $E_{1/2}$ = 0.92 V. This one-step 1e- reduction corresponds to the Mn(II/III) couple and is in good agreement with the reported value [3]. The electrochemical data for our complex clearly indicate the presence of the Mn(II/III) couple.

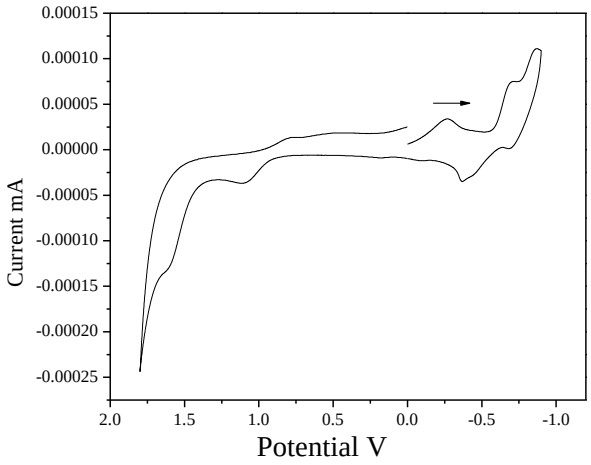

Figure 8b. Cyclic voltammograms of 0.1mM solution of $PW_{11}Mn$ in acetate buffer pH 5.

2.4 Catalytic Reaction

The catalytic activity was evaluated for oxidation of alkenes using hydrogen peroxide in one case and molecular oxygen as oxidant and TBHP as co-oxidant in other. Oxidation reaction was carried out in a batch type reactor operated under atmospheric pressure. In a typical reaction, measured amount of $PW_{11}Mn$ was added to a three necked flask containing alkenes and initiator TBHP (0.15mmol) at 80°C (for styrene) and 50°C (for cyclic alkenes). The reaction was started by bubbling O_2 into the liquid. In case of hydrogen peroxide, the reaction was started by adding a measured quantity of 30% aqueous H_2O_2 to the flask containing $PW_{11}Mn$ and alkenes. The reaction was carried out by varying different parameters such as mole ratio, reaction temperature, amount of the $PW_{11}Mn$ and reaction time.

In the oxidation of alkenes, after completion of reaction the reaction mixture was allowed to cool to room temperature and then 10% aqueous solution Na_2CO_3 was added with constant stirring. The resultant mixture (organic and aqueous) was allowed to stand for 15-20 minute in order to separate the two distinct layers. The aqueous layer was collected and concentrated HCl was added slowly with constant stirring. No white precipitates of benzoic acid were formed. The remained organic layer was extracted with dichloromethane and analyzed on Gas Chromatograph (Nucon 5700 model) having a flame ionization detector and BP-1 capillary column (30m, 0.25mm id), programmed oven (temperature range 353 – 473K) and N_2 as carrier gas. Product identification was done by comparison with authentic samples and finally by a combined Gas Chromatography Mass Spectrometer (Hewlett-Packard column) using HP-1 capillary column (30m, 0.5mm id) with EI and 70eV ion source. The conversion as well as selectivity was calculated on the basis of mole percent of alkenes.

$$\text{Conversion (\%)} = \frac{(\text{initial mol \%}) - (\text{final mol \%})}{(\text{intial mol (\%)})} \times 100$$

$$\text{Selectivity (\%)} = \frac{\text{moles of product formed}}{\text{moles of substrate consumed}} \times 100$$

The turn over number (TON) was calculated using the following equation

$$\text{TON} = \frac{\text{moles of product}}{\text{moles of catalyst}}$$

In order to optimize the conditions, oxidation of styrene was chosen as model reaction. Oxidation of styrene generally results in formation of five oxidation products as shown in scheme 2.

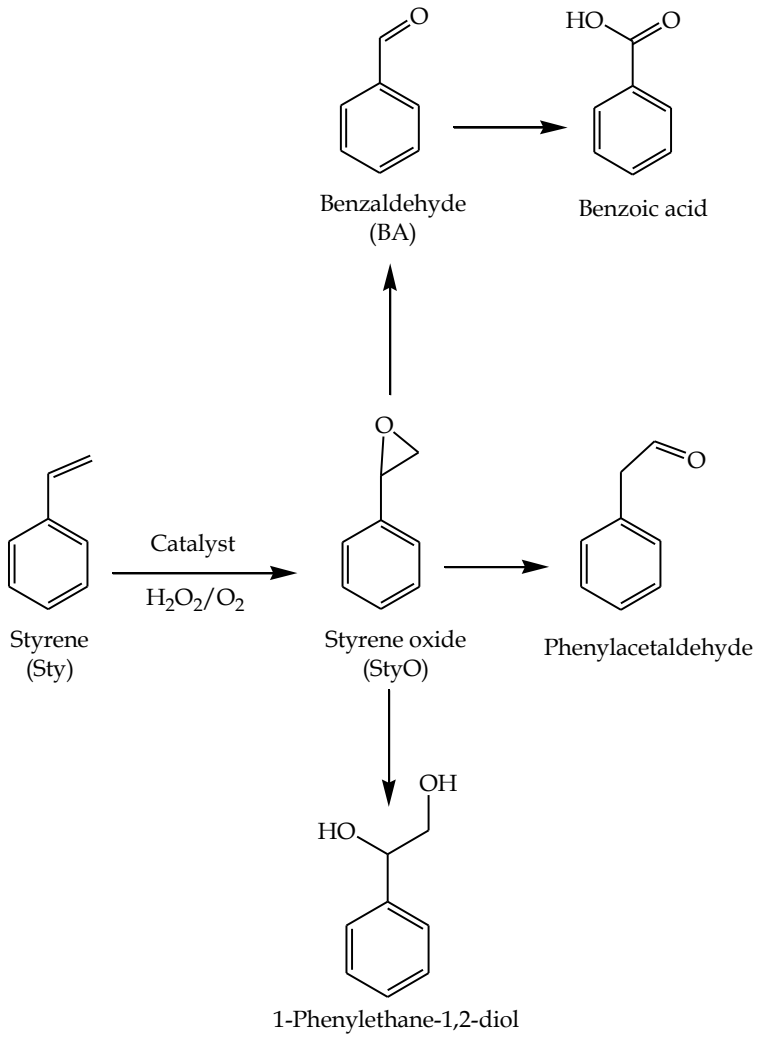

Scheme 2. Products for oxidation of Styrene

2.4.1 Oxidation of styrene using molecular oxygen

A detailed study on the oxidation of styrene with molecular oxygen as an oxidant and TBHP as co-oxidant was carried out. An experiment without catalyst was carried out and no conversion was obtained, indicating that there is no auto-oxidation taking place. In the present case, $PW_{11}Mn$ behaves as a heterogeneous catalyst. Further, the different parameters viz. amount of catalyst, reaction time and temperature were checked to get optimum reaction condition for oxidation of styrene.

Effect of the catalyst amount

The effect of catalyst amount on the conversion of styrene is illustrated in Figure 9. As the amount of catalyst was increased from 5 mg to 25mg, the conversion of styrene increased from 4 to 61%. With further increase in the catalyst amount from 25mg to 200mg, the conversion improves and reached up to 99%.

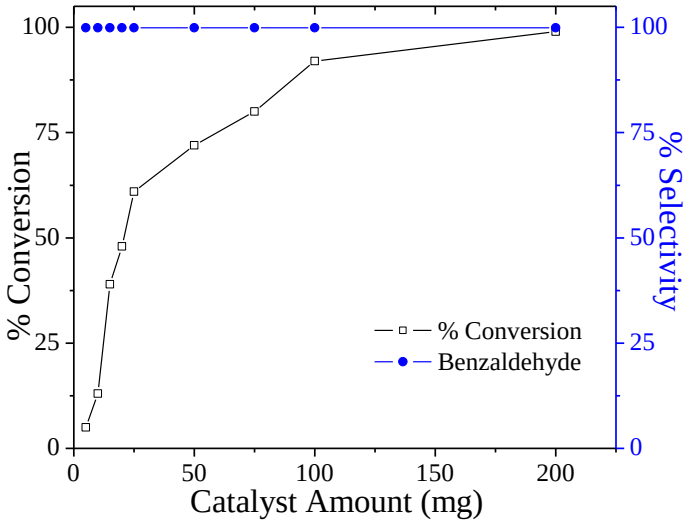

Figure 9. Effect of catalyst amount on oxidation of Styrene

With increase in the amount of the catalyst the number of active sites (i.e. amount of Mn increases) increases which results in increase % conversion. The obtained results clearly indicate that Mn functions as active

sites for oxidation. Vancheesan et al. have reported that the use of TBHP with transition metal-based catalysts activates the metal centre [21]. The activated catalyst then attacks the C=C bond. It follows bond cleavage mechanism rather than forming epoxidation. As a result, the formation of benzaldehyde is favoured. However, 25mg can be considered sufficient enough to carry out the reaction and further, effect of reaction time and temperature was studied.

Effect of reaction time

The effect of reaction time on the conversion was depicted in Figure 10 keeping other parameter constant. The degree of conversion increases with increases in reaction time. However within the reaction of 4h, about 61% styrene was converted. With prolonging the reaction time the conversion slowly increases to 100% in 24h.

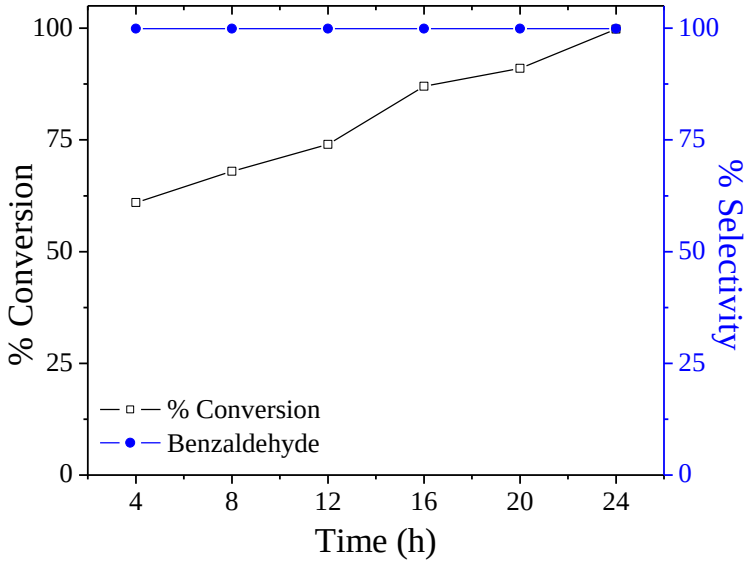

Figure 10. Effect of reaction time on oxidation of styrene

This may be due to the fact that initially styrene is consumed during the reaction, as a result the amount of the reactant decreases, which then requires time to reversibly bind with the oxidant. Further, the rate of desorption of the products formed from the catalyst surface is faster as a

result the overall rate of the reaction slows down resulting into slow increase in the conversion with time. Due to the improved catalytic activity of $PW_{11}Mn$ within the short period of time, 4h would be preeminent time period to carry out the oxidation of styrene.

Effect of temperature

The styrene oxidation was carried out at five different temperatures to find the effect of temperature on the catalytic activity, which is presented in Figure 11. The styrene conversion increases dramatically from 50°C to 80°C. But from 80°C to 90°C conversion was not significant but it drops beyond 90°C. Increasing in the reaction temperature can quicken the reaction rate, but at higher reaction temperature can leads to the polymerization of styrene.

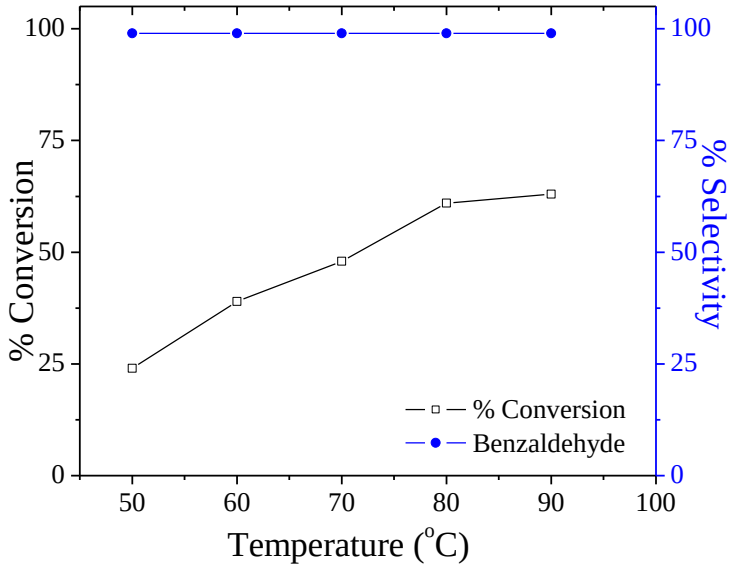

Figure 11. Effect of temperature on oxidation of styrene

Leaching and Heterogeneity Test

In the present case, $PW_{11}Mn$ remains insoluble under the present reaction conditions, so leaching and heterogeneity test was required.

The leaching of Mn from $PW_{11}Mn$ was confirmed by carrying out analysis of the used catalyst (EDAX) as well as the product mixtures (AAS) (Analysis of the used catalyst did not show appreciable loss in the manganese content as compared to the fresh catalyst). In addition, the product mixture was also analyzed by UV-visible spectroscopy. The absence of the absorption band indicates no leaching of Mn from the catalyst during the reaction.

For rigorous proof of heterogeneity, a test was carried out in which the catalyst was filtered from the reaction mixture after 2h at 80 ^oC and the filtrate was allowed to react up to the completion of the reaction time (4h). The reaction mixture after 2h and the final filtrate were analysed by GC (Table 3). No change in conversion or selectivity was found for the filtrate indicating that the present catalyst falls into category C [22].

Table 3. % Conversion and % selectivity for oxidation of styrene (with and without catalyst)

[a]Catalyst	Conversion (%)	Selectivity (%) (BA)
$PW_{11}Mn$ (2h)	28	>99
Filterate (4h)	28	>99

Conversion based on substrate; styrene, 100mmole; oxidant, O_2(4ml/min); TBHP, 0.15mmol; amount of catalyst, 25 mg; temperature, 80^oC

Regeneration and Recyclability

The catalyst remains insoluble in the present reaction conditions and can be separated easily by simple filtration. The separated catalyst was washed with dichloromethane and dried at 100^oC. Oxidation of styrene was then carried out with the recycled catalyst, under the optimized conditions. The results for the fresh as well as the regenerated catalysts are presented in Table 4. There was no appreciable change in selectivity of the products;

however, a small decrease in conversion was observed which shows that the catalysts are stable and can be reused for up to two catalytic cycles.

Table 4. Oxidation of styrene with fresh and recycled catalysts

[a]Catalyst	Conversion (%)	Selectivity (%) (BA)
$PW_{11}Mn$	61	>99
R1- $PW_{11}Mn$	59	>99
R2- $PW_{11}Mn$	56	>99

Conversion based on substrate; styrene, 100mmole; oxidant, O_2(4ml/min) ; TBHP, 0.15mmol; amount of catalyst, 25 mg; temperature, 80^{o}C; Time, 4h

2.4.2 Oxidation of styrene using H_2O_2

A detail study was carried out on oxidation of styrene by varying different parameters such as mole ratio of styrene to H_2O_2, reaction temperature, catalyst amount and reaction time to get optimum reaction condition for oxidation of styrene. An experiment without catalyst was carried out and no conversion was obtained, indicating that there is no auto-oxidation taking place. In the present case, $PW_{11}Mn$ behaves as a homogeneous catalyst.

Effect of mole ratio

Oxidation of Styrene was carried out by varying the mole ratio of Sty to H_2O_2 from 1:1 to 1:3. As illustrated in Figure 12. The oxidation of styrene improved from 59 to 100% upon increasing the styrene to H_2O_2 mole ratio from 1:1 to 1:3. Further increases in the amount of H_2O_2 from 1:3 to 1:4 did not result in the styrene conversion as well as selectivity of benzaldehyde. Thus, suggesting that a large amount of oxidant is not an essential condition to improve the oxidation of styrene. Therefore, 1:3 styrene to H_2O_2 mole ratio was considered the optimized condition for the oxidation of styrene.

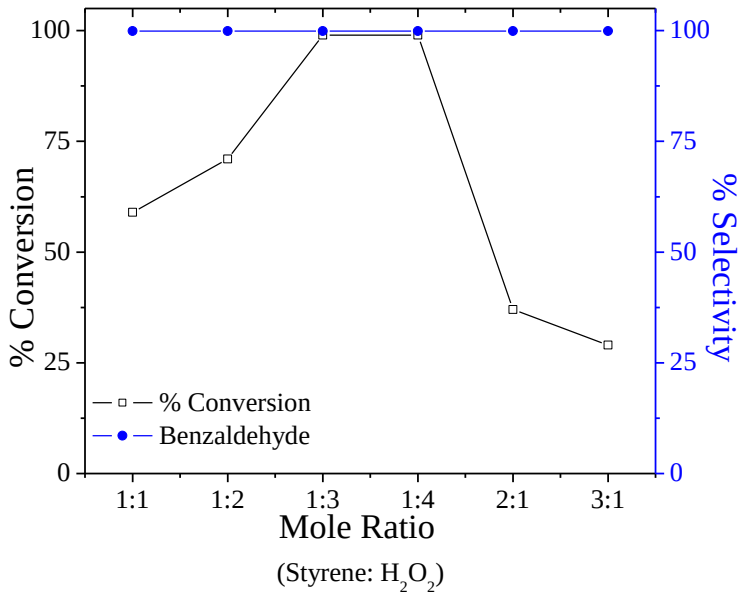

Figure 12. Effect of mole ratio on oxidation of styrene

Effect of amount of catalyst

The effect of catalyst amount on the conversion of styrene is illustrated in Figure 13. As the amount of catalyst was increased from 5 mg to 25mg, the conversion of styrene increased from 30 to 100%. With further increase in the catalyst amount from 25mg to 30mg, the conversion and selectivity does not change. As the amount of catalyst increases the number of active sites (i.e. amount of Mn increases) increases which results in increase % conversion. The obtained results clearly indicate that Mn functions as active sites for oxidation. However, 25mg can be considered sufficient enough to carry out the reaction and further, effect of reaction time and temperature was studied.

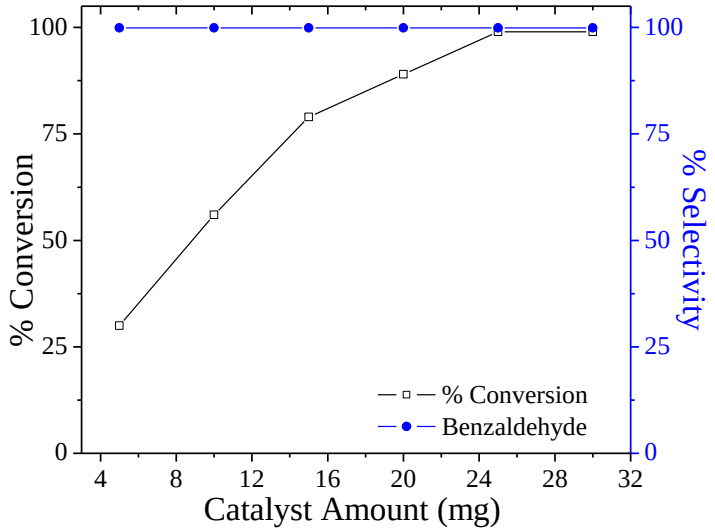

Figure 13. Effect of amount of catalyst on oxidation of styrene

Effect of reaction time

The effect of reaction time on the conversion was depicted in Figure 14 keeping other parameter constant. The degree of conversion increases with increases in reaction time. However within the time of 14h, 100% styrene was converted. However, the selectivity to benzaldehyde remained unchanged basically throughout the entire reaction procedure. Due to the improved catalytic activity of $PW_{11}Mn$ within the short period of time, 14h would be preeminent time period to carry out the oxidation of styrene.

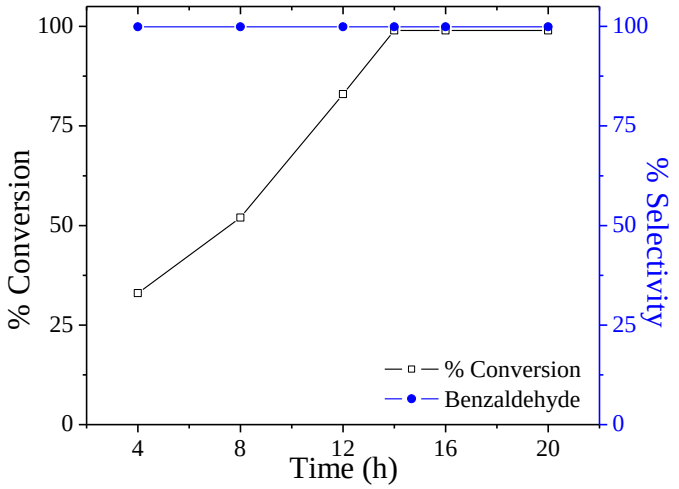

Figure 14. Effect of reaction time on oxidation of styrene

Effect of temperature

The styrene oxidation was carried out at different temperatures to find the effect of temperature on the catalytic activity, which is presented in Figure 15. The styrene conversion increases dramatically from 50°C to 80°C. But from 80°C to 90°C conversion and selectivity does not change.

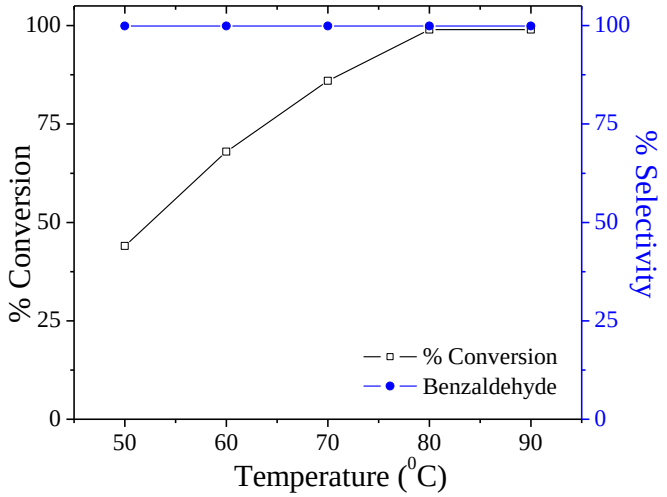

Figure 15. Effect of temperature on oxidation of styrene

These results indicate that higher temperature was required to achieve better conversion. Due to the higher catalytic activity of $PW_{11}Mn$ at

80°C, it was chosen as the best temperature to carry out the oxidation of styrene.

It has been reported that in case of TMSPOMs, oxidation proceeds through formation of metal peroxo species [23]. This formed metal-peroxo species attacks alkenes resulting into products. In the present case the Mn peroxo species are highly reactive and have good tendency to accommodate the active oxygen from the peroxide to form the metal peroxo species into the cavity of POMs. As a result the substrate is easily oxidized giving rise to oxygenated products. In the present case, single selective product is obtained this is due to the high reactivity of the catalyst which results in formation of the more stable product (i.e. BA) rather than the less stable intermediate (i.e. StyO). The highest selectivity of BA might be due to further oxidation of styrene oxide by the nucleophilic attack of H_2O_2 on styrene oxide.

Leaching and Heterogeneity Test

In the present case, $PW_{11}Mn$ behaves as homogeneous catalyst as a result leaching and heterogeneity test was not required.

Regeneration and Recycling

In the present case, $PW_{11}Mn$ behaves as homogeneous catalyst. Even though the catalyst was soluble in the aqueous phase, it could regenerated and reused after a simple workup. The products were separated by extraction with dichloromethane and the aqueous phase (containing catalyst) was dried at 100°C to collect the solid catalyst. The catalytic activity of the regenerated catalyst was evaluated under the optimized conditions. The results for the same are represented in Table 5. As seen from table, slight decrease in conversion may be due to the little loss of the catalyst during the workup. The obtained results show that the catalyst is stable and can be regenerated and reused.

Table 5. Oxidation of styrene using hydrogen peroxide with fresh and regenerated catalyst

Catalyst	Conversion (%)	Selectivity for BA (%)	TON
$PW_{11}Mn$	100	>99	1393
R1- $PW_{11}Mn$	99	>99	1380
R2- $PW_{11}Mn$	99	>99	1380

Conversion based on substrate; substrate, 10mmole; oxidant H_2O_2 (30 mmole), amount of catalyst, 25 mg; reaction time 14h; reaction temperature 80^0C

2.4.3 Kinetics Study

A study on the kinetic behaviour was carried out for $PW_{11}Mn$. In all the experiments, reaction mixtures were analyzed at fixed interval of time using gas chromatography.

Determination of Order as Well as Rate of Reaction

The plot of log C_0/C versus time (Figure 16) shows a linear relationship of styrene consumption with respect to time. With an increase in reaction time, there is a gradual decrease in the styrene concentration.

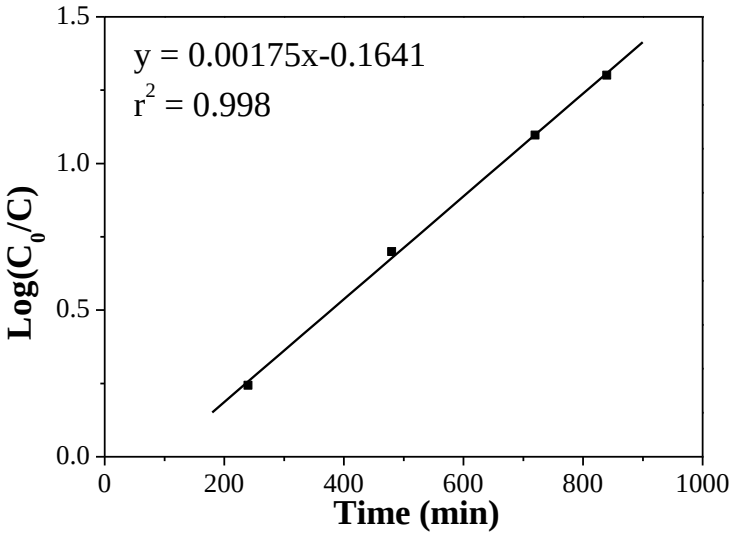

Figure 16. Styrene consumption as a function of reaction time

The linearity in the plot of Log(C_0/C) verses time indicate that the oxidation of styrene is expected to follow first-order. This was further supported by the study of the effect of catalyst concentration on the rate of the oxidation of styrene. The catalyst amount was varied from 5 to 25 mg at a fixed substrate concentration of 10mmol and at a temperature of 80°C. The plot of reaction rate versus catalyst amount (Figure 17) also shows a linear relationship for $PW_{11}Mn$. As the concentration of the active species, increased from 5 to 25 mg, the rate of reaction also increased.

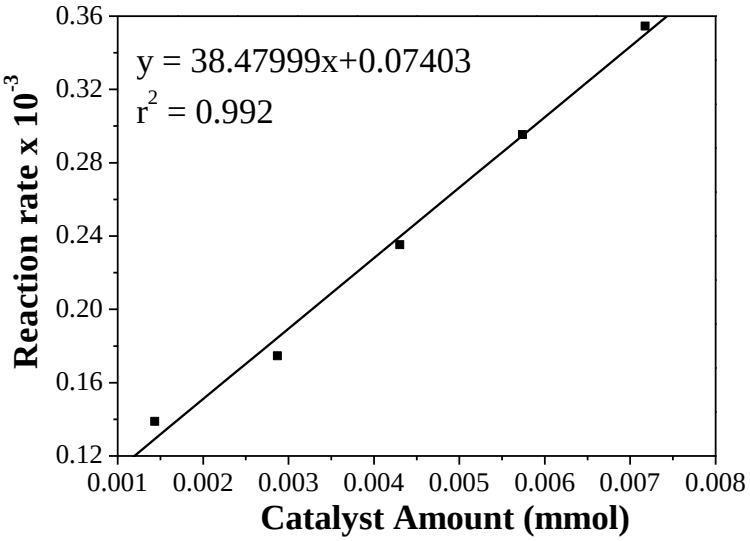

Figure 17. Effect of catalyst concentration on rate of reaction

The above study confirms that the initial rate of oxidation of styrene follow first-order kinetics with respect to the substrate as well as the catalyst. Based on the above results, the rate law was also deduced for $PW_{11}Mn$ catalysts and was found to obey Eq. 1.

$$\frac{-d[BA]}{dt} = k[Sty][Cat] \qquad (1)$$

As most of the oxidation reactions are temperature sensitive, the effect of temperature on the oxidation of styrene was also studied by varying the temperature between 313 and 363 K, keeping the styrene: H_2O_2 ratio of 1:3 and catalyst amount of 25 mg. As the temperature increases from 313 to 363 K, the conversion of styrene also increases drastically. This may be due to the activation of the catalytic species with temperature.

The graph of lnk versus 1/T was plotted (Figure 18) and the value of activation energy (Ea) was determined from the plot.

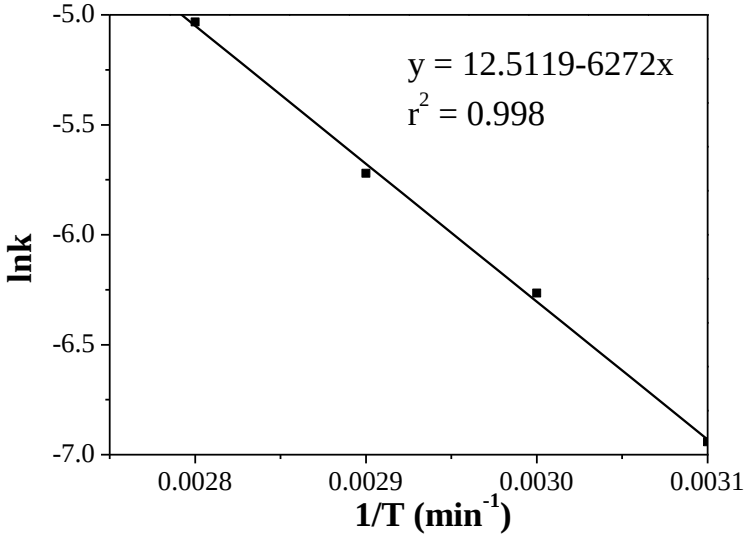

Figure 18. Arrhenius plot for $PW_{11}Mn$

From the value of activation energy (Ea), the pre-exponential factor (A) was determined using Arrhenius equation and the values are presented in Table 6.

Table 6. Kinetic parameters for oxidation of styrene

Activation energy (Ea)(kJ/mol)	**Pre-exponential factor (A) (min^{-1})**
52.2	2.7×10^5

Effect of oxidants on oxidation of alkenes

Under the optimized conditions, oxidation of cyclic alkenes viz. Cyhexene (Cy6) and Cyclooctene (Cy8) was carried out using both the oxidants. The results for the same are presented in Table 7.

Table 7. Effect of oxidants on oxidation of alkenes

Oxidant	[a]Alkene	Products	Conversion (%)	Selectivity (%)	TON
[b]O_2	Styrene	BA	61	> 99	8507
	Cy6	-	NC	-	-
	Cy8	-	NC	-	-
[b]H_2O_2	Styrene	BA	33	> 99	460
	Cy6	-	NC	-	-
	Cy8	-	NC	-	-

[a]Alkene, 100mmol, Alkene : H_2O_2, 1:3, O_2, 1 atm; TBHP, 0.15mmol; reaction time, [b]4h (styrene) 24h (Cyclic Olefins), catalyst amount, 25mg, temp, 80^oC; NC = No significant conversion

In case of styrene oxidation 61% conversion was obtained with O_2 and 33% conversion was obtained with H_2O_2. In both the cases BA was obtained as single selective product. The difference in conversion can be explained on the basis of the reactivity of oxidants.

It is known that O_2 has the highest content of active oxygen (i.e. singlet oxygen) [24]. The activation of metal centre by O_2 occurs in a single step via formation of M-O_2 species. Where as in case of oxidation involving H_2O_2 the activation of the metal centre occurs in two steps (i) via formation of hydroperoxo or peroxo species and (ii) these formed hydroperoxo or peroxo species rearranges to form oxo intermediate which attacks the substrate resulting in oxidation of substrate. In case of H_2O_2, the activation of the catalyst takes place in two steps, as a result it requires more time as compared to O_2. Hence, more conversion is expected in the case of molecular oxygen and the obtained results are in good agreement with the explanation.

No significant conversion was obtained for cyclic alkenes under the optimized conditions. This may be due to the reason that eventhough Mn^{II}

species are good oxidation catalysts they require activation to initiate the reaction. As the reaction was carried out under optimized conditions, the concentration of TBHP (an intiator) used (with O_2) was not sufficient to activate the Mn^{II} species. In case of H_2O_2, it is well reported that the utilization of H_2O_2 with tungsten based compounds is low especially for cyclic alkenes [25]. Hence, the results are as expected.

Reaction Mechanism

In order to study the reaction mechanism the same sets of reactions were carried under at two different conditions; (i) styrene + oxidant + TBHP and (ii) styrene + oxidant + $PW_{11}Mn$. In both the cases the reaction did not progress significantly. These observations indicate that the liberation of O_2 from TBHP was not sufficient to proceed the reaction as well as activation of Mn^{2+} to Mn^{3+} being necessary for provoking the reaction under the optimized conditions. Hence it may be concluded that in present study TBHP acts as an initiator only.

Based on the above observations the reaction mechanism for styrene involving TBHP as an initiator (Scheme 3) has been proposed. It has been reported that for TMSPOMs catalysts containing metal cations in low valency states and involving O_2 as an oxidant follow the radical chain mechanism induced by M-O_2 intermediate [26, 27]. In the present catalytic system, the mechanism involving the Mn species is expected to follow the same path.

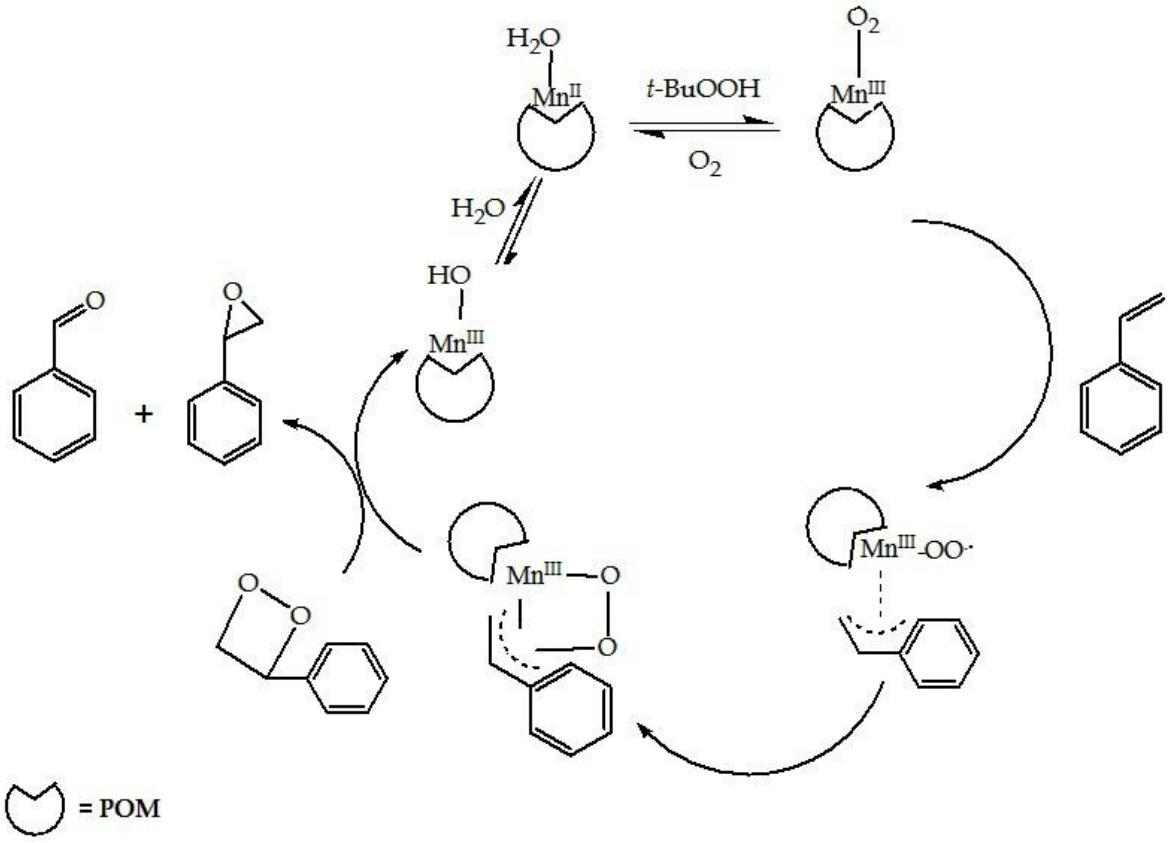

Scheme 3. Proposed reaction mechanism for oxidation of styrene using O_2

The role of TBHP is as an initiator. The activation of Mn^{2+} species takes place through a formation of $\cdot OMn^{3+}PW_{11}$. This activated species ($\cdot OMn^{3+}PW_{11}$) gets attached with O_2 species and forms $\cdot OOMn^{3+}PW_{11}$ radical which then attack the substrate. The metal-superoxo intermediate reversibly binds styrene attacking the reaction site which results in oxidation of substrate to form products. A tentative reaction mechanism for styrene, as an example, is proposed in Scheme 3. As described in the proposed reaction mechanism, the activation of the catalyst takes place through attack of TBHP following the formation of an active intermediate, $\cdot OMn^{3+}PW_{11}$. It is expected that TBHP gets reduced to form tert-butyl alcohol and in turn oxidizes Mn^{2+} to Mn^{3+} in situ. The liberated oxygen from TBHP attacks Mn^{3+} to form $\cdot OMn^{3+}PW_{11}$. This formed intermediate may be responsible for the activation of alkenes.

A similar mechanism is expected with H_2O_2, but the only difference is in the formation of the active species. The reaction of the metal centre with H_2O_2 results in the generation of the active species which may be hydroperoxo or peroxo species. In oxidation of styrene, the unstable intermediate (StyO) rearranges to form the more stable product (BA). The highest selectivity of benzaldehyde results due to further oxidation of styrene oxide by the nucleophilic attack of H_2O_2 on styrene oxide.

CONCLUSIONS

1. One-pot *in situ* synthetic approach for caesium salt of mono Mn(II) substituted phosphotungstate starting from a commercially available $H_3PW_{12}O_{40}$ and $MnCl_2.4H_2O$ was introduced.
2. The X-ray analysis shows double disorder in the crystal: (i) Mn and W atoms were distributed over the 12 positions and the Mn atom could not be distinguished from the 11W atoms distributed equally over the 12 addenda atoms in the Keggin structure (ii) Keggin polyanion is distributed over the two orientations related by a centre of symmetry.
3. The presence of Mn^{II} was confirmed by FT-IR, UV-visible, ESR as well as ^{31}P NMR spectroscopy. Electrochemical studies confirmed the presence of Mn(II/III) couple.
4. In case of styrene oxidation 61% conversion in 4h with O_2 and 100% conversion in 14 h with H_2O_2 were obtained with benzaldehyde as a single selective product under liquid phase solvent free condition.
5. $PW_{11}Mn$ acts as a homogeneous catalyst with H_2O_2 while as a heterogeneous catalyst with O_2.
6. In case of H_2O_2 a method for regeneration of $PW_{11}Mn$ from homogeneous medium was successfully developed.
7. $PW_{11}Mn$ can be successfully regenerated and reused upto 2 cycles without any significant loss in the catalytic activity.
8. $PW_{11}Mn$ is an efficient as well as selective catalyst for solvent free liquid phase oxidation of styrene under mild reaction conditions using environmentally benign oxidants.
9. The oxidation of styrene follows first order in presence of H_2O_2 as an oxidant.
10. The calculated activation energy (from Arrhenius Plot) for oxidation of styrene was found to be 52.2kJ/mol.

References

1. C. M. Torne, G. F. Tourne, S. A. Malik, T. G. R. Weakly, *J. Inorg. Nucl. Chem.,* 32, 3875 (1970).
2. D. E. Katsoulis, M.T. Pope, *J. Chem., Chem. Commmun.*, 1186 (1986).
3. X. Zhang, M. T. Pope, M. R. Chance, G.B. Jameson, *Polyhedron* 14, 1381 (1995).
4. J. R. Galan-Mascaros, C. Gimenez-Saiz, S. Triki, C. J. Gomez-Garcia, E. Coronado, L. Ouahab, *Angew. Chem. Int. Ed.*, 34, 1460 (1995).
5. J. R. Galan-Mascaros, C. Gimenez-Saiz, S. Triki, C. J. Gomez-Garcia, E. Coronado, *J. Am. Chem. Soc.*, 120, 4671 (1998).
6. K. Nowinska, A. Waclaw, W. Masierak, A. Gutsze, *Catal. Lett.*, 92, 157 (2004).
7. S. S. Balula, I. Santos, A. F. Gamelas Jose, A. M. V. Cavaleiro, N. Binsted, W. Schlindwein, *Eur. J. Inorg. Chem.,* 1027 (2007).
8. C. L. Hill and R. B. Brown, *J. Am. Chem. Soc.*, 108, 536, (1986)
9. C. L.Hill, C. M. Prosser-McCartha, *Coord. Chem. Rev.*, 143, 407 (1995).
10. Bruker, SADABS, SMART, SAINT and SHELXTL, Bruker AXS Inc., Madison, (2000).
11. G. M. Sheldrick, SHELX-97, *Program for crystal structure solution and analysis,* University of Gottingen, Gottingen, (1997).
12. T. G. R. Weakly, *J. Cryst. Spectroscop. Res.* 17, 383 (1987).
13. M. Sadakane, D. Tsukuma, M. H. Dickman, B. Bassil, U. Kortz, M. Higashijima, W. Ueda, *Dalton Trans.,* 4271 (2006).
14. A. Vogel, *A textbook of quantitative inorganic analysis*, 5th edn. Longmans, Green and Co, London, 491 (1989).
15. C. Rocchiccioli-Deltcheff, R. Thouvenot, *J. Chem. Res. Synop.,* 2, 46 (1977).
16. C. Rocchiccioli-Deltcheff, R. Thouvenot, *J. Chem. Res., (*M), 0555 (1977).
17. I. Bar-Nahum, H. Cohen, R. Neumann, *Inorg. Chem.,* 42, 3677 (2003).
18. C. Brevard, R. Schimpf, G. Tourne, C. M. Tourne, *J. Am. Chem. Soc.,* 105, 7059 (1983).

19. S. Xuan Guo, A. W. A. Mariotti, C. Schlipf, A. M. Bond, A. G. Wedd, *Inorg. Chem.*, 45, 8563 (2006).
20. M. Sadakane, E. Steckhan, *J. Mol. Catal. A Chem.*, 114, 221 (1996).
21. S. Kanmani, S. Vancheesan, *J. Mol. Catal. A Chem.,* 150, 95 (1999).
22. A. Sheldon, M. Walau, I. W. C. E. Arends, U. Schuchurdt, *Acc. Chem. Res.,* 31, 485 (1998).
23. N. Mizuno, K. Yamaguchi, K. Kamata, *Coord. Chem. Rev.,* 249, 1944, (2005).
24. L. Smith, M. Kulig, *J. Am. Chem. Soc.*, 98, 4, (1976).
25. N. Mizuno, *Science*, 130, 964, (2003).
26. L. Xinrong, X. Jinyu, L. Huizhang, Y. Bin, J. Songlin, X. Gaoyang, *J. Mol. Catal.,* 161, 163, (2000).
27. X. Zhang, Q. Chen, D.C. Duncan, R. J. Lachicotte, C. L. Hill, *Inorg. Chem.,* 36, 4381, (1997).

CHAPTER

3

Di-Manganese(II) Substituted Phosphotungstate: Synthesis, Structural, Spectroscopic Characterization and Solvent free Liquid Phase Oxidation of Alkenes

Mn(II) substituted compound based on dilacunary POMs

In the family of POMs, the class of di-lacunary POMs $[\gamma\text{-}XW_{10}O_{36}]^{n-}$ (X = P, Si, Ge) [1-3] is significantly interested as it exhibit an exciting and versatile solution chemistry. When two triads of the plenary Keggin polyanion $[XW_{12}O_{40}]^{n-}$ ($X= P^{V}$, Si^{IV}) are rotated by 60^{0}, two WO_6 octahedra (one from each triad) end up being edge-shared. Loss of these two octahedral results in the dilacunary polyanion $[\gamma\text{-}XW_{10}O_{36}]^{n-}$, with C_s point group symmetry.

The reaction of the di-lacunary phosphotungstate $[PW_{10}O_{36}]^{n-}$ with transition-metal cations M in aqueous solution leads to the formation of di transition-metal-substituted phosphotungstate. These di-metal substituted structures contain the two or more than two d-metals in adjacent positions as either “in-pocket” or “out-of-pocket” isomers (Figure 1).

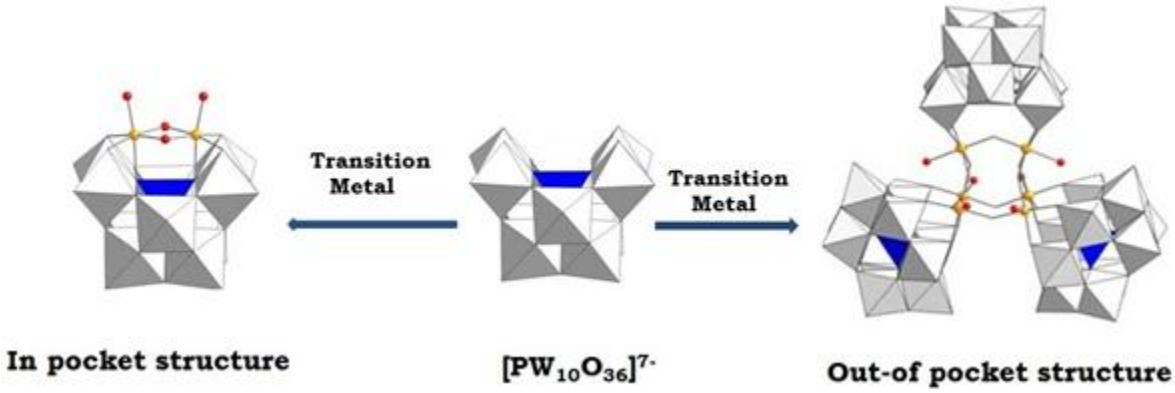

Figure 1. In pocket and out-of pocket structure

The in-pocket isomers contain bonds between the central hetero atom oxygens and the incorporated d- electron metal centre [4]. In contrast, the out-of-pocket isomers do not contain this bond, and consequently the d-electron metals are displaced from the centre of the polyoxoanion and frequently multiply bonded to other adjacent polyoxoanions or distinct structural units [4]. Usually, the in-pocket structure forms a monomer in solution, while out-of-pocket structure yields dimer, trimer and tetramer which is consistent with the considerable structural differences between these two coordination patterns.

To the date number of the articles are available in the literature presenting the in-pocket di-metal substituted structures having general formula $[\gamma\text{-}M_2(H_2O)_2XW_{10}O_{36}]^{n-}$ (X=P, Si; M= V, Fe, Cu, Ti) [4-7]. Despite of their appealing potential, the synthesis is not straight forward and presents a number of problems in which di-lacunary precursors are readily isomerize to other isomer.

Literature survey shows that although Mn(II) is a commonly used transition metal, till the date no work has been carried out for synthesis, characterization and catalytic aspect of di-manganese substituted phosphotungstate. So, it was thought of interest to synthesize in pocket di-manganese substituted phosphotungstate with their systematic characterization and evaluate catalytic activity for solvent free liquid phase oxidation of alkenes.

Considering the above aspects, in the present work, one-pot *in situ* synthesis of the cesium salt of air stable di-manganese substituted phosphotungstate ($PW_{10}Mn_2$) was synthesized, starting from a commercially available $H_3PW_{12}O_{40}$ and $MnCl_2.4H_2O$. The synthesized complex was systematically characterized in solid as well as in solution by elemental analysis, TGA, FT-IR, UV-Visible, ESR, ^{31}P NMR and Cyclic voltammetry. The catalytic activity was evaluated for solvent free liquid phase oxidation of alkenes under mild reaction conditions using environmentally benign oxidants, viz. H_2O_2 and O_2. Oxidation of alkenes was carried out by varying different parameters such as mole ratio of alkene: H_2O_2, catalyst amount, reaction time and reaction temperature. A method for regeneration was proposed and the catalyst was reused upto 2 cycles. The kinetics of the reaction was also studied. The rate of reaction and order of reaction was determined. The effect of temperature on rate constant was studied, and the activation energy was calculated by fitting the results in to Arrhenius equation.

3.1 Experiment

Materials

All chemicals used were of A. R. grade. $H_3PW_{12}O_{40}.29H_2O$ (Loba Chemie, Mumbai), $MnCl_2.4H_2O$, CsCl, NaOH, acetone, dichloromethane, 30% aqueous H_2O_2 and Styrene were obtained from Merck and used as received. Cyclohexene and Cis-cyclooctene were obtained from Spectrochem.

Synthesis of di-manganese substituted phosphotungstate

2.88gm of $H_3PW_{12}O_{40}.nH_2O$ was dissolved in 10ml of water and pH of the solution was strictly adjusted to 6.4 using 3M NaOH solution. The solution was heated to 90°C with stirring. To this hot solution, 0.4 g of $MnCl_2.4H_2O$ dissolved in 10 ml water was added. The solution was heated at 90°C with stirring for 1h and filtered hot, and 2gm solid CsCl was immediately added. The resulting orange yellow precipitates were filtered and dried at 50°C. The synthetic approach was presented in Scheme 1.

Scheme 1. Synthesis of $PW_{10}Mn_2$

3.2 Characterization

Elemental analysis was carried out using a JSM 5610 LV instrument combined with an INCA EDX-SEM analyzer for the quantitative identification of metals. TGA was carried out with a Mettler Toledo Star SW 7.01 up to 600^{o}C. FTIR spectra were recorded as KBr pellets on a Perkin-Elmer instrument. UV–Vis spectra were recorded at ambient temperature on Perkin–Elmer 35 LAMDA instrument using 1 cm quartz cells. ESR spectra were recorded on a Varian E-line Century series X-band ESR spectrometer (liquid nitrogen temperature scanned from 2,000 to 3,200 Gauss). ^{31}P solution NMR spectra were recorded in D_2O on a Bruker ACF 300-MHz instrument. Cyclic voltammetry was performed on a CH-660 instrument, USA at room temperature. A glassy carbon working electrode and an Ag/AgCl reference electrode were used. The analysis of the product mixtures for any leaching of Mn was carried by using atomic absorption spectrometer AAS GBC-902 instrument.

3.3 Results and Discussion

Unfortunately we could not get good quality crystals for di Mn-substituted phosphotungstate suitable for X-ray analysis because of tiny size; however, we have provided enough evidence for the presence of two Mn(II) into the dilacunary phosphotungstate.

Elemental analysis

The observed values for the elemental analysis in the isolated complex are in good agreement with the theoretical values. Anal Calc: Cs, 25.12; W, 49.52; P, 0.84; Mn, 2.96; O, 21.12; Found: Cs, 24.93; W, 50.20; P, 0.85; Mn, 2.92; O, 21.78. The number of water molecules was calculated from TGA curve, based on total weight loss, corresponds to loss of 9 water molecules. From the elemental as well as the thermal analysis the chemical formula of the complex is proposed as, $Cs_7[PW_{10}(Mn(H_2O))_2O_{38}].7H_2O$.

FT-IR

The frequencies of FT-IR bands for $[PW_{12}O_{40}]^{3-}$, PW_{12}; $[PW_{10}O_{36}]^{7-}$, PW_{10} and $[PW_{10}Mn_2(H_2O)_2O_{38}]^{7-}$, $PW_{10}Mn_2$ are presented Table 1 and the spectra for PW_{12} as well as $PW_{10}Mn_2$ are presented in Figure 2.

Table 1. FT-IR Spectra

FT-IR Frequency (cm^{-1})	**$PW_{12}O_{40}$**	**$PW_{10}O_{36}$**	**$PW_{10}Mn_2$**
P-O	1080	1086	1090
		1053	1068
		1023	1050
W=O	982	965	991
		954	952
W-O-W	893	892	894
	812	830	801
Mn-O-W	-		443

As shown in the Table 1 vibrational spectra of the $PW_{10}Mn_2$ is not similar to the PW_{12} and PW_{10}.

The central PO_4 group is a good probe to determine the symmetry of a phosphotungstate as characteristic vibration of P-O group is clearly separated [8]. There is a splitting and shifting for $PW_{10}Mn_2$ as compared to that of PW_{12} (Figure 2, Table 1). The P-O band 1080cm^{-1} for PW_{12} is splits into the three bands, characteristics bands of PW_{10} [1, 9], indicating the in-situ formation of dilacunary phosphotungstate in the synthesized material i.e. $PW_{10}Mn_2$. These three well-resolved bands of low symmetry central PO_4 confirm the retainment of its original C_{2v} symmetry of PW_{10} [5, 10, 11]. The frequency data for P-O band of $PW_{10}Mn_2$ shows the shifting as compared to PW_{10} due to the incorporation of Mn(II) into the distorted *Oh* lacuna.

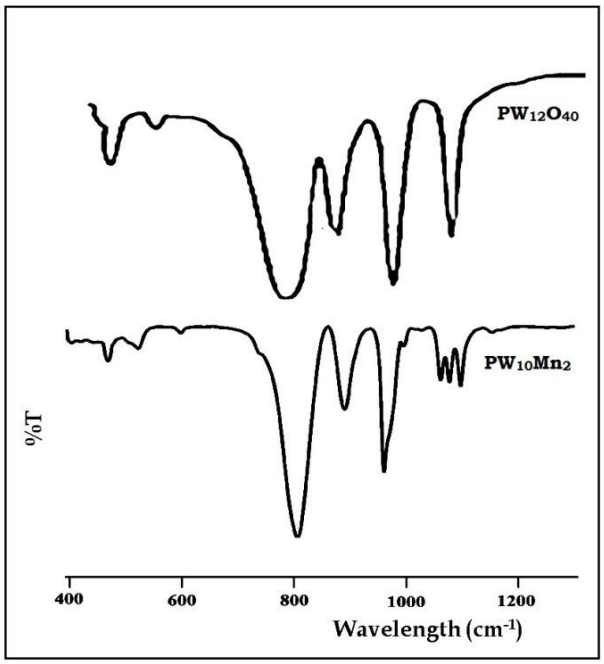

Figure 2. FT-IR spectra of (i) $PW_{12}O_{40}$ (ii) $PW_{10}Mn_2$

There is also a shift in the stretching vibration of W=O and W-O-W vibration indicating the complaxation of the Mn(II). An additional band at 443 cm^{-1} in $PW_{10}Mn_2$ is attributed to the Mn–O vibration. Thus, the FTIR spectra clearly indicate the incorporation of manganese into the Keggin framework and provide clear evidence for the presence of single isomer of $PW_{10}Mn_2$, which is further confirm by ^{31}P solution NMR.

UV-Vis Spectra

The UV–vis spectrum of $PW_{10}Mn_2$ recorded in water showed two peaks (Figure 3). An intense peak at 297 nm is assigned to O → W charge transfer. A broad band in the visible region around 390–405 nm corresponds to the presence of Mn(II) in the complex (Figure 3). No bands were observed in the region of 450–500 nm, typical of Mn(IV) and Mn(III) [12]. The presence of Mn(II) was further confirmed by ESR and ^{31}P NMR.

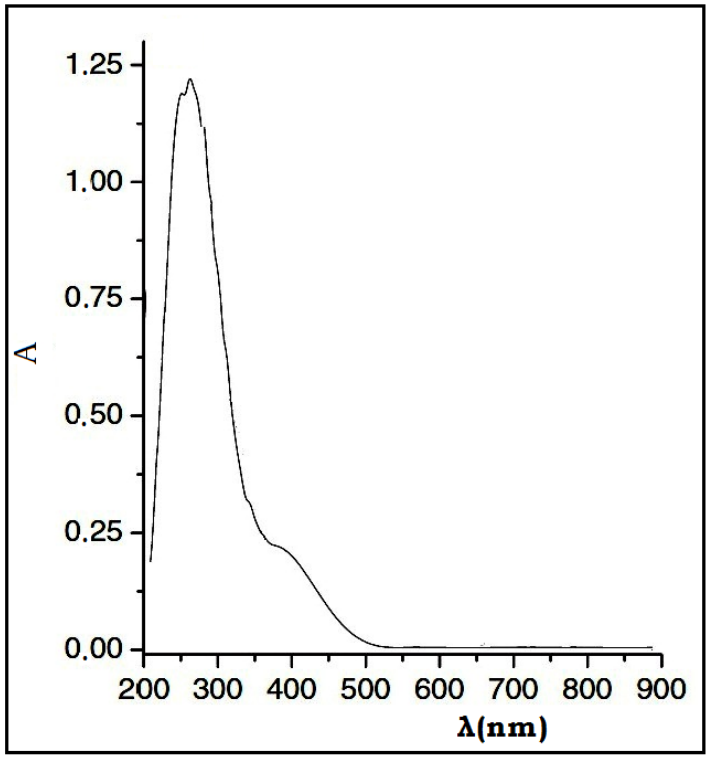

Figure 3. UV-Vis spectra

ESR

ESR spectroscopy provides a good probe to understand the environmental symmetry of transition metal ion. In present case, ESR study indicating presence of Mn(II) ion either in octahedral position of lacuna or remain as countercation. The parameters of the ESR spectra gives the information about the location and the environmental symmetry of Mn(II) ion in lacunary POMs, i.e. either Mn(II) is really present in the lacuna or exist as counter ion. Nowinska et al. reported the ESR spectra of Mn(II) modified POMs at X-band, showed signals with g ≈ 2 and g ≈ 4.3, which corresponds to Mn(II) in octahedral environmental (i.e. Mn(II) ion present in the lacuna) and Mn(II) in tetrahedral environment (i.e. Mn(II) exist as counter ion) respectively [13].

The full-range (4,000–2,000 G) X-band room temperature ESR spectrum of $PW_{10}Mn_2$ shows one broad, weak and poorly resolved signal at g ≈ 1.98, which can be assigned to Mn(II). However, the broadness of the signal may be

due to the fast relaxation of unpaired electrons [12]. Since the fast relaxation of electrons can be restricted by low-temperature ESR. Hence low temperature ESR spectrum (Figure 4) was recorded. Well-resolved six-line spectrum with g ≈ 2.1, corresponding to the octahedral environment of Mn(II) clearly depicting the incorporation Mn(II) ion into the Keggin framework. Thus absence of signal at g ≈ 4.3 confirms the absence of Mn(II) as counter ion.

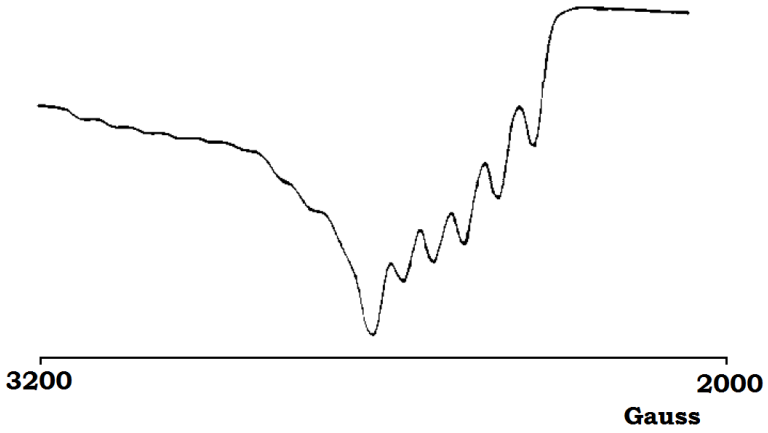

Figure 4. Low temperature ESR spectra

^{31}P NMR

^{31}P NMR spectroscopy is a commanding and useful probe to identify the change in the environment around the phosphorous. Further, it can also determine the isomers present in the reaction product. During synthesis of disubstituted POMs it is difficult to obtain pure isomer of the product in aqueous media as accompanied by uncharacterized species and hence resulting into the two to three lines in ^{31}P NMR spectrum which is well supported by literature [14, 15].

In the present case only single peak is observed confirming the formation of single pure isomer of the $PW_{10}Mn_2$.

The δ value for PW_{12} is observed at -14.55 ppm [16]. The in-situ replacement of one W by Mn leads to the formation of $PW_{11}Mn$ and having

chemical shift at -13.65 ppm. Substitution of two W from PW_{12} by two Mn cation leads to the formation of $PW_{10}Mn_2$ and having chemical shift at -12.31 ppm (Figure 5). The shift in the δ value is attributed to the change in the chemical environment around the central P atom. The current synthetic procedure overcome the disadvantage of getting mixture of products [15] during the preparation of disubstituted phosphotungstate

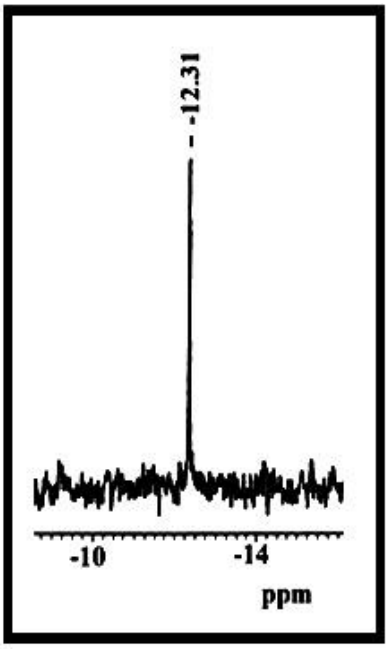

Figure 5. ^{31}P Solution NMR

Cyclic Voltametry

The cyclic voltammograms of PW_{10} (Figure 6a), $PW_{10}Mn_2$ (Figure 6b) and $PW_{11}Mn$ (Figure 6c) were recorded in acetate buffer at pH 5.

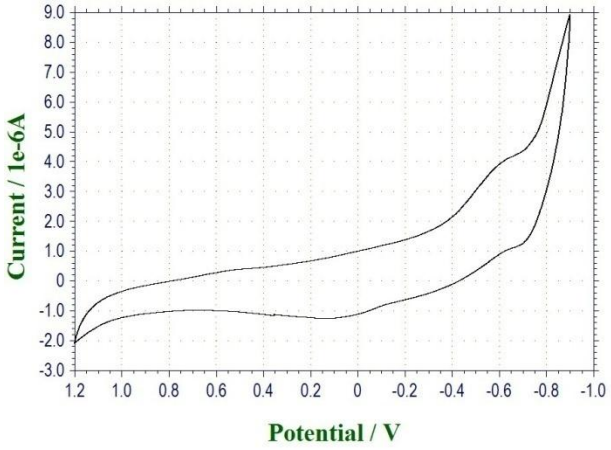

(a)

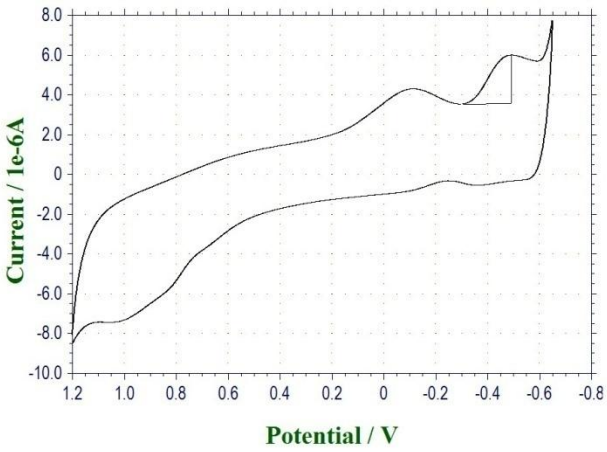

(b)

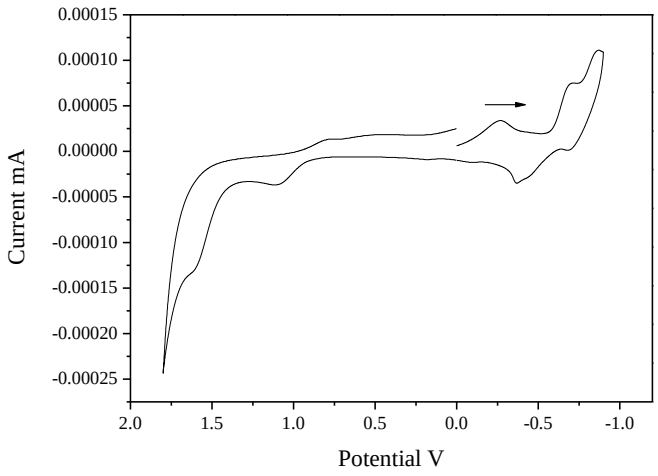

(c)

Figure 5. Cyclic voltammogram in acetate buffer (pH 5)
(a) PW_{10} (b) $PW_{10}Mn_2$ (c) $PW_{11}Mn$

The cyclic voltammogram of $PW_{11}Mn$ showed three redox potentials. The reversible redox wave at +1.1 V in the positive potential corresponds to the Mn(II) species, and the other two reversible redox couples obtained at -0.8 and -0.4 V in the negative potential correspond to $PW_{11}O_{39}$ species. The cyclic

voltammogram of $PW_{10}Mn_2$ also showed three redox potentials. The reversible redox wave at +0.9 V in the positive potential corresponds to the Mn(II) species, and the other two reversible redox couples obtained at -0.6 and -0.1 V in the negative potential correspond to PW_{10} species. It can be seen that as WO octahedra are lost the reduction generally shifts to more negative values, that means reduction is more difficult. This is due to the increased charge of the cluster making the addition of electrons harder. So, the potential values being negative for $PW_{10}Mn_2$ than that of $PW_{11}Mn$. It has been reported by Sadakane et al. [17] that the Mn(II/III) redox potential is pH independent in the pH range of 3–7. This one-step, $1e^-$ reduction corresponds to the Mn(II/III) couple and is in good agreement with the reported value [17]. The electrochemical data for our complex clearly indicates the presence of the Mn(II/III) couple as also confirmed by one step electron reduction in $PW_{10}Mn_2$.

The PW_{10} showed reversible redox process in aqueous buffered media with Epa and Epc values (-0.65 and -0.6 V, respectively,).The presence of reversible redox couples obtained at -0.6V in $PW_{10}Mn_2$ further support the formation of dilacunary phosphotungstate.

3.4 Catalytic Reaction

3.4.1 Oxidation of styrene using molecular oxygen

A detailed study on the oxidation of styrene with molecular oxygen as an oxidant and TBHP as co-oxidant was carried out. An experiment without catalyst was carried out and no conversion was obtained, indicating that there is no auto-oxidation taking place. In the present case, $PW_{10}Mn_2$ behaves as a heterogeneous catalyst. Further, the different parameters viz. amount of catalyst, reaction time and temperature were checked to get optimum reaction condition for oxidation of styrene.

Effect of the catalyst amount

The effect of catalyst amount on the conversion of styrene is illustrated in Figure 7. As the catalyst amount increased from 5 mg to 25mg, the conversion of styrene increased from 6 to 54%. With further increase in the catalyst amount from 25 to 100mg, the conversion improves and reached up to 64%.

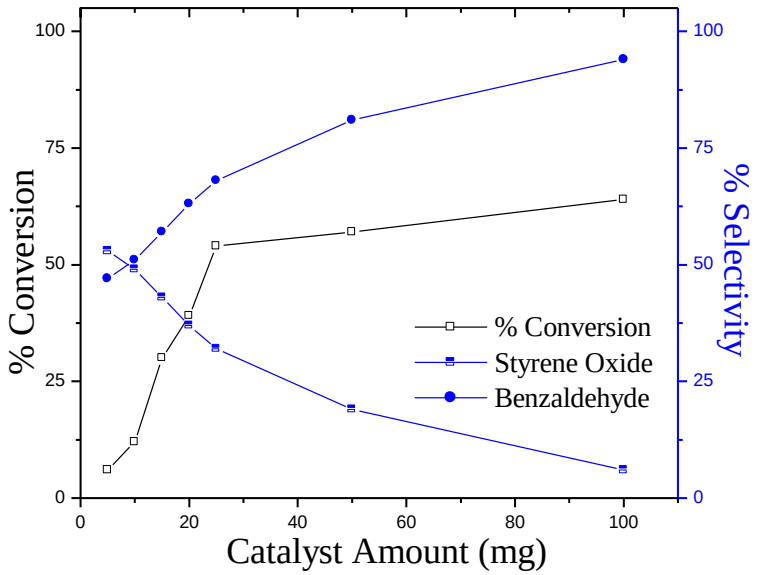

Figure 7. Effect of catalyst amount

With increase in the amount of the catalyst the number of active sites (i.e. amount of Mn increases) available for the reaction to progress increases, which results in a difference in the selectivity of products.

Increasing the amount of the catalyst the product selectivity shifts from the less stable intermediate (epoxide) to the more stable product (benzaldehyde). This may be due the fact that with increase in the amount of the active species the reaction becomes fast which favours the conversion of the formed styrene oxide (less stable intermediate) to benzaldehyde (more stable product) (Scheme-2, Chapter-2).

Due to the industrial importance of styrene oxide, 25mg can be considered sufficient enough to carry out the reaction and further, effect of reaction time and temperature was studied.

Effect of reaction time

The effect of reaction time on the conversion was depicted in Figure 8 keeping other parameter constant. The degree of conversion increases with increases in reaction time. However within the time of 4h, about 54% styrene was converted with 32% selectivity towards styrene oxide and 68% selectivity towards BA.

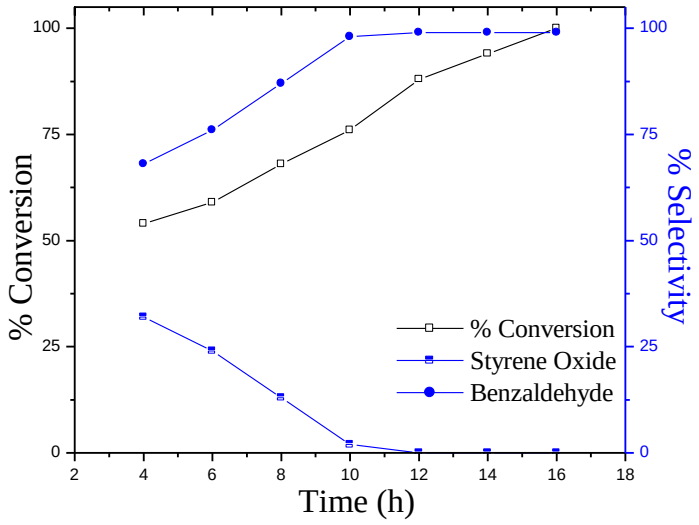

Figure 8. Effect of reaction time

With prolonging the reaction time the conversion slowly increases to 100% in 16h with single selective product (BA). This may be due to the fact that the styrene is consumed during the reaction, as a result the amount of the reactant decreases, which then requires time to reversibly bind with the oxidant. Further, the rate of desorption of the products formed from the catalyst surface is faster as a result the overall rate of the reaction slows down resulting into slow increase in the conversion with time. The distribution of the product selectivity changes with increase in the reaction time. Initially, after 4h, 32 % selectivity towards styrene oxide and 68% selectivity for BA were observed. As the reaction time increases the product selectivity shifts towards BA. With an increase in the reaction time the unstable intermediate, styrene oxide, is converted to the more stable product BA.

Due to the improved catalytic activity of $PW_{10}Mn_2$ within the short period of time and known industrial importance of styrene oxide, 4h would be preeminent time period to carry out the oxidation of styrene.

Effect of temperature

The styrene oxidation was carried out at five different temperatures to find the effect of temperature on the catalytic activity (Figure 9).

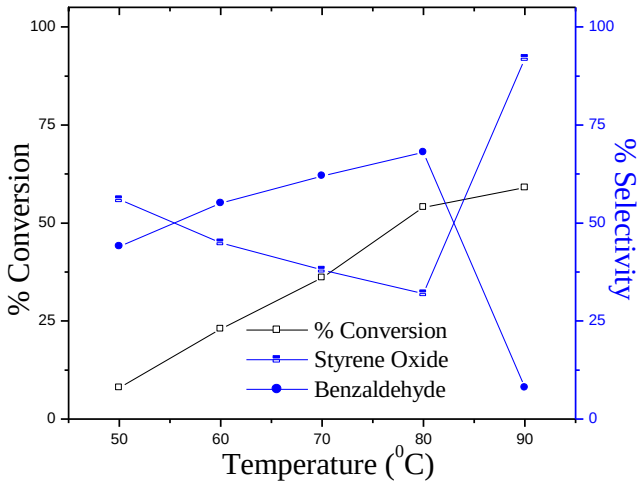

Figure 9. Effect of temperature

The styrene conversion increases dramatically from 50°C to 80°C. But from 80°C to 90°C conversion was not significant but it drops beyond 90°C. These results indicate that higher temperature was required to achieve better conversion. Increasing in the reaction temperature can quicken the reaction rate, but at higher reaction temperature (100°C) can leads to the polymerization of styrene. Due to the higher catalytic activity of $PW_{10}Mn_2$ at 80°C, it was chosen as the best temperature to carry out the oxidation of styrene.

Leaching and Heterogeneity Test

The leaching and heterogeneity test was carried as mentioned in Ch-2. The obtained results indicate no leaching was observed for Mn from the catalyst during the reaction. The results for heterogeneity test are presented in Table 2.

Table 2 % Conversion and % selectivity for oxidation of styrene (with and without catalyst)

Catalyst	**Conversion (%)**	**Selectivity (%)**	
		StyO	**BA**
$PW_{10}Mn_2$ (2h)	19	59	41
Filtarate (4h)	19	58	42

Conversion based on substrate; styrene, 100mmole; oxidant, O_2(4ml/min) ; TBHP, 0.15mmol; amount of catalyst, 25 mg; Reaction time, 4h; temperature 80°C

Regeneration and Recyclability

The regeneration of the catalyst was carried out as described in Ch-2. The results for the fresh as well as the regenerated catalysts are presented in Table 3. There was no appreciable change in selectivity of the products; however, a small decrease in conversion was observed which shows that the catalysts are stable and can be reused for up to two catalytic cycles.

Table 3. Oxidation of styrene with fresh and recycled catalysts

Catalyst	Conversion (%)	Selectivity (%)	
		StyO	BA
$PW_{10}Mn_2$	54	32	68
R1- $PW_{10}Mn_2$	52	31	69
R2- $PW_{10}Mn_2$	51	30	70

Conversion based on substrate; styrene, 100mmole; oxidant, O_2(4ml/min) ; TBHP, 0.15mmol; amount of catalyst, 25 mg; Reaction time, 4h; temperature 80^oC

3.4.2 Oxidation of styrene using H_2O_2

A detail study was carried out on oxidation of styrene by varying different parameters such as mole ratio of styrene to H_2O_2, reaction temperature, catalyst amount and reaction time and in order to get optimum reaction condition for oxidation of styrene. An experiment without catalyst was carried out and no conversion was obtained, indicating that there is no auto-oxidation taking place. In the present case, $PW_{10}Mn_2$ behaves as a homogeneous catalyst.

Effect of mole ratio

Oxidation of Styrene was carried out by varying the mole ratio of Styrene to H_2O_2 from 1:1 to 1:3. As illustrated in Figure 10, oxidation of styrene improved from 66 to 100% upon increasing the styrene to H_2O_2 mole ratio from 1:1 to 1:3. Further styrene to H_2O_2 mole ration increased from 1:1 to 3:1 the conversion gradually decrease from 66% to 43%. Therefore, 1:3 styrene to H_2O_2 mole ratio was the optimum for the oxidation of styrene.

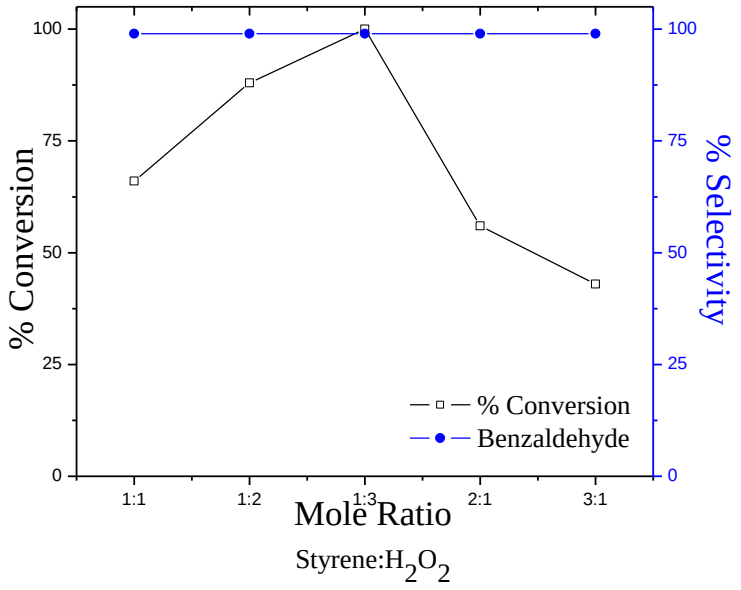

Figure 10. Effect of mole ratio

Effect of amount of catalyst

The effect of catalyst amount on the conversion of styrene is described in Figure 11. Thus, for different amount of catalyst, the styrene: H_2O_2 (1:3) mole ratio was taken. When the amount of catalyst was increased from 5 mg to 25mg, the conversion of styrene increased from 51 to 100%. With increase in the amount of the catalyst the number of active sites (i.e. amount of Mn increases) increases which results in increase % conversion. The obtained results clearly indicate that Mn functions as active sites for oxidation. However, 25mg can be considered sufficient enough to carry out the reaction and further, effect of reaction time and temperature was studied.

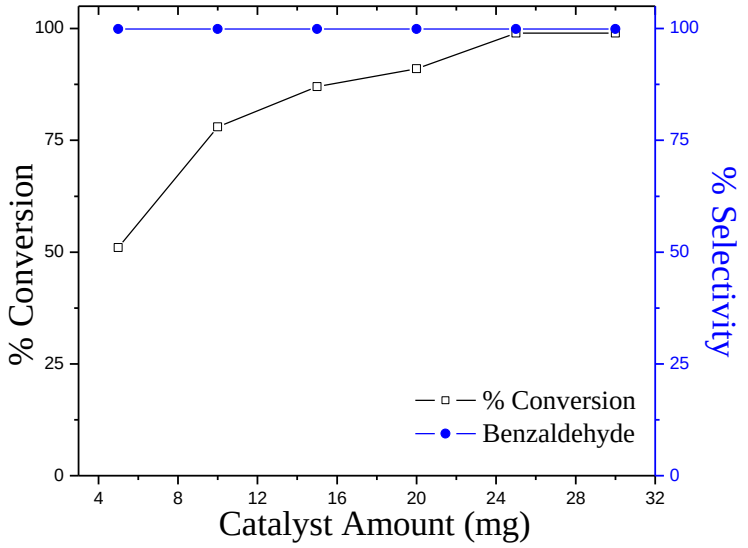

Figure 11. Effect of amount of catalyst

Effect of reaction time

The effect of reaction time on the conversion was depicted in Figure 12 keeping other parameter constant. The degree of conversion increases with increases in reaction time. However within the time of 14h, 100% styrene was converted. However, the selectivity to benzaldehyde remained unchanged throughout the reaction. Due to the high catalytic activity of $PW_{10}Mn_2$ within the moderate

period of time, 14h would be prominent time period to carry out the oxidation of styrene.

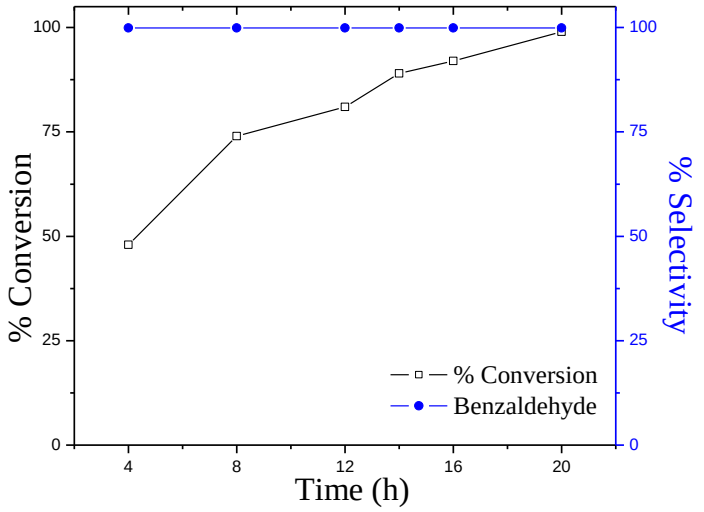

Figure 12. Effect of reaction time

Effect of temperature

The styrene oxidation was carried out at different temperatures to find the effect of temperature on the catalytic activity, which is presented in Figure 13.

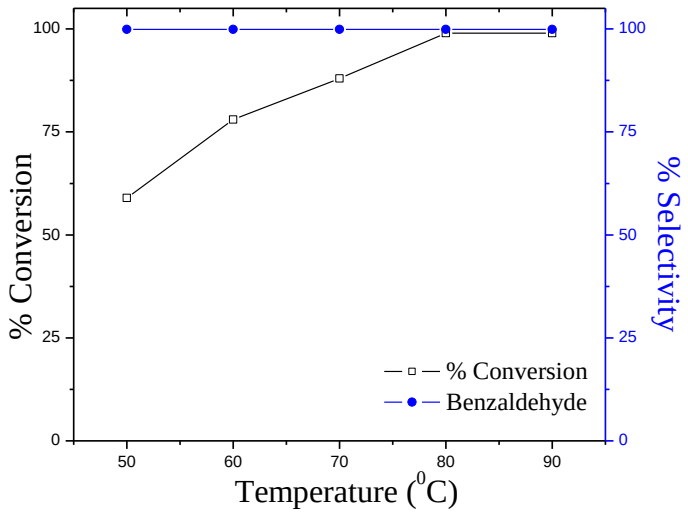

Figure 13. Effect of temperature

The styrene conversion increases dramatically from 50°C to 80°C. These results indicate that higher temperature was required to achieve better conversion. Due to the higher catalytic activity of $PW_{10}Mn_2$ at 80°C, it was chosen as the best temperature to carry out the oxidation of styrene.

It has been reported that in case of TMSPOMs, oxidation proceeds through formation of metal peroxo species [18]. This formed metal-peroxo species attacks alkenes resulting into products. In the present case the Mn peroxo species are highly reactive and have good tendency to accommodate the active oxygen from the peroxide to form the metal peroxo species into the cavity of POMs. As a result the substrate is easily oxidized giving rise to oxygenated products. In the present case, single selective product is obtained this is due to the high reactivity of the catalyst which results in formation of the more stable product (i.e. Benzaldehyde) rather than the less stable intermediate (i.e. epoxide). The highest selectivity of benzaldehyde might be due to further oxidation of styrene oxide by the nucleophilic attack of H_2O_2 on styrene oxide.

Regeneration and Recycling

The regeneration and recycling of the catalyst was carried out as mentioned in Ch-2 and the results for the same are presented in Table 4.

Table 4. Oxidation of styrene using hydrogen peroxide with fresh and regenerated catalyst

Catalyst	Conversion (%)	Selectivity (%) BA	TON
$PW_{10}Mn_2$	100	>99	1469
R1- $PW_{10}Mn_2$	98	>99	1439
R2- $PW_{10}Mn_2$	97	>99	1425

Conversion based on substrate: styrene (10mmole); oxidant, H_2O_2 (30mmole); catalyst amount, 25mg; temperature 80°C; reaction time14h

3.4.3 Kinetics Study

A study on the kinetic behaviour was carried out for $PW_{10}Mn_2$. In all the experiments, reaction mixtures were analyzed at fixed interval of time using gas chromatography.

Determination of Order as Well as Rate of Reaction

The plot of log C_0/C versus time (Figure 14) shows a linear relationship of styrene consumption with respect to time. With an increase in reaction time, there is a gradual decrease in the styrene concentration.

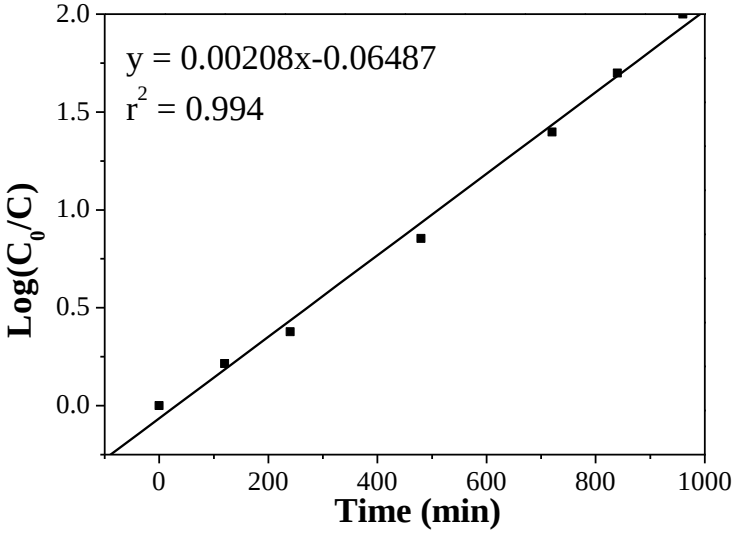

Figure 14. Styrene consumption as a function of reaction time

The linearity in the plot of Log(C_0/C) verses time shows that the oxidation of styrene is expected to follow first-order. This was further supported by the study of the effect of catalyst concentration on the rate of the oxidation of styrene. The catalyst amount was varied from 5 to 30 mg at a fixed substrate concentration of 10mmol and at a temperature of 80°C. The plot of rate of reaction versus catalyst amount (Figure 15) also shows a linear relationship for $PW_{10}Mn_2$. As the concentration of the active species, increased from 5 to 30 mg, the rate of reaction also increased.

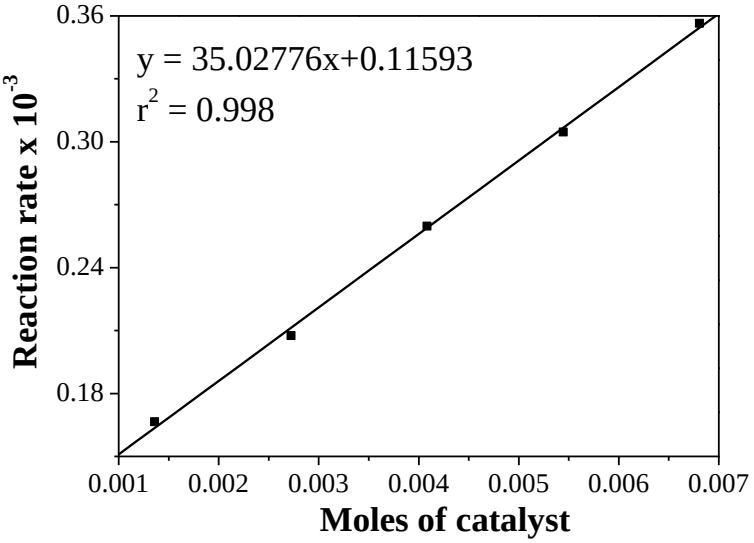

Figure 15. Effect of catalyst concentration on rate of reaction

The graph of lnk versus 1/T was plotted (Figure 16) and the value of activation energy (Ea) was determined from the plot.

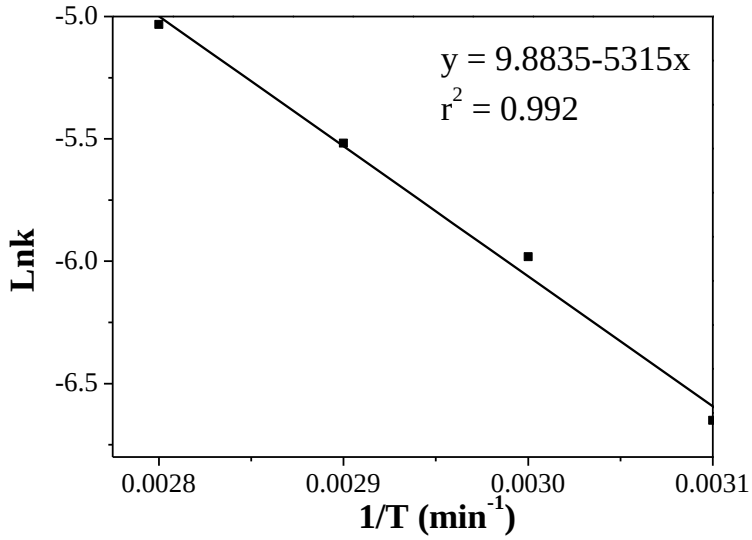

Figure 16. Arrhenius plot

From the value of activation energy (Ea), the pre-exponential factor (A) was determined using Arrhenius equation and the values are reported in Table 5.

Table 5. Kinetic parameters for oxidation of styrene $PW_{1o}Mn_2$

Activation energy (Ea)(kJ/mol)	**Pre-exponential factor (A) (min^{-1})**
44.2	1.9×10^4

Effect of oxidants on oxidation of alkenes

Under the optimized conditions, oxidation of cyclic alkenes viz. Cy6 and Cy8 was carried out using both the oxidants. The results for the same are presented in Table 6.

It is seen from Table 6 that in case of styrene oxidation 54% conversion is obtained with O_2 while 48% conversion is obtained with H_2O_2. The difference in conversion can be explained on the basis of the reactivity of oxidants. As discussed in the previous chapter, O_2 has the highest content of active oxygen (i.e. singlet oxygen). The activation of metal centre by O_2 occurs in a single step and oxidation involving H_2O_2 the activation of the metal centre occurs in two steps.

Table 6. Effect of oxidants on oxidation of alkenes

[a]Oxidant	Alkene	Products	Conversion (%)	Selectivity (%)	TON
[b]O_2	Sty	StyO	54	32	7933
		BA		68	
	Cy6	Cy6O	5	> 99	734
	Cy8	Cy8O	2	> 99	293
[c]H_2O_2	Sty	BA	48	> 99	705
	Cy6	Cy6O	3	> 99	44
	Cy8	Cy8O	NC	-	

[a]Alkene, 100mmol, alkene : H_2O_2, 1:3, O_2, 1 atm; TBHP, 0.15mmol; reaction time, [b]4h (styrene) 24h (Cyclic olefins), [c]14h; catalyst amount, 25mg, temp, 80°C

As it is seen from Table 6, in case of O_2, 32% StyO was obtained, while BA was obtained as single selective product with H_2O_2. This difference in the selectivity of products can also be explained on the basis of the nature of oxidant. In the oxidation of Sty, StyO is formed as an intermediate product which is then converted to BA. It has been reported by Kamata *et al.* [19, 20] that the efficiency of H_2O_2 utilization, by the POMs as well as the tungsten

compounds is low. Further, the reaction with H_2O_2 is a fast and exothermic resulting in nucleophilic attack of H_2O_2 on StyO giving rise to higher selectivity for BA. As a result, BA is expected as a major product. On the other hand, the reaction with O_2 is slow and a controlled one resulting in stabilization of intermediate, StyO. Thus the selectivity for the products is as expected.

For oxidation of cyclic alkenes no significant conversion was obtained. As the reaction was carried out under optimized conditions, the concentration of TBHP (an intiator) used (with O_2) was not sufficient to activate the Mn^{II} species. In case of H_2O_2, it is well reported that the utilization of H_2O_2 with tungsten based compounds is low especially for cyclic alkenes [21]. Hence, the results are as expected.

The $PW_{10}Mn_2$ is expected to follow the same reaction mechanism for O_2 and H_2O_2 as discussed in previous chapter 2 for $PW_{11}Mn$.

CONCLUSIONS

1. One Pot in situ in-pocket category based ceasium salt of di Mn(II)-substituted phosphotungstate was synthesized directly from commercially available $H_3PW_{12}O_{40}$ and $MnCl_2.4H_2O$.
2. FT-IR and ^{31}P NMR spectroscopy successfully evidenced for the in-situ formation of di-manganese substituted phosphotungstate.
3. ESR and Electrochemical studies confirmed the presence of Mn(II).
4. In case of styrene oxidation 54% conversion with 32% selectivity towards styrene oxide in 4h with O_2 and 100% conversion with benzaldehyde as a single selective product in 14h with H_2O_2 was obtained.
5. $PW_{10}Mn_2$ acts as a homogeneous catalyst with H_2O_2 while as a heterogeneous catalyst with O_2.
6. In case of H_2O_2 a method for regeneration of $PW_{10}Mn_2$ from homogeneous medium was successfully developed.
7. $PW_{10}Mn_2$ can be successfully regenerated and reused upto 2 cycles without any significant loss in the catalytic activity.
8. $PW_{10}Mn_2$ is an efficient as well as selective catalyst for solvent free liquid phase oxidation of alkenes under mild reaction conditions using environmentally benign oxidants.
9. The oxidation of styrene follows first order in presence of H_2O_2 as an oxidant.
10. The calculated activation energy (from Arrhenius Plot) for oxidation of styrene was found to be 44.3 kJ/mol.

References

1. W. H. Knoth, R. L. Harlow, *J. Am. Chem. Soc.*, 103, 1865 (1981).
2. J. Canny, A. Teze, R. Thouvenot, G. Herve, *Inorg. Chem.,* 25, 2114 (1986).
3. N. H. Nsouli, B. S. Bassil, M. H. Dickman, U. Kortz, B. Keita, L. Nadjo, *Inorg. Chem.,* 45, 3858 (2006).
4. B. S. Bassil, U. Kortz, *Dalton Trans.*, 40, 9649 (2011).
5. P. J. Domaille, R. L. Harlow, *J. Am. Chem. Soc.*, 108, 2108 (1986).
6. C. J. Gomez-Garcia, E. Coronado, P. Gomez-Romero, N. Casan-Pastor, *Inorg. Chem.*, 32, 89 (1993).
7. T. Ozeki, T. Yamase, *Acta. Cryst.*, C47, 693 (1991).
8. C. Rocchiccioli-Deltcheff, M. Fournier, R. Franck, R. Thouvenot, *Inorg. Chem.*, 22, 209 (1983).
9. P. J. Domaille, *Inorg. Synth.*, 27, 96 (1990).
10. E. Cadot, V. Bereau, F. Secheresse, *Inorg. Chim. Acta.*, 252, 101 (1996).
11. C. Rocchiccioli-Deltcheff, R. Thouvenot, *Spectrosc. Lett.*, 12, 127 (1979).
12. I. Bar-Nahum, H. Cohen, R. Neumann, *Inorg. Chem.,* 42, 3677 (2003).
13. K. Nowinska, A. Waclaw, W. Masierak, A. Gutsze, *Catal. Lett.*, 92, 157 (2004).
14. P. J. Domaille, W. H. Knoth, *Inorg. Chem.*, 22, 818 (1983).
15. K. Nomiya, M. Takahashi, J. A. Widegren, T. Aizawa, Y. Sakai, N. C. Kasuga, *Dalton trans.*, 3679 (2002).
16. M. T. Pope, *Heteropoly and Isopoly Oxometalates*, Springer-Verlag, Berlin, Germany, (1983).
17. Sadakane, E. Steckhan, *J. Mol. Catal. A Chem.*, 114, 221 (1996).
18. N. Mizuno, K. Yamaguchi, K. Kamata, *Coord. Chem. Rev.,* 249, 1944, (2005).

19. K. Kamata, K. Yohehara, Y. Sumida, K. Yamaguchi, S. Hikichi and N. Mizuno, *Science*, 300, 964, (2003).
20. K. Kamata, M. Kotani, K. Yamaguchi, S. Hikichi and N. Mizuno, *Chem.–Eur. J.*, 13, 639, (2007).
21. N. Mizuno, *Science*, 130, 964, (2003).

CHAPTER

4

Manganese(II) Substituted Sandwich type Phosphotungstate: Synthesis, Structural Characterization and Catalytic Activity towards Liquid Phase Oxidation of Alkenes

- **Paper Published**

  Eur. J. Inorg. Chem. 1871- 1875, (2011).

DOI: 10.1002/ejic.201001285

A Manganese(II) Sandwich-Type Phosphotungstate Complex – Synthesis, Structural Characterization and Catalytic Activity towards Liquid-Phase Aerobic Epoxidation of Alkenes

Ketan Patel,[a] Bharat Kumar Tripuramallu,[b] and Anjali Patel*[a]

Keywords: Manganese / Tungsten / Sandwich complexes / Epoxidation / Heterogeneous catalysis / Phosphotungstate

The dimeric, tetranuclear manganese(II)-substituted sandwich-type phosphotungstate complex has been synthesized in high yield using a straightforward one-pot synthesis by reacting commercially available $H_3[PW_{12}O_{40}]$ with $MnCl_2$. The complex has been characterized by single-crystal X-ray structure analysis. The complex is oxidatively and solvolytically stable and has been used as a heterogeneous catalyst in the efficient, selective aerobic epoxidation of styrene, cyclohexene and *cis*-cyclooctene.

Sandwich type compound based on trilacunary POMs

In the family of POMs, trivacant lacunary POMs are of particular interest because they present the opportunity to modify the surface properties of metal-oxide-like structural units via the replacement of several adjacent high-valent tungsten centres with low-valent transition metals [1-10]. The sandwich-type POMs accommodate a number of transition metal cations between the two lacunary polyoxoanions [11].

Even though, Mn(II) is most commonly used transition metal, tetranuclear Mn^{2+} sandwich type POMs complexes are comparatively less documented. The available literature reports the synthesis of sandwich type complexes either from dilacunary [12] or trilacunary [13] POMs or from the individual salts [14, 15], in a very complex and tedious processes. In 1993 Coronado et. al. reported synthesis and structural characterization of Keggin type tetranuclear sandwich complex $(Mn_4(H_2O)_2(PW_9O_{34}))^{10-}$ with detailed magnetochemistry [13]. The reported compound was the first example of an oxo bridged manganese cluster in (+2) oxidation state with potassium ions as counter cations. Pope et. al. prepared different manganese substituted sandwich complexes (from individual salts) with low valence $[Mn^{II}_4(H_2O)_2(PW_9O_{34})_2]^{10-}$, mix valence $[Mn^{II,III}_4(H_2O)_2(PW_9O_{34})_2]^{10-}$ and high valence $[Mn^{III}_4(H_2O)_2(PW_9O_{34})_2]^{10-}$ and suggested that later two species are one- and three-electron oxidized derivatives of $[Mn^{II}_4(H_2O)_2(PW_9O_{34})_2]^{10-}$ [15].

The catalytic activity of the manganese substituted sandwich type phosphotungstate, has been explored for oxidation of various substrates by Hill and Neumann, where presence of a set of manganese cations in sandwich complexes was used in epoxidation of alkenes in presence of solvent [16-20].

To the best of our knowledge, one pot synthesis for Keggin type tertranuclear sandwich complex $[Mn_4(H_2O)_2(PW_9O_{34}))^{10-}]$ (PW_9Mn_4) has not been in literature. Nevertheless, up to now catalytic epoxidation using sandwich type phosphotungstate is limited to alkenes due to its complication in the synthesis of the material.

In the present work an advantage was taken to synthesize same complex by introducing a new one pot synthesis of tetranuclear sandwich complex $(Mn_4(H_2O)_2(PW_9O_{34}))^{10-}$ (PW_9Mn_4) from commercially available $H_3PW_{12}O_{40}$ and $MnCl_2$ to present a straightforward path. The further intention is to use the tailored, effective and nontoxic material $(Mn_4(H_2O)_2(PW_9O_{34}))^{10-}$ as catalyst to achieve industrially reduced costs and eco-benign conditions, with high product selectivity and reaction rates at ambient temperatures. The synthesized complex was isolated as a cesium salt and characterized by Elemental analysis, TGA, FT-IR and ESR, and unambiguously by single crystal X-ray analysis. This material was employed as catalysts for solvent free liquid phase oxidation of styrene using O_2 and H_2O_2 as oxidants under mild reaction conditions. The catalyst was regenerated after a simple workup and reused. The kinetics of the reaction was also studied. The rate of reaction and order of reaction was determined. The effect of temperature on rate constant was studied, and the activation energy was calculated by fitting the results in to Arrhenius equation.

4.1 Experimental

Material

All chemicals used were of A. R. grade. 12-Tungstophosphoric acid, $H_3PW_{12}O_{40}.nH_2O$ (Loba Chemie, Mumbai), NaOH, $MnCl_2.4H_2O$, CsCl, styrene, cyclohexene, Cis-cyclooctene, TBHP, 30% aqueous H_2O_2 and dichloromethane were obtained from Merck and used as received.

Synthesis of sandwich type POMs

2.88 g of $H_3PW_{12}O_{40}.nH_2O$ was dissolved in 10ml of water and pH of the solution was adjusted to 7.2 using 3M NaOH solution. The solution was heated to 90°C with stirring. To this hot solution, 0.396 g of $MnCl_2.4H_2O$ dissolved in 10 ml water was added. The solution was heated at 90°C with stirring for 1h and filtered hot, and 10ml saturated solution of CsCl was added. The resulting mixture was allowed to stand overnight at room temperature, filtered and the obtained yellow colored crystals (yield= 87.9%) were dried at 50°C. The isolated solid was designated as PW_9Mn_4. The synthesis was presented in Scheme 1.

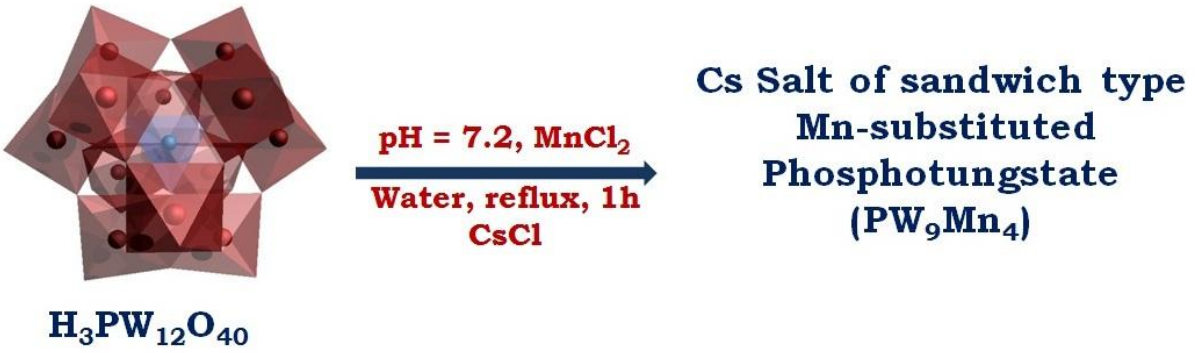

Scheme 1. Synthesis of PW_9Mn_4

4.2 Characterization

Elemental analysis was carried out using a JSM 5610 LV instrument combined with an INCA EDX-SEM analyzer for the quantitative identification of metals. TGA was carried out with a Mettler Toledo Star SW 7.01 up to 600°C. FTIR spectra were recorded as KBr pellets on a Perkin-

Elmer instrument. ESR spectra were recorded on a Varian E-line Century series X-band ESR spectrometer (liquid nitrogen temperature scanned from 2,000 to 3,200 Gauss). The analysis of the product mixtures for any leaching of Mn was carried by using atomic absorption spectrometer AAS GBC-902 instrument.

4.3 Results and Discussion

4.3.1 X-Ray Diffraction Technique

Crystal structure

The single crystal X-ray analysis were performed at 298(2) K on a Bruker SMART APEX CCD area detector system [λ(Mo-K_α) = 0.71973 Á], graphite monochromator, 2400 frames were recorded with an ω scan width of 0.3°, each for 10 s, crystal-detector distance 60 mm, collimator 0.5 mm. The data were reduced by using SAINTPLUS and a multi-scan absorption correction using SADABS [21] was performed. Structure solution and refinement were done using programs of SHELX-97 [22]. All non hydrogen atoms were refined anisotropically. During the crystallography, 39039 reflections were collected amongst which 8981 were unique ones used to solve the structure [R (int) = 0.0495].

PW_9Mn_4 was crystallized in triclinic space group P-1, with a=11.977(2) Å, b=12.664(3)Å, c=16.234(3) Å. The details of the recorded crystal data are presented in Table 1.

Table 1. Crystal Data and Structural Refinement

Empirical formula	$Cs_{9.37}$ Mn_4 O_{74} P_2 W_{18} H_{12}
Formula weight	6116.20
Crystal system, space group	Triclinic, P-1
Unit cell dimensions	a = 11.97 (2) A α= 102.10(3)
	b = 12.66 (3) A β= 102.69(3)
	c = 16.23(3) A γ= 105.66(3)
Temperature	293(2) K
Volume	2216.2(8) A^3
Z, Calculated density	1, 4.583 Mg/m^3
Absorption coefficient	27.972 mm^-1
F(000)	2616
Crystal size	0.20 x 0.16 x 0.10 mm
Theta range for data collection	1.34 to 26.41 deg.
Reflections collected / unique	39039 / 8981 [R(int) = 0.0495]
Completeness to theta = 26.41	98.9 %
Absorption correction	Empirical
Max. and min. transmission	0.1663 and 0.0713
Refinement method	Full-matrix least-squares on F^2
Data / restraints / parameters	8981 / 0 / 548
Goodness-of-fit on F^2	1.080
Final R indices [I>2sigma(I)]	R1 = 0.0467, wR2 = 0.1084
R indices (all data)	R1 = 0.0568, wR2 = 0.1130
Largest diff. peak and hole	3.246 and -1.875 e.A^-3

Single-crystal X-ray diffraction analysis shows that PW_9Mn_4 exhibits an asymmetric dimeric structure, composed of the association of two [α-PW_9O_{34}]$^{9-}$ anions with four rhomb like Mn^{2+} ions leading to a sandwich type structure (Figure 1a) with idealized C_{2h} point symmetry. Bond valence sum (BVS) calculations of all the manganese atoms in PW_9Mn_4 (2.14, 2.17 for Mn1 and Mn2 respectively) indicates these Mn atoms are all +2 valence.

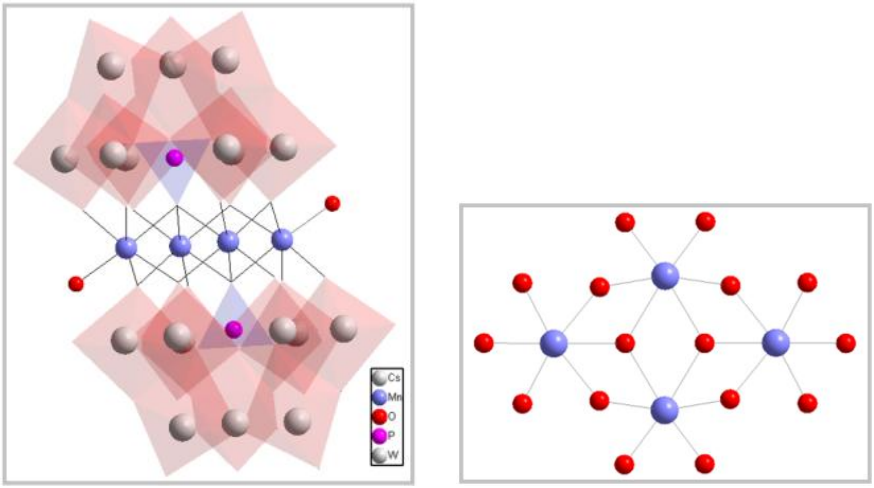

Figure 1. (a) PW_9Mn_4 (b) the rhomb like {Mn_4O_{16}}

Bond-valence sum calculations for PW_9Mn_4 indicate that the terminal oxygen atoms associated with two of the four transition-metal ions (Mn^{2+}) in the central plane are the only protonation sites of the polyanion [23]. The rhomb like {Mn_4O_{16}} (Figure 1b) group in the core of PW_9Mn_4 contains four edge-sharing Mn^{2+} octahedra with coplanar manganese atoms, which are sandwiched by two unprecedented [α-PW_9O_{34}]$^{9-}$ building units. The basic building block [α-PW_9O_{34}]$^{9-}$ in sandwich complex is similar to the well defined structure of trivacant Keggin-type polyoxoanions, which comprises a tetrahedral PO_4 group surrounded by three edge sharing W_3O_{13} triads.

The bond distances of P-O are in the range of 1.527(11)-1.545(11) Å with an average of 1.53 Å and the O-P-O angles range from 107.6(5) to 112.0(5). Moreover, the O_{34} oxygen atom links the centro-symmetric Mn atom in each [α-PW_9O_{34}]$^{9-}$ with three octahedrally coordinated Mn^{2+} centres in the core of PW_9Mn_4 on each side of the plane. Thus the arrangement of the central, rhomb like Mn_4O_{16} group formed by four edge-sharing Mn^{2+} ions

in the “belt” are all octahedrally coordinated. Two of them are in the two internal positions and coordinated by two [α-PW_9O_{34}]$^{9-}$ ligands; the other two Mn^{2+} ions are in the two external positions, and have a bonding interaction with terminal water molecules. The relevant bond lengths of Mn-O are in the range of 2.082(11)-2.325(12) Å. Furthermore, the four Mn atoms lie at the corners of the rhomb like Mn_4O_{16} group, two opposite sides of which differ slightly in length.

The crystal structure analysis shows that manganese ions are not present as counter cations only the Cs atoms were found to be present as counter cations. The crystallographic refinement of the PW_9Mn_4, suggests the presence of 9.37 Cs atoms as counter cations, while the elemental analysis confirms the presence of 10 Cs atoms around the polyanion. So, based on the structural and elemental analysis, the final formula of the PW_9Mn_4 is proposed as:

$$Cs_{10}[Mn_4(H_2O)_2(PW_9O_{34})_2].13H_2O.$$

Further, the number of water molecules determined from structural analysis shows the presence of $6H_2O$ molecules in the coordination sphere, while the thermal analysis indicates the presence of $13H_2O$. The difference in the value may be due to the loss of water in the process of single crystal XRD data collection. The elemental composition of the PW_9Mn_4 based on X-ray diffraction is fully supported by the results of elemental analysis.

Powdered X-Ray Diffraction

The powder XRD pattern of PW_9Mn_4 is presented in Figure 2 together with simulated pattern using the data set obtained by single crystal analysis. The experimental and simulated patterns are similar indicating that single crystal and bulk structures are identical.

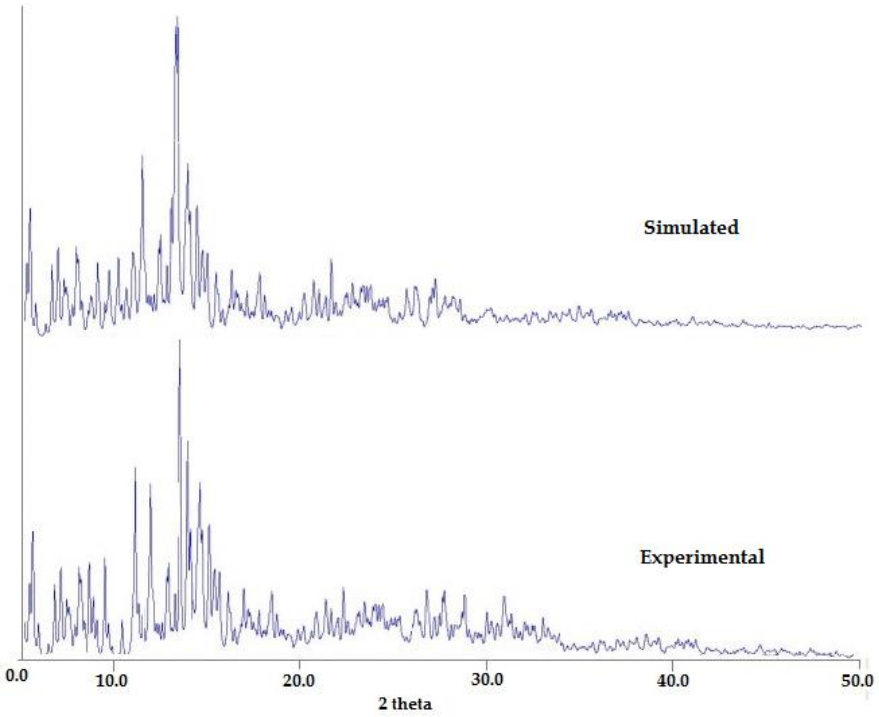

Figure 2. PXRD patterns for PW_9Mn_4

4.3.2 Spectral Analysis

Elemental Analysis

The observed values for the elemental analysis in the isolated complex are in good agreement with the theoretical values. Anal Calc: Cs, 21.18; W, 52.69; P, 0.98; Mn, 3.50; O, 21.14; Found: Cs, 20.83; W, 52.38; P, 0.96; Mn, 3.32; O, 20.58. The number of water molecules was calculated from TGA curve, based on total weight loss, corresponds to loss of 13 water molecules. From the elemental as well as the thermal analysis the chemical formula of the PW_9Mn_4 is proposed as, $Cs_{10}[Mn_4(H_2O)_2(PW_9O_{34})_2].13H_2O$. The elemental analysis for tungsten was carried out in the filterate. The observed % of W in

the filterate was 16.56%, which corresponds to loss of three equivalent of tungsten from $H_3PW_{12}O_{40}.nH_2O$.

FT-IR

All the characteristic vibrational frequencies for PW_9Mn_4 (Table 2) decreases as compared with those of $PW_{12}O_{40}$ which is attributed to the increase of the negative charges of the anions [24-26]. The characteristic vibrational modes of the PO_4 unit show that there is a loss of local symmetry as expected for the trivacant Keggin unit. The asymmetry stretching vibration of W-O-W splits into 3 peaks when the corresponding sandwich species are formed. In addition, the terminal W-O and bridging W-O-W stretches characteristic of all POMs are present.

Table 2. FT-IR frequency data

POMs	**FT-IR band frequencies (cm^{-1})**			
	P-O	**W=O**	**W-O-W**	**Mn-O-W**
$H_3PW_{12}O_{40}$	1080	982	893, 812	-
PW_9Mn_4	1032	940	877, 771,740	499

ESR

Low temperature ESR spectra were recorded for PW_9Mn_4 in the range of 3200 to 2000 G. The low temperature ESR shows a well resolved six lines ESR (Figure 3) spectrum with g ~ 2.1, which indicates the presence of Mn (II) ion into *Oh* environment.

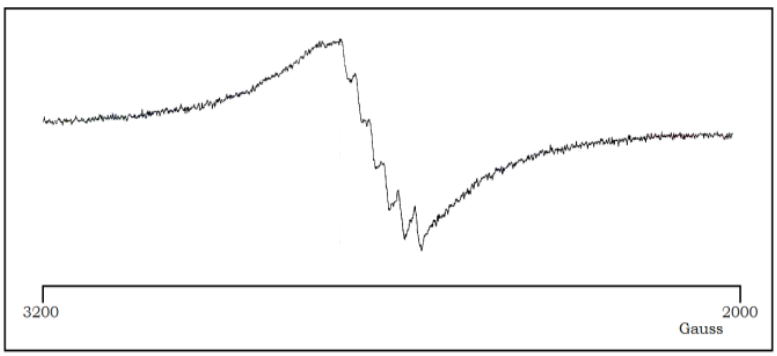

Figure 3. ESR spectra of PW_9Mn_4

4.4 Catalytic Reaction

4.4.1 Oxidation of styrene using molecular oxygen

A detailed study on the oxidation of styrene with molecular oxygen as an oxidant and TBHP as co-oxidant was carried out. An experiment without catalyst was carried out and no conversion was obtained, indicating that there is no auto-oxidation taking place. In the present case, PW_9Mn_4 behaves as a heterogeneous catalyst. Further, the different parameters viz. amount of catalyst, reaction time and temperature were checked to get optimum reaction condition for oxidation of styrene.

Effect of the catalyst amount

The effect of catalyst amount on the conversion of styrene is illustrated in Figure 4. As the amount of catalyst was increased from 5 mg to 25mg, the conversion of styrene increased from 9 to 58%. With further increase in the catalyst amount from 25mg to 100mg, the conversion improves and reached up to 72%. With increase in the amount of the catalyst the number of active sites (i.e. amount of Mn increases) available for the reaction to progress increases which results in a difference in the selectivity of products.

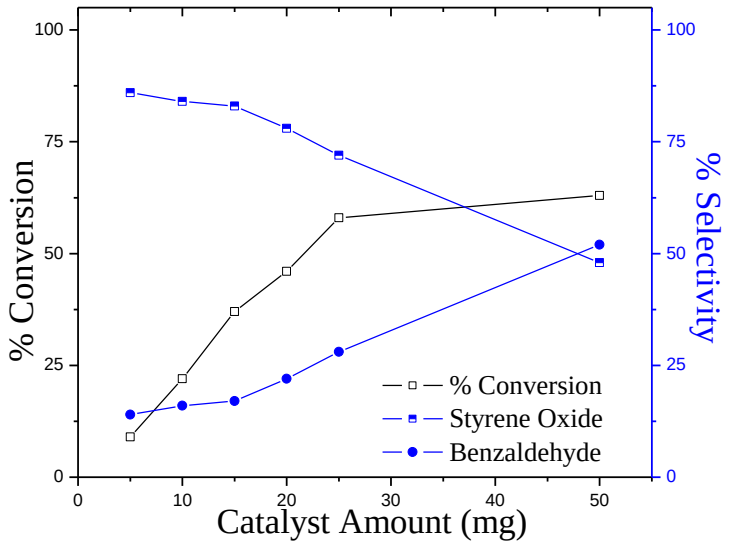

Figure 4. Effect of catalyst amount

Further, increasing the amount of the catalyst the product selectivity changes from the styrene oxide to benzaldehyde. Due to the known industrial importance of styrene oxide as well as looking to a reduced amount of catalyst, 25mg can be considered sufficient enough to carry out the reaction and effect of reaction time and temperature was studied.

Effect of reaction time

The effect of reaction time on the conversion was depicted in Figure 5, keeping other parameter constant. The degree of conversion increases with increases in reaction time. However within the time of 4h, about 58% styrene was converted with 72% selectivity towards styrene oxide and 28% selectivity towards benzaldehyde. With prolonging the reaction time the conversion slowly increases to 100% in 16h with single selective product (benzaldehyde). The distribution of the product changes with increase in the reaction time. Initially, after the completion of 4h, the 72% selectivity towards styrene oxide and 28% selectivity for benzaldehyde were observed.

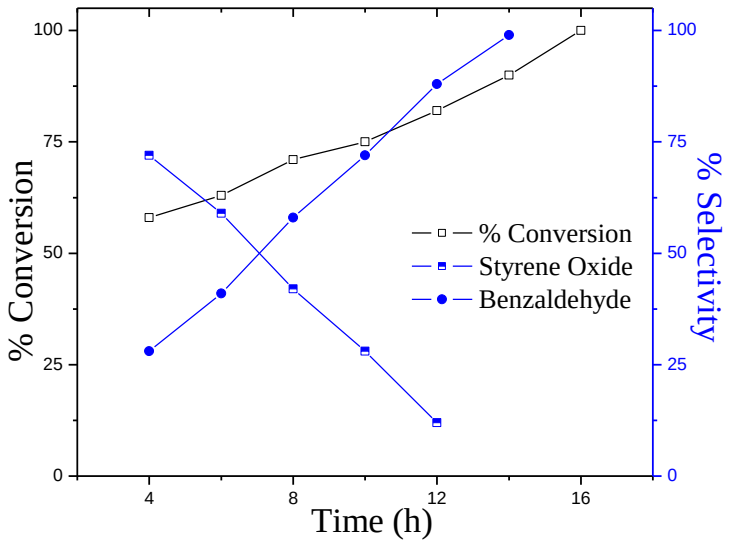

Figure 5. Effect of reaction time

As the reaction time increases the product selectivity shifts towards benzaldehyde. With an increase in the reaction time the unstable intermediate, styrene oxide, is converted to the more stable product

benzaldehyde. Due to the improved catalytic activity of PW_9Mn_4 within the short period of time and known industrial importance of styrene oxide, 4h would be preeminent time period to carry out the oxidation of styrene.

Effect of temperature

The effect of temperature for oxidation of styrene is presented in Figure 6. The styrene conversion was increases from 50°C to 80°C. But from 80°C to 90°C conversion was not significant and it drops beyond 90°C. These results indicate that higher temperature was required to achieve better conversion. Increasing in the reaction temperature can quicken the reaction rate, but at higher reaction temperature (100°C) can leads to the polymerization of styrene. Due to the superior catalytic activity of PW_9Mn_4 at 80°C , it was chosen as the best temperature to carry out the oxidation of styrene.

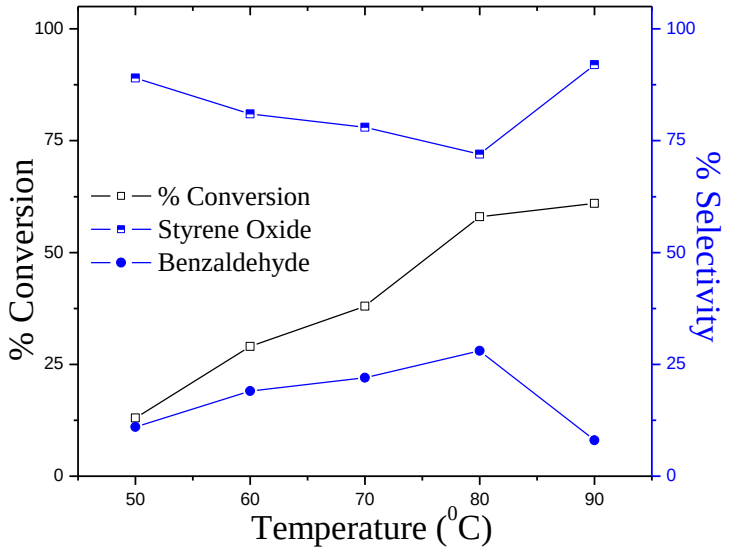

Figure 6. Effect of reaction temperature

Leaching and Heterogeneity Test

The leaching and heterogeneity test was carried as mentioned in Ch-2. The obtained results indicate no leaching was observed for Mn from the catalyst during the reaction. The results for heterogeneity test are presented in Table 3.

Table 3. % Conversion and % selectivity for oxidation of styrene (with and without catalyst)

Catalyst	Conversion (%)	Selectivity (%)	
		Styrene oxide	Benzaldehyde
PW_9Mn_4 (2h)	26	83	17
Filtrate (4h)	26	82	18

Conversion based on substrate; styrene, 100mmole; oxidant, O_2(4ml/min) ; TBHP, 0.15mmol; amount of catalyst, 25 mg; time, 4h; temperature 80^{o}C

Regeneration and Recyclability

The regeneration of the catalyst was carried out as described in Ch-2. The results for the fresh as well as the regenerated catalysts are presented in Table 4. There was no appreciable change in selectivity of the products; however, a small decrease in conversion was observed which shows that the catalysts are stable and can be reused for up to two catalytic cycles.

Table 4. Oxidation of styrene with fresh and recycled catalysts

Catalyst	Conversion (%)	Selectivity (%)	
		StyO	BA
PW_9Mn_4	58	72	28
R1-PW_9Mn_4	56	70	30
R2-PW_9Mn_4	54	69	31

Conversion based on substrate; styrene, 100mmole; oxidant, O_2(4ml/min) ; TBHP, 0.15mmol; amount of catalyst, 25 mg; time, 4h; temperature 80^{o}C

Oxidation of Cyclic alkenes using Molecular Oxygen

A detailed study for oxidation of cyclic alkenes with molecular oxygen as an oxidant and TBHP as co-oxidant was carried out. An experiment without catalyst was carried out and no conversion was obtained, indicating that there is no auto-oxidation taking place. In the present case, PW_9Mn_4 behaves as a heterogeneous catalyst. Further, the different parameters viz. amount of catalyst and reaction time were checked to get optimum reaction condition for oxidation of cyclic alkenes.

Effect of catalyst amount

The effect of catalyst amount on the conversion of cyclic alkenes is illustrated in Figure 7. As the amount of catalyst was increased from 5 mg to 25mg, the conversion of cyclohexene and cyclooctene increased from 9 to 42% and 2 to 34% respectively with the single selective product. With further increase in the catalyst amount from 25mg to 100mg, the conversion did not improve at much extent. However, 25mg of catalyst can be considered sufficient enough to carry out the reaction and further effect of reaction time was studied.

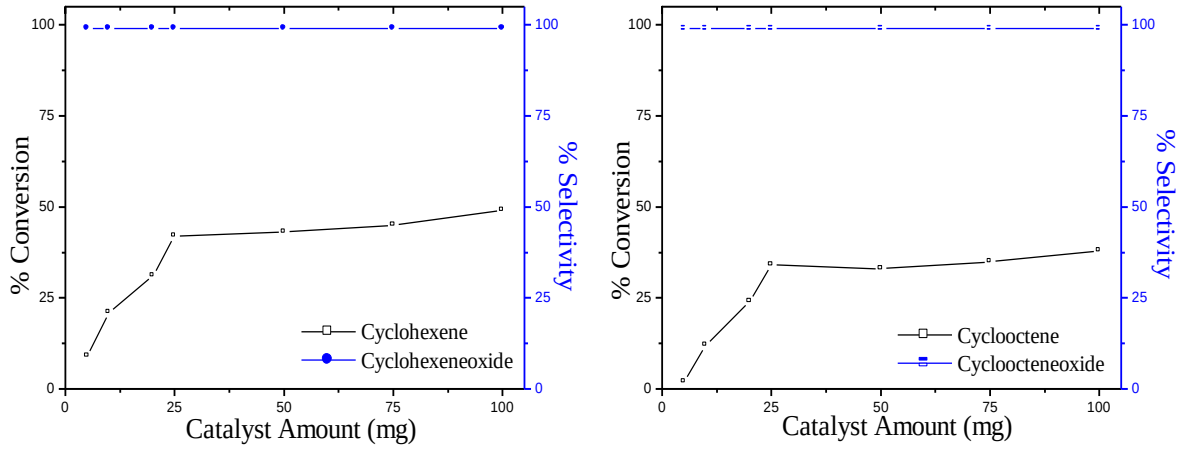

Figure 7. Effect of the catalyst amount for oxidation of Cyclic alkenes

Effect of reaction time

The effect of reaction time on the conversion was depicted in Figure 8, keeping other parameter constant. The degree of conversion increases with increases in reaction time. However within the time period of 4h, about no conversion was observed for cyclohexene as well as cyclooctene. With prolonging the reaction time the conversion slowly increases to 44% in case of cyclohexene and 36% in case of cyclooctene in 30h.

The mechanistic pathway for the oxidation of cyclic alkenes using a dioxygen species has been reported by Neumann and Dahan [27]. It has been proposed that oxidation of the alkenes in the presence of transition metal compound proceeds by a metal-catalyzed auto-oxidation reaction by forming an M-O_2 intermediate. This type of auto-oxidation reaction therefore, gives possibility of achieving epoxidation of alkenes by an addition reaction. The activation time required for the catalyst in the case of cyclic alkenes is more as compared to alkenes [27, 28], so as a result in the present case, 30 h reaction time was required to optimize the parameters. The observed order for the reactivity of cyclic olefins was cyclohexene > cyclooctene. The lower conversion for cyclooctene is mainly due the bulkiness of the cyclic ring. The large ring size, as well as ring strain, partially prevents the oxidation process which results in lower conversion of the substrate.

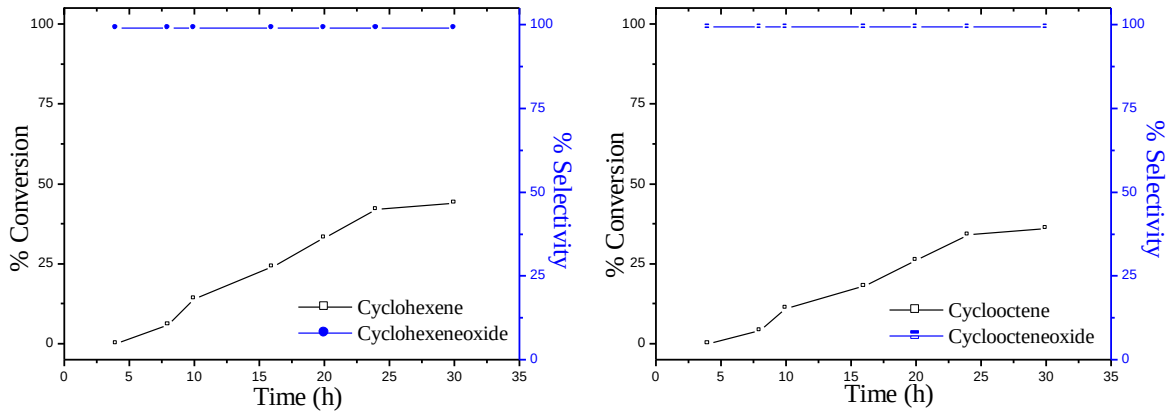

Figure 8. Effect of reaction time for oxidation of cyclic alkenes

4.4.2 Oxidation of styrene using H_2O_2

A detail study was carried out for oxidation of styrene by varying different parameters such as mole ratio of styrene to H_2O_2, reaction temperature, catalyst amount and reaction time in order to get optimum reaction condition for oxidation of styrene. To ensure the catalytic activity, all reactions were carried out without catalyst. No conversion was obtained. In the present case, PW_9Mn_4 behaves as a homogeneous catalyst.

Effect of mole ratio

Oxidation of Styrene was carried out by varying the mole ratio of Styrene to H_2O_2 from 1:1 to 1:3. As illustrated in Figure 9, oxidation of styrene improved from 73 to 100% upon increasing the styrene to H_2O_2 molar ratio from 1:1 to 1:3. Further styrene to H_2O_2 mole ration increased from 1:1 to 3:1 the conversion gradually decrease from 73% to 51%. Therefore, 1:3 styrene to H_2O_2 molar ratio was considered the optimum condition for the oxidation of styrene.

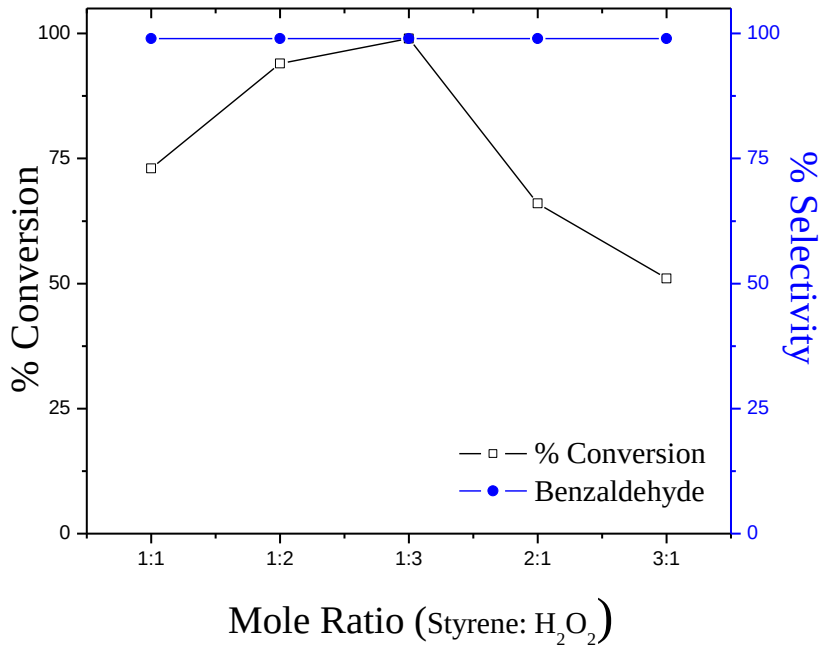

Figure 9. Effect of mole ratio

Effect of amount of catalyst

The effect of catalyst amount on the conversion of styrene was presented in Figure 10. As the amount of catalyst was increased from 5 mg to 25mg, the conversion of styrene increased from 58 to 100%.

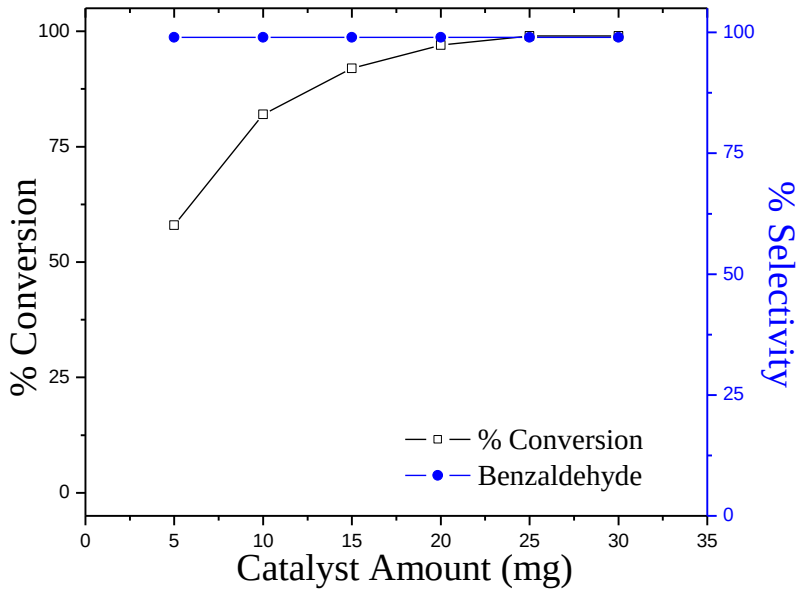

Figure 10. Effect of amount of catalyst

With increase in the amount of the catalyst the number of active sites (i.e. amount of Mn increases) increases which results in increase % conversion. The obtained results clearly indicate that Mn functions as active sites for oxidation. However, at the reduced amount of catalyst, 25mg can be considered sufficient enough to carry out the reaction and further effect of reaction time and temperature was studied.

Effect of reaction time

The effect of reaction time on the conversion was depicted in Figure 11, keeping other parameter constant. The degree of conversion increases with increases in reaction time. However within the reaction of 14h, 100% styrene was converted. However, the selectivity to benzaldehyde remained unchanged throughout the entire reaction. Due to the maximum conversion activity of PW_9Mn_4 within the moderate period of time, 14h would be preeminent time period to carry out the oxidation of styrene.

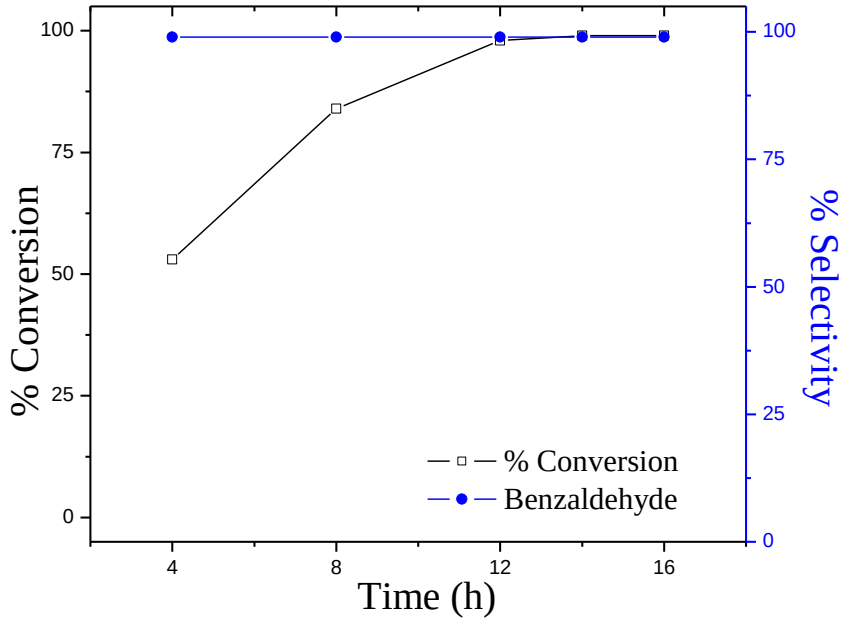

Figure 11. Effect of reaction time

Effect of temperature

The styrene oxidation was carried out at different temperatures to find the effect of temperature on the catalytic activity, which is presented in Figure 12. The styrene conversion increases dramatically from 50°C to 80°C. These results indicate that higher temperature was required to achieve better conversion. Due to the higher catalytic activity of PW_9Mn_4 at 80°C, it was chosen as the best temperature to carry out the oxidation of styrene.

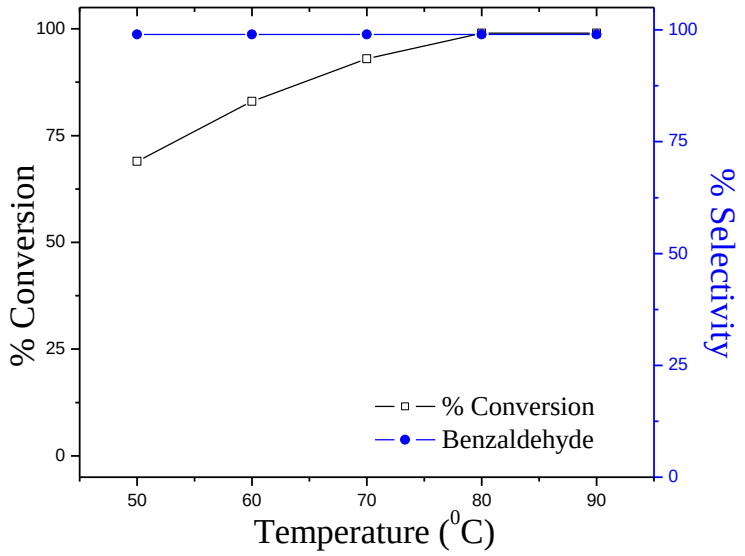

Figure 12. Effect of temperature on oxidation of styrene

It has been reported that in case of TMSPOMs, oxidation proceeds through formation of metal peroxo species [29]. This formed metal-peroxo species attacks alkenes resulting into products. In the present case the Mn peroxo species are highly reactive and have good tendency to accommodate the active oxygen from the peroxide to form the metal peroxo species into the cavity of POMs. As a result the substrate is easily oxidized giving rise to oxygenated products. In the present case, single selective product is obtained this is due to the high reactivity of the catalyst which results in formation of the more stable product (i.e. Benzaldehyde) rather than the less stable intermediate (i.e. epoxide). The highest selectivity of benzaldehyde might be due to further oxidation of styrene oxide by the nucleophilic attack of H_2O_2 on styrene oxide.

Leaching and Heterogeneity Test

In the present case, PW_9Mn_4 behaves as homogeneous catalyst as a result leaching and heterogeneity test was not required.

Regeneration and Recycling

The methodology for regeneration and recycling of the catalyst was carried out as mentioned in Ch-2 and the results for the same are presented in Table 5.

Table 5. Oxidation of styrene using H_2O_2 with fresh and regenerated catalyst

Catalyst	**Conversion (%)**	**Selectivity for BA (%)**	**TON**
PW_9Mn_4	100	> 99	2446
R1- PW_9Mn_4	98	> 99	2397
R2- PW_9Mn_4	97	> 99	2373

Conversion based on substrate; substrate, 10mmole; oxidant H_2O_2 (30 mmole), amount of catalyst, 25 mg; reaction time 14h; reaction temperature 80^0C

4.4.2 Kinetics Study

A study on the kinetic behaviour was carried out for PW_9Mn_4. In all the experiments, reaction mixtures were analyzed at fixed interval of time using gas chromatography.

Determination of Order as Well as Rate of Reaction

The plot of log C_0/C versus time (Figure 13) shows a linear relationship of styrene consumption with respect to time. With an increase in reaction time, there is a gradual decrease in the styrene concentration.

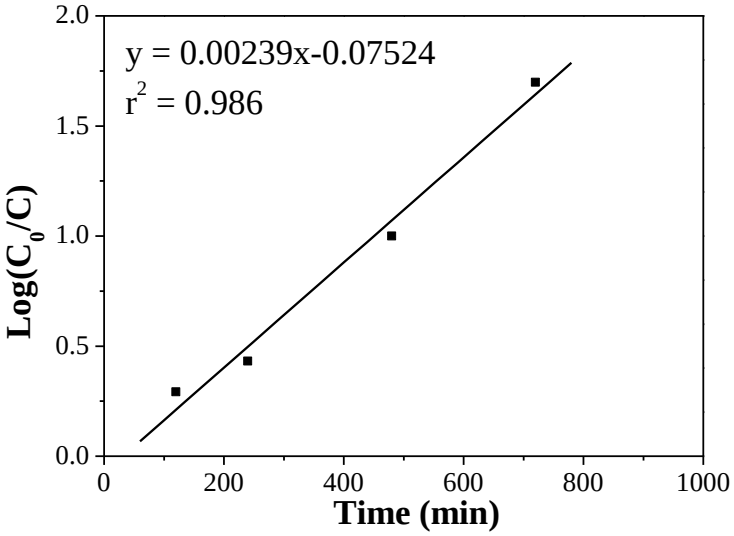

Figure 13. Styrene consumption as a function of reaction time

The linearity in the plot of Log(C_0/C) verses time indicate that the oxidation of styrene is expected to follow first-order. This was further supported by the study of the effect of catalyst concentration on the rate of the oxidation of styrene. The catalyst amount was varied from 5 to 25 mg at a fixed substrate concentration of 10mmol and at a temperature of 80°C.

The plot of reaction rate versus catalyst amount (Figure 14) also shows a linear relationship for $PW_{11}Mn$. As the concentration of the active species, increased from 5 to 25 mg, the rate of reaction also increased.

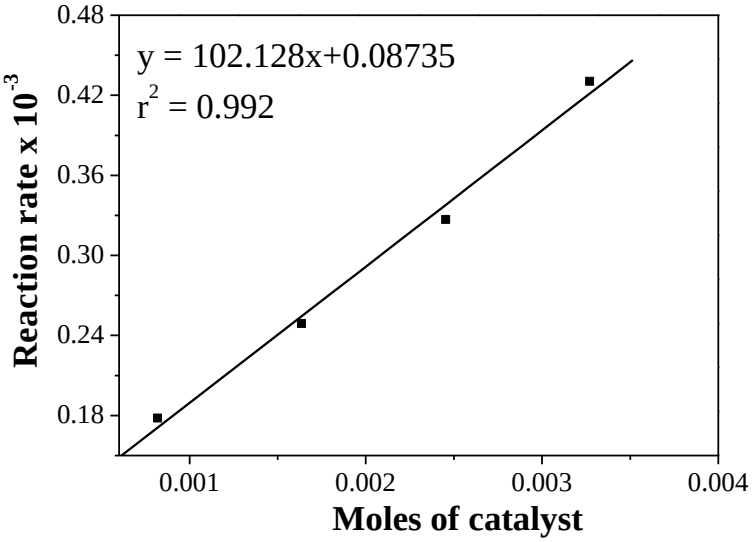

Figure 14. Effect of catalyst concentration rate of reaction

The above study confirms that the initial rate of oxidation of styrene follow first-order kinetics with respect to the substrate as well as the catalyst.

As most of the oxidation reactions are temperature sensitive, the effect of temperature on the oxidation of styrene was also studied by varying the temperature between 313 and 363 K, keeping the styrene: H_2O_2 ratio of 1:3 and catalyst amount of 25 mg. As the temperature increases from 313 to 373 K, the conversion of styrene also increases drastically. This may be due to the activation of the catalytic species with temperature.

The graph of lnk versus 1/T was plotted (Figure 15) and the value of activation energy (Ea) was determined from the plot.

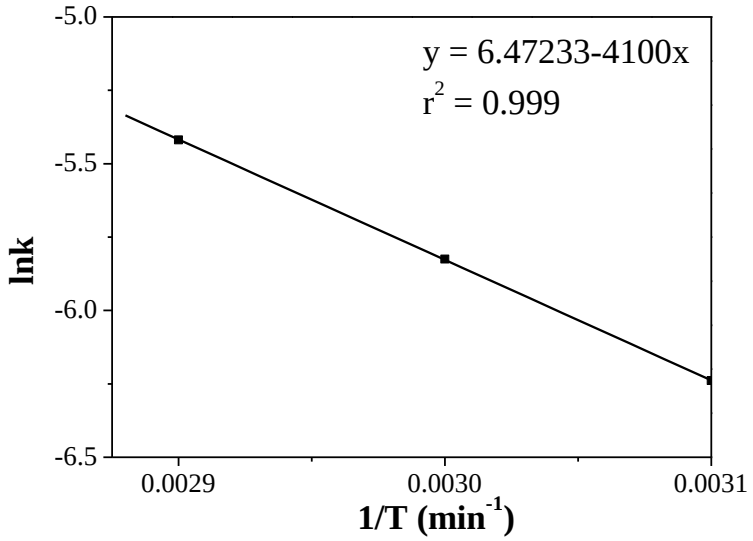

Figure 15. Arrhenius plot

From the value of activation energy (Ea), the pre-exponential factor (A) was determined using Arrhenius equation and the values are reported in Table 6.

Table 6. Kinetic parameters for oxidation of styrene

Activation energy (Ea)(kJ/mol)	**Pre-exponential factor (A) (min^{-1})**
34.1	6.47×10^2

4.4.2 Oxidation of cyclic alkenes using H_2O_2

A detailed study for oxidation of cyclic alkenes with H_2O_2 as an oxidant was carried out. An experiment without catalyst was carried out and no conversion was obtained, indicating that there is no auto-oxidation taking place. In the present case, PW_9Mn_4 behaves as a homogeneous catalyst. Further, the different parameters viz. amount of catalyst and reaction time were checked to get optimum reaction condition for oxidation of cyclic alkenes.

Effect of mole ratio

Oxidation of Cy6 and Cy8 was carried out by varying the mole ratio of 1:1 to 1:3 (Cyclic alkenes: H_2O_2) and presented in Figure 16. It is observed from Figure 16 that with increase in the mole ratio from 1:1 to 1:3, there was a change in the % conversion. With 1:3 mole ratio 18% conversion with >99% selectivity towards Cy6oxide for Cy6 and 12% conversion with > 99% selectivity towards Cy8oxide for Cy8 was obtained. No significant change in conversion was obtained with further increase in cyclic alkenes to H_2O_2 mole ratio. Hence, further optimization of the conditions was carried out with 1:3 molar ratio of styrene to H_2O_2.

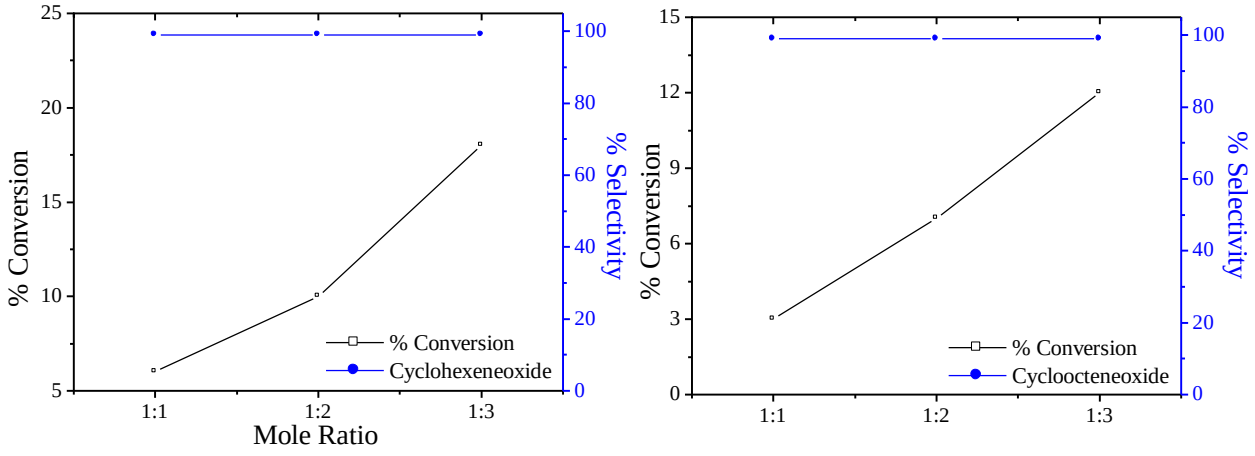

Figure 16. Effect of mole ratio

Effect of amount of catalyst

The effect of amount of catalyst on the conversion of cyclic alkenes is represented in Figure 17. It is seen from Figure that the activity of cyclic alkenes increases initially up to 25mg. There was no remarkable difference in the progress of reaction was observed when catalyst amount increase from 25mg or 100mg. So, 25mg amount of catalyst was taken to be optimal.

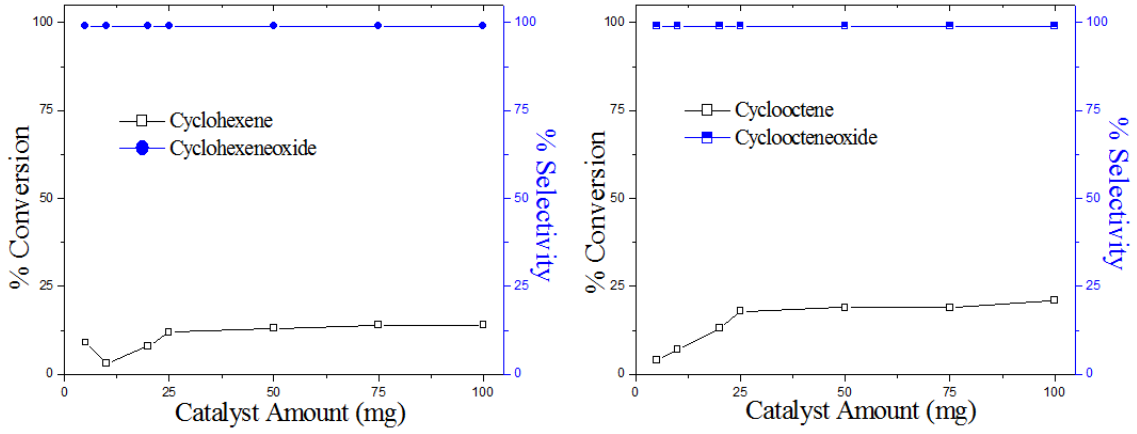

Figure 17. Effect of amount of catalyst

Effect of reaction time

The effect of reaction time was also studied under the optimized conditions of mole ratio and catalyst amount (Figure 18). On increasing the reaction time from 4h to 24h the conversion for Cy6 and Cy8 slowly increased. With further increase in reaction time no significant conversion was observed. This could be due to the attainment in the stability of the formed peroxo intermediate.

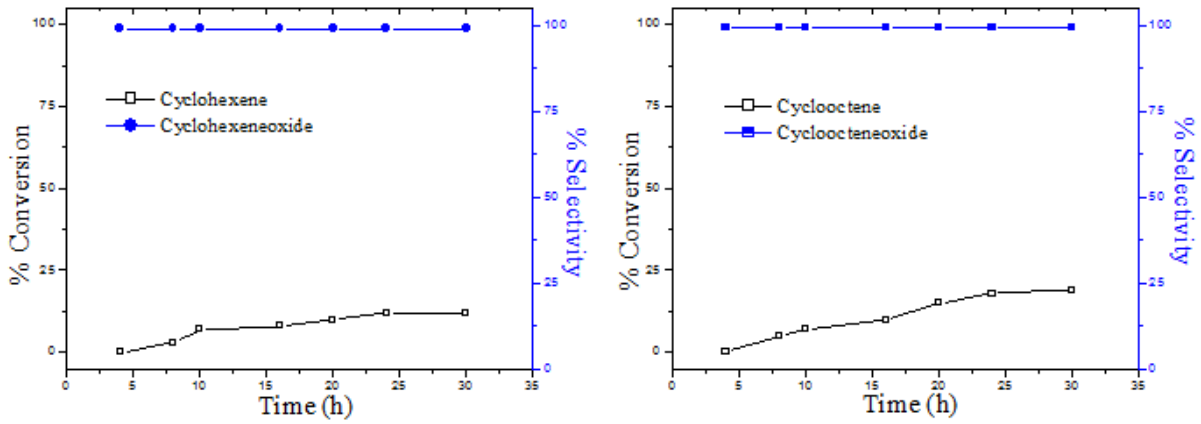

Figure 18. Effect of reaction time

Effect of oxidants on oxidation of alkenes

As seen from Table 7, O_2 gives higher conversions for all the alkenes as compared to H_2O_2. This difference in the reactivity can be explained on the basis of nature of oxidants.

Table 7. Effect of oxidants on oxidation of alkenes

[a]Oxidant	Alkene	Products	Conversion (%)	Selectivity (%)	TON
[b]O_2	Styrene	StyO	58	72	17614
		BA		28	
	Cy6	Cy6 oxide	42	> 99	10294
	Cy8	Cy8 oxide	34	> 99	8333
[c]H_2O_2	Styrene	Benzaldehyde	49	> 99	1296
	Cy6	Cy6 Oxide	18	> 99	440
	Cy8	Cy8 Oxide	12	> 99	293

[a]Alkene, 100mmol, alkene : H_2O_2, 1:3, O_2, 1 atm; TBHP, 0.15mmol; reaction time, [b]4h (styrene) 30h (Cyclic olefins), [c]14h; catalyst amount, 25mg, temp, 80^oC

As discussed earlier O_2 has the highest content of active oxygen (i.e. singlet oxygen). The activation of metal centre by O_2 occurs in a single step via formation of M-O_2 species while in case of H_2O_2, activation of metal centre by H_2O_2 occurs in two steps, as a result it requires more time as compared to O_2, to achieve high conversion.

It is also seen from Table 7 that in case of O_2, StyO was obtained as major product, while BA was obtained as single selective product with H_2O_2. This difference in the selectivity of products can also be explained on the basis of the nature of oxidant. In the oxidation of Sty, StyO is formed as an intermediate product which is then converted to BA. It has been reported by Kamata *et al.* that the efficiency of H_2O_2 utilization, by the POMs as well as the tungsten compounds is low. Also their selectivity towards epoxides using H_2O_2 as oxidant is poor. Further, the reaction with H_2O_2 is fast and exothermic resulting in nucleophilic attack of H_2O_2 on StyO giving rise to higher selectivity for BA. The obtained result is as expected. On the other hand, the reaction with O_2 is slow and a controlled one resulting in

stabilization of intermediate, StyO. Thus the selectivity for the products is as expected.

Oxidation of cyclic alkenes also showed the similar behaviour as styrene. As mentioned above, the efficiency of H_2O_2 utilization, by tungsten based compounds is low with poor reactivity for cyclic alkenes. The obtained results are as expected.

The observed order for the reactivity of cyclic alkenes is Cy6 > Cy8. The higher conversion for the lower number of cyclic carbon indicates that the cis-cyclooctene is more strained and does not easily coordinate to the metal centre during the oxidation process. The bulkiness of cyclic ring as well as the ring strain makes it difficult to coordinate with the metal centre and thus partially prevents the oxidation process.

The PW_9Mn_4 is expected to followe the same reaction mechanism for O_2 and H_2O_2 as discussed in previous chapter of $PW_{11}Mn$.

Effect of Mn(II) centre in oxidation of alkenes

(I) Oxidation of styrene using O_2

The effect of Mn substitution in the conversion is shown in Table 8. 12 % conversion was obtained with benzaldehyde as single selective product in case of $PW_{12}O_{40}$. All the Mn(II)- substituted phosphotungstates show higher conversion as compare to unsubstituted phosphotungstate. This suggests that Mn functions as active sites for oxidation.

Table 8. Effect of Mn centre on oxidation of styrene using O_2

Catalyst	Conversion	Selectivity		TON
		Styrene oxide	Benzaldehyde	
$PW_{11}Mn$	61	-	>99	8507
$PW_{10}Mn_2$	54	32	68	7826
PW_9Mn_4	58	72	28	17614

Conversion based on styrene(100mmole); oxidant, amount of catalyst, 25 mg;O_2(4ml/min) ; TBHP, 0.15mmol catalyst, temperature 80^{o}C, 4h

61% conversion was obtained in case of $PW_{11}Mn$, whereas not much difference in the conversion was observed in the case of $PW_{10}Mn_2$ as well as PW_9Mn_4. However, it is very interesting to observe the difference in the selectivity of the products with change in the degree of substitution. Single selectivity was obtained for $PW_{11}Mn$ where as 32% and 72% selectivity towards styrene oxide was obtained for $PW_{10}Mn_2$ and PW_9Mn_4 respectively.

It has been reported that for TMSPOMs catalysts containing metal cations in low valency states and involving O_2 as an oxidant always follow the radical chain mechanism induced by M-O_2 intermediate. In the present catalytic system, the mechanism involving the Mn species is expected to follow the same path. The role of TBHP is as an initiator. The activation of Mn^{2+} species takes place through a formation of $\cdot OMn^{3+}PW_{11}$. This activated

species (**.**$OMn^{3+}PW_{11}$) gets attached with O_2 species and forms $\cdot OOMn^{3+}PW_{11}$ radical which then attack the substrate. The metal-superoxo intermediate reversibly binds styrene attacking the reaction site which results in oxidation of substrate to form products. The distribution of the product in oxidation of styrene is dependent on the reactivity of the superoxo intermediate.

The selectivity of the products depends upon the reactivity of the superoxo species. If the superoxo species is more reactive, the formed styrene oxide gets immediately converted to benzaldehyde and if superoxo species is less reactive, it stabilized the formation of the styrene oxide.

It is known that the presence of high electron density decreases the reactivity of the superoxo species. In the present case PW_9Mn_4 is more –ve (i.e. high electron density) and hence formed superoxo species is expected to be less reactive which will in turn to stabilize the epoxide. The obtained results are as expected.

(II)Oxidation of styrene using H_2O_2

The effect of Mn centre on oxidation of styrene was presented in Table 9. $PW_{12}O_{40}$ gave 28 % conversion with single selective product (BA) in 12h.

Table 9. Effect of Mn centre on oxidation of styrene using H_2O_2

Catalyst	Conversion	Selectivity		TON	Ea (kJ/mol)
		StyO	BA		
$PW_{11}Mn$	83	-	>99	1128	52.2
$PW_{10}Mn_2$	89	-	>99	1307	44.2
PW_9Mn_4	98	-	>99	2421	34.1

Conversion based on styrene(10mmole); oxidant, H_2O_2 (30mmole); amount of catalyst, 25 mg; temperature 80°C; 12h

The reaction of the Mn centre with H_2O_2 results in the generation of the active species which may be hydroperoxo or peroxo species. In oxidation of styrene, the unstable intermediate (StyO) rearranges to form the more stable product (BA). The highest selectivity of benzaldehyde results due to further oxidation of styrene oxide by the nucleophilic attack of H_2O_2 on styrene oxide. So, in all the cases benzaldehyde was obtained as single selective product. The activation energy for PW_9Mn_4 is lower than that of other two catalysts. It means that it requires lower energy as compared to other two catalysts and achieves maximum conversion in less period of time.

(III) Oxidation of Cyclic alkenes

A comparative data for oxidation of alkenes using O_2 and H_2O_2 for $PW_{11}Mn$, $PW_{10}Mn_2$ and PW_9Mn_4 (Table 10) are as follows.

Table 10. Effect of Mn centre on oxidation of Cyclic alkenes

Catalyst	Oxidant	Alkenes	Conversion	Selectivity (%)		TON
				Cy6O	Cy8O	
$PW_{11}Mn$	O_2	Cy6	NC	-		-
		Cy8	NC		-	-
	H_2O_2	Cy6	NC	-		-
		Cy8	NC		-	-
$PW_{10}Mn_2$	O_2	Cy6	5	>99	-	734
		Cy8	2	-	>99	293
	H_2O_2	Cy6	3	>99	-	44
		Cy8	NC	-	-	-
PW_9Mn_4	O_2	Cy6	42	>99	-	10294
		Cy8	34	-	>99	8333
	H_2O_2	Cy6	18	>99	-	440
		Cy8	12	-	>99	293

Alkene, 100mmol, Alkene : H_2O_2, 1:3, O_2, 1 atm; TBHP, 0.15mmol; reaction time, 30h (Cyclic Olefins); catalyst amount, 25mg, temp, 80^{o}C; NC = No significant conversion

As seen from Table 10, no significant conversion was obtained with $PW_{11}Mn$ using O_2 and H_2O_2. $PW_{10}Mn_2$ gave 5% and 2% conversion for Cy6 and Cy8 in presence of O_2 and 3% conversion for Cy6 in presence of H_2O_2.

PW_9Mn_4 gave 42% and 34% in presence of O_2 and 18% and 12% in presence of H_2O_2 for Cy6 and Cy8. Oxidation of cyclic olefins generally follows two types of mechanism, (i) oxidation (ii) bond cleavage, e.g. in case of cyclohexene if allylic attack is preferred, which results in further oxygenated products. Further it is also known that if the oxidation is carried out, over an acidic catalyst using a strong oxidant having high content of active oxygen, the bond cleavage mechanism is preferred over allylic attack

resulting in formation of cyclohexanol or cyclohexanone [30]. In the present study oxidation was observed giving rise to cyclohexene oxide. This could be explained on the basis of the nature of the PW_9Mn_4. The present catalyst is not acidic in nature and as well as presence of high electron density on the catalyst is responsible for stabilization of the formed epoxide. However previously it is shown that, the decreased catalytic activity was observed when Mn(II) is substituted into the POMs [16, 17]. The presence of two sets of two adjacent Mn(II) centers in PW_9Mn_4 and their effect on the catalytic activity were therefore of interest.

For transition metal substituted polyoxometalates, the catalytically active site is at the substituted transition metal centre while the polyoxometalates function as a ligand with strong capacity for accepting electrons. The incoming reactant (i.e.alkenes) directly bind to the Mn(II) centre, responsible for conversion. So higher activity is observed, which is as expected.
For oxidation of cyclic alkenes, PW_9Mn_4 was found to be more reactive as compared to other two catalysts.

CONCLUSION

1. We present the first example of tetranuclear Mn(II)-substituted sandwich type phosphotungstate, synthesized directly from commercially available $H_3PW_{12}O_{40}$ and $MnCl_2.4H_2O$ which may open up a new route to establish the well-known sandwich type structure directly from Keggin analogue.
2. The structural analysis shows the formation of rhomb like tetranuclear Mn cation sandwich between the two trilacunary POMs (without disorder). It also indicates that the terminal oxygen atoms associated with two of the four Mn^{2+} ions in the central plane are the only protonation sites in PW_9Mn_4. The presence of Mn^{II} was confirmed by ESR study.
3. In the oxidation of Styrene 58% conversion was obtained with 72% selectivity towards styrene oxide in 4h with O_2 and 98% conversion with benzaldehyde as a single selective product in 12h with H_2O_2. It is a choice for the chemists to select the reaction, with 98% conversion and single selective product or with 58% conversion and 72% selectivity towards styrene oxide.
4. In case of epoxidation of Cy6 and Cy8 42% and 34% conversion was obtained with single selective product of Cy6O and Cy8O respectively.
5. PW_9Mn_4 acts as a homogeneous catalyst with H_2O_2 while as a heterogeneous catalyst with O_2.
6. In case of H_2O_2 a method for regeneration of PW_9Mn_4 from homogeneous medium was successfully developed.
7. PW_9Mn_4 can be successfully regenerated and reused upto 2 cycles without any significant loss in the catalytic activity.
8. PW_9Mn_4 is an efficient as well as selective catalyst for solvent free liquid phase oxidation of alkenes under mild reaction conditions using environmentally benign oxidants.
9. The oxidation of styrene follows first order in presence of to H_2O_2 as an oxidant.

10. The calculated activation energy (from Arrhenius Plot) for oxidation of styrene was found to be 34.1kJ/mol.
11. The superiority of the present catalyst lies in obtaining good conversion with high TON as well as single selective products towards cyclic olefins.

References

1. M. T. Pope, *Heteropoly and Isopoly Oxometalates*, Springer-Verlag, Berlin, Germany, (1983).
2. C. L. Hill, C. M. Prosser-McCartha, *Coord. Chem. Rev.*, 143, 407 (1995)
3. T. J. R Weakley, H. T. Evans, Jr. J. S. Showell, G. F. Tourne, C. M. Tourne, *J. Chem. Soc. Chem. Comm.*, 139, (1973).
4. R. G.Finke, M. Droege, *J.Am.Chem.Soc.*, 103, 1587 (1981)
5. R. G.Finke, M. W.Droege, P. J. Domaille, *Inorg.Chem.*, 26, 3886 (1987)
6. T. J. R. Weakley, R. G. Finke, *Inorg. Chem.*, 29, 1235 (1990)
7. J. M. Clemente-Juan, E. Coronado, J.R. Galan-Mascaros, C. J. Gomez-Garcıa, *Inorg. Chem.*, 38, 55 (1999)
8. X. Zhang, Q.Chen, D. C. Duncan, R.J. Lachicotte, C. L. Hill., *Inorg. Chem.*, 36, 4381 (1997)
9. L. Bi, U. Kortz, B. Keita, L. Nadjo, H. Borrmann, *Inorg. Chem.*, 43, 8367 (2004).
10. J. G. Liu, F. Ortega, P. Sethuraman, D. E. Katsoulis, C. E. Costello, M. T. Pope, *J. Chem. Soc., Dalton Trans.*, 1901 (1992).
11. Y. Hou, L. Xu, M. Cichon, S. Lense, K. I. Hardcastle, C. L. Hill, *Inorg. Chem.*, 49, 4125 (2010).
12. U. Kortz, S. Isber, M. H. Dickman, D. Ravot, *Inorg. Chem.*, 39, 2915 (2000).
13. C. J. Gomez Garcia, E. Coronado, P. Gomez Romero, N. Pastor, *Inorg. Chem.*, 32, 3378 (1993).
14. U. Kortz, S. Nellutla, A. C. Stowe, N. S. Dalal, U. Rauwald, W. Danquah, D. Ravot, *Inorg. Chem.*, 43, 2308 (2004).
15. X. Zhang, G. B. Jamesonu, C. J. Oconnor, M T. Pope, *Polyhedron*, 43, 917 (1996).
16. M. D. Ritortho, T. M. Anderson, W. A. Neiwert, C. L. Hill, *Inorg. Chem.*, 43, 44 (2004).

17. R. Ben-Daniel, L. Weiner, R. Neumann, *J. Am. Chem. Soc.*, 124, 8788 (2002).
18. X. Zhang, T. M. Anderson, Q. Chen, C. L. Hill, *Inorg. Chem.*, 40, 418 (2001).
19. R. Neumann, M. Gara, *J. Am. Chem. Soc.*, 116, 5509 (1994).
20. R. Neumann, M. Gara, *J. Am. Chem. Soc.*, 117, 5066 (1995).
21. SADABS, SMART, SAINT and SHELXTL, Bruker AXS Inc., Madison, Wisconsin, USA, (2000).
22. G. M. Sheldrick, SHELX-97, *Program for Crystal Structure Solution and Analysis*, University of Gottingen, Gottingen, Germany, (1997).
23. I. D. Brown, D. Altermatt, *Acta. Crystallogr., Sect. B*, 41, 244 (1985).
24. U. Kortz, I. M. Mbomekalle, B. Keita, L. Nadjo, B. Patrick, *Inorg. Chem.*, 41, 6412 (2002).
25. L.-H. Bi, E. Wang, J. Peng, R. D. Huang, L. Xu, C. W. Hu, *Inorg. Chem.*, 39, 671 (2000).
26. R. Contant, R. Thouvenot, *Can. J. Chem.*, 69, 1498 (1991).
27. R. Neumann, M. Dahan, *J. Am. Chem. Soc.*, 120, 11969 (1998).
28. P. Shringarpure, A.Patel, *Ind. Engg. Chem. Res.*, 50, 9069 (2011).
29. N. Mizuno, K. Yamaguchi, K. Kamata, *Coord. Chem. Rev.*, 249, 1944 (2005).
30. P. Shringarpure, A. Patel, *J. Mol. Chem. A*, 321, 22 (2010).

Main Conclusion

- Synthesis of Mn(II) substituted phosphotungstate *using an easy, simple and straightforward in-situ "one pot" approach.*
- This synthetic approach may open up a new synthetic route for TMSPOMs (mono, di and tetra-substituted sandwich type POMs) directly from commercially available Keggin analogue.
- The use of all synthesized complexes as catalysts were established for the solvent free oxidation of alkenes under mild reaction conditions.
- $PW_{11}Mn$ is an efficient catalyst for selective oxidation of styrene to benzaldehyde.
- PW_9Mn_4 is an efficient catalyst for selective epoxidation of styrene as well as cyclic alkenes.
- All the catalysts were regenerated and reused successfully upto two cycles. They could also be used for more number of cycles.
- The oxidation of styrene follows first order in presence of H_2O_2 as an oxidant for all the catalysts.

PART B

Functionalization of Transition Metal Substituted Polyoxometalates

CHAPTER

5

Introduction

The tailoring and synthesis of Functionalized (organic–inorganic hybrid) materials constructed from distinctive building blocks represents an outstanding research area in inorganic chemistry, coordination chemistry, crystal engineering and materials science, which is of great interest owing to their extensive theoretical and practical applications in molecular recognition, non-linear materials, absorption, magnetic and photosensitive materials [1-13]. In this field, an efficient and widely adopted route with interesting and meaningful properties is the combination of multiple well defined inorganic building blocks and organic moieties, generally by synergetic interactions [14-16].

In this regards, POMs can act as an excellent inorganic multidentate O-donor ligands to assemble various inorganic–organic hybrid compounds with a vast range of structural properties. The obtained materials having potential applications in the fields of medicine, magnetism, optics, biology and catalysis [17-19].

The concept of functionalized materials has been explored and applied to either non-crystalline materials isolated under mild synthetic conditions following the method of 'Chimie Douce' [20, 21] or crystalline materials synthesized at room temperature or under hydrothermal conditions [22-24]. The structure and properties obtained from such materials depend on the nature of both the components. In the field of catalysis, the study of functionalized materials based on POMs can help in understanding the nature of interactions between organic moiety and the surface of oxides and lead to more efficient recyclable multifunctional catalysts. The synthesis of such functionalized materials can result in the formation of amorphous or crystalline materials that are isolated under mild conditions or under hydrothermal conditions.

Functionalized materials can be mainly of two classes depending upon nature of the interaction between the organic and inorganic components [25] (Figure 1).

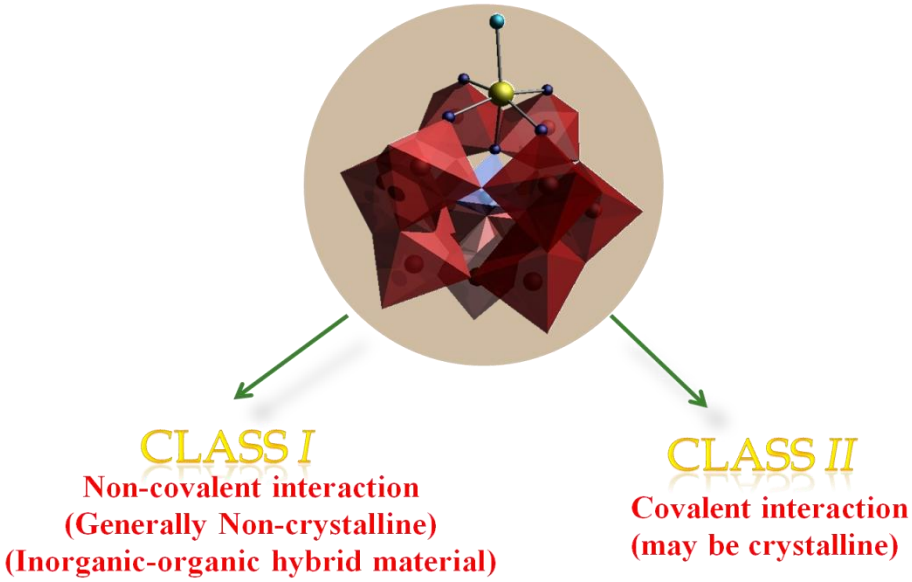

Figure 1. Nature of Interaction

Class I gathers all the complexes where no covalent bonds are shared between the organic and the inorganic moieties. Only electrostatic interactions, hydrogen bonds, or van der Waals interactions are involved. In the class II, the organic and inorganic moieties are linked via strong covalent or iono-covalent bonds.

Functionalization of POMs with organic moiety remains a synthetic challenge, as the two parts (the POMs and the organic functionalizing moiety) present very different chemical and structural properties.

Four different strategies were explored to date for the synthesis of functionalized material based on POMs [26, 27].

(I) Coordination competition

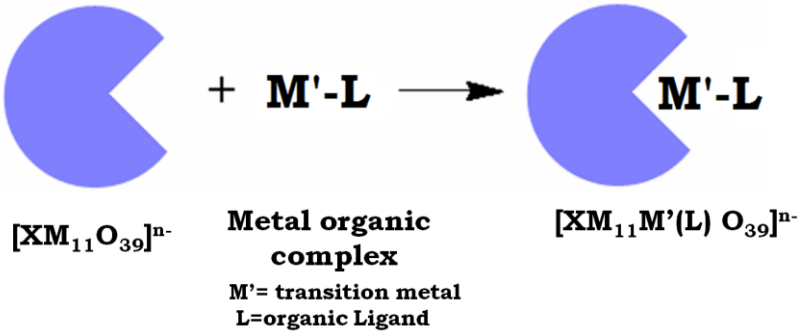

Figure 2. Coordination competition

This approach consists of lacunary POMs (LPOMs) as ligands. These LPOMs react with organic metal complexes through coordination competition (Figure 2) to form new POMs coordinated metal complexes [28-30].

(II) Terminal modification

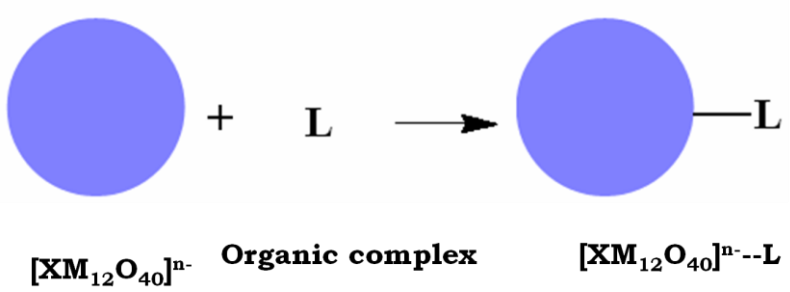

Figure 3. Terminal modification

This route involves modification of the POMs surface by substituting terminal O atoms of POMs with organic species (Figure 3). Generally, such kind of synthesis was carried out in organic solvents [16, 31, 32].

(III) In situ synthesis

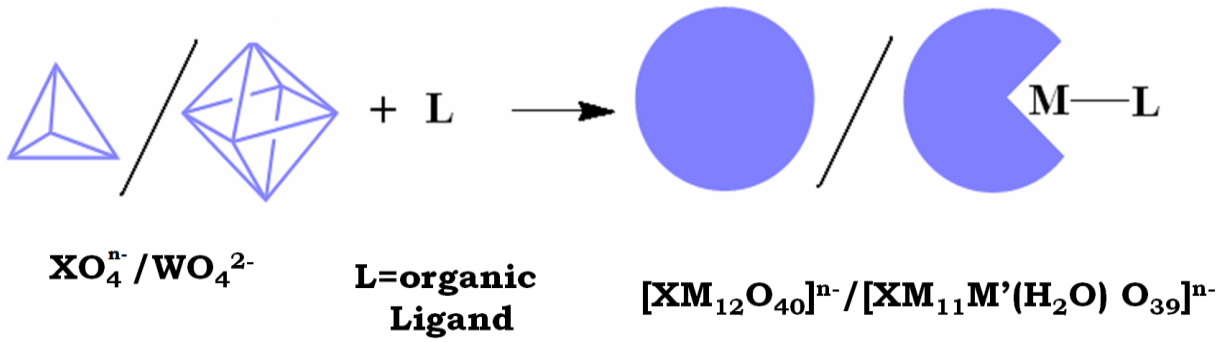

Figure 4. In-situ synthesis

This strategy consists of self-condensation of the simple inorganic and organic units (sometimes pre-synthesized POMs/TMSPOMs) (Figure 4). Most of the successful syntheses using this route were carried out under hydrothermal conditions [33, 34].

(IV) Ligand substitution

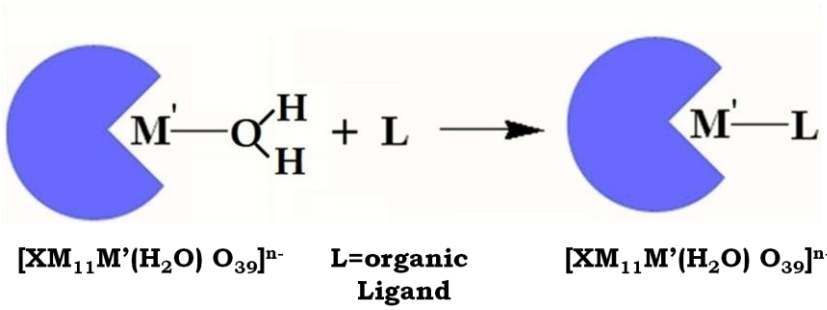

Figure 5. Ligand substitution

This method consists of TMSPOMs as starting materials. In TMSPOMs the transition metal is coordinated with available five oxygen atoms of the POMs, while the sixth coordination site on the metal is occupied by an aqua ligand. Thus aqua ligand is labile and can be replaced by any organic group or even by organometallic groups [35 - 40].

Due to the numerous papers in this field, we will focus our attention only on the functionalization of mono transition metal substituted Keggin type POMs with targeted properties and emergent applications in the field of catalysis.

In 1970, Baker and Figgis [37] first studied substitution of the coordinated water molecule by ammonia and pyridine in cobalt substituted silicotungstate, $[SiW_{11}Co^{X}(L)O_{39}]^{n-}$ (X= II, n = 6; X = III, n = 5, L= ammonia or Pyridine) and characterized by ligand-field spectra, elemental analysis, redox titration, potentiometric titration, cryoscopy and polarography. After wards, in 1973 Weakley studied replacement of aqua ligand by pyridine and ammonia in cobalt and nickel substituted POMs, $[XW_{11}M(H_2O)\ O_{39}]^{n-}$ (X= P, B, As ; M= Co(II), Co(III) and X=P; M=Ni(II)) using diffuce reflectance spectra [38]. Klemperer et. al. reported solid oxide-supported organometallic derivative of titanium substituted phosphotungstate, $[PW_{11}Ti^{IV}(C_5H_5)O_{39}]^{4-}$ by reacting lacunary phosphotungstate and $Ti^{IV}(C_5H_5)$ and charcaterized by ^{17}O NMR and IR spectroscopy [39].

Subsequently, replacement of the water molecule in iron substituted POMs, $[XW_{11}Fe^{III}(H_2O)O_{39}]$ (X=B, Si, Ge, P, As) by various inorganic groups ($[Fe(CN)_6]^{4-}$, SCN-, SO_3^{2-}) was studied by Zonnevijlle and Tourne´[40]. In 1986 Keana et al. functionalized Ti(IV)-substituted POMs using cyclopentadienyl group [41,42] and characterized using various spectroscopic techniques.

In 1992 Pope group studied substitution of water molecules in ruthenium substituted phosphotungstate ($[PW_{11}Ru(H_2O)O_{39}]^{4-}$) using pyridine, sulfoxides, dialkyl sulfides, and various active alkenes (maleic, fumaric, crotonic acids, 1-4-dihydroxybut-2-ene) and characterized by electronic absorption spectroscopy and NMR spectroscopy (^{31}P and ^{183}W) [43].

So and Co-workers reported complexes of TMSPOMs ($[SiW_{11}M(H_2O)O_{39}]^{n-}$ ($M=Co^{II}$ and Ni^{II})) with nitrogeneous ligand (pyridine or imidazole) and studied by means of ^{1}H NMR [44-46]. Wei and Pope isolated functionalized POMs $[XW_{11}O_{39}RhCH_2COOH]$ (where X=P, Si) with Rh-C bonds under hydrothermal condition and characterized by means of X-ray analysis and NMR spectroscopy (^{31}P and ^{183}W) [47].

In 2000 Bonchio and co-workers reported fast and selective method for replacement reaction towards $[PW_{11}Ru^{II}(DMSO)O_{39}]^{5-}$ [48] using $[PW_{11}O_{39}]^{7-}$ with cis-$[Ru(DMSO)_4Cl_2]$ in water, under microwave irradiation.

Peng group reported various functionalized materials comprising transition metal substituted silicotungstate ($[SiW_{11}MO_{39}]^{n-}$, where M= Mn(II), Co(II), Ni(II) and Zn(II)) with $H_3P_2O_7$ and H_2PO_4 as pendant ligand [49, 50]. Zorrilla and Lezama studied functionalized polymeric POMs made up of copper-oxalate dimers and POMs entities by means of X-ray analysis and magnetic susceptibility [51].

Proust and co-workers reported the synthesis of nitride functionalized POMs $[PW_{11}O_{39}(MN)]^{n-}$ (M= Os, Re) [52] and organiimido functionalized POMs $[PW_{11}O_{39}\{Re^{V}NPh\}]^{4-}$ (Ph= C_6H_5) in presence of triethylene amine [53].
Further, the same author reported reactivity of $[PW_{11}O_{39}]^{7-}$ towards $[Ru^{II}(arene)Cl_2]_2$ (arene= benzene, toluene, *p*-cymene, hexamethylbenzene) leads to the formation of monomeric or dimeric compounds [54, 55] where, cationic $\{(arene)Ru(H_2O)\}^{2+}$ groups are covalently bound to the nucleophilic oxygen atoms of lacunary phosphotungstate.

Zorrilla and Lezama in 2005 reported effect of alkaline acetate/acetic acid buffer solution nature on the dimensionality of a series of functionalized compounds, comprising copper substituted POMs and copper(II)-bipyridine-oxalate complexes [56]. In the same year Peng et al. crystallize a new derivative of rare organic capped-structure of phosphotungstate with a pendant π-conjugated organic ligand, $([PW_{11}O_{39}Co^{II}(pbpy)]^{5-}$ (pbpy)5-phenyl-2-(4-pyridinyl)pyridine) [57]. They also found that the organic ligand was not only capable of functionalizing POMs, but also assembling POMs clusters into the supramolecular framework under hydrothermal conditions.

Kortz et. al. reported unusual bipodal attachment of an organometallic moiety to ruthenium substituted silico and germane tungstate ($[Ru^{II}(DMSO)_3(H_2O)\text{-}XW_{11}O_{39}]^{6-}$, X= Si, Ge) and characterized the complexes using single crystal XRD and multinuclear NMR (^{183}W, ^{13}C, ^{1}H, ^{29}Si) [58]. Further, Sadakane and Kortz provided the crystallographic evidence for the DMSO derivative of ruthenium substituted silicotungstate $[SiW_{11}Ru^{III}(DMSO)O_{39}]^{5-}$ with large excess of dmso, isolated by heating the aqua derivative [59].

Proust and co-workers synthesized functionalized POMs of ruthenium-nitrido derivative $[PW_{11}O_{39}\{Ru^{VI}N\}]^{4-}$ [60] by reacting $[PW_{11}O_{39}]^{7-}$ and $[Ru^{VI}NCl_5]^{2-}$ or $[Ru^{VI}NCl_4]^{-}$ and characterized the complex using multinuclear NMR (^{31}P and ^{183}W NMR) together with an EXAFS, XANES analysis. Further, the same group explored the potentiality of nitrido derivative of phosphotungstate $[PW_{11}O_{39}\{Ru^{VI}N\}]^{4-}$ compound in N-atom transfer reactions to release bis(triphenylphosphane) iminium cation [60]. Proust and co-workers isolated two other closely related species $[(Ru^{III}N(OH)PPh_3)PW_{11}O_{39}]^{4-}$ and $[(Ru^{III}OPPh_3)PW_{11}O_{39}]^{4-}$ while working with ruthenium-nitrido derivative [61].

In 2008 Sadakane and Kortz reported carbonyl–ruthenium substituted undecatungstosilicate $[SiW_{11}O_{39}Ru^{III}(CO)]^{5-}$ and represents the first example of metal–carbonyl moiety being fully incorporated into the POMs by means of various spectroscopic techniques [62].

Afterwards Peng group provided complete structural analyses of functionalized complexes (($[SiW_{11}M(L)O_{39}]^{n-}$ (where M=Ni(II), Mn(II), Co(II) and L = imidazole and 4,4' bipyridine) comprising transition metal substituted silicotungstate with imidazole and 4,4'-bipyridine as pendant ligands [27, 63] using coordination competition approach. Poblet et. al. provided reactivity of various transition metal nitrido POMs derivative by means of DFT calculations. [64]. Pope et. al. recorded EPR spectra of a series of Ru-containing compounds $[PW_{11}Ru^{III}(L)O_{39}]^{5-}$, (where L=$H_2O$, pyridine or DMSO) and suggested S-type coordination mode of the DMSO molecule to the Ru center [65]. Wang and co-workers synthesized two enantiomerical chainlike POMs (D and L) $[Cu(en)_2]$-$[Cu(en)_2(H_2O)_2][SiW_{11}CuO_{39}]$ (where en=ethylene diamine) and suggested the presence of asymmetric coordination of metal-organic units is responsible for chirality in the POMs chain [66].

Proust group reported stable manganese(V)-nitrido POMs derivative $[PW_{11}O_{39}\{Mn^{V}N\}]^{5-}$ [67] synthesized by means of photochemical activation of the manganese(III)-azido derivative $[PW_{11}O_{39}Mn^{III}N_3]^{5-}$. The same group reported potentiality of chromium(V)-nitrido derivative $[PW_{11}O_{39}\{CrN\}]^{5-}$ towards trifluoroacetic anhydride and forming the acylimido derivative $[PW_{11}O_{39}\{Cr^{V}NCOCF_3\}]^{4-}$ [68].

Thouvenot and co-workers proved coordination interaction between POMs-porphyrin complex by means of steady-state and time-resolved luminescence measurements and ^{1}H NMR [69]. Proust and co-workers in 2011 extended the concept of N-atom transfer from the electrophilic ruthenium(VI) nitrido containing POMs to the N-heterocyclic carbene $\{CH_2(Mes)N\}_2C$ to synthesized functionalized ruthenium(III)-containing POMs $[PW_{11}O_{39}Ru^{III}\{NC\{N(Mes)CH_2\}_2\}]^{5-}$ [70].

Recently, Sadakane and Kortz stabilized high-valence Ru(III)-substituted silicotungstates with pyridine based ligands,$[SiW_{11}O_{39}Ru^{III}(Py)]^{5-}$, (Py = pyridine, 4-pyridine-carboxylic acid, 4,4'-bipyridine, 4-pyridine-acetamide and 4-pyridine-methanol) and extensively studied using various spectroscopic techniques, XANES analysis and X-ray analysis [71].

A Literature survey shows that the group of Pope, Proust, Kortz, and Peng have significantly contributed towards the synthesis and characterization of functionalized POMs. However, no work has been reported on catalytic aspect of the same.

Meanwhile in 2003, Bar-Nahum and Neumann reported synthetic pathway for the synthesis, especially for organometallic-POMs functionalized compound, [72] in which, the two components are connected by an alkylene group (Scheme 1). A series of metallosalen (M-salen, M = Mn, Co, Ni, and Pd) compounds were attached to a Keggin type silico tungstate through an alkyl bridging spacer, and characterized by various spectral techniques. This synthesis method found to be most useful, especially when the synthesized complexes have been used for catalytic applications.

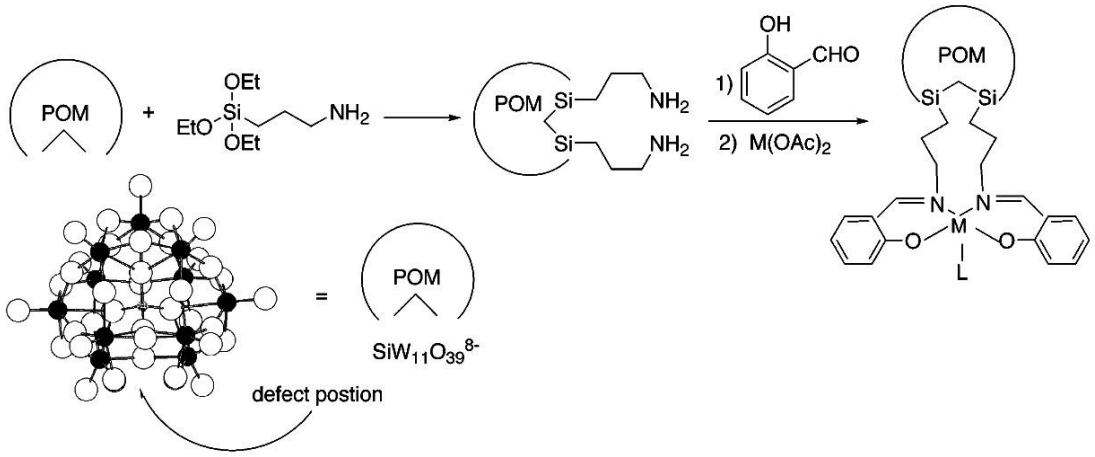

Scheme 1. Synthetic pathway for the preparation of the M-Salen-POMs Compounds [72]

Literature survey shows that, only Mirkhani group studied the catalytic properties of functionalized material of metallosalen-POMs (M-salen-POMs (M=Fe, Ni, Co, Cu and Mo)) complexes in homogeneous medium using hydrogen peroxide and tert-butyl hydroperoxide as an oxygen source in presence of solvent [73-77].

To the best of our knowledge, the reported articles in functionalized POMs comprising phosphotungstate as well as silicotungstates derivative with Ru, Co, Fe, Ti, Ni. At the same time studies on the phosphotungstates consist of Mn are very scarce. It also shows that no reports are available in the literature for oxidation reaction in solvent free condition. So, it was thought of interest, to functionalize the Mn(II)-substituted phosphotungstate with various organic ligands. The catalytic activity of synthesized functionalized materials was evaluated for oxidation of alkenes under

solvent free liquid phase conditions in presence of environmentally benign oxidants i.e. O_2 and H_2O_2.

Considering all the aspects, following work has been planned.

Objectives

1. To functionalize Mn(II) substituted phosphotungstate using various organic ligands via non-covalent and covalent approach.
2. To prove nature of interaction, various spectroscopic techniques were used.
3. To evaluate catalytic activity of synthesized functionalized material in solvent free liquid phase aerobic oxidation of styrene.
4. To study effect of functionalizing organic ligand in aerobic oxidation reaction.

Chapter 6 consist of functionalization of $PW_{11}Mn$ by salen while **Chapter 7** consist of functionalization $PW_{11}Mn$ by (S)-(+)-sec-butylamine and (R)-(-)-cyclohexylethylamine.

The synthesized complexes were characterized in solid as well as solution by various spectral techniques. The catalytic activity was evaluated for solvent free liquid phase aerobic oxidation of styrene using all synthesized complexes. Recycling, regeneration and heterogeneity test was carried out.

References

1. M. T. Pope, A. Muller (Eds.), *Polyoxometalates: From Platonic Solids to Anti-Retroviral Activity*, Kluwer, Dordrecht, The Netherlands, (1994).
2. Issue on "Polyoxometalates", *Chem. Rev.* 98, 1, (1998).
3. M. T. Pope, A. Muller (Eds.), Polyoxometalate Chemistry: From Topology via Self-Assembly to Applications, Kluwer, Dordrecht, (2001).
4. *Polyoxometalate Chemistry for Nano-Composite Design*, ed. T. Yamase, and M. T. Pope, Kluwer, Dordrecht, The Netherlands, (2002).
5. J. J. Borras-Almenar, E. Coronado, A. Mueller, M. T. Pope (Eds.), *Polyoxometalate Molecular Science*, Kluwer, Dordrecht, The Netherlands, (2004).
6. D. L. Long, E. Burkholder, L. Cronin, *Chem. Soc. Rev. 36*, 105, (2007).
7. D. Hagrman, P.Hagrman, J. Zubieta, *Angew. Chem., Int. Ed.*, 38, 3165, (1999).
8. P. Hagrman, D. Hagrman, J. Zubieta, *Angew. Chem., Int. Ed.*, 38, 2638, (1999).
9. D. Loy, K. Shea, *Chem. Rev.*, 95, 1431, (1995).
10. A. P. Wight, M. E. Davis, *Chem. Rev.*, 102, 3589, (2002).
11. C. R. Kagan, D. B. Mitzi, C. D. Dimitrakopoulos, *Science*, 286, 945, (1999).
12. H. J. Bolink, E. Coronado, J. Orozco, M. Sessolo, *Adv. Mater.*, 21, 79, (2009).
13. U. Kortz, F. Hussain,M. Reicke, *Angew. Chem. Int. Ed.*, 44, 3773, (2005).
14. A. Stein, B. Melde, R. Schroden, *Adv. Mater.*, 12, 1403, (2000).
15. P. Gomez-Romero, *Adv. Mater.*, 13, 163, (2001).
16. Z. H. Peng, *Angew. Chem., Int. Ed.*, 43, 930, (2004).
17. A. Dolbecq, E. Dumas, C. R. Mayer, P. Mialane, *Chem. Rev.*,110, 6009, (2010)
18. A. Proust, B. Matt, R.Villaneau, G. Guillemot, P. Gouzerh, G.Izzet, Coord. Chem. Rev., DOI 10.1039/c2cs35119f

19. D. L. Long, R. Tsunashima, L. Cronin, *Angew. Chem., Int. Ed.*, 49, 1736, (2010).
20. D. A. Loy, K. J. Shea. *Chem. Rev.* 95, 1431, (1995).
21. J. P. Corriu, *Eur. J. Inorg. Chem.* 1109, (2001).
22. A. Bagno, M. Bonchio, A. Sartorel, G. Scorrano, *Eur. J. Inorg. Chem.,* 17, (2000).
23. C. Dablemont, A. Proust, R. Thouvenot, C. Afonso, F. Fournier, J. C. Tabet, *Inorg. Chem.* 43, 3514, (2004).
24. V. L. Lahootun, C. Besson, R. Villanneau, F. Villain, L. M. Chamoreau, K. Boubekeur, S. Blanchard, R. Thouvenot, A. Proust, *J. Am. Chem. Soc.,* 129, 7127, (2007).
25. C. Sanchez, F. Robot, *New. J. Chem.* 18, 1007, (1994).
26. P. Gouzerh, A. Proust, *Chem. Rev.* 98, 77, (1998).
27. H. liu, C.J. Gomez-Garcia, J. Peng, J. Sha, Y. Li, Y. Yan, *Dalton Trans.* 6211, (2008).
28. J. C. Duhacek, D. C. Duncan, *Inorg. Chem.*, 46, 7253, (2007).
29. C. Dablemont, A. Proust, R. Thouvenot, C. Afonso, F. Fournier, J. C. Tabet, *Inorg. Chem.*, 43, 3514, (2004).
30. K. Nomiya, H. Torii, K. Nomura, Y. Sato, *J. Chem. Soc., Dalton Trans.*, 1506 (2001).
31. Q. Li, Y. G. Wei, J. Hao, Y. L. Zhu, L. S. Wang, *J. Am. Chem. Soc.*, 129, 5810, (2007).
32. H. Kang, J. Zubieta, *J. Chem. Soc., Chem. Commun.*, 1192, (1988).
33. Y. Lu, Y. Xu, E. B. Wang, J. Lu, C. W. Hu, L. Xu, *Cryst. Growth Des.*, 5, 257, (2005).
34. X. Y. Wei, M. H. Dickman, M. T. Pope, *Inorg. Chem.*, 36, 130, (1997).
35. C. Rong, M. T. Pope, *J. Am. Chem. Soc.*, 114, 2932, (1992).
36. O. A. Kholdeeva, T. A. Trubitsina, G.M.Maksimov, A. V. Golovin, R. I. Maksimovskaya, *Inorg. Chem.*, 44, 1635, (2005).

37. L. C. W. Baker, J. S. Figgis, *J. Am. Chem. Soc.*, 92, 3794, (1970).
38. T. J. R. Weakley, *J. Chem. Soc., Dalton Trans.* 341, (1973).
39. R. K. C. Ho, W. G. Klemperer, *J. Am. Chem. Soc.,* 100, 6772, (1978).
40. F. Zonnevijlle, C. M. Tourne, G. F. Tourne, *Inorg. Chem.*, 22, 1198, (1983).
41. J. F. W. Keana, M. D. Ogan., *J. Am. Chem. Soc.*, 108, 7951, (1986).
42. J. F. W. Keana, M. D. Ogan, L. U. YiXin, M. Beer, J. Varkeyt, *J. Am. Chem. Soc.*, 108, 7957, (1986).
43. C. Rong, M. T. Pope, *J. Am. Chem. Soc.*, 114, 2932, (1992).
44. M. Ko, G. I. Rhyu, H. So, *Bull. Korean. Chem. Soc.*, 14, 500, (1993).
45. J. Y. Kim, S. M. Park, H. So, *Bull. Korean. Chem. Soc.*, 18, 369, (1997).
46. J. Park, J. Y. Kim, H. So, J. Liu, *Inorg. Chim. Acta.,* 319, 8, (2001).
47. X. Wei, M. H. Dickman, M. T. Pope, *J. Am. Chem. Soc.,* 120, 10254, (1998).
48. A. Bagno, M. Bonchio, A. Sartorel, G. Scorrano, *Eur. J. Inorg. Chem.*, 17 (2000).
49. J. Peng, W. Li, E. Wang, Q. Bai., *J. Chem. Soc.*, *Dalton Trans.*, 3668, (2001).
50. J. Peng, H. Y. Ma, Z. G. Han, B. X. Dong, W. Z. Li, J. Lu, E. B. Wang., *Dalton. Trans.*, 3850, (2003).
51. S. Reinoso, P. Vitoria, L. Lezama, A. Luque, J. M. Gutierrez-Zorrilla., *Inorg. Chem.*, 42, 3709, (2003).
52. H. Kwen, S. Tomlinson, E. A. Matta, C. Dablemont, R. Thouvenot, A. Proust, P. Gouzerh, *Chem. Comm.*, 2970, (2002)
53. C. Dablemont, A. Proust, R. Thouvenot, C. Afonso, F. Fournier, J. C. Tabet, *Inorg. Chem.,* 43, 3514, (2004).
54. V. Artero, D. Laurencin, R. Villanneau, R. Thouvenot, P. Herson, P. Gouzerh, A. Proust, *Inorg. Chem.*, 44, 2826, (2005).
55. D. Laurencin, R. Villanneau, H. Gerard, A. Proust, *J. Phys. Chem. A*, 110, 6345, (2006).
56. S. Reinoso, P. Vitoria, J. M. Gutierrez-Zorrilla, L. Lezama, L. S. Felices, J. I. Beitia, *Inorg. Chem.*, 44, 9731, (2005).

57. Z. Han, Y. Zhao, J. Peng, H. Ma, Q. Liu, E. Wang, *J. Mol. Struct.*, 738, 1, (2005).
58. L. H. Bi, U. Kortz, B. Keita, L. Nadjo, *Dalton. Trans.*, 3184, (2004).
59. M. Sadakane, D. Tsukuma, M. H. Dickman, B. Bassil, U. Kortz, M. Higashijima, W. Ueda, *Dalton Trans.*, 4271, (2006).
60. V. L. Lahootun, C. Besson, R. Villanneau, F. Villain, L.M. Chamoreau, K. Boubekeur, S. Blanchard, R. Thouvenot, A. Proust, *J. Am. Chem. Soc.*, 129, 7127, (2007).
61. C. Besson, Y. V. Geletii, F. Villain, R. Villanneau, C. L. Hill, A. Proust, *Inorg. Chem.*, 48, 9436, (2009).
62. M. Sadakane, Y. Iimuro, D. Tsukuma, B. S. Bassil, M. H. Dickman, U. Kortz, Y. Zhang, S. Ye, W. Ueda, *Dalton Trans.,* 6692, (2008).
63. H. Liu, C. J. Gomez-Garcıa, J. Peng, J. Sha, L. Wang, Y. Yan, *Inorg. Chim. Acta*, 362, 1957, (2009).
64. S. Romo, N. S. Antonova, J. J. Carbo, J. M. Poblet, *Dalton Trans.*, 5166, (2008).
65. C. C. Rong, H. So, M. T. Pope, *Eur. J. Inorg. Chem.*, 5211, (2009).
66. H. fu, Y. G. Li, Y. H. Wang, X. L. Wang, X. J. Feng, E. B. Wang, *Inorg. Chim. Acta*. 362, 3231, (2009).
67. G. Izzet, E. Ishow, J. Delaire, C. Afonso, J. C. Tabet, A. Proust, *Inorg. Chem.*, 48, 11865, (2009).
68. V. Lahootun, J. Karcher, C. Courillon, F. Launay, K. Mijares, E. Maatta, A. Proust, *Eur. J. Inorg. Chem.*, 4899, (2008).
69. D. Schaming, C. Costa-Coquelard, I. Lampre, S. Sorgues, M. Erard, X. Liu, J. Liu, L. Sun, J. Canny, R. Thhouvenot, L. Ruhlmann, *Inorg. Chim. Acta.,* 363, 2185, (2010)
70. C. Besson, J. H. Mirebeau, S. Renaudineau, S. Roland, S. Blanchard, H. Vezin, C. Courillon, A. Proust, *Inorg. Chem.*, 50, 2501, (2011).
71. M. Sadakane, S. Moroi, Y. Iimuro, N. Izarova, U. Kortz, S. Hayakawa, K. Kato, S. Ogo, Y. Ide, W. Ueda, T. Sano, *Chem. Asian J.*, 7, 1331, (2012).
72. I. Bar-Nahum, H. Cohen, R. Neumann, *Inorg. Chem.*, 42, 3677, (2003).

73. V. Mirkhani, M. Moghadam, S. Tangestaninejad, I. Mohammadpoor-Baltork, N. Rasouli, *Inorg. Chem. Commun.*, 10, 1537, (2007).
74. V. Mirkhani, M. Moghadam, S. Tangestaninejad, I. Mohammadpoor-Baltork, E. Shams, N. Rasouli, *Appl. Catal. A*, 334, 106, (2008).
75. V. Mirkhani, M. Moghadam, S. Tangestaninejad, I. Mohammadpoor-Baltork, N. Rasouli, *Catal. Commun.*, 9, 219, (2008).
76. V. Mirkhani, M. Moghadam, S. Tangestaninejad, I. Mohammadpoor-Baltork, N. Rasouli, *Catal. Commun.*, 9, 2171, (2008).
77. M. Moghadam, V. Mirkhani, S. Tangestaninejad, I. Mohammadpoor-Baltork, M. Javedi, *Polyhedron.*, 29, 648, (2010).

CHAPTER

6

Functionalization of Manganese Substituted Phophotungstate by Salen: Synthesis, Spectroscopic Characterization and Liquid Phase Solvent free Oxidation of Styrene

- **Paper Published**

Supramolecule. Chem., 24, 149-156, (2012).

Supramolecular Chemistry
Vol. 24, No. 3, March 2012, 149–156

Taylor & Francis
Taylor & Francis Group

Synthesis, characterisation and catalytic activity of non-crystalline organic–inorganic hybrid material comprising Keggin-type manganese(II)-substituted phosphotungstate and salen

Ketan Patel, Pragati Shringarpure and Anjali Patel*

Chemistry Department, Faculty of Science, M.S. University of Baroda, Vadodara 390 002, India

(*Received 25 May 2011; final version received 24 October 2011*)

A new inorganic–organic hybrid material comprising Keggin-type mono manganese-substituted phosphotungstate and salen was synthesised. The synthesised hybrid material was systematically characterised by various physicochemical techniques such as elemental analysis, thermal gravimetric analysis, FT-IR, UV–vis, electron spin resonane, ^{1}H NMR, ^{13}C MAS NMR and ^{31}P NMR. The catalytic activity was evaluated for non-solvent liquid phase oxidation of styrene using O_2. The novelty of the present work lies in obtaining 42% conversion with 41% selectivity for styrene oxide with O_2 under solvent-free mild reaction conditions only in 4 h.

As mentioned earlier, functionalization is a matter for POMs reactivity and provides structural and spectroscopic model which display selective recognition of substrates as well as products [1-7]. While synthesizing such kind of hybrid material, the desired inorganic and organic units should not only stable in various reactions system but also possess controllable and operability structures for the production of new materials with unique properties and structures [8-11].

Schiff-base metal complexes represent excellent metal–organic candidates to fabricate various functional complexes due to their easily modified structures and various applications in the field of catalysis chemistry as well as bioinorganic chemistry [12-20]. Among numerous metal complexes, manganese schiff base catalysts are preferred because manganese itself is relatively nontoxic metal and superior for the selective oxidation of styrene, chiefly because of fewer side reactions over manganese complexes. Especially Mn(III) salen complexes have proven to be highly active and selective for epoxidation of alkenes[21-27].

Till the date, chemistry of Mn-Schiff-base and POMs both independently involved in numerous fields, but the reports about the combinations of these two interesting fields to generate new hybrid materials have been less explored. Neumann and coworkers reported hybrid compounds with two functional centers consisting of a metallosalen moiety (M-salen; M) Mn, Co, Ni, and Pd) connected by an alkylene bridging group to a lacunary Keggin type silicotungstate [28] and characterized by various spectroscopic techniques. Recently, Wang et al. reported functionalized aggregates of Anderson type of POMs and metal – schiff base [29] and provide first single-crystal structures of metal–schiff-base decorated POMs compounds. To the best of our knowledge, only Mirkhani group studied the catalytic properties of functionalized material of metallosalen-POMs (M-salen-POMs (M=Fe, Ni, Co, Cu and Mo)) complexes in homogeneous medium using hydrogen peroxide and tert-butyl hydroperoxide as an oxygen source in presence of solvent [30-34].

A Literature survey shows that limited efforts have been paid to combine unique physical and chemical properties of metal-salen and POMs to display applications in the field of materials science as well as catalysis. Most of the work was carried out with silicotungstates, and studies on the phosphotungstates are very less. So, it was thought of interest, to functionalize the Mn(II)-substituted phosphotungstate with an organic ligand, like salen, which would result in interesting catalytic properties.

In the present work, an attempt was made to synthesise a new non-crystalline functionalized material, comprising Keggin-type manganese substituted phosphotungstate ($PW_{11}Mn$) and salen (S). The synthesised functionalized compound was systematically characterised by elemental analysis, TGA, FT-IR, UV–vis, ESR, multinuclear NMR (^{1}H, ^{13}C MAS and ^{31}P NMR. This material was employed as catalysts for solvent free liquid phase oxidation of styrene using O_2 and H_2O_2 as oxidants under mild reaction conditions. Key reaction parameters such as amount of catalyst, reaction temperature and reaction time were evaluated to optimize the condition. Further, Oxidation of cyclohexene and cyclooctene was also carried out under optimized condition. But as no significant conversion was obtained, hence results have not been included.

6.1 Experimental section

Materials

All chemicals used were of A.R. grade. $Na_2WO_4.nH_2O$, Na_2HPO_4, NaOH, $MnCl_2{\cdot}4H_2O$, CsCl, acetone, ethylene diamine, salicyaldehdyde, styrene, cyclohexene, Cis-cyclooctene, 30% H_2O_2 and dichloromethane were obtained from Merck.

Synthesis of salen

The salen ligand (Schiff base) was synthesised followed by the reported method [35], by refluxing the ethanolic solution of the ethylenediamine and salicylaldehyde for 2h (Scheme 1).

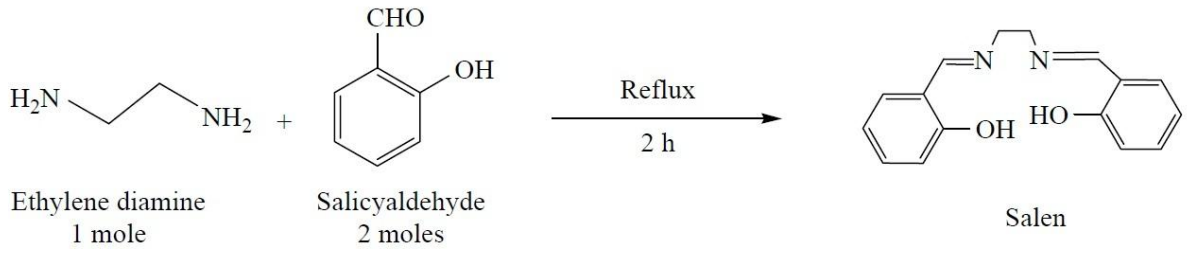

Scheme 1. Synthesis of S.

Synthesis of functionalized material ($PW_{11}Mn$--S)

The cesium salt of $PW_{11}Mn$ (0.8985 g, 0.04mmol) was dissolved in a minimum amount of water, and S (0.067 g, 0.04 mmol) was dissolved in a minimum amount of absolute alcohol. The alcoholic solution of S was added dropwise to the aqueous solution of $PW_{11}Mn$. The resultant mixture was refluxed for 10h with constant stirring, filtered to obtain pale yellow powder. The isolated material was washed with water as well as ethanol and dried at room temperature (35-40^oC) (Scheme 2).

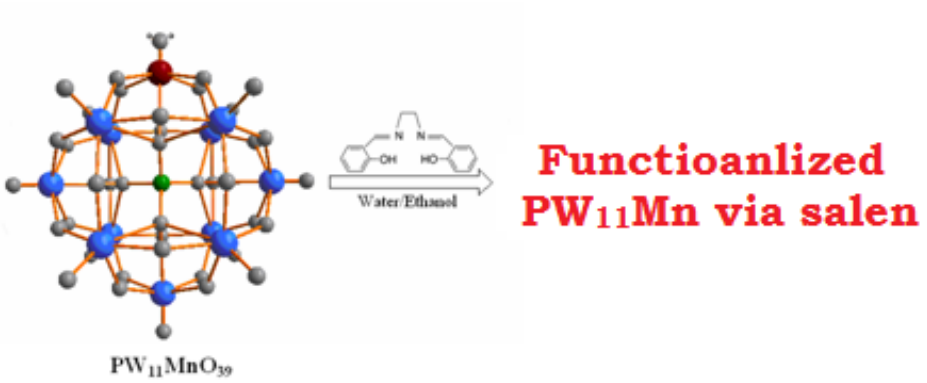

Scheme 2. Synthesis of $PW_{11}Mn$--S

Synthesis of physical mixture of $PW_{11}Mn$ and S

The physical mixture was synthesised by mixing equimolar amount of $PW_{11}Mn$ and salen. Salen(0.067 g, 0.04 mmol) and the caesium salt of $PW_{11}Mn$ (0.8985 g, 0.04mmol) were mixed and grinded properly in a mortar and pestle till it becomes homogeneous in nature. The obtained mixture was designated as $PW_{11}Mn$+S.

6.2 Characterisation

Elemental analysis was carried out using JSM 5610 LV combined with INCA instrument for EDX-SEM analyser for the quantitative identification of metal ions. C, H and N analyses were carried out using PerkinElmer 2400. The total weight loss was calculated by the TGA method on the Mettler Toledo Star SW 7.01 upto 6008C. FT-IR spectra of the samples were recorded as the KBr pellet on the PerkinElmer instrument. The UV–visible spectrum was recorded at an ambient temperature on PerkinElmer 35 LAMDA instrument using the 1 cm quartz cell. The ESR spectra was recorded on a Varian E-line Century series X-band ESR spectrometer (liquid nitrogen temperature and scanned from 2000 to 3200 Gauss). ^{1}H solution NMR was recorded in DMSO on Varian Mercury plus 300 instruments. ^{13}C MAS NMR was recorded on Bruker DSX 300MHz instrument. ^{31}P solution NMR was recorded in D_2O on Bruker ACF 300MHz instrument.

6. 3 Results and Discussion

6. 3.1 Spectroscopic Analysis

Elemental analysis

The observed values for S are in good agreement with the theoretical values. Anal Calc: C, 71.64; H, 5.97; N, 10.44. Found: C, 71.53; H, 5.94; N, 10.40. The values of elemental analysis data for $PW_{11}Mn$--S are in good agreement with the theoretical values. Anal Calc: Cs, 14.32; W, 54.50; P, 0.84; Mn, 1.48; O, 21.98; C, 5.1; H, 0.43; N, 0.75. Found: Cs, 14.28; W, 54.45; P, 0.81; Mn, 1.47; O, 21.49; C, 5.0; H, 0.43; N, 0.74.

The number of water molecules calculated from TGA curve shows 4.6% weight loss corresponding to loss of 10 water molecules. From the elemental as well as thermal techniques, the chemical formula of the isolated hybrid material is proposed as $Cs_5[PW_{11}O_{39}Mn\ (H_2O)]\cdot 9H_2O$--(S) .

FT-IR

The FT-IR stretching vibration for S, $PW_{11}Mn$ and $PW_{11}Mn$--S are presented in Table 1. The FT-IR spectrum of $PW_{11}Mn$--S shows that all the stretching vibrations correspond to P-O, W=O and W-O-W without any significant shift except in the W-O-W bridges. There was a slight shift from 820 to 813cm^{-1} observed in case of $PW_{11}Mn$--S. In addition to these vibrations, FT-IR spectrum can be helpful in obtaining structural information concerning the organic groups.

Table 1. FT-IR Frequency data

	P-O	**W=O**	**W-O-W**	**Mn-O**	**C-N**	**C=N**	**C-H**	**C-O**
$PW_{11}Mn$	1078 1053	956	882 820	507	-	-	-	-
S	-	-	-	-	1149	1634	1497 1459	1525
$PW_{11}Mn$--S	1077 1054	955	884 813	513 -	1150	1631	1496 1460	1545 -

A pair of the weak peaks at 1496 and 1460cm^{-1} was obtained for S and $PW_{11}Mn$--S, which is attributed to both symmetric- and asymmetric-

stretching vibrations of aliphatic C-H bonds. Furthermore, the stretching vibration of $PW_{11}Mn$--S for C-N, C=N and aliphatic as well as for aromatic CH_2 region can also be observed. The results ensure a successful functionalization of $PW_{11}Mn$ with salen. At the same time it has also been observed that there is a shift in the peak position from 1525 to 1545cm^{-1} corresponding to the C-O stretching vibration. This interesting observation indicates some interaction of salen with the $PW_{11}Mn$. It is well known that the POMs are polydentate ligand with high negative charge, which may favoured the formation of hydrogen bond. Hence, in the present case, it may be possible that the salen ligand gets bind to the large cluster of POMs via hydrogen bond.

UV-Visible

The UV–vis spectra of Mn(III)-salen (MnS) and $PW_{11}Mn$--S are shown in Figures 1 and 2. It is well known that metalation of salen ligand with Mn(II) yields the corresponding MnS complex distinctly identified by UV–vis as well as by colour (brown) [35]. As seen from the UV–vis spectra for MnS (Figure 1), two absorption bands were observed at 500 and 420 nm corresponding to the typical d–d transition band for MnS complex, indicating the presence of Mn(III) in the square pyramidal environment.

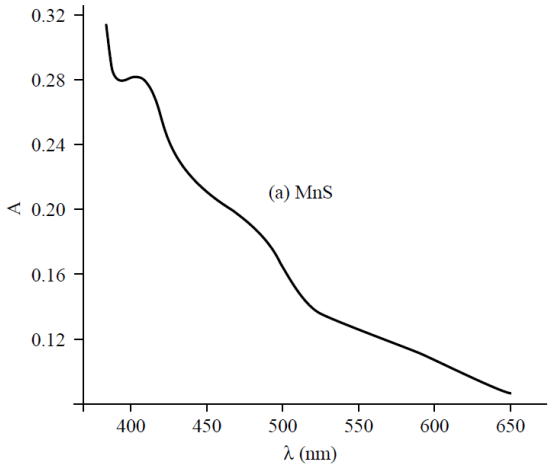

Figure 1. UV-Vis spectra of MnS

Whereas, UV–vis spectrum for $PW_{11}Mn$--S (Figure 2) shows two absorption bands, one strong at 291 nm corresponding to the $[PW_{11}O_{39}]^{7-}$

species. The other broad and weak absorption band at around 393-400 nm, associated with d–d transition, which is a typical value for Mn(II).

The absence of any absorption bands at 420 and 500 nm, which is the typical region for MnS complex, indicates that salen moiety is not covalently coordinated to the Mn centre. The presence of Mn(II) species was further confirmed by ESR spectroscopy.

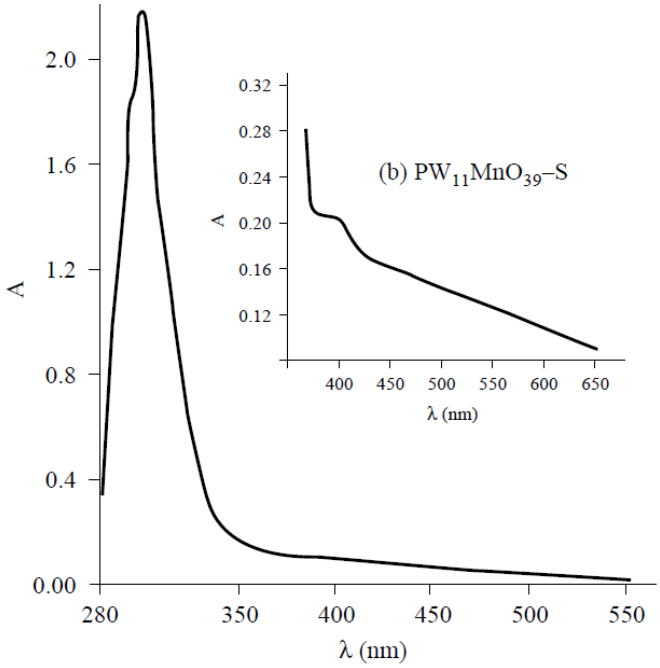

Figure 2. UV-Vis spectra of $PW_{11}Mn$--S

ESR

Paramagnetic compounds have different relaxation times. If the electronic relaxation is slow, good ESR spectra can be obtained at room temperature while, if the electronic relaxation is fast, good ESR spectra can be obtained only at low temperature. MnS compounds are known to be ESR silent in the normal X-band mode but absorb at g = 8 in the high-field ESR spectroscopy [28]. If salen is covalently coordinated to Mn, ESR is expected to be silent. However, a well resolved six line hyperfine spectrum for $PW_{11}Mn$--S indicating the presence of Mn(II) species (Figure 3). Thus UV–vis and ESR studies indicate the presence of salen in the synthesised material and support the observation drawn from FT-IR, i.e. the formation of the hydrogen bond.

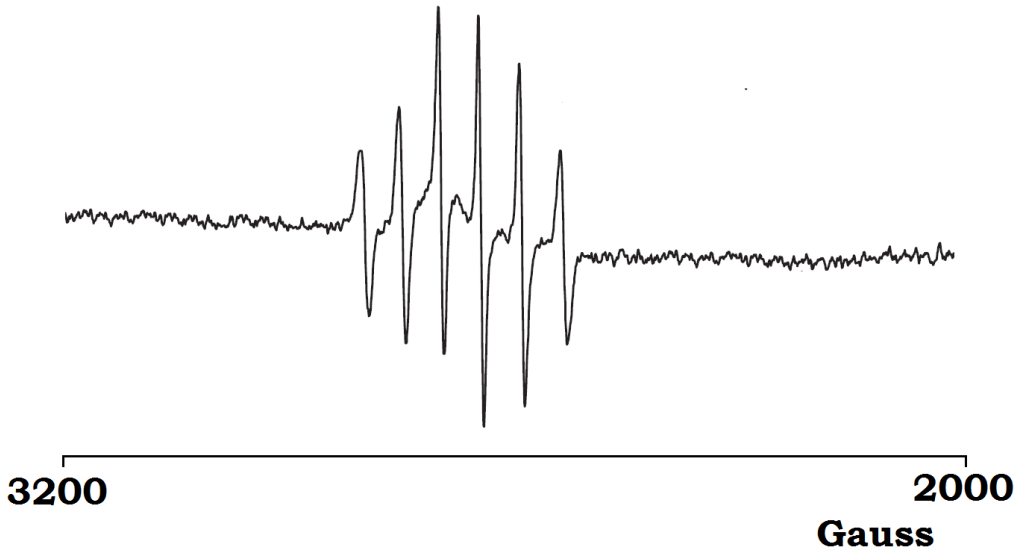

Figure 3. ESR Spectra of $PW_{11}Mn$--S

Magnetic spectroscopy

It is known that the presence of paramagnetic metal centre generally results in a poorly defined NMR spectrum. As mentioned earlier, for paramagnetic compounds electronic relaxation is fast, good ESR spectrum cannot be obtained at room temperature, while good NMR spectrum can be obtained at room temperature.

In order to study the interaction between $PW_{11}Mn$ species and the salen moiety, solution (^{1}H and ^{31}P) and solid (^{13}C) NMR spectra were recorded. The ^{1}H NMR spectrum of S and $PW_{11}Mn$--S was recorded in D_2O and $CDCl_3$ respectively (Figure 4a and 4b). The chemical shifts for all protons of the organic moiety (i.e. salen) in $PW_{11}Mn$--S did not show any significant shift as compared to S.

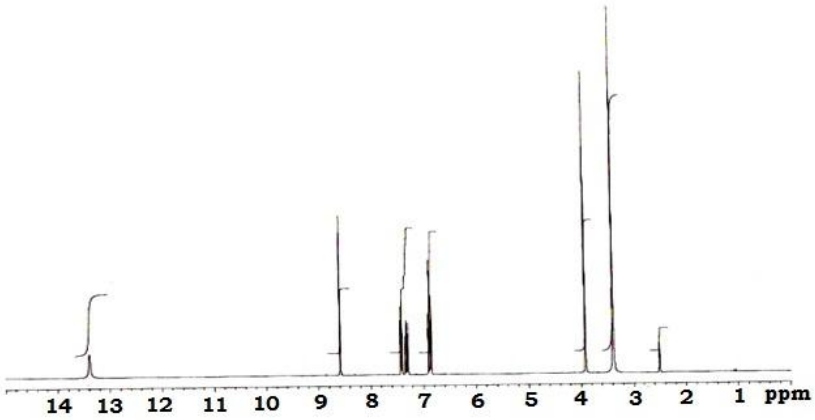

Figure 4a. ^{1}H NMR of S

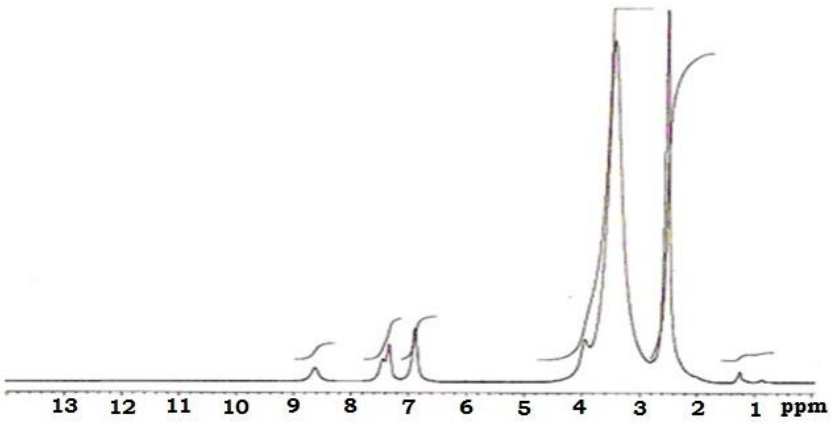

Figure 4b. ^{1}H NMR spectra of $PW_{11}Mn$--S

However, broadening of the signal in case of $PW_{11}Mn$--S is observed. If the Mn centre forms the covalent bond with the salen moiety, significant chemical shift is expected. The absence of any shift in the signals indicate that S is not coordinate to Mn but is present in the chemical environment of $PW_{11}Mn$ as an individual moiety. The chemical shift of the ^{13}C MAS NMR values for S and $PW_{11}Mn$--S (Figure 5) is presented in Table 2.

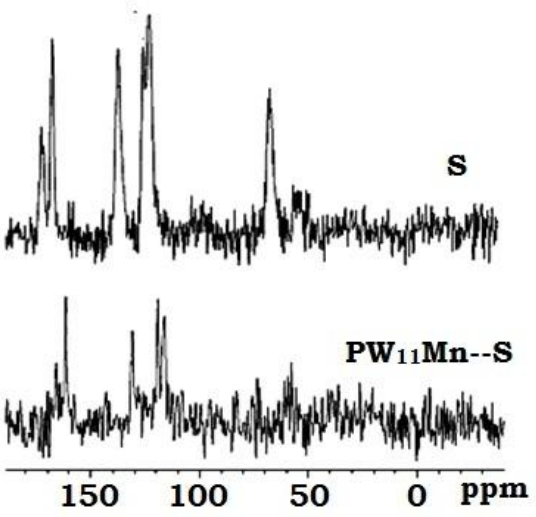

Figure 5. ^{13}C MAS NMR for S and $PW_{11}Mn$--S

Table 2. ^{13}C MAS NMR chemical shifts for S and $PW_{11}Mn$--S

Functional Group	**Chemical shift (ppm)**	
	S	**$PW_{11}Mn$--S**
CH_2 (bridge carbon)	54.81	57.82
CH_2 (ring carbon)	121.53	116.22
	124.4	119.20
	135.08	130.84
C-O	171.52	161.91
C=N	166.51	165.91

As shown in Table 2, the ring C atoms (-CH_2-) as well as C-OH were significantly shielded and appeared upfield with respect to the salen moiety.

A very significant shifting from +171.5 to +161.9 ppm can be attributed to the shift of the electron density from O-H of salen to the bridging O of $PW_{11}Mn$. It is known that for transition metal-substituted POMs, the bridging O atom is expected to generate basic sites and as a consequence they attract the protonated species towards them. In the present case, O-H of the S is attracted towards oxygen atoms of the $PW_{11}Mn$ and form hydrogen bond. Hence upfield shifts for the C atom of the C-OH are observed.

In addition to this, NMR signal of the C=N does not show any shift from the parent value. This indicates that the N atom of the salen does not coordinate with the Mn centre of $PW_{11}Mn$. Upon comparison of the ^{1}H and ^{13}C NMR spectrum of $PW_{11}Mn$--S, it was observed that the proton of the C-O-H group is not deprotonated. This observation indicates that the S moiety is not coordinated with the Mn of the $PW_{11}Mn$, but is intactly attracted towards $PW_{11}Mn$ via some chemical interaction. From the above study, it may be proposed that salen is present in the complex via H-bonding. The H of C-O-H from salen forms hydrogen bond with the bridging O of the Mn of the $PW_{11}Mn$ without disturbing the Mn-substituted Keggin structure.

The presence of intact Keggin unit is further supported by ^{31}P solution NMR (Figure 6). A strong single-line ^{31}P NMR spectrum δ = -13.7 ppm was obtained. The value of -13.7 ppm is the typical region for the mono metal-substituted Keggin type POMs, indicating the presence of intact Keggin unit. Thus spectral as well as the magnetic studies confirm the presence of strong H-bonding between S and $PW_{11}Mn$.

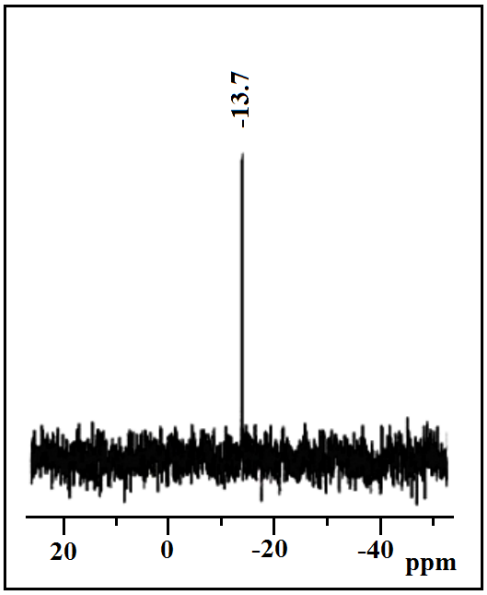

Figure 6. ^{31}P NMR Spectra of $PW_{11}Mn$--S

6.3.2 Catalytic activity

Oxidation of styrene using H_2O_2

A detail study was carried out on oxidation of styrene by varying different parameters such as mole ratio of styrene to H_2O_2, reaction temperature, catalyst amount and reaction time to get optimum reaction condition for oxidation of styrene. An experiment without catalyst was carried out and no conversion was obtained, indicating that there is no auto-oxidation taking place.

Effect of mole ratio

Oxidation of styrene was carried out by varying the mole ratio of Sty to H_2O_2 from 1:1 to 1:3. As presented in Figure 7, the oxidation of styrene increases from 62 to 100% upon increasing the styrene to H_2O_2 mole ratio from 1:1 to 1:3. Further increases in the amount of H_2O_2 from 1:3 to 1:4 did not result in the styrene conversion as well as selectivity of benzaldehyde. Therefore, 1:3 styrene to H_2O_2 mole ratio was considered the optimized condition for the oxidation of styrene.

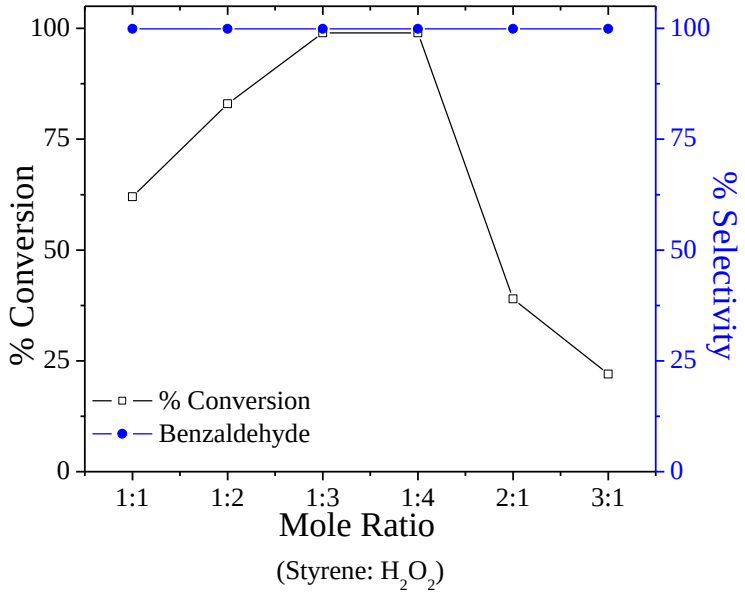

Figure 7. Effect of mole ratio on oxidation of styrene

Effect of amount of catalyst

The effect of catalyst amount on the conversion of styrene is demonstrated in Figure 8. The amount of catalyst was increased from 5 mg to 25mg, the conversion of styrene increased from 39 to 100%. With increase in the catalyst amount from 25mg to 30mg, the conversion and selectivity does not change. The obtained results clearly indicate that Mn functions as active sites for oxidation. However, 25mg can be considered sufficient enough to carry out the reaction and further, effect of reaction time and temperature was studied.

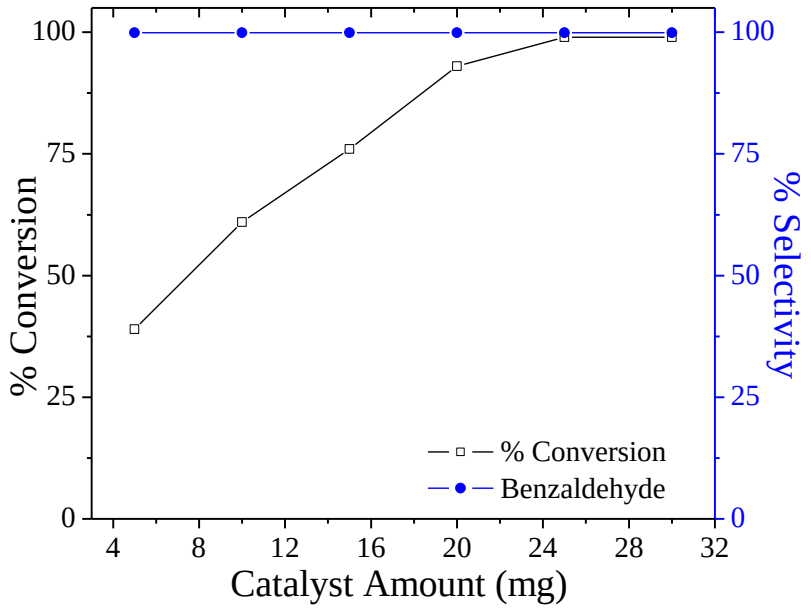

Figure 8. Effect of amount of catalyst on oxidation of styrene

Effect of reaction time

The effect of reaction time on the conversion was depicted in Figure 9 keeping other parameter constant. The degree of conversion increases with increases in reaction time. However within the time of 20h, 100% styrene conversion was observed. However, the selectivity to benzaldehyde remained unchanged throughout the entire reaction procedure. Due to the improved catalytic activity of $PW_{11}Mn$--S within the short period of time, 20h would be preeminent time period to carry out the oxidation of styrene.

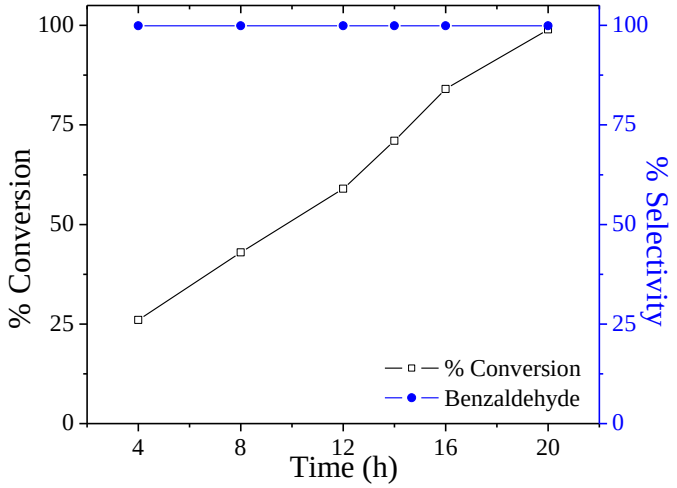

Figure 9. Effect of reaction time on oxidation of styrene using H_2O_2

The optimum conditions for 100% conversion with >99% selectivity for BA are; mole ratio of styrene to H_2O_2 as 1:3; catalyst amount = 25mg; reaction temperature = 80^{o}C and reaction time = 20h.

Regeneration and Recycling

The regeneration and recycling of the catalyst was carried out as mentioned in Ch-2 and the results for the same are presented in Table 3.

Table 3. Oxidation of styrene using hydrogen peroxide with fresh and regenerated catalyst

Catalyst	Conversion (%)	Selectivity (%) BA	TON
$PW_{11}Mn$--S	100	>99	1500
R1- $PW_{11}Mn$--S	98	>99	1470
R2- $PW_{11}Mn$--S	97	>99	1455

Conversion based on substrate: styrene (10mmole); oxidant, H_2O_2 (30mmole); catalyst amount, 25mg; temperature 80^oC; reaction time14h

$PW_{11}Mn$ gave 100% conversion in 14h whereas $PW_{11}Mn$--S gave 71% conversion with single selective product (i.e. BA) in 14h. This may be due to the fact that, Mn(II) sites are the catalytic active sites which are responsible for effective oxidation of styrene. In case of $PW_{11}Mn$--S, these active sites Mn(II) are surrounded by S moiety. As a result, the Mn(II) centre becomes sterically hindered. This steric hindrance around the active metal centre leads to the partial prevention of the oxidation process. In $PW_{11}Mn$ these Mn(II) active sites are easily available for oxidation reaction.

In case of $PW_{11}Mn$--S single selective product (i.e.BA) was obtained. This is because the reaction with H_2O_2 is fast and exothermic resulting in nucleophilic attack of H_2O_2 on StyO opens the ring and giving rise to BA. So, higher selectivity for BA was observed.

Oxidation of styrene using O_2

A detailed study on the oxidation of styrene with O_2 and TBHP (co-oxidant) was carried out to optimise conditions. A neat reaction (without catalyst) was carried out and it showed no conversion for the substrate, indicating that there is no auto-oxidation taking place.

Effect of amount of catalyst

The effect of the amount of catalyst on the conversion of styrene is represented in Figure 10. It is seen from the figure that the conversion increases up to 75 mg, after that it stays almost constant. The non-polar molecules such as hydrocarbons just adsorb on the surface without entering the bulk. Thus, on further increase in the amount, there may be blocking of the active sites and thus increase in conversion is not significant. This shows that it follows the adsorption phenomenon rather than the typical pseudo-liquid behaviour. In the present catalytic system, as the concentration of the catalyst increases the number of active sites available for the reaction to progress increases which results in a difference in the selectivity of products.

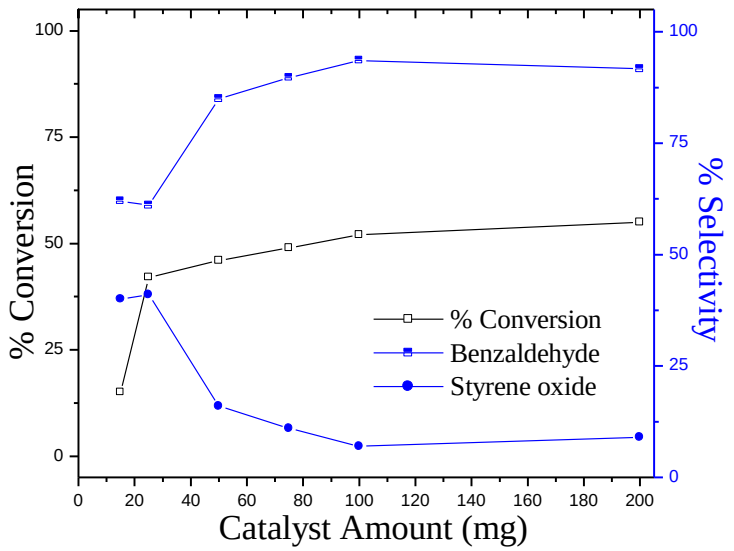

Figure 10. Effect of amount of catalyst

On further increase in the concentration of the catalyst the distribution of selectivity of products towards the more stable product (i.e. BA). Due to the known importance of epoxide, the amount of the catalyst was optimised at 25 mg. Furthermore, the effect of reaction time on oxidation of styrene was also studied.

Effect of reaction time

It is seen from Figure 11 that with the increase in reaction time the conversion also increases. Initially, the increase in the conversion is fast, and after 16 h a slow increase in the conversion is observed. This may be due to the fact that the styrene is consumed during the reaction, as a result the amount of the reactant decreases, which then requires time to reversibly bind with the oxidant. Furthermore, the rate of desorption of the products formed from the catalyst surface is faster, as a result the overall rate of the reaction slows down resulting in a slow increase in the conversion with time. As a result the overall rate of the reaction slows down and results in a slow increase in the percentage conversion with time.

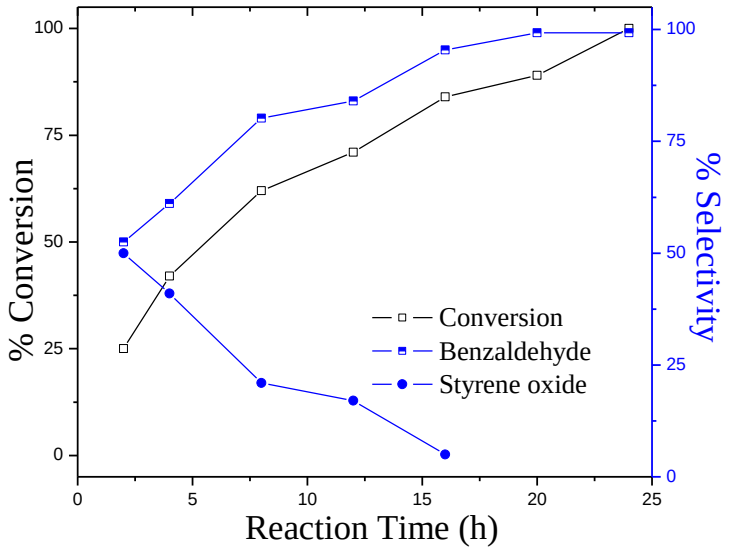

Figure 11. Effect of reaction time

The distribution of the product changes with increase in the reaction time. Initially, after the completion of 2h, the equimolar of both products

was observed. As the reaction time increases the product selectivity shifts towards BA. With an increase in the reaction time the unstable intermediate, epoxide, is converted to the more stable product BA. Due to the known industrial importance of styrene oxide, the reaction time was optimized at 4 h.

Effect of salen

Oxidation of styrene involves the formation of styrene oxide and BA. It is known that if the oxidation reaction is fast the product selectivity shifts towards the more stable product (BA) rather than the less stable intermediate (StyO). While if the reaction is slow and controlled, one styrene oxide is obtained as a major product. In order to see the effect of salen and to confirm the chemical interaction, the catalytic activity of $PW_{11}Mn$, MnS and the physical mixture ($PW_{11}Mn$+S) was evaluated for oxidation of styrene under the optimised conditions of $PW_{11}Mn$--S. The obtained results are represented in Table 4.

Table 4. Comparison of conversion and selectivity values for oxidation of styrene

Catalyst	**% Conversion**	**% Selectivity**	
		BA	**StyO**
*MnS	24	29	71
$PW_{11}Mn$	58	>99	-
$PW_{11}Mn$--S	42	59	41
$PW_{11}Mn$+S	56	>99	-

Styrene: 100mmol; amount of catalyst: 25mg; Oxidant: O_2(1 atm), TBHP:0.2 ml; reaction time:4h; temperature, 80°C

* Equivalent amount of catalyst was taken

As seen from Table 4, in case of MnS, only 24% conversion with 71% selectivity for styrene oxide and 29% selectivity for BA was obtained in 4h. However, 61% conversion with single selective product (i.e. BA) was obtained when $PW_{11}Mn$ was used as a catalyst in 4 h. On the other hand, moderate conversion of 42% was obtained for $PW_{11}Mn$--S with 41% selectivity towards

styrene oxide and 59% selectivity towards BA was obtained. The difference in the conversion as well as selectivity for the functionalized material can be explained on the basis of S. Mn(II) sites are the catalytic active sites which are responsible for effective oxidation of styrene. In case of $PW_{11}Mn$--S, these active sites Mn(II) are surrounded by S moiety. As a result, the Mn(II) centre becomes sterically hindered. This steric hindrance around the active metal centre leads to the partial prevention of the oxidation process. Hence, the overall reaction becomes a controlled reaction, resulting in the formation of styrene oxide.

Furthermore, the almost same conversion as well as selectivity towards BA for $PW_{11}Mn$+S and $PW_{11}Mn$ indicates the presence of salen as a separate moiety. Thus, for $PW_{11}Mn$+S, the salen moiety is free and not attached to $PW_{11}Mn$ via chemical interaction, as a result the Mn(II) active sites are easily available for oxidation which results in a single selective product with almost the same percentage conversion as that of $PW_{11}Mn$. The above data clearly indicates that the formed hydrogen-bonded molecular assembly (formed by salen and $PW_{11}Mn$) is the real active species responsible for selectivity towards styrene oxide. As seen from Table 4, $PW_{11}Mn$--S gives higher conversion as compared to MnS, while better selectivity towards epoxide than $PW_{11}Mn$. It is also observed from Figure 11 that the hybrid material gives 100% conversion with single selective product in 24 h. So the present catalyst is superior as compared to MnS and $PW_{11}Mn$. Thus, there is a choice for the chemists to select the reaction, with 100% conversion and single selective product or with 42% conversion and 41% selectivity towards styrene oxide.

Test for leaching and heterogeneity.

Any leaching of the active species makes the catalyst unattractive and hence it is necessary to study the stability as well as leaching of $PW_{11}Mn$--S. The catalyst was filtered after the completion of the reaction and the filtrate was characterised for UV–Visible spectroscopy. For comparison, UV–Vis spectra of $PW_{11}Mn$--S in water were also recorded (Figure 12). The absence of

characteristic peaks in filtrate (Figure 13) indicates that there is no leaching of $PW_{11}Mn$--S, and the catalyst remains completely insoluble under reaction condition and could be reused.

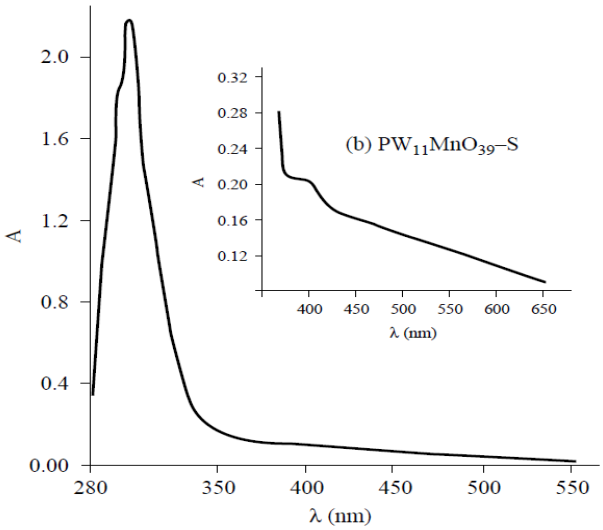

Figure 12. UV–vis spectra of $PW_{11}Mn$--S.

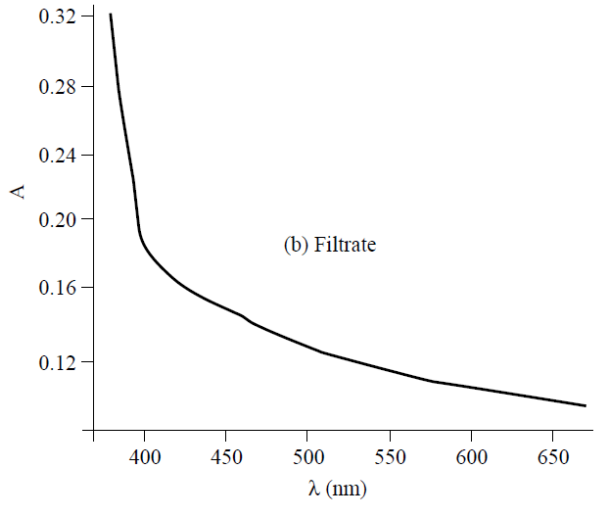

Figure 13. UV-Vis spectra of filtrate

Furthermore, for the rigorous proof of heterogeneity, a test was carried out by a filtering catalyst from the reaction mixture at 80°C after 2h and the filtrate was allowed to react up to 4h. The reaction mixture was kept for 2h and filtrate was analysed on gas chromatogram. No change in % conversion as well as % selectivity was observed. On the basis of the results, it can be

concluded that there is no leaching of the $PW_{11}Mn$--S, and the present catalysts are truly heterogeneous in nature and fall into the category C [36].

Regeneration and recycling

The catalyst remains insoluble in the present condition and hence can be easily separated by simple filtration followed by washing. As in present case, the amount of catalyst is very less (25 mg), hence recycling of the catalyst was not very efficient. There is difficulty in the collection of catalyst due to the loss during filtration. But if a large amount of catalyst is used, the recycling of the catalyst was significant. The recycle catalyst shows a decrease in the conversion value upto 3%, whereas the distribution of the products remains the same.

CONCLUSION

1. A new functionalized material was synthesized by non-covalent interaction that combines the unique physical and chemical properties of $PW_{11}Mn$ and salen.
2. Spectral and magnetic studies show that the Keggin unit retains its structure even after the introduction of S.
3. Based on FT-IR and multinuclear NMR (^{31}P, ^{1}H, ^{13}C) study, the interaction (Hydrogen bonding between hydrogen from salen and oxygen from $PW_{11}Mn$) and the structure has been proposed (Figure 14).

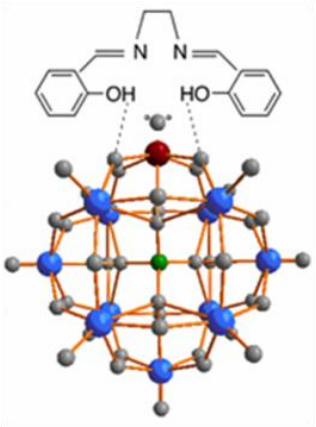

Figure 14 Functionalized $PW_{11}Mn$ via Salen

4. The presence of Mn^{II} was confirmed by FT-IR, UV-visibleas well as ESR .
5. The superiority of the present catalyst lies in obtaining 42 % conversion with 41% selectivity for styrene oxide using molecular oxygen in short period of time (4h).
6. The catalyst was regenerated and *reused up to 3* cycles after simple workup.
7. To prove the non-covalent interaction, *catalysis* is used as *one of the characterization method.*
8. It is a choice for the chemists to select the reaction, with 100% conversion and single selective product (BA) or with 42% conversion and 41% selectivity towards styrene oxide

References

1. M. T. Pope, A. Muller (Eds.), *Polyoxometalates: From Platonic Solids to Anti-Retroviral Activity*, Kluwer, Dordrecht, The Netherlands, (1994).
2. Issue on "Polyoxometalates", *Chem. Rev.* 98, 1, (1998).
3. M. T. Pope, A. Muller (Eds.), *Polyoxometalate Chemistry: From Topology via Self-Assembly to Applications*, Kluwer, Dordrecht, (2001).
4. Polyoxometalate Chemistry for Nano-Composite Design, ed. T. Yamase, and M. T. Pope, Kluwer, Dordrecht, The Netherlands, (2002).
5. J. J. Borras-Almenar, E. Coronado, A. Mueller, M. T. Pope (Eds.), *Polyoxometalate Molecular Science*, Kluwer, Dordrecht, The Netherlands, (2004).
6. D. L. Long, E. Burkholder, L. Cronin, *Chem. Soc. Rev.* ,36, 105, (2007).
7. D. Hagrman, P.Hagrman, J. Zubieta, *Angew. Chem., Int. Ed.*, 38, 3165, (1999).
8. A. Stein, B. Melde, R. Schroden, *Adv. Mater.*, 12, 1403, (2000).
9. P. Gomez-Romero, *Adv. Mater.*, 13, 163, (2001).
10. Z. H. Peng, *Angew. Chem., Int. Ed.*, 43, 930, (2004).
11. A. Dolbecq, E. Dumas, C. R. Mayer, P. Mialane, *Chem. Rev.*,110, 6009, (2010)
12. M. Hitoshi, C. Rodolphe, W. Wolfgang, L. Lollita, B. Claire, S. Kenichi , Y. Masahiro, *Angew. Chem., Int. Ed.*, 43, 2801, (2004).
13. K. C. Gupta, A. K. Sutar, *Coord. Chem. Rev.*, 252, 1420, (2008).
14. H. Miyasaka, A. Saitoh ,S. Abe, *Coord. Chem. Rev.*, 251, 2622, (2007).
15. W. Radecka-Paryzek, V. Patroniak, J. Lisowski, *Coord. Chem. Rev.*, 249, 2156, (2005).
16. P. Cozzi, *Chem. Soc. Rev.*, 43, 410, (2004).
17. F. Bedioui, *Coord. Chem. Rev.*, 144, 39, (1995).
18. M. Sigman, E. Jacobsen, *J. Am. Chem. Soc.*, 120, 4901, (1998).
19. J. Tchou, A. Grollman, *J. Biol. Chem.*, 270, 11671, (1995).
20. C. Buser, L. Thompson, B. Diner, G. Brudvig, *Biochemistry*, 29, 8977, (1990).

21. T. Hamada, T Fukuda, H. Imanishi, T Katsuki, *Tetrahedron.*, 52, 515, (1995).
22. F. Fache, E. Schulz, M. L. Tommasino, M. Lemaire, *Chem. Rev.*, 100, 2159, (2000).
23. W. Zhang, J. L. Loebach, S. R. Wilson, E. N. Jacobsen, *J. Am. Chem. Soc.*, 112, 2801, (1990).
24. K. Srinivasan, P. Michaud, J. K. Kochi, *J. Am. Chem. Soc.*, 108, 2309 (1986).
25. E. N. Jacobson, W. Zhang, M. L. Guler, *J. Am. Chem. Soc.*, 113, 6703, (1991).
26. T. Katsuki, *J. Mol. Catal: A. Chem.*, 113, 87, (1996).
27. W. Zhang and E. N. Jacobson, *J. Org. Chem.*, 56, 2296, (1991).
28. I. Bar-Nahum, H. Cohen, R. Neumann, *Inorg. Chem.*, 42, 3677, (2003).
29. Q. Wu, W. Chen, D. Liu, C. Liang, Y.G.Li, S. W. Lin, E. Wang, *Dalton.Trans.*, 40, 56, (2011).
30. V. Mirkhani, M. Moghadam, S. Tangestaninejad, I. Mohammadpoor-Baltork, N. Rasouli, *Inorg. Chem. Commun.*, 10, 1537, (2007).
31. V. Mirkhani, M. Moghadam, S. Tangestaninejad, I. Mohammadpoor-Baltork, E. Shams, N. Rasouli, *Appl. Catal. A*, 334, 106, (2008).
32. V. Mirkhani, M. Moghadam, S. Tangestaninejad, I. Mohammadpoor-Baltork, N. Rasouli, *Catal. Commun.*, 9, 219, (2008).
33. V. Mirkhani, M. Moghadam, S. Tangestaninejad, I. Mohammadpoor-Baltork, N. Rasouli, *Catal. Commun.*, 9, 2171, (2008).
34. M. Moghadam, V. Mirkhani, S. Tangestaninejad, I. Mohammadpoor-Baltork, M. Javedi, *Polyhedron.*, 29, 648, (2010).
35. A. R.Silva, C. Freire, B. de Castro, *New. J. Chem.*, 28, 253, (2004).
36. R. A. Sheldon, M. Walau, I. W. C. E. Arends, U. Schurdt, *Acc. Chem. Res.*, 31, 485, (1998).

CHAPTER

7

Functionalization of Manganese Substituted Phosphotungstate by various organic ligands: Synthesis, Spectroscopic Characterization and Solvent free Liquid Phase Oxidation of styrene

- **Papers Published**

Mat. Res. Bull. , 47, 425-431 (2012).

Inorg. CHim. Acta., 382, 79-83 (2012).

Materials Research Bulletin 47 (2012) 425–431

Contents lists available at SciVerse ScienceDirect

Materials Research Bulletin

journal homepage: www.elsevier.com/locate/matresbu

Keggin type inorganic–organic hybrid material containing Mn(II) monosubstituted phosphotungstate and S-(+)-sec-butyl amine: Synthesis and characterization

Ketan Patel, Anjali Patel *

Chemistry Department, Faculty of Science, M.S. University of Baroda, Vadodara 390 002, India

ARTICLE INFO

Article history:
Received 29 April 2011
Received in revised form 23 August 2011
Accepted 26 October 2011
Available online 6 November 2011

Keywords:
A. Inorganic compounds
C. Nuclear magnetic resonance (NMR)
D. Catalytic properties

ABSTRACT

A new inorganic–organic POM-based hybrid material comprising Keggin type mono manganese substituted phosphotungstate and enantiopure S-(+)-sec-butyl amine was synthesized in an aqueous media by simple ligand substitution method. The synthesized hybrid material was systematically characterized in solid as well as solution by various physicochemical techniques such as elemental analysis, TGA, UV–vis, FT-IR, ESR and multinuclear solution NMR (^{31}P, ^{1}H, ^{13}C). The presence of chirality in the synthesized material was confirmed by CD spectroscopy and polarimeter. The above study reveals the attachment of S-(+)-sec-butyl amine to Keggin type mono manganese substituted phosphotungstate through N → Mn bond. It also indicates the retainment of Keggin unit and presence of chirality in the synthesized material. An attempt was made to use the synthesized material as a heterogeneous catalyst for carrying out aerobic asymmetric oxidation of styrene using molecular oxygen. The catalyst shows the potential of being used as a stable recyclable catalytic material after simple regeneration without significant loss in conversion.

Inorganica Chimica Acta 382 (2012) 79–83

Contents lists available at SciVerse ScienceDirect

Inorganica Chimica Acta

journal homepage: www.elsevier.com/locate/ica

Functionalization of Keggin type manganese substituted phosphotungstate by *R*-(−)-1-cyclohexylethylamine: Synthesis and characterization

Ketan Patel, Anjali Patel*

Chemistry Department, Faculty of Science, M.S. University of Baroda, Vadodara 390002, India

ARTICLE INFO

Article history:
Received 31 August 2010
Received in revised form 29 September 2011
Accepted 5 October 2011
Available online 20 October 2011

Keywords:
Manganese
Phosphotungstate
R-(−)-1-Cyclohexylethylamine

ABSTRACT

A new chiral polyoxometalates based functionalized material comprising Keggin type mono manganese substituted phosphotungstate and enantiopure *R*-(−)-1-cyclohexylethylamine was synthesized in an aqueous media by simple ligand substitution method. The POM-based synthesized material was systematically characterized in solid as well as solution by various physicochemical techniques such as elemental analysis, TGA, UV–Vis, FT-IR, ESR and multinuclear solution NMR (^{31}P, ^{1}H, ^{13}C). The presence of chirality in the synthesized material was confirmed by CD spectroscopy and polarimeter. The above study reveals the attachment of *R*-(−)-1-cyclohexylethylamine to Keggin type mono manganese substituted phosphotungstate through N → Mn dative bond. It also indicates the retainment of Keggin unit and chirality in the synthesized material.

The increasing use of POMs in the fields of catalysis [1-9], material science [10-12] and biology [13, 14] has attracted the worldwide scientists to develop chiral POMs. The preparation of chiral POMs, or chiral structures including POMs, is consequently a goal for many polyoxometalate chemists, as it would provide ultimate control for the synthesis such complexes. Chirality in POMs can manifest itself in several distinct ways, and the development of organic hybrids creates even more possibilities. It can derive from stereogenic arrangements in the solid state or at the supramolecular level. The chiral POMs structure can be intrinsically chiral (chiral metal framework), or chirality can derive from *Functionalization of the organic ligands* or from introduction of stereogenic side-chains [15].

As number of strategies have been used for the synthesis of such functionalized materials based on POMs [16-19]. This includes transition metal-substituted POMs [20, 21], lacunary POMs [22-24], saturated POMs and simple inorganic units as the starting materials [25-27]. Since the POMs and organic moiety have different chemical and structural properties, their synthesis remains a challenge. The reported syntheses include hydrothermal conditions [28] self-assembly reactions starting with the minimal building blocks [25-27] or the use of organic solvent [29-32].

Wang and coworkers synthesized two enantiomerical pure POMs (D and L) $[Cu(en)_2]$-$[Cu(en)_2(H_2O)_2][SiW_{11}CuO_{39}]$ (where en=ethylene diamine) and with asymmetric coordination of metal-organic units [33].

In 2009 Peng et al. has synthesized the such functionaized materials, containing manganese substituted silicotungstate and imidazol as well as cobalt substituted silicotungstate and 4,4'-bipyridine as an antenna ligand and fully characterized by spectroscopically as well as crystallographycally [19, 34]. They have carried out the synthesis in aqueous media under normal bench conditions using *coordination competition approach*.

At the same time, synthesis using *ligand substitution approach* was not much used at all. Further, it was also found that no reports were available on the functionalization of $PW_{11}Mn$ with SBA and Cy. So, it was thought of interest to synthesize POMs based functionalized material using SBA and Cy by ligand substitution approach. As (S)-(+)-Secbutylamine (SBA)

and (R)-(-)-Cyclohexylethylamine (Cy) having N atom as potential coordination sites which may play important role to extend the structure with chiral centre, it was select as an organic ligand.

The present work consists of synthesis of a new functionalized material comprising Keggin type manganese substituted phosphotungstate and SBA and Cy by ligand substitution method. The synthesized functionalized material was systematically characterized by elemental analysis, TGA, UV-Vis, ESR, FT-IR, multinuclear NMR (^{1}H, ^{13}C, ^{31}P), CD Spectroscopy and Polarimeter. Oxidation of styrene was carried out by varying different parameters such as mole ratio of alkene to H_2O_2, catalyst amount, and reaction time. An attempt was made to use the synthesized functionalized material for carrying out asymmetric aerobic oxidation of styrene at ambient temperature under mild reaction condition. The catalyst was regenerated and reused. Further, Oxidation of cyclohexene and cyclooctene was also carried out under optimized condition. But as no significant conversion was obtained, hence result has not been included.

7.1 Experimental Section

Materials

All the chemicals used were of A. R. grade. $H_3PW_{12}O_{40}.nH_2O$, (Loba Chemie, Mumbai), NaOH, $MnCl_2.4H_2O$, CsCl, styrene, 30% H_2O_2 dichloromethane were obtained from Merck and used as received. (S)-(+)-secbutylamin (SBA) and (R)-(-)-cyclohexylethylamin (Cy) were obtained from Sigma and used as received.

Synthesis of POMs based functionalized material

(a) Synthesis of $PW_{11}Mn$-SBA

0.8985gm of $PW_{11}Mn$ was dissolved in 10 ml of distilled water. 0.1314 gm of SBA was dissolved in 15 ml of ethanol. The ethanolic solution of SBA was added drop wise to the aqueous solution of $PW_{11}Mn$. The pH of the solution was found to be 6.4. This resulted mixture was refluxed for 10 h and then allowed to cool, filtered and washed with water: ethanol (1:1) mixture. The obtain powder was designed as $PW_{11}Mn$-SBA. The synthesis was presented in Scheme 1.

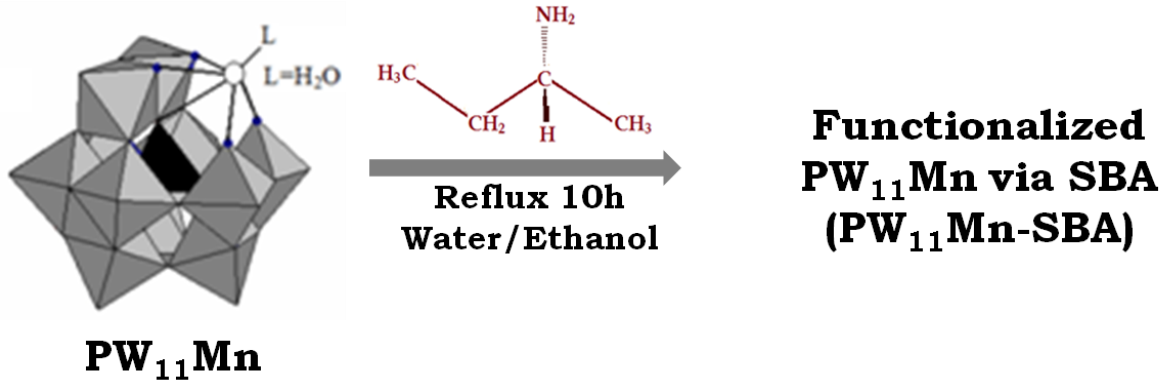

Scheme 1. Synthesis of $PW_{11}Mn$-SBA

(b) Synthesis of $PW_{11}Mn$-Cy

0.8985gm of $PW_{11}Mn$ was dissolved in 10 ml of distilled water. 0.127gm of Cy was dissolved in 15 ml of ethanol. The ethanolic solution of Cy was added drop wise to the aqueous solution of $PW_{11}Mn$. The pH of the solution was found to be 6.4. This resulted mixture was refluxed for 10 h and then allowed to cool, filtered and washed with water: ethanol (1:1) mixture. The obtain powder was designed as $PW_{11}Mn$-Cy. The synthesis was presented in Scheme 2.

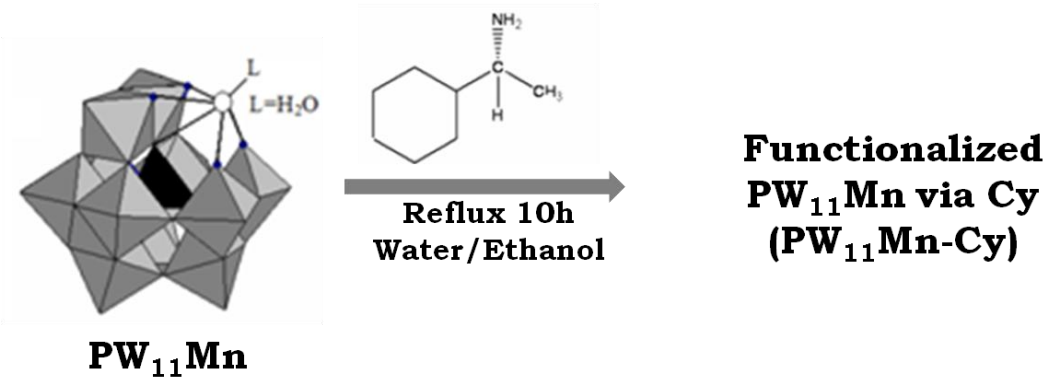

Scheme 2. Synthesis of $PW_{11}Mn$-Cy

7.2 Characterization

Elemental analysis was carried out using JSM 5610 LV combined with INCA instrument for EDX-SEM analyzer for the quantitative identification of metal ions. Thermo Gravimetric Analysis was carried out on the Mettler Toledo Star SW 7.01 upto 600°C in air with the heating rate of 5°C/min. FT-IR spectra of the samples were recorded as the KBr pellet on the Perkin Elmer instrument. The UV-visible spectrum was recorded at ambient temperature on Perkin Elmer 35 LAMDA instument using the 1cm quartz cell. The ESR spectra were recorded on a Varian E-line Century series X-band ESR spectrometer (liquid nitrogen temperature and scanned from 2000 to 3200 Gauss). Solution NMR (^{1}H, ^{13}C, ^{31}P) was recorded in D_2O as well as in $CDCl_3$ on Bruker ACF 300 MHz instrument. Optical activity was carried out using JASCO (J- 815 CD Spectrometer, model no: J-815-150L) and JASCO (P-

2000 Digital Polarimeter). The optical rotation was carried out for neat S-SBA as well as for PW_{11}Mn-SBA in methanol and water respectively. The 5% solution was used to carry out optical rotation.

Catalytic activity

The catalytic activity was carried out as mentioned in Ch-2. The reaction mixture was extracted in dichloromethane and analyzed by Agilent Technologies 6890N gas chromatography (FID, 19091G-B213 chiral capillary column (30 m × 0.32 mm × 0.25 um)) using nitrogen as a carrier gas with flow rate 30 ml/min. The injector temperature, detector temperature, and oven temperature were 250, 250, and 100 ◦C, respectively. The authentic samples of benzaldehyde, R- and S-configuration styrene epoxides were used as the standard product to determine the yields by comparison of peak height and area.

7.3 Results and Discussion

The present work divided in two parts. First part involving the discussion involving the functionalization of PW_{11}Mn by SBA and second part involving the functionalization of PW_{11}Mn by Cy.

(I) Functionalization of PW_{11}Mn by SBA (PW_{11}Mn-SBA)

7.3.1a Spectroscopic Analysis

Elemental analysis

The observed values for the elemental analysis in the isolated complex (PW_{11}Mn-SBA) are in good agreement with the theoretical values. Anal Calc: Cs,18.11 ; W, 55.13; P,0.84; Mn,1.49; O,21.81 ; C,1.30; H, 0.89; N,0.38. Found: Cs, 17.92 ; W,54.84; P,0.83; Mn,1.47; O,21.49 ; C,1.20 ; H,0.80 ; N,0.35. The number of water molecules was calculated from TGA curve, based on total weight loss (4.3%), correspond to loss of 11 water molecules. From elemental as well as thermal analysis the chemical formula of the isolated complex is proposed as, $Cs_5[PW_{11}O_{39}Mn(C_4H_{11}N)].11H_2O$.

FT-IR

The frequencies of FT-IR bands for $PW_{11}Mn$; SBA, $PW_{11}Mn$-SBA and R1-$PW_{11}Mn$-SBA (reused catalyst) are shown in Table 1. SBA gives characteristic IR fingerprint region for C-N vibration (1290, 1259 and 1148cm^{-1}), symmetric and asymmetric stretching vibrations of aliphatic C-H bonds (2928, 2850 and 1450cm^{-1}) and N-H stretching vibration (1598cm^{-1}). $PW_{11}Mn$-SBA complex shows IR vibration bands correspond to $PW_{11}Mn$ as well as SBA. It displays a characteristic IR fingerprint in the region of 1000-700cm^{-1}, attributed to the stretching vibration of the tetrahedral P-O bonds (1075 and 1054cm^{-1}), terminal W=O bonds (952cm^{-1}) and the two types of bridging W-O-W bonds of the cluster (880 and 812cm^{-1}). These characteristic IR data indicating the retainment of Keggin structure even after introduction of SBA. However, little shift was observed which may due to the introduction of SBA in the coordination sphere of $PW_{11}Mn$.

Table 1. FT-IR Frequency data

Materials	**FT-IR frequencies**						
	P-O	**W=O**	**W-O-W**	**Mn-N**	**C-N**	**N-H**	**C-H**
$PW_{11}Mn$	1078 1053	955	884 813	-	-	-	-
SBA	-	-	-	-	1290 1259 1148	1598	2928 2850 1450
$PW_{11}Mn$-SBA	1075 1054	952	880 812	672	1200 1173	1541	2922 2852 1448
R_1-$PW_{11}Mn$-SBA	1078 1055	953	882 815	670	1201 1171	1541	2920 2848 1451

In addition, from the FT-IR spectra we can obtain the structural information about the organic ligand. A pair of weak peaks at 2922 and 2852cm^{-1} for the synthesized material is attributed to the symmetric and asymmetric stretching vibrations of aliphatic C-H bonds. These results ensure the successful formation of POMs based hybrid material with $PW_{11}Mn$ and SBA.

It is interesting to note down that after introduction of an organic moiety (i.e. for $PW_{11}Mn$-SBA), the vibration bands that originated from C-N bond gives two broad bands at 1200 and 1273 cm^{-1} instead of three characteristic bands. Further a very significant shift, from 1598 cm^{-1} to 1541 cm^{-1} for N-H stretching is observed. This indicates the formation of dative bond from N→Mn. As a result of decreases in electron density on N atom, N-H bond length decreases which leads to the significant shift. In addition, the formation of new band at 672 cm^{-1} also supports the formation of N→Mn bond.

UV-Visible

The UV-vis spectrum of $PW_{11}Mn$ and in water, shows a W→O charge-transfer peak at 291 nm accompanied by another λ_{max} at 398 nm (Figure 1a), which can be attributed to the d–d electronic transition of the Mn center in the $[PW_{11}O_{39}Mn(H_2O)]$ anion. While the UV-vis spectrum of $PW_{11}Mn$-SBA in water, shows two peaks. One at 289 nm corresponding to the W→O charge-transfer and another λ_{max} at 407nm (Figure 1b) which can be attributed to the d–d electronic transition of the Mn center in the $[PW_{11}O_{39}Mn$-SBA] anion. The shift in λ_{max} from 398nm to 407nm may be due to the replacement of the labile aquo ligand by SBA.

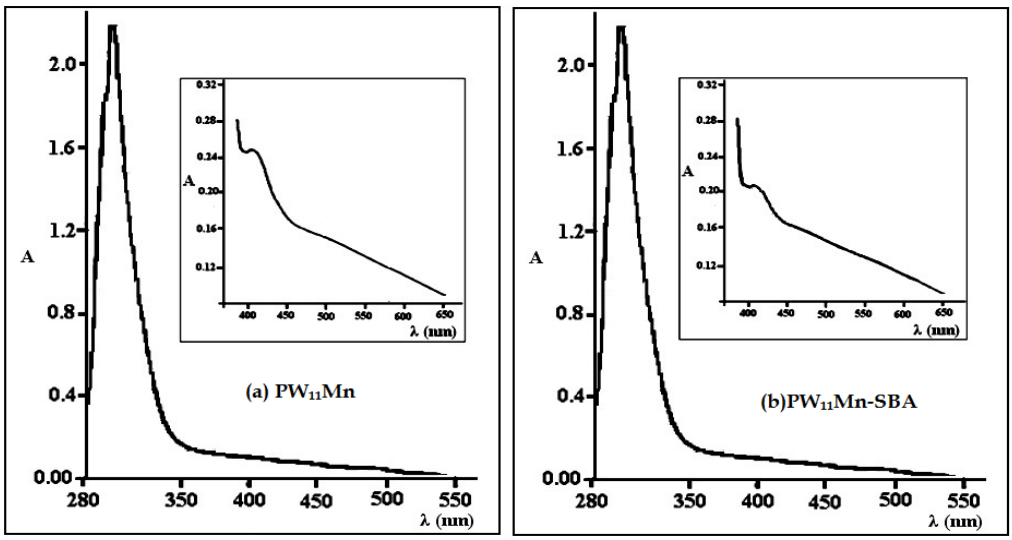

Figure 1. UV-VIS Spectra of (a) $PW_{11}Mn$ (b) $PW_{11}Mn$-SBA

The ability of the manganese polyoxometalate to coordinate with the organic ligand is well documented in the literature [19] and it was reported that, changes in the position or shape or increase in intensity of ligand field band was observed when aquo ligand was replaced by any ligand. The change of the ligand field band was observed for number of ligand in case Co(II) undecatungstocobalto(II) by Weakly et al [35]. The obtained result is as expected.

ESR

Paramagnetic compounds have different relaxation times. If the electronic relaxation is slow, good ESR spectra can be obtained at room temperature while, if the electronic relaxation is fast, good ESR spectra can be obtained only at low temperature. The low temperature ESR for $PW_{11}Mn$ and $PW_{11}Mn$-SBA were recorded in the range of 3200 to 2000 G. The low temperature ESR shows (Figure 2a and 2b) a well resolved six lines ESR spectrum with g ~ 2.3 and 2.1 which is as expected and confirms the presence of Mn(II) in the synthesized material. The slight shift in g value may be due to the change in the environment around the Mn(II) centre.

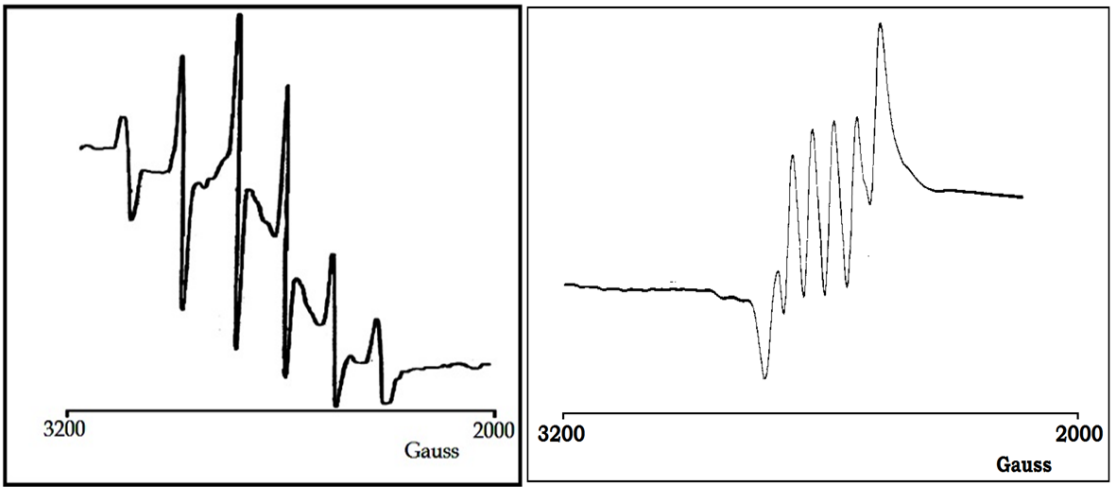

Figure 2. ESR Spectra of (a) $PW_{11}Mn$ (b) $PW_{11}Mn$-SBA

Thus the FT-IR, UV-Vis and ESR spectrum supports the formation of POMs based functionalized material through N→Mn bond.

Nuclear Magnetic Resonance Spectra

It is known that the presence of paramagnetic metal centre generally results in a poorly defined NMR spectrum. In present case, well resolved NMR spectra (^{13}C, ^{31}P) are obtained. This may be due to the two facts; the concentration of paramagnetic metal centre (present case 1.53% Mn(II)), the electronic relaxation for paramagnetic compound is fast. So ESR spectra can not be obtained at room temperature but NMR spectrum can be obtained at room temperature.

^{31}P NMR spectra for $PW_{11}Mn$ and $PW_{11}Mn$-SBA are shown in Figure 3a and 3b. ^{31}P NMR spectroscopy is a useful method to identify the change in the environment around the transition metal centre incorporated into the POMs. Further, it also showed the purity of the formed product. However many a time it is well documented that in case of preparing such kind hybrid material there is lack of getting pure product in aqueous media resulting into the two to three line in ^{31}P NMR spectrum [36]. Such kind material exhibiting spectrum corresponds to the formed product along with presence of other species (i.e. monolacunary POMs and TMSPOMs).

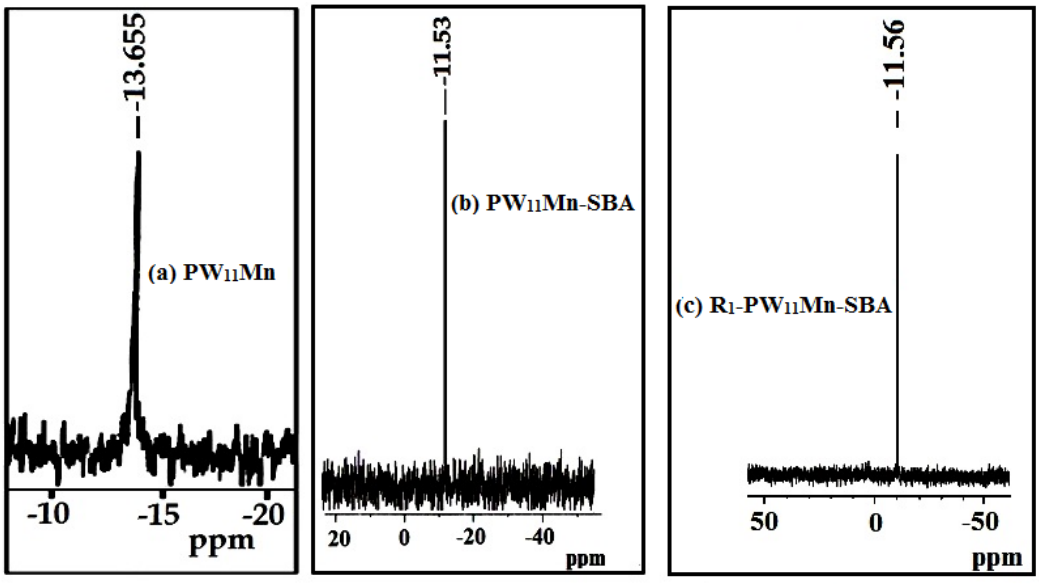

Figure 3. ^{31}P NMR of (a) $PW_{11}Mn$ (b) $PW_{11}Mn$-SBA (c) R1-$PW_{11}Mn$-SBA

In the present case only single peak is observe confirming the formation of single pure products. The significant up field shift in $PW_{11}Mn$-SBA as compared to $PW_{11}Mn$ in may be due to the change in the

environment around the Mn(II)-centre. This also changes the central P environment, i.e. PO_4-Mn-H_2O becomes PO_4-Mn-SBA. Thus ^{31}P NMR indicates the successful replacement of aquo ligand by SBA.

Figure 4 presents the structure of SBA. The chemical shift of ^{13}C NMR spectrum for SBA as well as $PW_{11}Mn$-SBA (Figure 5) are presented in Table 2. As shown in Table 2, no significant shift in $^{a}CH_3$ carbon indicates the amine remain intact in the synthesized material. The considerable upfield shift was observed for $^{b}CH_3$ and $^{c}CH_2$ and downfield shift was observed for ^{d}CH. This may be due to the bond formation between N atom of SBA and Mn of $PW_{11}Mn$. Once, dative bond form between Mn-N, the electron density on N atom decreases, which leads to the downfield shift for ^{d}CH carbon. The result is as expected. The NMR study confirms the formation of N→Mn bond.

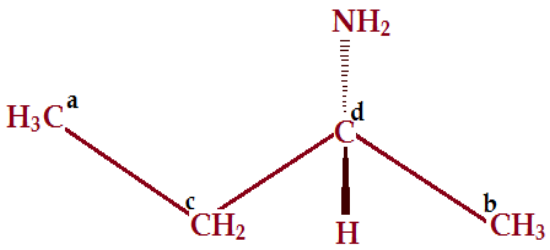

Figure 4. Structure of SBA

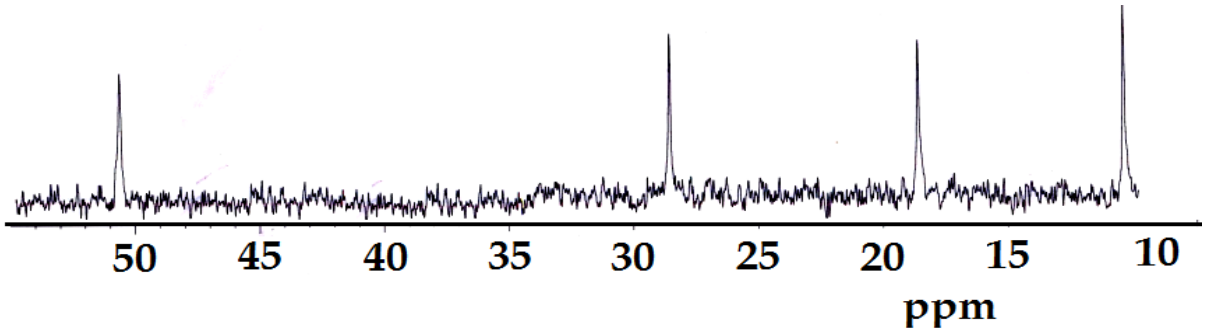

Figure 5. ^{13}C NMR $PW_{11}Mn$-SBA

Table 2. Chemical Shift for ^{13}C NMR

Chemical Shift	SBA	$PW_{11}Mn$-SBA
$^{a}CH_3$	10.8	10.6
$^{b}CH_3$	23.6	18.83
$^{c}CH_2$	33.8	28.76
^{d}C-H	48.6	50.84

^1H NMR spectra of the $PW_{11}Mn$-SBA (Figure 6) show broadened peaks or very poorly defined spectra corresponding to the CH_3 and CH_2 protons. This indicates the presences of SBA moiety into the coordination sphere of $PW_{11}Mn$. Presence of paramagnetic centre will responsible to give broadened peaks or very poorly defined spectra.

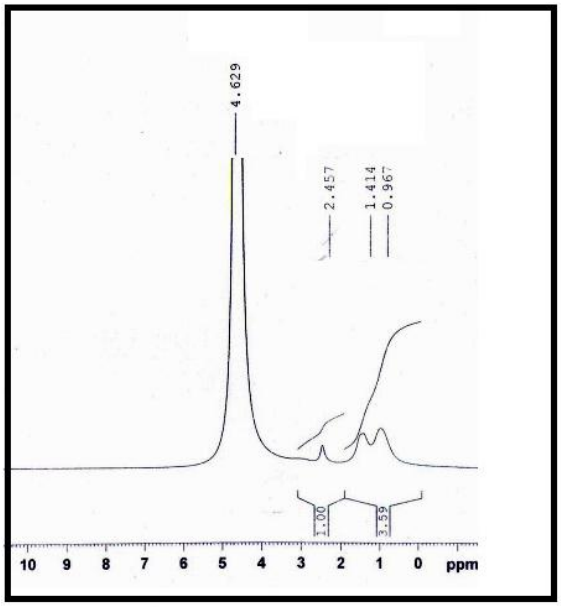

Figure 6. ^1H NMR spectra of $PW_{11}Mn$-SBA

CD spectroscopy

To examine the chiroptical and stable activities of synthesized material in the solution state, the CD spectra was carried out in water (Figure 7). The spectrum of the synthesized material exhibits Cotton effect at 250 nm. This is region for characteristic of the oxygen-to-tungsten charge-transfer bands of Keggin polyoxoanions [37]. The induced circular dichroism in the POM clusters can be clearly seen in the CD spectra. Optical rotation of SBA & PW_{11}Mn-SBA was found to be [α] 20/D+1.49 and [α]20/D+0.4 respectively. This result ensures that the synthesized material is chiral.

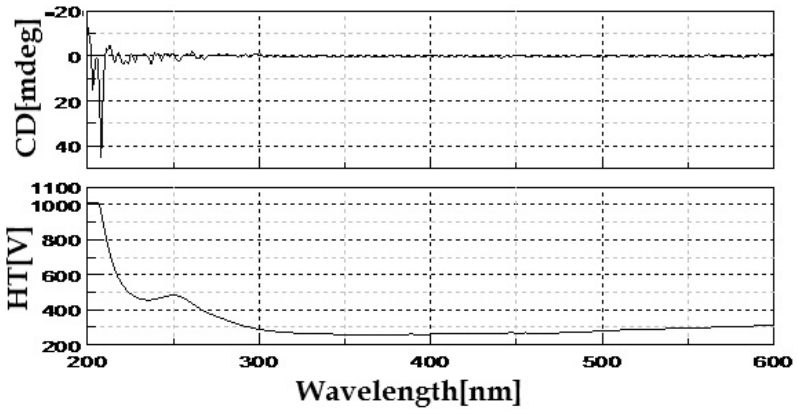

Figure 7. CD Spectra of PW_{11}Mn-SBA

7.3.1a Catalytic activity

Oxidation of styrene using H_2O_2

A detail study was carried out on oxidation of styrene by varying different parameters such as mole ratio of styrene to H_2O_2, catalyst amount and reaction time to get optimum reaction condition for oxidation of styrene. An experiment without catalyst was carried out and no conversion was obtained, indicating that there is no auto-oxidation taking place.

Effect of mole ratio

Oxidation of Styrene was carried out by varying the mole ratio of Sty to H_2O_2 from 1:1 to 1:3. As demonstrated in Figure 8, the oxidation of styrene improved from 63 to 100% upon increasing the styrene to H_2O_2 mole ratio from 1:1 to 1:3. Further increases in the amount of H_2O_2 from 1:3 to 1:4 did not result in the styrene conversion as well as selectivity of benzaldehyde. Thus, suggesting that a large amount of oxidant is not an essential condition to improve the oxidation of styrene. Therefore, 1:3 styrene to H_2O_2 mole ratio was considered the optimized condition for the oxidation of styrene.

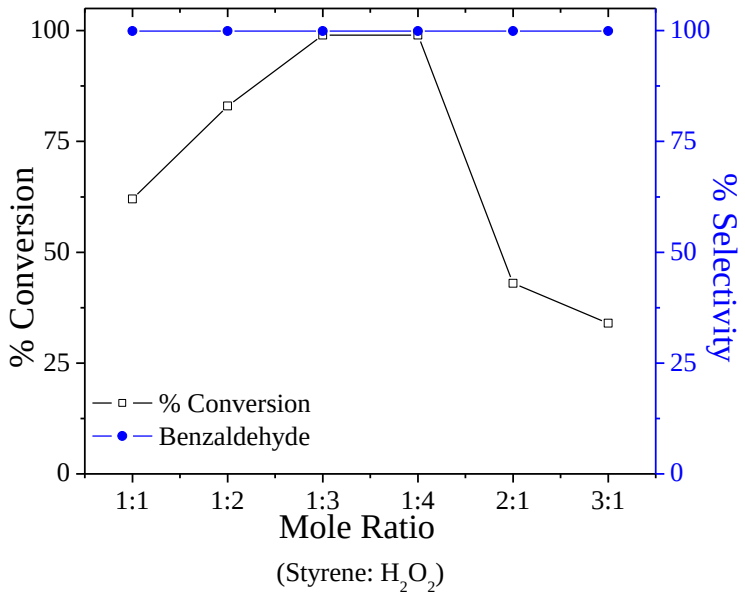

Figure 8. Effect of mole ratio on oxidation of styrene

Effect of amount of catalyst

The effect of catalyst amount on the conversion of styrene is illustrated in Figure 9. As the amount of catalyst was increased from 5 mg to 25mg, the conversion of styrene increased from 37 to 100%. With further increase in the catalyst amount from 25mg to 30mg, the conversion and selectivity does not change. The obtained results clearly indicate that Mn functions as active sites for oxidation. However, 25mg can be considered sufficient enough to carry out the reaction and further, effect of reaction time and temperature was studied.

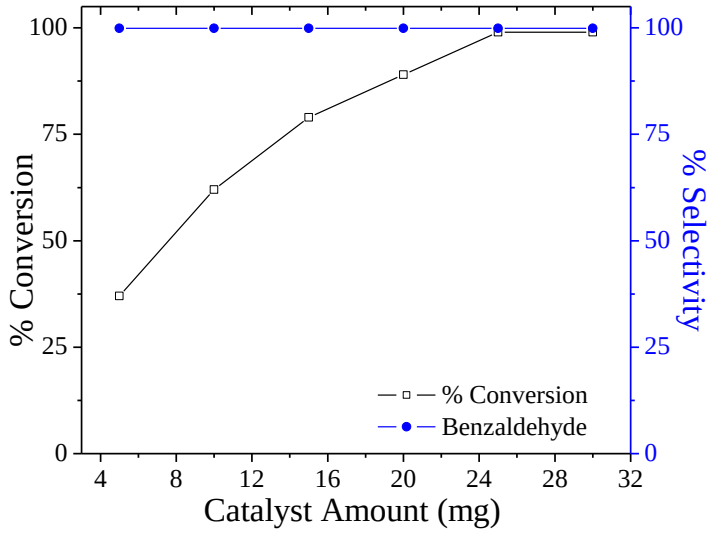

Figure 9. Effect of amount of catalyst on oxidation of styrene

Effect of reaction time

The effect of reaction time on the conversion was depicted in Figure 10 keeping other parameter constant. The degree of conversion increases with increases in reaction time. However within the time of 18h, 100% styrene conversion was observed. However, the selectivity to benzaldehyde remained unchanged basically throughout the entire reaction procedure. Due to the improved catalytic activity of PW_{11}Mn-SBA, 18h would be preeminent time period to carry out the oxidation of styrene.

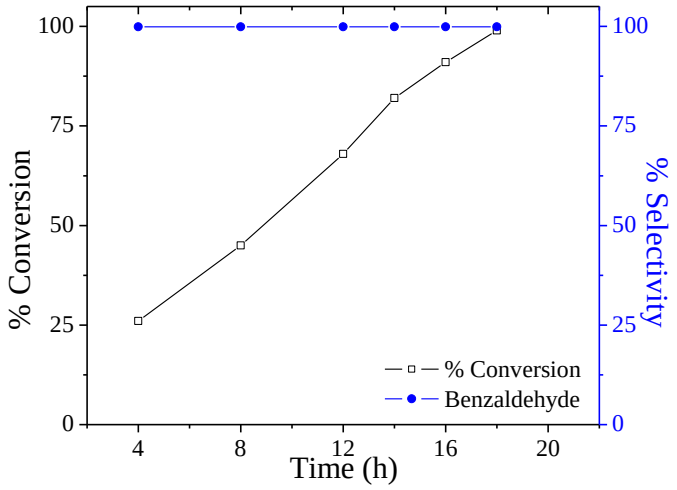

Figure 10. Effect of reaction time on oxidation of styrene using H_2O_2

Leaching and Heterogeneity Test

In the present case, PW_{11}Mn-SBA behaves as homogeneous catalyst as a result leaching and heterogeneity test was not required.

Regeneration and Recycling

The regeneration and recycling of the catalyst was carried out as mentioned in Ch-2 and the results for the same are presented in Table 3.

Table 3. Oxidation of styrene using hydrogen peroxide with fresh and regenerated catalyst

Catalyst	Conversion (%)	Selectivity for BA (%)	TON
PW_{11}Mn-SBA	100	>99	1428
R1- PW_{11}Mn-SBA	99	>99	1414
R2- PW_{11}Mn-SBA	99	>99	1414

Conversion based on substrate; substrate, 10mmole; oxidant H_2O_2 (30 mmole), amount of catalyst, 25 mg; reaction time 18h; reaction temperature 80^0C

Oxidation of styrene using O_2

A neat reaction (without catalyst) was carried out and it showed no conversion for the substrate indicating that there is no auto oxidation taking place. In order to study the role of TBHP the same sets of reactions were carried under two different conditions: (i) alkene + oxidant + TBHP and (ii) alkene + oxidant + PW_{11}Mn-SBA. In both the cases the reaction did not progress significantly. These observations indicate that the liberation of O_2 from TBHP was not sufficient to induce the reaction as well as the activation of manganese. Hence it may be concluded that in the present study TBHP acts as an initiator only.

Effect of amount of catalyst

The effect of concentration of the catalyst amount on the conversion and selectivity is shown in Table 4. In the present study epoxidation of styrene gives styrene oxide as well as benzaldehyde. However with an increase in the amount of catalyst, % conversion also increases. This suggests that the manganese centre functions as active sites for oxidation.

Table 4. Effect of amount of catalyst

Catalyst	**Amount (mg)**	**Conversion (%)**	**Selectivity (%)**		**ee (S) (%)**
			BA	**StyO**	
PW_{11}Mn-SBA	5	6	75	25	6
	10	19	78	22	8
	15	32	83	17	7
	20	41	86	14	9
	25	52	89	11	10
	30	58	> 99		

Substrate; styrene, 100mmole; oxidant, O_2(4ml/min) ; TBHP, 0.15mmol;reaction time 4h;temperature , 80^oC

It is very interesting to observe the difference in the selectivity of the products with an increase in the amount of the catalyst. As shown in Table 4, up to 25 mg of catalyst, epoxide was observed. On further increasing the amount of the catalyst, the product selectivity shifts from the less stable

intermediate (epoxide) to the more stable product (benzaldehyde). This may be due to the fact that with increase in the amount of the active species the reaction becomes very fast which favours the conversion of the formed styrene oxide to benzaldehyde. Due to the known importance of epoxide, the amount of the catalyst was optimized at 25 mg.

Effect of reaction time

It is seen from the Table 5 that the distribution of the product changes with increase in the reaction time. As the reaction time increases the product selectivity shifts towards BA. With increase in the reaction time the unstable intermediate, epoxide, is converted to the more stable product BA. Due to the known industrial importance of styrene oxide, the reaction time was optimized at 4 h.

Table 5. Effect of reaction time

Catalyst	**Reaction time (h)**	**Conversion (%)**	**Selectivity (%)**		**ee (S) (%)**
$PW_{11}Mn$-SBA			**BA**	**StyO**	
	2	27	81	19	10
	4	52	89	11	10
	6	56	>99		

substrate; styrene, 100mmole; oxidant, O_2(4ml/min) ; TBHP, 0.15mmol catalyst, 25mg; temperature , 80^oC

Effect of SBA

To examine the effect organic ligand, the oxidation of styrene was carried out using $PW_{11}Mn$ as well as $PW_{11}Mn$-SBA in optimize condition and the distribution of products are reported in Table 6. $PW_{11}Mn$ showed 61% conversion for styrene with >99% selectivity towards benzaldehyde where as $PW_{11}Mn$-SBA showed 52 % converstion with 11 % selectivity towards 89 % selectivity towards benzaldehyde. The difference in the catalytic activity can be explained on the basis of the structural difference between $PW_{11}Mn$ and $PW_{11}Mn$-SBA. This could be explained on the basis of the nature of the catalyst. The catalytic performances of the $PW_{11}Mn$-SBA catalysts are

mainly due to the easy electron-donating ability of the organic ligand, which facilitate the formation of stabilization of the formed styrene oxide.

Table 6. Oxidation of styrene using $PW_{11}Mn$ and $PW_{11}Mn$-SBA (under optimized condition)

[c]Alkenes	Conversion (%)	Products	Selectivity (%)	ee (S)	[d]TON
Styrene	[a]52/[b]61	StyO BA	[a]11 [a]89/ >[b]99	10	[a]7251/[b]8507

[a]Epoxidation of alkenes catalyzed by $PW_{11}Mn$-SBA; [b]Epoxidation of alkenes catalyzed by $PW_{11}Mn$; [c]Conversion based on substrate; styrene, 100mmole; oxidant, O_2(4ml/min) ; TBHP, catalyst ,25mg;reaction time 4h; [d]TON: Turnover number based on conversion

Leaching as well as heterogeneity test

Any leaching of the active species makes the catalyst unattractive and hence it is necessary to study the stability as well as leaching of $PW_{11}Mn$-SBA. The catalyst was filtered after completion of reaction and the filtrate was characterized for UV-Vis spectroscopy. For comparison, UV-Vis spectrum of $PW_{11}Mn$-SBA recorded (Figure 11). The absence of characteristic peaks in filtrate indicates that there is no leaching of $PW_{11}Mn$-SBA and the catalyst remains completely insoluble under reaction condition and could be reused.

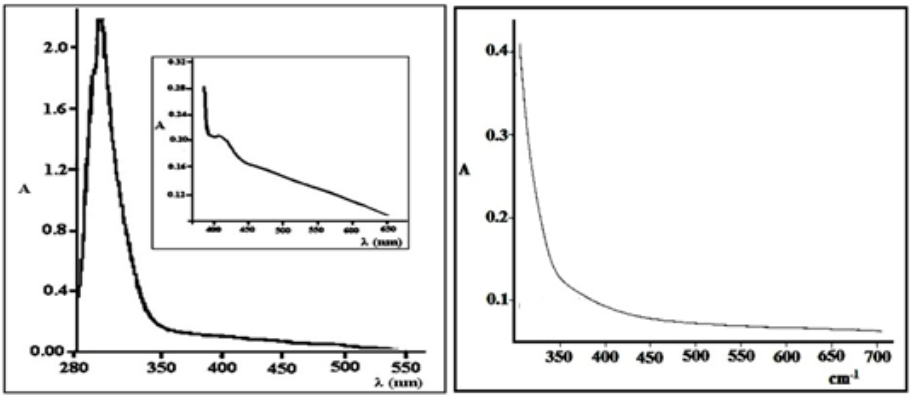

Figure 11. UV-Vis spectra of (a) $PW_{11}Mn$-SBA (b) filtrate

For rigorous proof of heterogeneity, a test was carried out by filtering catalyst from the reaction mixture at 80°C after 2h and the filtrate was allowed to react up to completion of reaction (4h). The reaction mixture of 2h

and filtrate was analyzed on Gas Chromatogram. The results are presented in Table 7. No change in % conversion as well as % selectivity was found. On the basis of the results, it can be the present catalysts are truly heterogeneous in nature.

Table 7. % Conversion and % selectivity for oxidation of styrene (with and without catalyst)

Catalyst	**Reaction time (h)**	**Conversion (%)**	**Selectivity**		**ee (S)(%)**
			BA	**StyO**	
PW_{11}Mn-SBA	2	27	81	19	10
Filterate	4	27	81	19	10

Substrate; styrene, 100mmole; oxidant, O_2(4ml/min) ; TBHP, amount of catalyst, 25mg ; reaction time 4h; temperature , 80^{o}C

Regeneration and recycling of the catalyst

In order to investigate the stability of the catalyst during oxidation reaction, the catalyst was separated by simple filtration after completion of reaction. The separated catalyst was washed with dichloromethane and dried at 100^{o}C (designated as R_1-PW_{11}Mn-SBA). Oxidation of styrene was then carried out with the recycled catalyst, under the optimized conditions (R_1-PW_{11}Mn-SBA). The obtained results are presented in Table 8. As seen from Table 8, the recycled catalyst did not show any appreciable change in the activity, indicating that the catalyst is stable and can be regenerated for repeated use.

Table 8. Recycling of the catalyst

Catalyst	Reaction time (h)	Conversion (%)	Selectivity (%)		ee (S) (%)
			BA	StyO	
PW_{11}Mn-SBA	4	52	89	11	10
R1-PW_{11}Mn-SBA	4	50	90	10	9

Substrate; styrene, 100mmole; oxidant, O_2(4ml/min) ; TBHP, 25 mg catalyst;reaction time 4h; temperature , 80^oC

Further the recycled catalyst (R1-PW_{11}Mn-SBA) was characterized by FT-IR (Table 1) and ^{31}P NMR (Figure 3c) spectroscopy. The FT-IR spectra of the R1-PW_{11}Mn-SBA display the all the characteristic bands for the C-N, N-H stretching and N→Mn bond.

Further, the ^{31}P NMR spectra of R_1-PW_{11}Mn-SBA show the chemical shift at -11.56 ppm (Figure 3c). No shift in FT-IR bands and the chemical shift indicate that the PW_{11}Mn-SBA remains stable in the present reaction condition.

(II) Functionalization of $PW_{11}Mn$ by Cy ($PW_{11}Mn$-Cy)

7.3.2a Spectroscopic Analysis

Elemental analysis

The values of elemental analysis data for $PW_{11}Mn$-Cy are in good agreement with the theoretical values. Anal Calc: Cs, 15.82; W, 60.29.50; P, 0.92; Mn, 1.64; O, 20.98; C, 2.67; H, 0.47; N, 0.39. Found: Cs, 15.58; W, 60.05; P, 0.89; Mn, 1.60; O, 20.49; C, 2.62; H, 0.43; N, 0.34.

The number of water molecules was calculated from TGA curve for $PW_{11}Mn$-Cy which shows 4.7% loss in weight corresponding to loss of 9 water molecules. As thermal as well as elemental analysis reveals the chemical formula of the isolated complex is proposed as, $Cs_5[PW_{11}O_{39}Mn(C_8H_{17}N)].9H_2O$.

UV-Visible

The UV-Vis spectra of $PW_{11}Mn$ as well as $PW_{11}Mn$-Cy are presented in Figure 12. The UV–vis spectrum of $PW_{11}Mn$-Cy in water shows two peaks: one at 291 nm corresponding to the W =O charge-transfer and another λ_{max} at 406 nm which can be attributed to the d–d electronic transition of the Mn center in the $PW_{11}Mn$-Cy.

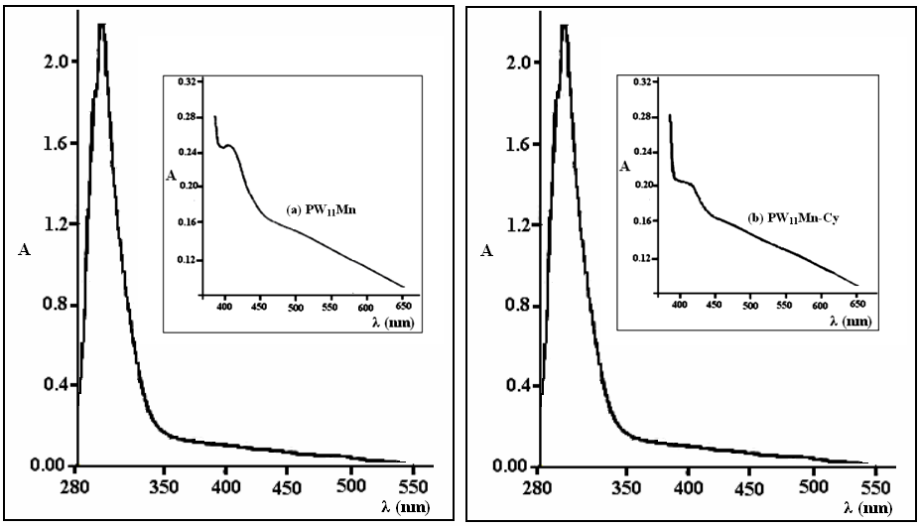

Figure 12. UV-Vis Spectra of (a) $PW_{11}Mn$ (b) $PW_{11}Mn$-Cy

The shift in λ_{max} from 398 nm to 406 nm may be due to the replacement of the labile aquo ligand by Cy.

ESR

The full range (4000 – 2000 G) X-band room temperature ESR spectrum for $PW_{11}Mn$ and $PW_{11}Mn$-Cy were recorded. The room temperature ESR signal shows one broad, weak and poorly resolved signal at g ~ 2.3 and 2.01 which may be due to the presence of Mn(II). It has been reported by K. Nowinska et al. that Mn(II) ion introduced into octahedral lacuna of the Keggin structure should be responsible for the signal in the range of g parameter of about 2, which is attributed to octahedral or distorted octahedral environment [38]. The obtained broad ESR spectrum may be due to the fast relaxation of unpaired electrons. It is known that the fast relaxation of electrons can be restricted by Low Temperature ESR. So in the present case low temperature ESR for $PW_{11}Mn$ and $PW_{11}Mn$-Cy were recorded in the range of 3200 to 2000 G. The low temperature ESR shows (Figure 13a and 13b) a well resolved six lines ESR spectrum with g ~ 2.3 and 2.01 which is as expected and confirms the presence of Mn(II) in the synthesized material.

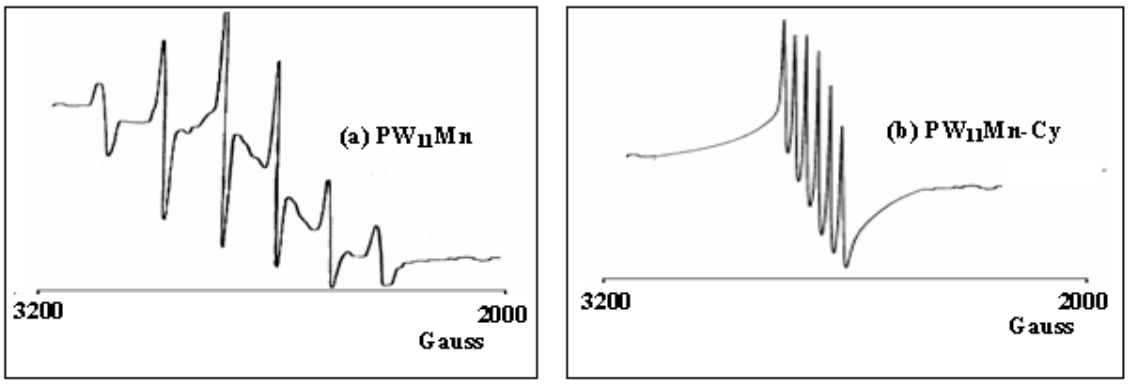

Figure 13. ESR Spectra of (a) $PW_{11}Mn$ (b) $PW_{11}Mn$-Cy

FT-IR

The frequencies of FT-IR bands for $[PW_{11}O_{39}Mn]^{5-}$; $PW_{11}Mn$; Cy and $[PW_{11}O_{39}Mn\text{-}Cy]^{5-}$; $PW_{11}Mn$-Cy are shown in Table 9.

Table 9. FT-IR Frequency data

	P-O	W=O	W-O-W	Mn-N	C-N	N-H	C-H
$PW_{11}Mn$	1078 1053	956	882, 820		-		-
Cy	-	-	-	-	1296 1264 1154	1599	2922 2852 1449
$PW_{11}Mn$ - Cy	1074 1051	952	879, 810	664	1201	1508	2926 2852 1449
R1-$PW_{11}Mn$ -Cy	1072 1050	954	880, 813	662	1204	1510	2928 2850 1451

$PW_{11}Mn$-Cy cluster displays a characteristic IR fingerprint in the region of 1000-700 cm^{-1}, attributed to the stretching vibration of the tetrahedral P-O bonds (1074 and 1051 cm^{-1}), terminal W=O bonds (952 cm^{-1}) and he two types of bridging W-O-W bonds of the cluster (879 and 810 cm^{-1}). These characteristic IR data indicating the retainment of Keggin structure even after introduction of Cy. However little shift was observed in bridging oxygen of $PW_{11}Mn$-Cy, which may due to the introduction of Cy in the coordination sphere of Mn centre by replacing aqua ligand.

In addition, from the FT-IR spectra we can obtain the structural information about the organic ligand. A pair of weak peaks at 2924 and 2852cm^{-1} for the synthesized material is attributed to the symmetric and asymmetric stretching vibrations of aliphatic C-H bonds. These results ensure the successful functionalization of $PW_{11}Mn$ with Cy.

As shown in Table 9 Cy gives characteristic (C-N) vibration at 1296, 1264, 1154 cm^{-1}. It is interesting to note down that after functionalization (i.e. for PW_{11}Mn-Cy), the vibration bands that originated from C-N bond are merged and an only one broad bond 1201cm^{-1} is developed. Further a very significant shift, from 1599cm^{-1} to 1508 cm^{-1} for N-H stretching is observed. This indicates the formation of dative bond from N→Mn. As a result of decreases in electron density on N atom, N-H bond length decreases which leads to the significant shift. In addition, the formation of new band at 664cm^{-1} also supports the formation of N→Mn bond.

Nuclear Magnetic Spectroscopy

^{31}P NMR spectra for $PW_{11}Mn$ and $PW_{11}Mn$-Cy are shown in Figure. 14a and 14b. No significant change in the chemical shift confirms that the Keggin unit remains intact after introduction of Cy to $PW_{11}Mn$.

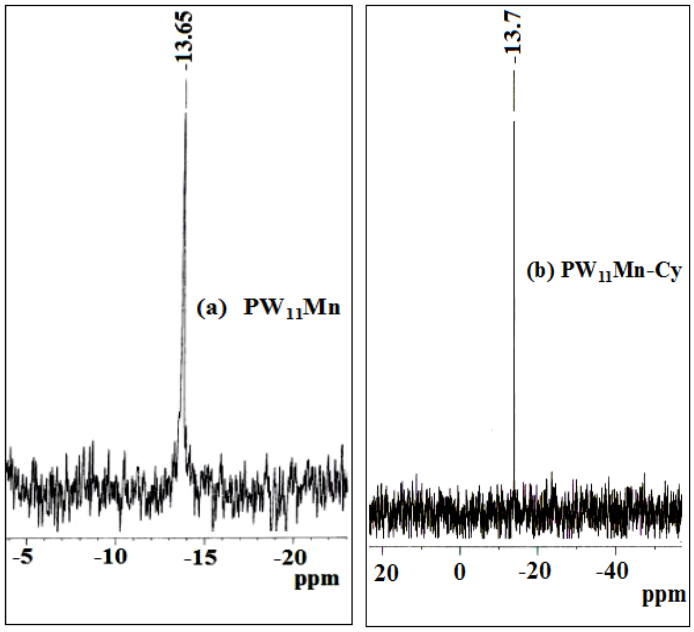

Figure 14. ^{31}P NMR of (a) $PW_{11}Mn$ (b) $PW_{11}Mn$-Cy

Figure 15a and 15b shows ^{13}C NMR spectrum for Cy as well as $PW_{11}Mn$-Cy. The values for chemical shift are presented in Table 10. As shown in Table 10, no significant shift in the cyclic ring carbon $^{(a\text{-}e)}CH_2$ indicates the amine remain intact in the synthesized material. The observed significant upfield shift for $^{h}CH_3$ and $^{f}C\text{-}C\text{-}NH_2$ may be due to the bond formation between N atom of Cy and Mn of $PW_{11}Mn$. Once, dative bond form between Mn-N, the electron density on N atom decreases, which leads to the downfield shift. The N atom attached to the stereogenic centre shows the downfield shift of 0.9 ppm. The result is as expected. NMR study confirms the formation of N→Mn bond.

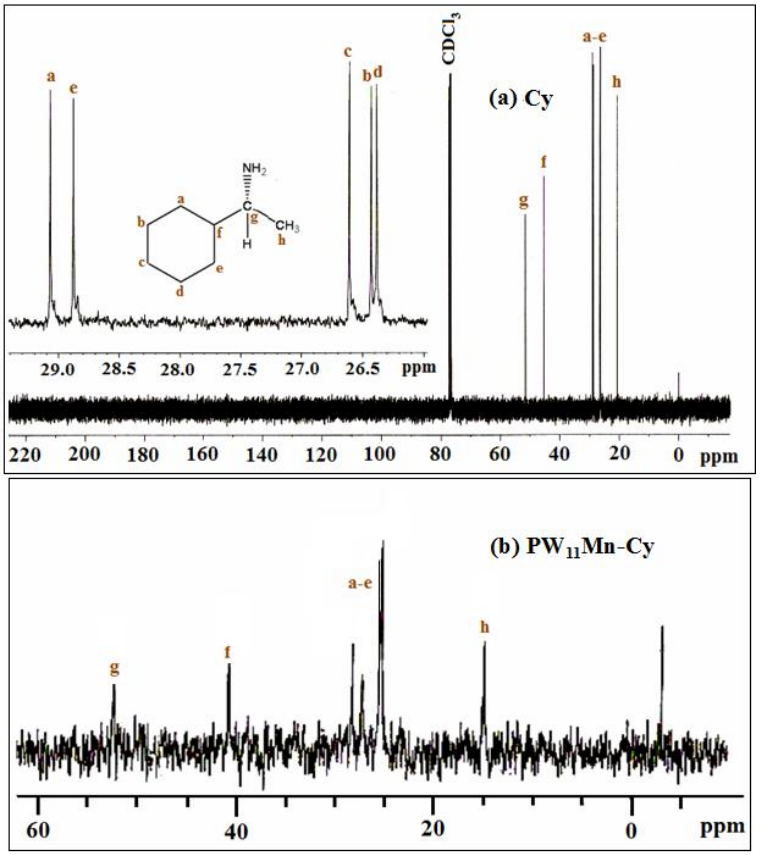

Figure 15. ^{13}C NMR of (a) Cy (b) $PW_{11}Mn$-Cy

Table 10. Chemical Shift for ^{13}C NMR

Functional Group	Chemical shift (ppm)	
	$PW_{11}Mn$-Cy	**Cy**
$^{h}CH_3$	14.986	20.797
$^{(a-e)}CH_2$ (ring carbon)	25.318 – 28.297	26.384 – 29.069
^{g}C-NH_2	52.436	51.573
^{f}C-C-NH_2	40.789	45.443

CD spectroscopy

The circular dichroism spectra of $PW_{11}Mn$-Cy in the solution state show significant induced optical rotation activity in the POMs moieties may be due to the presence of chiral organic ligand, which imparts chirality to the whole framework. The spectrum of the functionalized material displays strong cotton effects at 250nm (Figure 16), the characteristic spectral region of oxygen-to-tungstate charge transfer bands of Keggin polyoxoanions [37]. Further, chirality in the synthesized material was supported by carrying out out optical rotation. Optical rotation of Cy and $PW_{11}Mn$-Cy was found to be [α] 20/D-3.8 and [α] 20/D-2.65 respectively. This result ensures that the formed functionalized material is chiral.

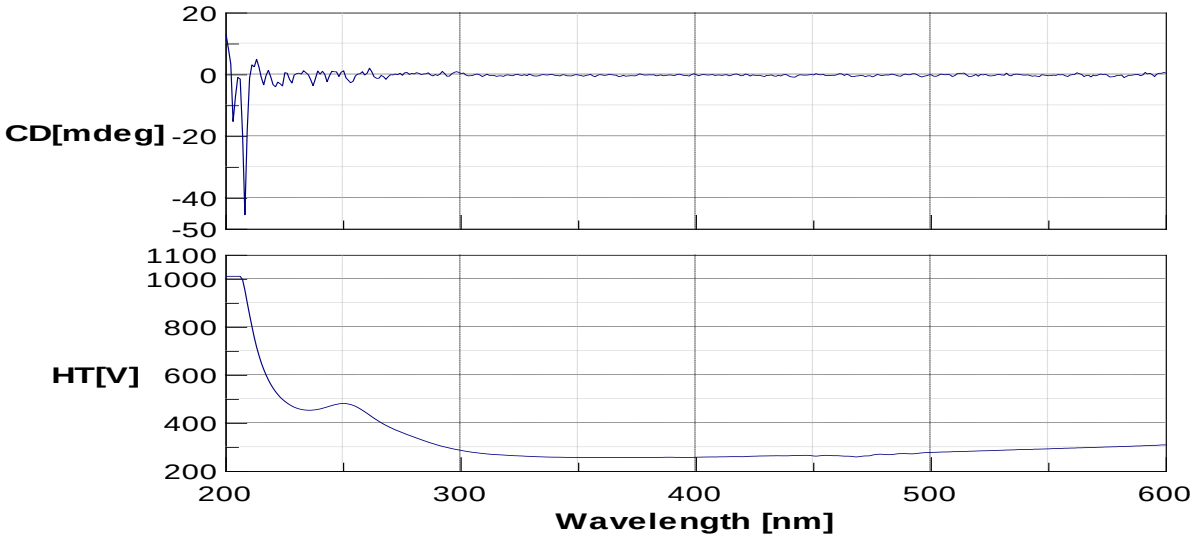

Figure 16. CD Spectra of $PW_{11}Mn$-Cy

7.3.2b Catalytic activity

Oxidation of styrene using H_2O_2

A detail study was carried out on oxidation of styrene by varying different parameters such as mole ratio of styrene to H_2O_2, catalyst amount and reaction time to get optimum reaction condition for oxidation of styrene. An experiment without catalyst was carried out and no conversion was obtained, indicating that there is no auto-oxidation taking place.

Effect of mole ratio

Oxidation of Styrene was carried out by varying the mole ratio of Sty to H_2O_2 from 1:1 to 1:3. As demonstrated in Figure 17, the oxidation of styrene improved from 67 to 100% upon increasing the styrene to H_2O_2 mole ratio from 1:1 to 1:3. Further increases in the amount of H_2O_2 from 1:3 to 1:4 did not result in the styrene conversion as well as selectivity of benzaldehyde. Thus, suggesting that a large amount of oxidant is not an essential condition to improve the oxidation of styrene. Therefore, 1:3 styrene to H_2O_2 mole ratio was considered the optimized condition for the oxidation of styrene.

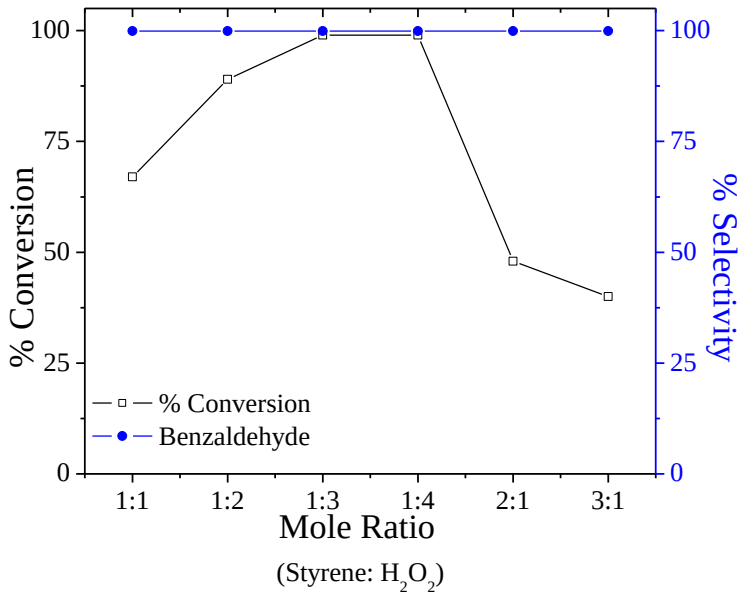

Figure 17. Effect of mole ratio on oxidation of styrene

Effect of amount of catalyst

The effect of catalyst amount on the conversion of styrene is illustrated in Figure 18. As the amount of catalyst was increased from 5 mg to 25mg, the conversion of styrene increased from 41 to 100%. With further increase in the catalyst amount from 25mg to 30mg, the conversion and selectivity does not change. The obtained results clearly indicate that Mn functions as active sites for oxidation. However, 25mg can be considered sufficient enough to carry out the reaction and further, effect of reaction time and temperature was studied.

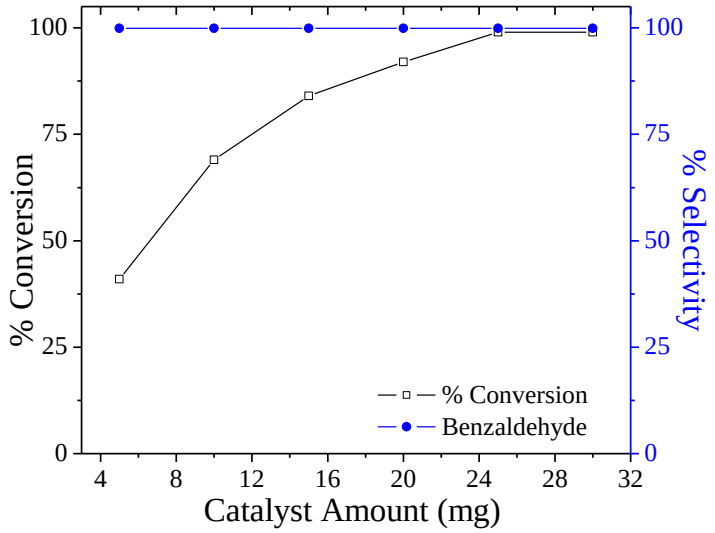

Figure 18. Effect of amount of catalyst on oxidation of styrene

Effect of reaction time

The effect of reaction time on the conversion was depicted in Figure 19 keeping other parameter constant. The degree of conversion increases with increases in reaction time. However within the time of 18h, 100% styrene was converted. However, the selectivity to benzaldehyde remained unchanged basically throughout the entire reaction procedure. Due to the improved catalytic activity of $PW_{11}Mn$-Cy, 18h would be preeminent time period to carry out the oxidation of styrene.

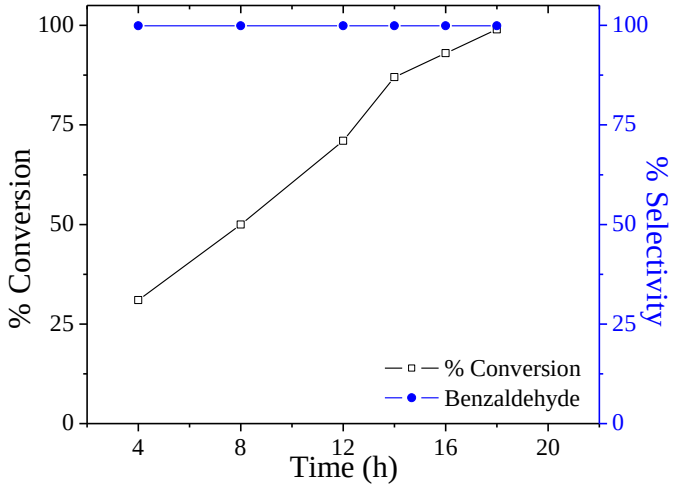

Figure 19. Effect of reaction time on oxidation of styrene

The optimum conditions for 100% conversion with >99% selectivity for BA are; mole ratio of styrene to H_2O_2 as 1:3; catalyst amount = 25mg; reaction temperature = 80^{o}C and reaction time = 18h.

Leaching and Heterogeneity Test

In the present case, $PW_{11}Mn$-Cy behaves as homogeneous catalyst as a result leaching and heterogeneity test was not required.

Regeneration and Recycling

The regeneration and recycling of the catalyst was carried out as mentioned in Ch-2 and the results for the same are presented in Table 11.

Table 11. Oxidation of styrene using hydrogen peroxide with fresh and regenerated catalyst

Catalyst	Conversion (%)	Selectivity for BA (%)	TON
$PW_{11}Mn$-Cy	100	>99	1416
R1- $PW_{11}Mn$- Cy	99	>99	1402
R2- $PW_{11}Mn$- Cy	99	>99	1402

Conversion based on substrate; substrate, 10mmole; oxidant H_2O_2 (30 mmole), amount of catalyst, 25 mg; reaction time 18h; reaction temperature 80^0C

$PW_{11}Mn$ gave 100% conversion in 14h whereas $PW_{11}Mn$-SBA and $PW_{11}Mn$-Cy gave 82% and 87% conversion with single selective product (i.e. BA) in 14h. As discussed in previous chapter that, Mn(II) sites are the catalytic active sites which are responsible for effective oxidation of styrene. The presence of steric hindrance leads to the partial prevention of the oxidation process. In case of $PW_{11}Mn$-SBA and $PW_{11}Mn$-Cy single selective product (i.e.BA) was obtained. This is because the reaction with H_2O_2 is fast and exothermic resulting in nucleophilic attack of H_2O_2 on StyO giving rise to BA. So, higher selectivity for BA was observed.

Oxidation of styrene using O_2

A neat reaction (without catalyst) was carried out and it showed no conversion for the substrate indicating that there is no auto oxidation taking place. In order to study the role of TBHP the same sets of reactions were carried under two different conditions: (i) alkene + oxidant + TBHP and (ii) alkene + oxidant + PW_{11}Mn-Cy. In both the cases the reaction did not progress significantly. These observations indicate that the liberation of O_2 from TBHP was not sufficient to induce the reaction as well as the activation of manganese. Hence it may be concluded that in the present study TBHP acts as an initiator only.

Effect of amount of catalyst

The effect of concentration of the catalyst amount on the conversion and selectivity is shown in Table 12. In the present study epoxidation of styrene gives styrene oxide as well as benzaldehyde. However with an increase in the amount of catalyst, % conversion also increases. This suggests that the manganese centre functions as active sites for oxidation. It is very interesting to observe the difference in the selectivity of the products with an increase in the amount of the catalyst. As shown in Table 12, up to 25 mg of catalyst, epoxide was observed. On further increasing the amount of the catalyst, the product selectivity shifts from the less stable intermediate (epoxide) to the more stable product (benzaldehyde). This may be due to the fact that with increase in the amount of the active species the reaction becomes very fast which favours the conversion of the formed styrene oxide to benzaldehyde. Due to the known importance of epoxide, the amount of the catalyst was optimized at 25 mg.

Table 12. Effect of amount of catalyst

Catalyst	Amount (mg)	Conversion (%)	Selectivity (%)		ee (R) (%)
			BA	StyO	
$PW_{11}Mn$-Cy	5	8	71	29	7
	10	20	75	25	9
	15	36	79	21	8
	20	44	84	16	10
	25	54	87	13	12
	30	64	> 99	-	-

substrate; styrene, 100mmole; oxidant, O_2(4ml/min) ; TBHP, 0.15mmol;reaction time 4h;temperature , 80^oC

Effect of reaction time

It is seen from the Table 13 that the distribution of the product changes with increase in the reaction time. Initially, after the completion of 2 h the 24 % of styrene oxide is observed. As the reaction time increases the product selectivity shifts towards BA. With increase in the reaction time the unstable intermediate, epoxide, is converted to the more stable product BA. Due to the known industrial importance of styrene oxide, the reaction time was optimized at 4 h.

Table 13. Effect of reaction time

Catalyst	Reaction time (h)	Conversion (%)	Selectivity (%)		ee (R) (%)
			BA	StyO	
$PW_{11}Mn$-Cy	2	34	76	24	10
	4	54	87	13	12
	6	60	>99	-	-

substrate; styrene, 100mmole; oxidant, O_2(4ml/min) ; TBHP, 0.15mmol catalyst, 25mg; temperature , 80^oC

Effect of Cy

To examine the effect organic ligand, the oxidation of styrene was carried out using $PW_{11}Mn$ as well as $PW_{11}Mn$-Cy in optimize condition and the distribution of products are reported in Table 14. $PW_{11}Mn$ showed 61% conversion for styrene with >99% selectivity towards benzaldehyde where as $PW_{11}Mn$-Cy showed 55 % converstion with 13 % selectivity towards styrene oxide and 87 % selectivity towards benzaldehyde. The difference in the catalytic activity can be explained on the basis of the structural difference between $PW_{11}Mn$ and $PW_{11}Mn$-Cy. This could be explained on the basis of the nature of the catalyst. The excellent catalytic performances of the $PW_{11}Mn$-Cy catalysts are mainly due to the easy electron-donating ability of the organic ligand, which facilitate the formation of stabilization of the formed styrene oxide.

Table 14. Oxidation of styrene using $PW_{11}Mn$ and $PW_{11}Mn$-Cy (under optimized condition)

[c]Alkenes	Conversion (%)	Products	Selectivity (%)	ee (R)	[d]TON
Styrene	[a]54/[b]61	StyO BA	[a]13 [a]87/ > [b]99	12	[a]7363/[b]8507

[a]Epoxidation of alkenes catalyzed by $PW_{11}Mn$-Cy; [b]Epoxidation of alkenes catalyzed by $PW_{11}Mn$; [c]Conversion based on substrate; styrene, 100mmole; oxidant, O_2(4ml/min) ; TBHP, catalyst ,25mg;reaction time 4h; [d]TON: Turnover number based on conversion

Leaching as well as heterogeneity test

Any leaching of the active species makes the catalyst unattractive and hence it is necessary to study the stability as well as leaching of $PW_{11}Mn$-Cy. The catalyst was filtered after completion of reaction and the filtrate was characterized for UV-Vis spectroscopy. For comparison, UV-Vis spectrum of $PW_{11}Mn$-Cy recorded (Figure 19). The absence of characteristic peaks in filtrate indicates that there is no leaching of $PW_{11}Mn$-Cy and the catalyst remains completely insoluble under reaction condition and could be reused.

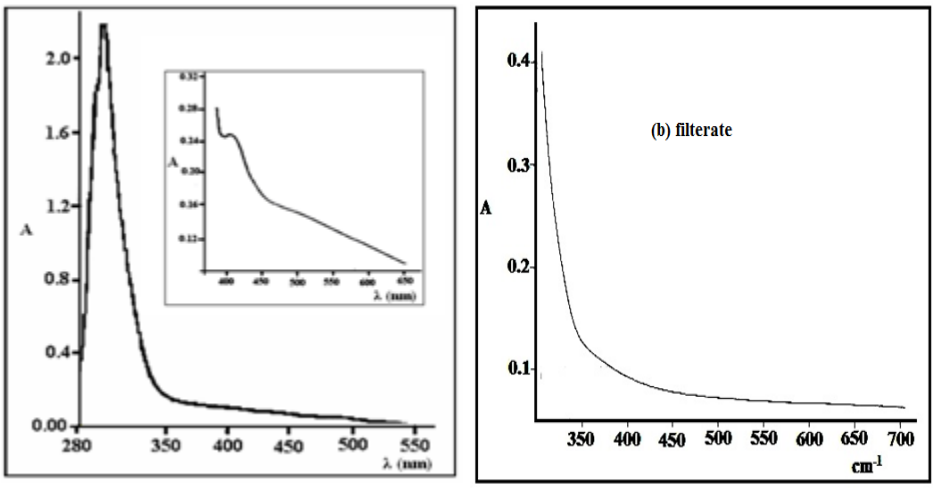

Figure 19. UV-Vis spectra of (a) $PW_{11}Mn$-Cy (b) filtrate

For rigorous proof of heterogeneity, a test was carried out by filtering catalyst from the reaction mixture at 80°C after 2h and the filtrate was allowed to react up to completion of reaction (4h). The reaction mixture of 2h and filtrate was analyzed on Gas Chromatogram. The results are presented in Table 15. No change in % conversion as well as % selectivity was found. On the basis of the results, it can be the present catalysts are truly heterogeneous in nature.

Table 15. % Conversion and % selectivity for oxidation of styrene (with and without catalyst)

Catalyst	Reaction time (h)	Conversion (%)	Selectivity		ee (R)(%)
			BA	StyO	
$PW_{11}Mn$-Cy	2	34	76	24	10
Filterate	4	34	78	22	9

Substrate; styrene, 100mmole; oxidant, O_2(4ml/min) ; TBHP, 25mg catalyst; reaction time 4h; temperature , 80°C

Regeneration and recycling of the catalyst

In order to investigate the stability of the catalyst during oxidation reaction, the catalyst was separated by simple filtration after completion of reaction. The separated catalyst was washed with dichloromethane and dried at 100^{o}C (designated as R_1-PW_{11}Mn-Cy). Oxidation of styrene was then carried out with the recycled catalyst, under the optimized conditions (R_1-PW_{11}Mn-Cy). The obtained results are presented in Table 16. As seen from Table 16, the recycled catalyst did not show any appreciable change in the activity, indicating that the catalyst is stable and can be regenerated for repeated use.

Table 16. Recycling of the catalyst

Catalyst	**Reaction time (h)**	**Conversion (%)**	**Selectivity (%)**		**ee (R) (%)**
			BA	**StyO**	
PW_{11}Mn-Cy	4	55	87	13	12
R1-PW_{11}Mn-Cy	4	54	89	11	11

Substrate; styrene, 100mmole; oxidant, O_2(4ml/min) ; TBHP, 25 mg catalyst; reaction time 4h; temperature , 80^{o}C

Further the recycled catalyst (R1-PW_{11}Mn-Cy) was characterized by FT-IR (Table 8). The FT-IR spectra of the R1-PW_{11}Mn-Cy display the all the characteristic bands for the C-N, N-H stretching and N→Mn bond.

Effect of organic ligand in aerobic oxidation of styrene

Under optimized condition, PW_{11}Mn-SBA gave 52% conversion with 89% selectivity towards benzaldehyde and 11% selectivity towards styrene oxide and PW_{11}Mn-Cy gave 55% conversion with 87% selectivity towards benzaldehyde and 13% selectivity towards styrene oxide. But, in 2h PW_{11}Mn-SBA gave 27% (Table 5) conversion with 19% (Table 13) selectivity towards styrene oxide and PW_{11}Mn-Cy gave 34% conversion with 24% selectivity towards styrene oxide. It is known that if the oxidation reaction is fast the product selectivity shifts towards more stable product (BA) rather than the less stable intermediate (StyO). The slow and controlled reaction can increase the selectivity of StyO. The difference in conversion and selectivity for the synthesized complexes can be explained on the basis of the incoming organic ligand. Mn(II) sites are the catalytic active sites which are responsible for oxidation of styrene. As in case of PW_{11}Mn-Cy, the presence of cyclic ring in Cy is responsible for higher selectivity towards StyO in 2h as compared to PW_{11}Mn-SBA. The obtained results are as expected.

Conclusion

1. New functionalized material was synthesized by covalent interaction that comprising $PW_{11}Mn$ and SBA as well as Cy.
2. Spectral studies show that the Keggin unit remain intact even after introduction of SBA and Cy.
3. The FT-IR and NMR (^{13}C and ^{31}P) studies indicate the formation of N→Mn dative bond in synthesized material (Figure 20).

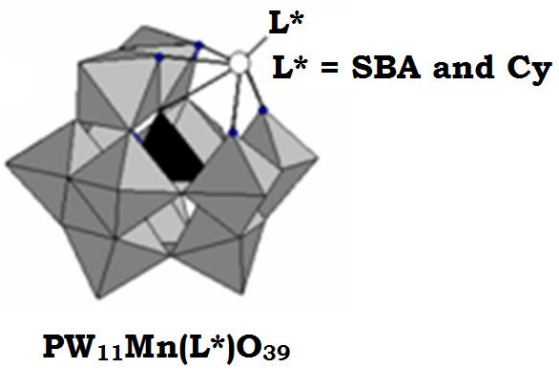

Figure 20. Functionalized $PW_{11}Mn$

4. The presence of Mn^{II} was confirmed by FT-IR, UV-visible as well as ESR spectroscopy
5. The presence of chirality in the synthesized material was confirmed by CD spectroscopy and polarimeter.
6. The synthesized functionalized material was successfully used as heterogeneous catalyst for carrying out asymmetric oxidation of styrene using O_2.
7. The catalyst was regenerated and *reused up to 2* cycles after simple workup.

References

1. M. T. Pope, A. Muller (Eds.), Polyoxometalates: From Platonic Solids to Anti-Retroviral Activity, Kluwer, Dordrecht, The Netherlands (1994).
2. Issue on "Polyoxometalates", *Chem. Rev.* 98, 1, (1998).
3. K. Y. Lee, M. Misono in Handbook of Heterogeneous Catalysis (2nd Edition), Vol.1 (Eds. G.Ertl, H. Knozinger, F. Schiuth, J. Weitkamp), Wiley-VCH, Weinheim, 318, (2008).
4. C. L. Hill, *J. Mol. Catal. A : Chem.*, 262, 1, (2007).
5. N. Mizuno, S. Hikichi, K. Yamaguchi, S. Uchida, Y. Nakagawa, K. Uchara, K. Kamata, *Catal. Today.*, 117, 32, (2006).
6. I.V. Kozhevinikov in Polyoxometalate Molecular Science Vol.98 (Eds. J. J. Borras-almendar, E. Coronado, A. Mullar, M. T. Pope), Kluwar Academics Publisher, Dordrecht, 2003, pp. 351-380.
7. R. Neumann in Polyoxometalate Molecular Science Vol.98 (Eds. J.J.Borras-almendar, E. Coronado, A. Mullar, M. T. Pope), Kluwar Academics Publisher, Dordrecht, pp. 327, (2003).
8. C. Boglio, G. Lemiere, B. Hasanknopf, S. Thorimbert, E. Lacote, M. Malacria, *Angew. Chem. Int. Ed.*, 45, 3324, (2006).
9. C. Boglio, K. Micoina, P. Remi, B. Hasanknopf, S. Thorimbert, E. Lacote, M. Malacria, C. Afonco, J-C Tabet, *Chem-Eur. J.*, 13, 5426, (2007).
10. Y.Kikukawa, S. Yamaguchi, K. Tsuchida, K. Uehara, K. Yamaguchi, N. Mizuno, *J. Am. Chem. Soc.*, 130, 5472, (2008).
11. N. Casan Pastor, P. Gomez Romero, *Front. Biosci.*, 9, 1759, (2004).
12. J. T. Rhule, C. L. Hill, D.A. Judd, R. F. Schinazi, *Chem. Rev.*, 98, 327, (1998).
13. B. Hasenknopf, *Front. Biosc.*, 10, 275, (2005).
14. T. Yamashe., *J. Mater. Chem.*, 15, 4773, (2005).
15. B. Hasenknopf, K. Micoine, E. Lacôte, S. Thorimbert, M. Malacria, R. Thouvenot, *Eur. J. Inorg. Chem.*, 5001, (2008).
16. A. Dolbecq , E. Dumas , C. R. Mayer, P. Mialane, *Chem. Rev.*, 110, 6009, (2010).

17. Z. Peng, *Angew. Chem. Int. Ed.,* 43, 930, (2004).
18. P. Gouzerh , A. Proust, *Chem. Rev.*, 98, 77, (1998).
19. H. liu, C. J. Gomez-Garcia, J. Peng, J. Sha, Y. Li, Y. Yan, *Dalton Trans.*, 6211, (2008).
20. C. Rong, M. T. Pope, *J. Am. Chem. Soc.*, 114, 2932, (1992)
21. O. A. Kholdeeva, T. A. Trubitsina, G. M. Maksimov, A. V. Golovin, R. I. Maksimovskaya, *Inorg. Chem.*, 44,1635, (2005).
22. J. C. Duhacek, D. C. Duncan, *Inorg. Chem.*, 46, 7253, (2007).
23. C. Dablemont, A. Proust, R. Thouvenot, C. Afonso, F. Fournier, J.C. Tabet, *Inorg. Chem.*, 43, 3514, (2004).
24. K. Nomiya, H. Torii, K. Nomura, Y. Sato, *J. Chem. Soc., Dalton Trans.*, 1506, (2001).
25. Q. Li, Y. G. Wei, J. Hao, Y. L. Zhu, L.S. Wang, *J. Am. Chem. Soc.*, 129, 5810, (2007).
26. H. Kang, J. Zubieta, *J. Chem. Soc., Chem. Commun.*, 1192, (1988).
27. Y. Lu, Y. Xu, E. B. Wang, J. Lu, C. W. Hu, L. Xu, *Cryst. Growth Des.*, 5, 257, (2005).
28. X. Y. Wei, M. H. Dickman, M. T. Pope, *Inorg. Chem.*, 36, 130, (1997).
29. J. F. W. Keana, M.D. Ogan, *J. Am. Chem. Soc.*, 108, 7951, (1986).
30. R. K. C. Ho, W. G. Klemperer, *J. Am. Chem. Soc.*, 100, 6772, (1978).
31. C. Dablemont, C. G. Hamaker, R. Thouvenot, Z. Sojka, M. Che, E. A. Maatta, A. Proust, *Chem.–Eur. J.*, 12, 9150, (2006).
32. H. Kwen, S. Tomlinson, E. A. Maatta, C. Dablemont, R. Thouvenot, A. Proust, P. Gouzerh, *Chem. Commun.*, 2970, (2002).
33. H. fu, Y. G. Li, Y. H. Wang, X. L. Wang, X. J. Feng, E. Wang., *Inorg.Chim.Acta.*, 362, 3231, (2009).
34. H. Li, C. J. Gómez-García, J. Peng, J. Sha, L. Wanga, Y. Yan, *Inorg. Chim. Acta.* 362, 1957, (2009).
35. T.J.R. Weakly, *J. Chem. Soc. Dalton Trans.*, 341, (1973).

36. V. Lahootun, C. Besson, R. Villanneau, F. Villain, L. Chamoreau, K. Boubekeur, S. Blanchard, R. Thouvenot, A. Proust, *J. Am. Chem. Soc.*, 129, 7127, (2007).
37. S. Allenmark, *Chirality*., 15, 409, (2003).
38. K. Nowinska, A. Waclaw, A. Gutsze, *Catal. Lett.*, 94,157, (2004).

NOVALTY OF WORK

1. For the first time easy one pot *in situ* synthesis of mono, di and sandwich type Mn(II)-substituted phosphotungstates were introduced.
2. The designed complexes were efficiently used as heterogeneous catalysts with O_2 as well as homogeneous catalysts with H_2O_2 for solvent free liquid phase oxidation reactions.
3. $PW_{11}Mn$ was proved to be an efficient catalyst for oxidation of styrene in achieving 61% and 100% conversion with BA as a single selective product with O_2 as well as H_2O_2 in 4h and 14h respectively.
4. PW_9Mn_4 was proved to be an efficient catalyst for epoxidation of alkenes, especially, in obtaining 42% conversion for oxidation of Cy6 in achieving 100% selectivity towards Cy6O with O_2 in 30h.
5. Functionalization $PW_{11}Mn$ was successfully carried out using non-covalent as well as covalent interaction with different organic ligands.
6. $PW_{11}Mn$--S was proved to be an efficient catalyst for oxidation of styrene in achieving 42% conversion with 41% selectivity towards StyO with O_2 in 4h under solvent free conditions.
7. To prove the non-covalent interaction, *catalysis* is used as *one of the characterization method.*
8. $PW_{11}Mn$-SBA and $PW_{11}Mn$-Cy was used as catalyst in asymmetric oxidation of styrene.

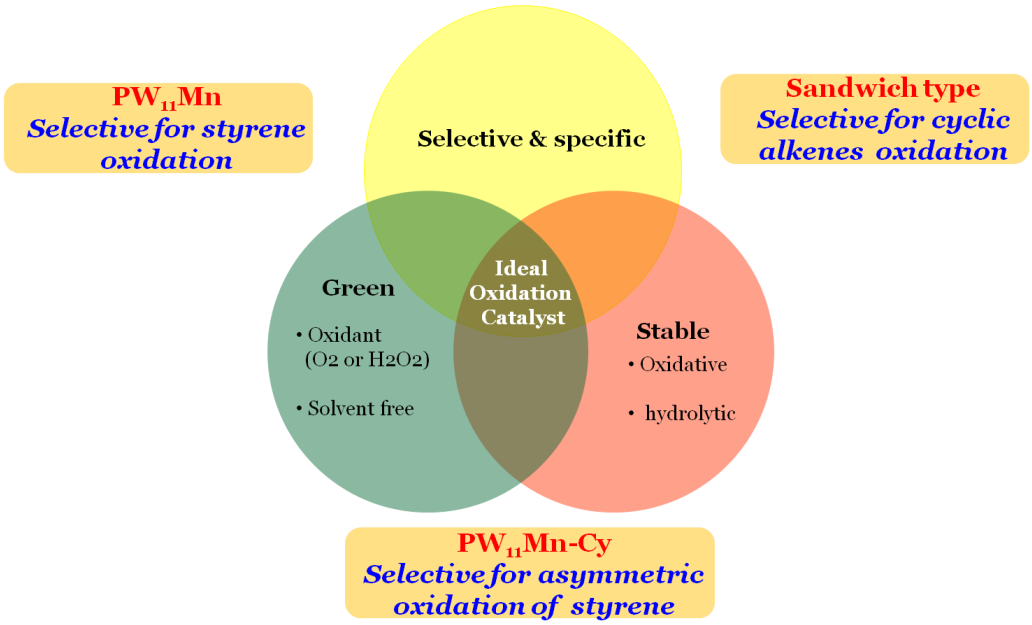

Paper presented in International/National Conferences, Symposium

1. "Manganese salen Supported onto Zirconia: Synthesis, Characterization and Aerobic Oxidation of alkenes", **Ketan Patel** and Anjali Patel presented at 11th CRSI National Symposium in Chemistry at National Chemical Laboratory, Pune, 6th -8th Feb 2009.

2. "Non-Solvent liquid phase oxidation of styrene over first transition metal substituted polyoxometalate: A comparative study", by Pragati Shringarpure, **Ketan Patel** and Anjali Patel presented at 6th WORLD CONGRESS ON OXIDATION CATALYSIS at University of Lille, France, 5th – 10th July 2009.

3. "Functionalized Keggin type Polyoxometalate: Synthesis and Characterization of a new Organic-Inorganic hybrid material containing Manganese substituted Phosphotungstate and Salen", by **Ketan Patel**, Pragati Shringarpure and Anjali Patel presented at INTERNATIONAL CONFERENCE ON POLYOXOMETALATE at Jacobs University, Bremen, Germany, 28th July- 1st Aug 2009.

4. "Functionalization of Manganese substituted Polyoxometalate with R-(-)-1-Cyclohexylethylamine: Synthesis and Characterization", by **Ketan Patel** and Anjali Patel presented at 12th International symposium on Inorganic Ring System at Holiday Inn Resort , Goa, 16th -20th August 2009.

5. "Functionalized Keggin type Polyoxometalate: Synthesis and Characterization of a new Organic-Inorganic hybrid material containing Ruthenium substituted Phosphotungstate and (R)-(-)-Cycohexylethylamin", by **Ketan Patel**, Soyeb Pathan and Anjali Patel presented at MTIC at IISC, Banglore, 3rd – 8th December 2009.

6. "Keggin type Mn(II) substituted phosphotungstate as a recyclable catalyst for the oxidation of alcohols with Hydrogen peroxide", by **Ketan Patel** and Anjali Patel presented at 13th CRSI ISER-KIIT, Bhubneswar, 3rd – 7th February 2011.

7. “A Keggin type inorganic-organic hybrid material containing Mn(II) monosubstituted phosphotungstate and S-(+)-Sec-butyl amine: Synthesis and Characterization”, by **Ketan Patel** and Anjali Patel presented International Symposium in Material Education at IISER PUNE, 24th – 29th March 2011.

8. “Supramolecular assembly of inorganic–organic hybrid material comprising Keggin-type Mn(II)-substituted phosphotungstate and salen: Synthesis, characterisation and catalytic activity”, by **Ketan Patel** and Anjali Patel at International Conference on Supramolecular and Nanomaterials- Research and Application at Gujarat University Ahmadabad, 6th – 8th February 2012.